THE UNIVERSITY
of EDINBURGH

The *Drosophila* E3 ubiquitin ligase Hyperplastic Discs interacts with Shaggy and regulates morphogen signalling in the developing eye

Sophie Moncrieff

Thesis presented for the Degree of Doctor of Philosophy

University of Edinburgh

2015

THE UNIVERSITY *of* EDINBURGH

Doctor of Philosophy – The University of Edinburgh – 2015

Declaration

I declare that this PhD thesis was composed by me, and that the work contained herein is original research carried out by myself. Where the work of others has been presented, this is stated and acknowledged accordingly. This work has not been submitted for any other degree or professional qualification.

Sophie Moncrieff, February 2015

Acknowledgements

I would first like to thank my supervisor Mark Ditzel for his guidance, support, and encouragement over the last four years. Thank you for always being approachable, and for being very thorough and quick at reading and correcting my thesis.

I would also like to thank my lab mates and friends, Elaine and Flavia, for many laughs and discussions to brighten up the long days in the lab. I don't know how I would've done it without you! Thank you for being my tea-drinking, amatriciana-eating, problem-solving and gossiping buddies. Also a really special thank you goes out to Flavia for always being there, for all the help and advice - you've taught me so much and I am very grateful!

Thank you to the Medical Research Council who have funded my PhD and given me this opportunity. Thanks also to Matthew Pearson and Paul Perry for all their help in the imaging suite. Matt, you always went out of your way to help - thank you for your patience. Thank you to Flavia Alves at the Institute of Cell Biology, Edinburgh, who performed the mass spectrometry on my samples. Last but not least, a big thank you must go to Marcos Vidal, for letting me be a student for a day in his lab at the Beatson Institute in Glasgow, and for Juan, who taught me how to dissect and stain *Drosophila* eye discs - without you I would not have all these colourful images to show off!

Of course I would like to thank my Mum and Dad, Christiane and Mirko, for their heartfelt support and encouragement, for always being there for a chat when I need it, and for keeping me positive - and of course for passing on their best qualities to me! Also thank you to all my friends and family, including my newly acquired

family in law, for helping me stay sane and always being interested and supportive. A special mention goes to Neil and Laura Hermon for their endless supply of highlighters - I think it's fair to say I put them to good use!

Finally, and most importantly, to my husband Jimmy: you have been through everything with me and I know I couldn't have done this without you. Thank you for being there for me when it was bad (making my dinner, calming me down when I got stressed, putting up with my late nights and erratic moods) and always believing in me.

This thesis is dedicated to my Grandad, Erhard Hempel, who would have been very proud of me.

Abstract

The expression of the *Drosophila melanogaster* morphogen Hedgehog (Hh) plays a key role in co-ordinating proliferation and differentiation during animal development. Tight spatial and temporal regulation of Hh expression is essential for its correct function in these essential processes. Both mis-expression of its mammalian orthologue Sonic Hedgehog (Shh) and aberrant stimulation of the associated signalling pathway occur in a wide range of human tumours. Although there is extensive knowledge of the signal transduction pathway that is activated in a Hh-stimulated cell, very little is known about pathways governing the expression of the morphogen itself.

The *Drosophila* tumour suppressor protein Hyperplastic Discs (Hyd), an E3 ubiquitin ligase, negatively regulates *hedgehog* (*hh*) expression and Hh pathway activity by independent mechanisms in the developing *Drosophila* eye. Genetically generated *hyd* mutant clones in the eye mis-express *hh* and the transcriptional activator of Hh target genes, Cubitus interruptus (Ci), and cause overgrowth of the surrounding wild-type tissue. However, the underlying molecular mechanism(s) by which Hyd regulates these morphogen regulatory pathways is not known. Hyd may be involved in ubiquitylating target proteins in these pathways, which could have degradative or non-degradative outcomes. In order to elucidate Hyd's molecular role in potential morphogen regulatory pathways, I applied a proteomics-based approach to identify novel Hyd binding partners and ubiquitylated substrates. Tandem affinity purification in combination with mass spectrometry was used to purify and identify Hyd and its complexed binding partners from *Drosophila* cells. Binding and ubiquitylation assays were subsequently used to verify and characterize the interactions. In addition, a biased, literature-guided approach was applied to identify likely Hyd binding partners based on their involvement in morphogen signalling and conservation across species. Finally, to assess the functional consequences of a newly identified interaction, I used a *Drosophila in vivo* model to determine whether the novel binding partner was capable of modifying the *hyd* mutant phenotype. For

this purpose, the Mosaic Analysis with a Repressible Cell Marker (MARCM) technique was used to generate *hyd* mutant clones in the developing larval eye, which were expressing transgenes resulting in either the over-expression or RNAi-mediated knockdown of the gene of interest.

My results indicate that Hyd is involved in regulating both Hh and Wg morphogen signalling in the *Drosophila* eye, and that the molecular mechanism of action may, at least in part, involve the protein kinase Shaggy (Sgg). Hyd interacts with the Hh and Wg transcriptional activator proteins Ci and Armadillo, respectively, as well as the Sgg kinase. Sgg is a negative regulator of both the Hh and Wg pathways, and acts to direct the proteolytic processing or degradation of the transcriptional effectors of these morphogen pathways. Sgg and its mammalian orthologue GSK3β were ubiquitylated *in vitro*, and GSK3β ubiquitylation was negatively regulated by the mammalian homologue of Hyd, EDD. Knockdown of *sgg* in eye disc cells mutant for *hyd* resulted in a dramatic rescue of the overgrowth phenotype. Loss of *hyd* in clones located in the anterior region of the eye disc resulted in low levels of the full-length Hh transcriptional activator protein Ci. This effect was reversed completely as a result of *sgg* knockdown. Furthermore, loss of *hyd* in eye disc clones resulted in elevated Hh and Wg morphogen expression. Mis-expression of *hh* in *hyd* mutant clones was significantly reduced upon over-expression of a constitutively active Sgg kinase. Hence *sgg* appears to genetically act downstream of *hyd* to regulate *hh* gene expression and Ci expression.

In summary my results identify Sgg as a novel regulator of *hh* gene expression, whose activity may be regulated by ubiquitylation, and which may be acting downstream of Hyd in a ubiquitin-regulated manner to control both *hh* gene expression and Hh pathway activity in the developing *Drosophila* eye. Hyd may also regulate Hh pathway activity by directly interacting with Ci and affecting its activity.

The results also indicate that Hyd may be a master regulator of both Hh and Wg morphogen signalling during *Drosophila* development.

Table of Contents

List of Figures

List of Tables

Amino Acid Code

Alanine	Ala	**A**
Arginine	Arg	**R**
Asparagine	Asn	**N**
Aspartic Acid	Asp	**D**
Cysteine	Cys	**C**
Glutamic Acid	Glu	**E**
Glutamine	Gln	**Q**
Glycine	Gly	**G**
Histidine	His	**H**
Isoleucine	Ile	**I**
Leucine	Leu	**L**
Lysine	Lys	**K**
Methionine	Met	**M**
Phenylalanine	Phe	**F**
Proline	Pro	**P**
Serine	Ser	**S**
Threonine	Thr	**T**
Tryptophan	Trp	**W**
Tyrosine	Tyr	**Y**
Valine	Val	**V**

Chapter 1: Introduction

1.1 The Ubiquitin Code

1.1.1 Ubiquitin and transfer of ubiquitin to substrates

Ten years ago, Avram Hershko, Aaron Ciechanover, and Irwin Rose discovered the functions of a small, highly conserved eukaryotic protein called ubiquitin. They were awarded the 2004 Nobel Prize in Chemistry for their work on ubiquitin, which increasing evidence suggests is involved in regulating almost every process in a cell [reviewed in (Welchman et al. 2005)].

Ubiquitin is a highly stable, 76-amino acid (aa) protein, which is almost structurally invariant from yeast to man. The high structural conservation of ubiquitin's compact β-grasp fold among eukaryotes suggests that it plays an important and central role in a cell's processes (Vijay-Kumar et al. 1987). Ubiquitin is covalently attached to substrate proteins through the action of a series of enzymes, a process known as ubiquitylation (**Figure 1.1**). Importantly, the modification of target proteins with ubiquitin is both reversible and dynamic, making it comparable to phosphorylation. Although ubiquitylation has classically been found to direct substrate protein degradation through a multi subunit protease called the 26S proteasome, more recent advances in the field have found that ubiquitylation can also affect protein conformation, activity, and interactions (Z. J. Chen & L. J. Sun 2009).

Ubiquitin is transferred to substrate proteins in a three-step mechanism involving three key enzymes: E1 activating enzymes, E2 conjugating enzymes and E3 ligase enzymes (**Figure 1.1**) (Deshaies & Joazeiro 2009; Schulman & Harper 2009; Ye & Rape 2009). In the first step, the E1 enzyme activates ubiquitin via its catalytic cysteine residue in an adenosine triphosphate (ATP)-dependent reaction, forming a high-energy thiol ester intermediate. The activated ubiquitin is then transferred to a

cysteine residue in the E2 enzyme, which interacts with different E3 ligase enzymes. The E3 ligase ultimately confers the specificity of the ubiquitylation reaction, as it is involved in recognizing the substrate protein. In humans, there are two E1 enzymes, 40 E2 enzymes, and 600 E3 enzymes, effectively increasing the specificity of the ubiquitylation cascade from E1 to E3 (Z. J. Chen & L. J. Sun 2009). The E3 ligase, in some cases with the help of the E2 enzyme, catalyses the covalent attachment of ubiquitin to the substrate in the final step. This involves the formation of an isopeptide bond between the carboxy-terminal of ubiquitin to the epsilon amino (NH_2)-group of an internal lysine residue of the substrate protein. In some cases, the isopeptide bond can also be formed at the extreme amino-terminal of the protein, effectively forming a covalent ubiquitin-Met1 linkage (also known as linear ubiquitylation) (Rieser et al. 2013).

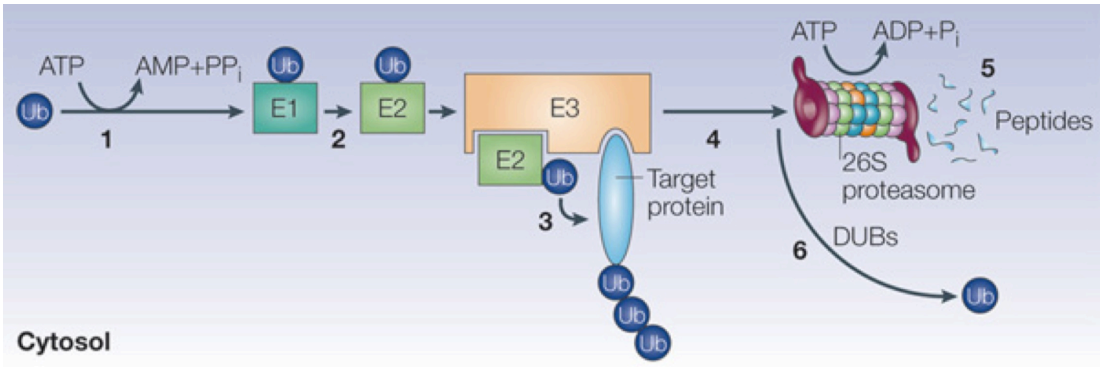

Figure 1.1: Transfer of Ubiquitin to substrates and degradation via the proteasome. Ubiquitin is activated by the E1 in an ATP-dependent reaction (1). The E1 then transfers ubiquitin to the E2 (2). In most cases, the E2 enzyme and the protein substrate both bind specifically to the E3 ligase, which transfers the activated ubiquitin moiety to the substrate (3). The E3 conjugates successive ubiquitin moieties to the substrate, which targets the substrate for degradation via the 26S proteasome (4). The substrate is degraded into peptides (5), and reusable ubiquitin is removed by deubiquitylating enzymes (DUBs) (6). Pi, inorganic phosphate; PPi, pyrophosphate; Ub, ubiquitin. Figure taken from **(Welchman et al. 2005)**.

Ubiquitination can result in the attachment of a single ubiquitin moiety, as well as multiple ubiquitin moieties, which can form polymeric chains (**Figure 1.2**). A substrate is monoubiquitylated if a single lysine residue is modified with ubiquitin, or

multi-monoubiquitylated if multiple lysine residues in the substrate protein are modified. Conversely, a substrate is polyubiquitylated if successive ubiquitin moieties are attached to internal lysine residues in the substrate-bound ubiquitin, resulting in the formation of polyubiquitin chains ranging from two to >10 ubiquitin moieties in length. Similarly, the substrate is multi-polyubiquitinated if multiple lysine residues in the substrate are modified with polyubiquitin chains [reviewed in (Komander & Rape 2012)]. Ubiquitin has seven lysine residues (K6, K11, K27, K29, K33, K48, and K63), which cover the surface of ubiquitin. Conjugation to these sites can result in polymeric chains of numerous topologies, composed of homogenous and/or mixed lysine linkages (**Figure 1.2**). In homogenous chains, the same ubiquitin residue is used for attachment of subsequent ubiquitin molecules during chain elongation. This results in the generation of, for example, Met1- (linear), Lys48- and Lys63-linked chains. Conversely, chains with mixed topology are generated if different lysine residues in the pre-attached ubiquitin are used for attachment of subsequent ubiquitin molecules during chain elongation. Consequently, polyubiquitin chains can adopt different structural conformations which are distinguished by ubiquitin-binding proteins that translate the different modifications into distinct cellular outcomes (Komander & Rape 2012; F. Ikeda & Dikic 2008). Although all possible linkages have been detected in cells, it is currently not known whether all have a physiological function (Peng et al. 2003; P. Xu et al. 2009). For example, the function of Lys6, Lys27, Lys29, and Lys33 chains is poorly understood.

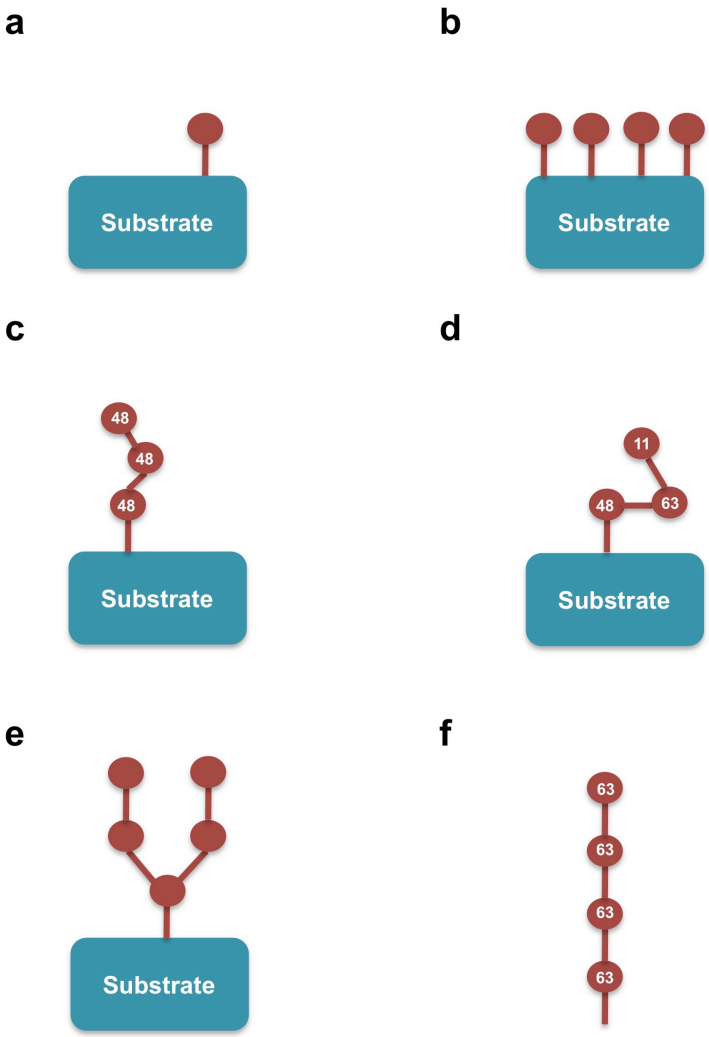

Figure 1.2: Ubiquitylation topologies. Distinct forms of ubiquitin (red balls) can be attached at multiple locations on a substrate. (a) Monoubiquitylation. (b) Multimonoubiquitylation. (c) Homogenous ubiquitin chain. (d) Mixed ubiquitin chain. (e) Branched ubiquitin chain. (f) Unanchored ubiquitin chain. Figure adapted from **(Komander & Rape 2012)**.

1.1.2 Types of E3 ubiquitin ligases

E3 ligase enzymes determine the specificity of the ubiquitin modification by selectively binding and ubiquitylating a specific substrate protein. They can be broadly categorized into two subfamilies: HECT (homology to E6AP C-terminus) domain E3 ligases (Rotin & S. Kumar 2009), and RING (really interesting new gene) domain E3 ligases (Joazeiro & Weissman 2000; Tyers & Willems 1999).

Additionally, each subfamily can be further classified into monomeric/homomeric and multi-protein complex E3 ligases.

1.1.2.1 HECT domain E3 ligases

HECT domain E3 ligases contain a 350-amino acid carboxy terminal domain with high homology to E6AP, the founding member of this subfamily (Huibregtse et al. 1993; Huibregtse et al. 1995). The defining feature of the HECT domain is a highly conserved, catalytic cysteine residue, which directly accepts the activated ubiquitin moiety from the E2, forming a HECT-ubiquitin intermediate. The E3 then directly binds the substrate, presumably through its amino terminal, and catalyses the transfer of ubiquitin to an acceptor lysine on the substrate, or pre-existing ubiquitin chains on the substrate (Scheffner et al. 1995; Huang et al. 1999). One example of a HECT domain E3 ligase is the *Drosophila* protein Hyperplastic Discs (Hyd) (Mansfield et al. 1994), and its human homologue E3 in Differential Display (EDD) (Honda et al. 2002), which form the basis of the work presented in this thesis. Although many HECT domain E3 ligases are thought to act as monomers, EDD can form a multi-protein complex with DNA-damage binding protein 1 (DDB1), Vpr-binding protein (VPRBP), and dual-specificity tyrosine-phosphorylation-regulated kinase 2 (DYRK2) to ubiquitylate the mitotic microtubule ATPase protein katanin p60 (Maddika & J. Chen 2009).

1.1.2.2 RING domain E3 ligases

In contrast to HECT domain E3 ligases, RING domain E3 ligases do not form an E3-ubiquitin intermediate. Instead, these E3 ligases bind different E2s via the RING domain, as well as interacting with the substrate. They therefore act as scaffolds that bring the E2 and the substrate into sufficient proximity, and position both proteins optimally for ubiquitylation to take place (Jackson et al. 2000). In this case, it is the E2 that catalyses the transfer of ubiquitin to the substrate (Lorick et al. 1999). The RING domain is characterized by a structural pattern of conserved cysteine and

histidine residues, which facilitates the binding of Zn^{2+} cations (N. Zheng et al. 2000).

RING domain E3 ligases can be further sub-divided into two groups. The first group consists of RING domain E3s that function as either monomers or homodimers, and that contain both the RING finger domain (i.e. the E2 binding domain) and a substrate recognition motif. Examples of members of this group include Mdm2 (Boyd et al. 2000; Geyer et al. 2000) and Parkin (Shimura et al. 2000). The second group consists of RING E3s that function as part of multi-subunit complexes, such as the APC complex, involved in the degradation of cell cycle regulators (Page & Hieter 1999), and the von-Hippel Lindau-Elongins B and C (VBC)-Cul2-RING finger complex, involved in the degradation of HIF1-alpha (Kamura et al. 2000; Maxwell et al. 1999). These E3 complexes are modular, and are based on a core scaffold that binds interchangeable substrate-targeting subunits, and different RING domain E3s to recruit the E2 (**Figure 1.3**). Members of the Cullin (CUL) protein family typically fulfill the role of the scaffold protein, and form the backbone of most E3 ligase complexes. Each Cullin protein associates with specific substrate adaptors and RING E3 ligases, generating a large possibility of different combinations with different substrates, as well as ubiquitin linkage specificities (Petroski & Deshaies 2005).

1.1.2.3 SCF ligase complexes

As mentioned above, many modular E3 ligases are based on a cullin scaffold, and are collectively referred to as cullin-RING ligase (CRL) family complexes (**Figure 1.3**). Of these, the CRL1 ligases, also known as the S-phase kinase-associated protein 1 (SKP1)-cullin 1 (CUL1)-F-box protein (SCF) complexes, are the best characterized. They specifically recognise phosphorylated signal- and cell cycle-induced proteins, mostly resulting in the degradation of the target protein (Petroski & Deshaies 2005; Skaar et al. 2013).

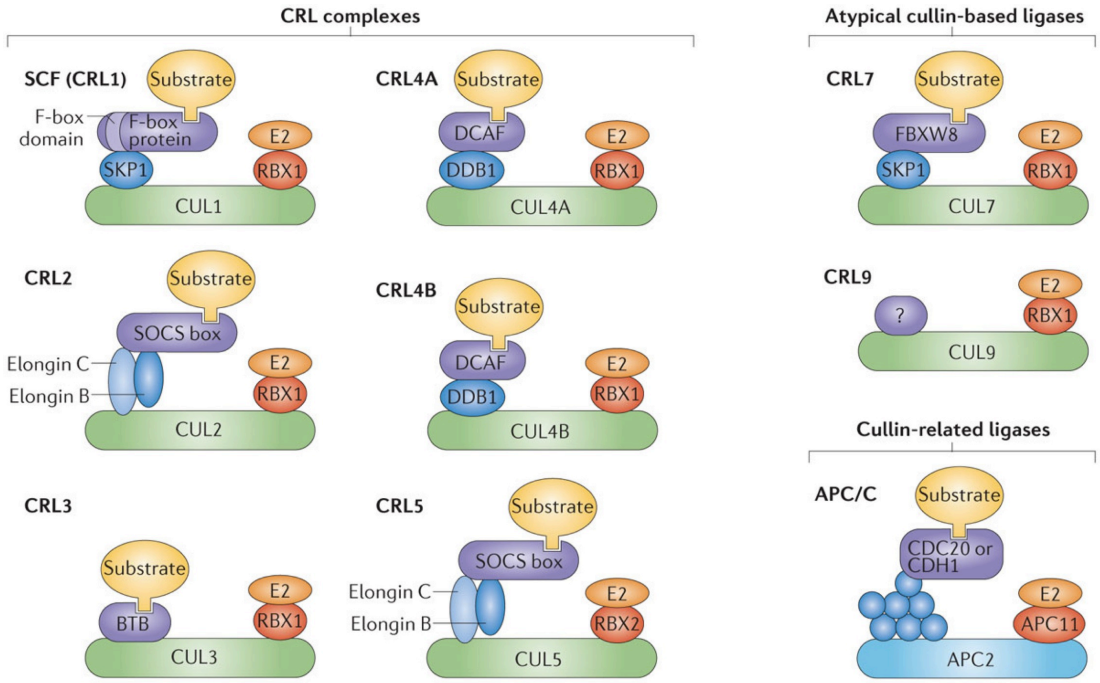

Figure 1.3: Members of the cullin–RING ligase (CRL) family. Cullin–RING ligase (CRL) complexes are modular multi-protein complexes, with variable substrate adaptors. The Cullin (CUL) proteins (green) form the backbone, and form a complex with RING-box protein 1 (RBX1; red), the E2 enzyme (orange), variable substrate adaptors (blue and purple), and the substrate (yellow). SKP1, S phase kinase-associated protein 1. SCF, SKP1–CUL1–F-box protein complex. DDB1, DNA damage-binding protein 1. DCAF, DDB1- and CUL4-associated factor. SOCS, suppressor of cytokine signalling. BTB, bric-a-brac-tramtrack-broad. FBXW8, F-box and WD40 domain 8. Figure taken from **(Skaar et al. 2013)**.

The core component of SCF complexes is the scaffold protein CUL1. The CUL1 carboxy terminus binds the small RING-box protein 1 (RBX1), which recruits the E2. The amino terminus of CUL1 interacts with S-phase kinase-associated protein 1 (SKP1), which recruits various F-box proteins (**Figure 1.3**). These different F-box proteins dictate the substrate specificity of SCF ligase complexes, and bind to SKP1 via their conserved F-box domain (Petroski & Deshaies 2005). There are sixty-nine F-box proteins in humans, and their interchangeability in SCF complexes enables these to target hundreds of different substrates (Jin et al. 2008; Skaar et al. 2009). The activity of SCF complexes is regulated on multiple levels, which includes phosphorylation of its individual components (Glickman & Ciechanover 2002), as

well as covalent modification with the ubiquitin-like protein NEDD8 (Skaar et al. 2013), although these mechanisms remain poorly understood.

F-box proteins typically recognize short degradation motifs, also known as degrons, in the substrate protein, and many bind specifically to phosphodegrons (Skaar et al. 2013). Some phosphodegrons are phosphorylated by a single kinase, whereas others require phosphorylation by multiple kinases and/or priming kinases, where one kinase must recognize a priming phosphate prior to phosphorylating the substrate. For example the F-box protein β-transducing repeat-containing protein (βTrCP) recognizes the consensus sequence Asp-Ser-Gly-Xaa-Xaa-Ser, where Xaa is any amino acid, and both Ser residues must be phosphorylated (Kitagawa et al. 1999; Lau et al. 2012).

1.1.3 Removal of ubiqitin: DUBs

The covalent modification of substrate proteins with ubiquitin is a reversible process. Deubiquitylating enzymes (DUBs) prevent the constitutive ubiquitylation of proteins by catalyzing the removal of ubiquitin and ubiquitin chains. DUBs can be categorized into five different families: ubiquitin-C-terminal hydrolases (UCHs), ubiquitin-specific proteases (USPs), Machado-Joseph Disease protein domain proteases (MJDs), ovarian tumour proteases (OTUs), and JAMM motif proteases (JAMMs) (Nijman et al. 2005). With the exception of JAMMs, which are metalloproteases, all DUBs are cysteine proteases that hydrolyse the penultimate amide bond at the ubiquitin carboxy terminus (Z. J. Chen & L. J. Sun 2009). UCHs remove short peptide chains from the carboxy terminus of ubiquitin, whereas USPs cleave the isopeptide bond between ubiquitin molecules, or between ubiquitin and the substrate (Glickman & Ciechanover 2002).

Several DUBs are proteasome-bound and play important housekeeping roles removing and recycling ubiquitin from substrates targeted for degradation. DUBs thereby protect ubiquitin from degradation and help maintain levels of free cellular ubiquitin (Finley 2009). Most USP family DUBs disassemble chains independently of the linkage, but instead recognize a specific set of substrates (Komander et al. 2009). Some DUBs, on the other hand, are linkage specific; for example JAMMs tend to be Lys63 specific, and several OTUs display specificity towards Lys48, Lys11, Lys29 and Lys33. Unlike non-linkage specific DUBs (e.g. USPs), linkage specific DUBs may not be able to remove the last ubiquitin on the substrate, possibly generating a monoubiquitylated substrate with distinct signaling properties and/or activity (Komander & Rape 2012). Finally, DUBs can be involved in the replacement of an existing ubiquitin chain with another ubiquitin chain that differs in topology, a process known as ubiquitin chain editing. During this process, DUBs and E3 ligases can form complexes, allowing them to act sequentially (Sowa et al. 2009). Interestingly, some proteins have both DUB and E3 activities - an example being the A20 protein, which is involved in the regulation of the transcription factor NF-κB (Wertz et al. 2004).

1.1.4 Ubiquitin-like proteins

Covalent modification of substrate proteins by small proteins such as ubiquitin is not unique to ubiquitylation. Several ubiquitin-like (UBL) proteins can also be conjugated to substrate lysine residues and utilise an analogous set of enzymes, which are mechanistically and structurally similar to E1, E2, and E3 proteins (Kerscher et al. 2006). UBLs increase the diversity of small-protein post-translational modifications and consequently the number of downstream effector proteins translating those modifications into specific cellular outcomes. Some UBL proteins share a very limited degree of sequence homology with ubiquitin, but all share the characteristic and highly conserved β-grasp ubiquitin superfold (Welchman et al. 2005).

At least eleven UBL proteins have been identified to date. Perhaps the most intensively studied UBL proteins include neuronal-precursor-cell-expressed developmentally downregulated protein-8 (NEDD8) and Small Ubiquitin-like Modifier (SUMO). NEDD8 is activated by the heterodimeric E1 APPBP1-UBA3 (Alzheimer-precursor-protein-binding protein-1-ubiquitin-activating enzyme-3), and transferred to substrates by the E2 UBC12 and the E3 ligase Mdm2 (mouse double minute-2) (Welchman et al. 2005; Xirodimas et al. 2004). NEDD8 is mainly involved in the regulation of E3 ligase proteins and complexes (Hori et al. 1999). For example, NEDD8 regulates SCF activity through modification of CUL1, which prevents the association of CUL1 with an inhibitor of SCF activity, CAND1 (cullin-associated and neddylation-dissociated-1). Conversely, deneddylation of CUL1 by the COP9 signalosome complex negatively regulates the activity of the SCF complex as it allows the binding of CAND1 and prevents the binding of the SKP1-F-box heterodimer (Cope & Deshaies 2003).

Another UBL protein, SUMO, mainly targets proteins involved in transcription, chromatin remodelling and DNA repair. The modification of proteins with SUMO mostly affects protein activity and localization (Gill 2004; Matunis et al. 1996). SUMO uses the E1 AOS1-UBA2, the E2 UBC9, and several E3 ligases, including RanBP2 (Ran-binding protein-2) for conjugation to target proteins. Interestingly, it has been suggested that protein sumoylation may oppose the function of ubiquitylation, as SUMO and ubiquitin can compete to modify the same site in some cases (Welchman et al. 2005; Gill 2004).

1.1.5 Functional outcomes of ubiquitination

Once a protein has been ubiquitylated, effector proteins with ubiquitin-binding domains (UBDs) translate the ubiquitin modification into specific cellular outcomes (Dikic et al. 2009). Different linkage topologies present different binding surfaces to effector proteins, and as a result affect the outcome of ubiquitylation. Classically, it is generally believed that K48-linked chains direct degradation of the modified protein, whereas K63-linked chains have various non-proteolytic functions, such as regulation of the protein's activity or sub-cellular localization (**Figure 1.4**). However, this view may be too simplified, as emerging evidence suggests that these chain types can both have proteolytic as well as non-proteolytic functions. In addition, the functional outcome of ubiquitylation is not solely dependent on chain topology, as it is also affected by several other factors such as timing, sub-cellular localization, reversibility of the modification, and cross-talk between E3s and effector proteins (Komander & Rape 2012).

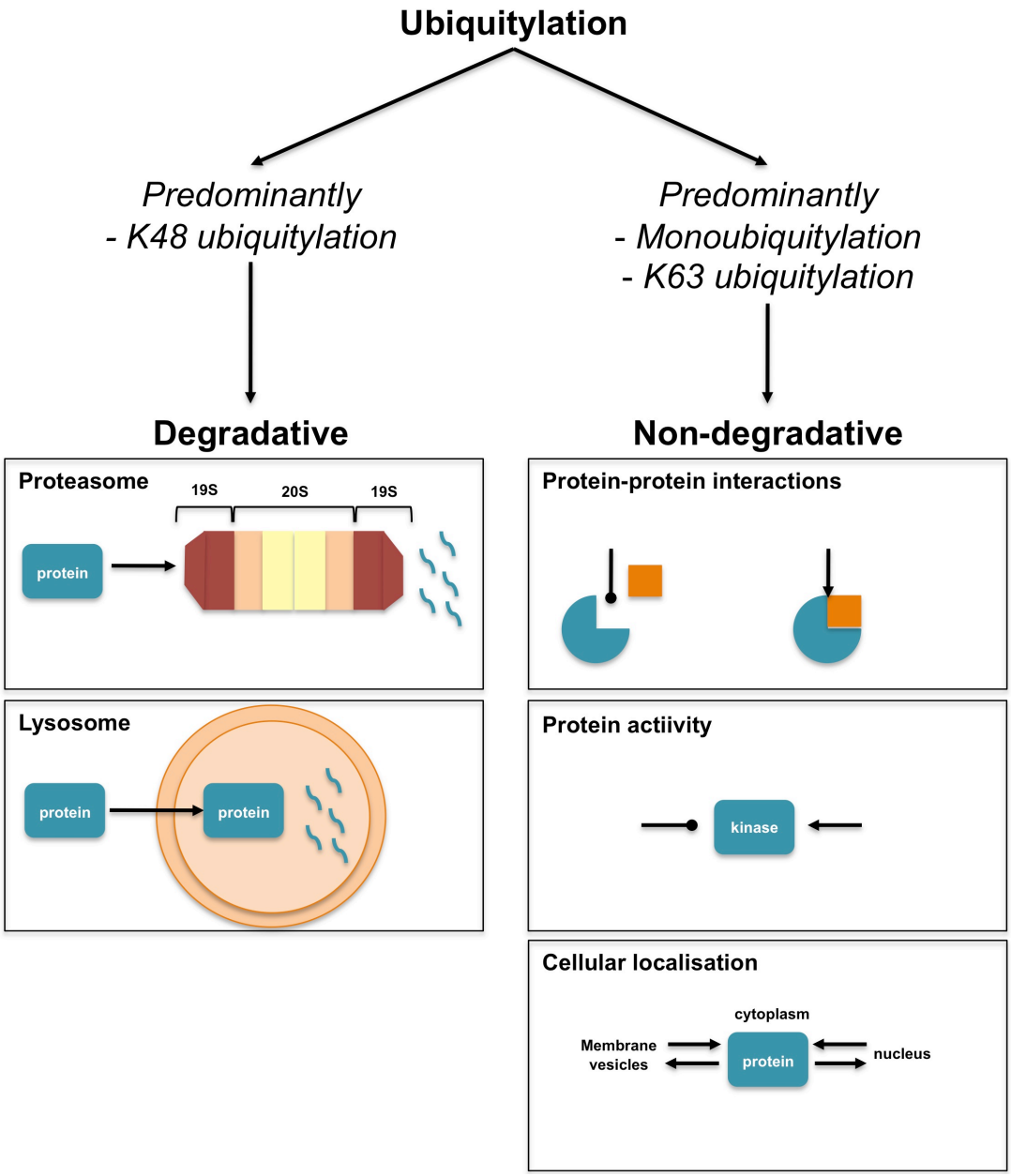

Figure 1.4: Cellular Outcomes of Ubiquitylation. Ubiquitylation can have both degradative and non-degradative outcomes. Ubiquitin-directed degradation occurs via the proteasome or the lysosome, whereas non-degradative ubiquitylation can positively (black arrows) or negatively (black circles) affect protein-protein interactions, protein activity, and cellular localisation.

1.1.5.1 Degradation via the proteasome

Historically, protein ubiquitylation was solely linked to protein degradation via the 26S proteasome, a large multi-subunit protease that is highly conserved among all eukaryotes (Finley 2009). This 2.5 MDa complex is composed of two sub-complexes: a 20S core particle (CP) and a 19S regulatory particle (RP) (**Figure 1.4**). The 20S CP harbours the catalytic protease activity and forms a barrel-shaped structure. The protease active sites face inward into the so-called proteolytic chamber, and degrade proteins into small peptides. One or two 19S regulatory particles can attach to either end of the 20S CP barrel to form the complete 26S proteasome. The function of the 19S RP is to recognize ubiquitylated proteins, partially unfold proteins destined for degradation, and to direct them into the 20S CP proteolytic chamber. Following protein degradation, small peptides as well as reusable ubiquitin are released from the 26S proteasome (Glickman & Ciechanover 2002).

Several ubiquitin linkages can result in protein degradation via the 26S proteasome. K48-linked ubiquitin chains were the first ubiquitin linkage found to direct protein degradation (Chau et al. 1989). Considering the importance of protein turnover in living cells, it is not surprising that quantitative proteomic analyses have revealed that K48-linked chains are the most abundant linkage type, and that inhibition of the 26S proteasome results in rapid accumulation of proteins modified with K48-linked ubiquitin chains (Kim et al. 2011; Kaiser et al. 2011). However, emerging evidence implicates other ubiquitin linkages in protein degradation via the 26S proteasome. For example, K11-linked chains conjugated by the E3 complex APC/C direct the degradation of cell cycle regulators during mitosis (Jin et al. 2008; Matsumoto et al. 2010), and, in some cases, K29- and K63-linked chains were also found to direct protein degradation (E. S. Johnson et al. 1995; Saeki et al. 2009).

Finally, proteins can also be targeted to the lysosome for degradation. The lysosome is a membrane-bound cellular compartment containing several proteases, in which proteins are engulfed and degraded. For example, membrane proteins are targeted to the lysosome through monoubiquitylation or K63-linked chains, which involves endocytosis of membrane proteins and fusion of endocytic vesicles with the lysosome (Mukhopadhyay & Riezman 2007).

1.1.5.2 Non-degradative outcomes of ubiquitylation

Ubiquitylation of proteins can also have many non-proteolytic outcomes, including the regulation of protein interactions, activity, and localization, all of which can affect various signalling pathways in the cell. These non-proteolytic functions of ubiquitin are most frequently associated with monoubiquitylation or linear (Met1) and K63-linked chains (Z. J. Chen & L. J. Sun 2009; Rieser et al. 2013; Komander & Rape 2012).

Ubiquitylation can both promote and inhibit protein interactions. For example, during the DNA damage response, monoubiquitylation of PCNA promotes its association with several DNA repair-specific DNA polymerases (Hoege et al. 2002; Bienko et al. 2010). K63-linked chains often play an important role in scaffolding, such as in the recruitment of several E3s to sites of DNA damage by K63-linked histone proteins (Al-Hakim et al. 2010). Conversely, ubiquitylation can also negatively affect interactions. For example, the transcription factor Smad4 is monoubiquitylated, which blocks its interaction with the transcriptional co-factor Smad2. De-ubiquitylation of Smad4 by USPX9 results in association with Smad2 and subsequent transcriptional activation (Dupont et al. 2009). In this example, ubiquitylation also affects protein activity indirectly.

Ubiquitylation can also direcly regulate protein activity by directing the proteolytic cleavage, or the partial proteolytic degradation of a protein. One such example is the Hh pathway transcriptional effector protein Cubitus interruptus (Ci), which is ubiquitylated and partially processed by the 26S proteasome, resulting in the removal of the transcriptional activation domain (Smelkinson & Kalderon 2006; J. Jiang & Struhl 1998; J. Jia et al. 2005; Noureddine et al. 2002). This generates a truncated, repressor protein, which translocates to the nucleus to inhibit the transcription of Hh pathway target genes (Méthot & Basler 1999). Changes in protein activity can also be the result of allosteric regulation through conformational changes following ubiquitylation (Ditzel et al. 2008).

Finally, ubiquitylation can regulate proteins by affecting their subcellular localization. As mentioned earlier, monoubiquitylation of plasma membrane proteins can result in their internalization into endosomes, as well as further re-routing to proteolytic lysosomes (Terrell et al. 1998; Stringer & Piper 2011). Additionally, the multimonoubiquitylation of the transcription factor p53 was shown to result in its nuclear export (M. Li et al. 2003).

1.2 Hedgehog (Hh) signalling in development and disease

When Christiane Nüsslein-Volhard and Eric Wieshaus performed a genetic screen to identify genes that are involved in the development of the fruit fly larval body plan in 1980, they came across *Drosophila* larvae that displayed disorganized bristles reminiscent of hedgehog spines (Nüsslein-Volhard & Wieschaus 1980). The distinctive phenotype was a result of a null allele of one gene, which they named *hedgehog* (*hh*), unknowingly establishing the Hedgehog signalling field and initiating a flood of research in developmental and cancer biology. Now, we know that the *hh* gene gives rise to a secreted protein that acts as a morphogen, diffusing

over relatively large distances to direct tissue patterning during development, and acting in a gradient-dependent manner to activate a signalling cascade in target cells (**Figure 1.5**). The ultimate target of the Hh signalling pathway is the regulation of the transcription factor Cubitus interruptus (Ci), which controls Hh target gene transcription and thus orchestrates a breadth of cellular outcomes depending on the concentration of Hh ligand and tissue type (Ingham & McMahon 2001).

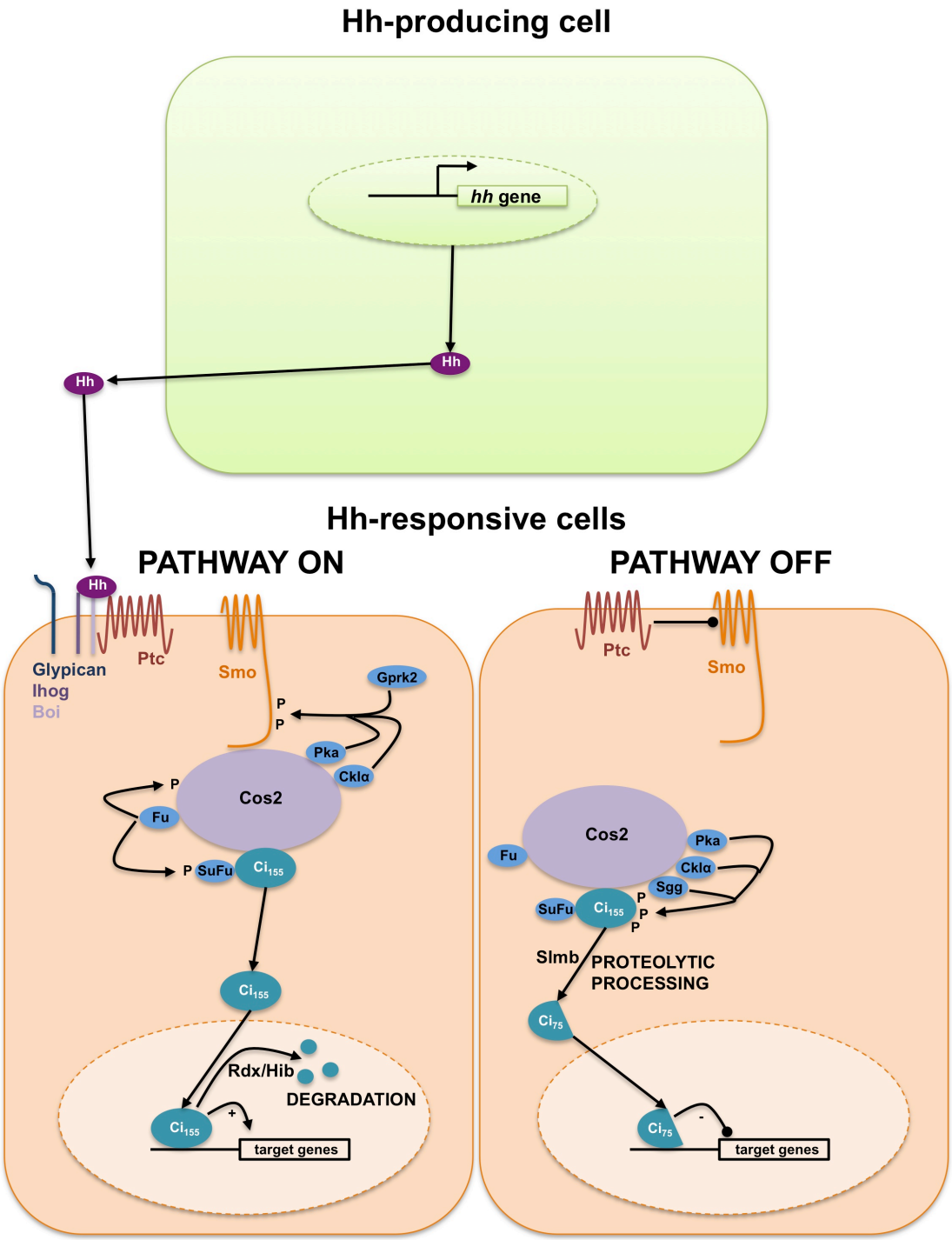

Figure 1.5: Hedgehog (Hh) signalling. (**Upper panel**) Hh ligand is expressed in, and secreted by, Hh-producing cells, and binds to its receptor Patched (Ptc) on Hh-responsive cells. (**Left panel**) This relieves inhibition of the trans-membrane protein Smoothened (Smo) by Ptc, which then initiates downstream signalling, and involves the phosphorylation of the Smo cytoplasmic tail by the kinases Gprk2, PKA, and CKI. This, in turn, results in the recruitment of the Hh signalling complex (HSC) to

the Smo cytoplasmic tail, consisting of the scaffold protein Costal 2 (Cos2), Fused (Fu), Supressor of fused (Sufu), and the transcriptional activator protein Ci_{155}. Fu phosphorylates the negative regulators of Ci_{155}, Cos2 and Sufu, resulting in the release of Ci_{155} from the complex, and its subsequent translocation into the nucleus to activate target gene expression. The Ci target gene *rdx/hib* (*Hs SPOP*) encodes a Cul3-based E3 ligase, which is responsible for the complete degradation of Ci_{155}, forming a negative feedback loop to control Hh pathway activity. (**Right panel**) In the absence of Hh ligand, Ptc inhibits Smo, which prevents its association with the HSC. Instead, Ci_{155} is retained by the HSC in the cytoplasm, which results in its sequential hyper-phosphorylation by multiple kinases that associate with the HSC, and include PKA, Sgg (*Hs* GSK3β), and CKI. Phosphorylated Ci_{155} is recognised by the Cul1-based E3 ligase Slimb (*Hs* βTrcP), which directs proteolytic processing of Ci_{155} via the 26S proteasome, resulting in the generation of a truncated Ci_{75} protein that lacks the transcriptional activation domain. Instead, Ci_{75} translocates to the nucleus to repress the transcription of target genes.

Hh signaling is largely conserved between flies and mammals, and plays a key role in embryonic development, as well as adult stem cell maintenance and tissue homeostasis (Wilson & Chuang 2010; Ingham & McMahon 2001; Beachy et al. 2004). Expression of *hh* and the resulting activation of the Hh pathway, which I will collectively refer to as Hh signalling, must therefore be tightly regulated in both a spatial and temporal manner. As a result, it is not surprising that defects in Hh ligand expression have been linked to tumour formation and maintenance in adults (L. L. Rubin & de Sauvage 2006; Scales & de Sauvage 2009). Although many components of the Hh pathway have been discovered using *Drosophila* and mouse genetics (Wilson & Chuang 2010; Forbes et al. 1993), the molecular mechanisms governing Hh ligand expression remain somewhat elusive.

The field of Hh signalling in *Drosophila* and vertebrates is vast, and thus beyond the scope of this thesis. As I am using the *Drosophila* eye as a developmental model system to determine the role of Hyd in the regulation of *hh* expression and the Hh pathway, I will concentrate on the molecular mechanisms underlying Hh ligand expression and Hh pathway transduction in the fruit fly, with a particular focus on the function of Hh signalling in the developing eye. Additionally, I will elaborate on

the pathological roles of Hh signalling in human cancer biology, to highlight the translational potential of the research presented in this thesis.

1.2.1 Expression and secretion of Hh ligand from Hh-producing cells

1.2.1.1 Transcriptional and epigenetic regulation

During *Drosophila* embryonic development, the homeodomain transcription factor Engrailed (En) positively regulates *hh* transcription in the posterior of each larval segment (Tabata et al. 1992). Similarly, En regulates *hh* expression in the posterior compartments of the larval leg and wing imaginal discs (Tabata et al. 1995; Zecca et al. 1995). The mechanism by which En regulates *hh* transcription is indirect, and involves the negative regulation of *ci* expression (Domínguez et al. 1996; Eaton & Kornberg 1990; Schwartz et al. 1995). The full-length Ci protein, Ci_{155}, is normally processed to the Ci_{75} transcriptional repressor form, which directly represses *hh* transcription in the wing disc (Domínguez et al. 1996; Méthot & Basler 1999). As a result, En-mediated repression of *ci* expression allows *hh* expression in the posterior compartment. Similarly, in the absence of En in the anterior compartment, Ci_{75} represses *hh* expression (Domínguez et al. 1996; Méthot & Basler 1999). Additionally, another target gene of Ci_{155}, *master of thickveins* (*mtv*), encodes a protein that, together with the co-repressor Groucho (Gro), represses *hh* and *en* expression in anterior cells (Bejarano et al. 2007; de Celis & Ruiz-Gómez 1995). However, En function is not required for *hh* expression in the eye-antennal disc (Strutt & Mlodzik 1996). Instead, the transcription factor Pointed, which is activated downstream of the Epidermal growth factor receptor (Egfr)/Ras pathway, binds an eye specific enhancer in the *hh* gene to drive expression of *hh* in the posterior compartment of the eye disc (Rogers et al. 2005).

Finally, *hh* expression in the wing disc is also controlled by an epigenetically regulated chromosomal element upstream of the *hh* gene known as a Cellular Memory Module (CMM) (Maurange & Paro 2002). The Trithorax-group (trxG) and Polycomb-group (PcG) proteins are epigenetic regulators that interact with CMMs, and act to maintain the active or silenced states of transcrption, respectively (Francis & Kingston 2001). Once activated or repressed in the respective compartments, *hh* expression in the wing disc is maintained through the action of trxG and PcG regulators on its CMM (Maurange & Paro 2002; Chanas & Maschat 2005).

1.2.1.2 Post-translational processing and modification

Following *hh* gene transcription and translation, the immature 45kDa Hh protein undergoes autoproteolytic cleavage and lipidation, which is mediated by the carboxy-terminal region of the protein (Hh-C). This involves recruitment of cholesterol by the Hh-C moiety, and subsequent covalent attachment of cholesterol to the amino-terminal (Hh-N) (Perler 1998; Mann & Beachy 2004). Following cleavage, Hh-C is degraded by the proteasome (X. Chen et al. 2011). Hh-N is then further post-translationally modified by the acyltransferase skinny hedgehog (SKI), which catalyses the attachment of a palmitic acid group to Hh-N (Chamoun et al. 2001), and this has been shown to increase Hh-N protein activity (F. R. Taylor et al. 2001; M.-H. Chen et al. 2004). This generates a dually lipid-modified 19kDa Hh-N protein that is cholesterol-modified at its carboxy-terminus and palmitoylated at its amino-terminus. As a result, Hh-N readily associates with sterol-rich microdomains on the plasma membrane (Rietveld et al. 1999), and its cholesterol modification in particular restricts Hh-N diffusion as it promotes its retention in the plasma membrane (Peters et al. 2004). The secretion of Hh-N requires the action of the multipass transmembrane protein Dispatched (DISP), which binds to the cholesterol moiety on Hh-N and promotes its release from the cell surface (Tukachinsky et al. 2012).

1.2.2 Activation of the Hh pathway in Hh-responsive cells

The secreted Hh ligand binds to its receptor, the transmembrane protein Patched (Ptc) (Nakano et al. 1989), on Hh-responsive cells, resulting in the activation of the Hh signaling cascade, and the transcription of tissue-specific Hh target genes by Ci (**Figure 1.5**). The transmembrane proteins Interference Hedgehog (Ihog) and Brother of Ihog (Boi) are thought to act as co-receptors (Camp et al. 2010; X. Zheng et al. 2010). Hh does not directly interact with Ptc, however it does directly interact with Ihog and Boi, suggesting that these co-receptors are required for the indirect binding of Hh to Ptc (McLellan et al. 2006; Yao et al. 2006). Hh signalling is also potentiated by glypicans on the plasma membrane, as their association with Hh enhances ligand stability and promotes the internalization of the Hh-Ptc complex (Yan & X. Lin 2009).

In the absence of bound Hh ligand, Ptc constitutively represses Hh pathway activity by inhibiting the action of the G-protein coupled receptor (GPCR) protein Smoothened (Smo) (Nakano et al. 1989; Hooper & Scott 1989). This triggers the removal of Smo from the plasma membrane, which is thought to occur through degradation and/or internalization of Smo into intracellular vesicles (Xia et al. 2012; S. Li et al. 2012). However, the molecular mechanism underlying Ptc-mediated Smo inhibition remains unclear.

The target of Ptc-mediated repression, Smo, is an orphan GPCR with no known ligand. However, Ptc may control the influx and/or efflux of a naturally occurring sterol-like ligand that controls Smo activity (Taipale et al. 2002), as several agonists and antagonists have been shown to control vertebrate Smo activity by binding to its membrane-integrated heptahelical domain (Mas & Ruiz i Altaba 2010). Ptc may

regulate Smo's potential sterol-ligand through its sterol-sensing domain (SSD) (Nikaido 2011).

Hh binding to Ptc relieves Ptc-mediated Smo inhibition, and initiates the intracellular signaling cascade (**Figure 1.5**). Smo accumulates at the plasma membrane, which is thought to be a result of increased trafficking from intracellular vesicles and/or an increase in Smo protein stability (Denef et al. 2000). Smo activation occurs through the phosphorylation of several residues on its cytoplasmic carboxy terminal tail by the sequential action of Protein Kinase A (PKA), Casein Kinase Iα (CKIα), and Gpcr Kinase 2 (GPRK2) (Y. Chen et al. 2010; H. Jia et al. 2010; J. Jia et al. 2004). This results in a conformational switch within the cytoplasmic region of Smo, which is required for Smo translocation to the plasma membrane and subsequent signalling activity (Zhao et al. 2007; Y. Chen et al. 2010). Interestingly, the level of Smo phosphorylation appears to be directly related to the strength of its signalling activity (J. Jia et al. 2004). Conversely, a group of protein phosphatases, including Pp1, Pp2a and Pp4, reverse Smo phosphorylation, thereby regulating the extent of Smo signalling activity (Y. Su et al. 2011b; H. Jia et al. 2009).

Phosphorylation of the Smo carboxy-terminal tail promotes its association with the normally microtubule-bound Hh signaling complex (HSC), which consists of the scaffold protein Costal 2 (Cos2), Fused (Fu), Suppressor of Fu (SuFu), and the transcription factor Cubitus interruptus (Ci) (**Figure 1.5**) (Kalderon 2004). The function of the HSC is to regulate the transcriptional activity of the zinc-finger protein Ci, which has the bi-functional ability to activate or repress target gene expression. In humans, a gene duplication event has given rise to three Ci orthologues, GLI1-3. In contrast to Ci, the GLI proteins have designated functions, where GLI1 acts as the transcriptional activator, whereas GLI3 is a transcriptional repressor; with GLI2 exhibiting both properties (Hui & Angers 2011). Ci consists of a zinc finger DNA binding domain, a C-terminal activation domain, and an N-terminal repressor domain (**Figure 1.6**). Importantly, Ci activity is regulated by three

key mechanisms: proteolytic processing, nuclear translocation, and degradation (J. Jiang 2006).

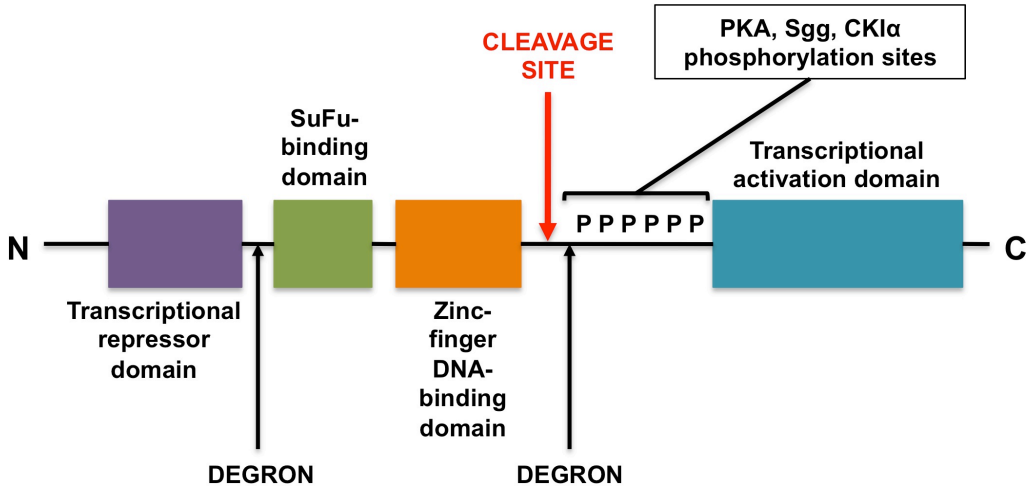

Figure 1.6: Domain structure of the full length Ci_{155} protein. Degrons represent binding/recognition sites for the Cul1-based Slimb/βTrcP E3 ligase complex, which targets Ci_{155} for partial proteolyic processing. Adapted from **(Briscoe & Thérond 2013).**

1.2.3 Proteolytic processing of Ci

In the absence of Hh pathway activation, the HSC associates with the kinases: protein kinase A (PKA), casein kinase Iα (CKIα), and glycogen synthase kinase 3β (GSK3β), also known as Shaggy in *Drosophila melanogaster*. This promotes the sequential phosphorylation of Ci on multiple residues of its carboxy terminus (**Figure 1.6**). PKA initially phosphorylates certain residues, also known as priming sites, which then serve as recognition sites for GSK3β and CKIα, resulting in further phosphorylation of nearby residues (J. Jiang 2002; Price & Kalderon 2002; J. Jia et al. 2005). The hyper-phosphorylation of Ci promotes its recognition by the F-box-containing protein Slimb [also known as β-transducing repeat-containing protein (βTrCP) in humans], which recruits an SCF E3 ubiquitin ligase complex, containing the S phase associated protein kinase 1 (SKP1) and Cullin 1 (CUL1), to catalyse Ci ubiquitylation. This, in turn, triggers the recognition, and subsequent partial proteolytic processing of Ci by the 26S proteasome, resulting in the removal of the

carboxy-terminal transcriptional activation domain (**Figure 1.7**) (Smelkinson & Kalderon 2006; J. Jiang & Struhl 1998; J. Jia et al. 2005; Noureddine et al. 2002). This processing event therefore gives rise to a truncated Ci transcriptional repressor protein (Ci_{75}), which translocates to the nucleus and represses Hh target gene transcription (Méthot & Basler 1999).

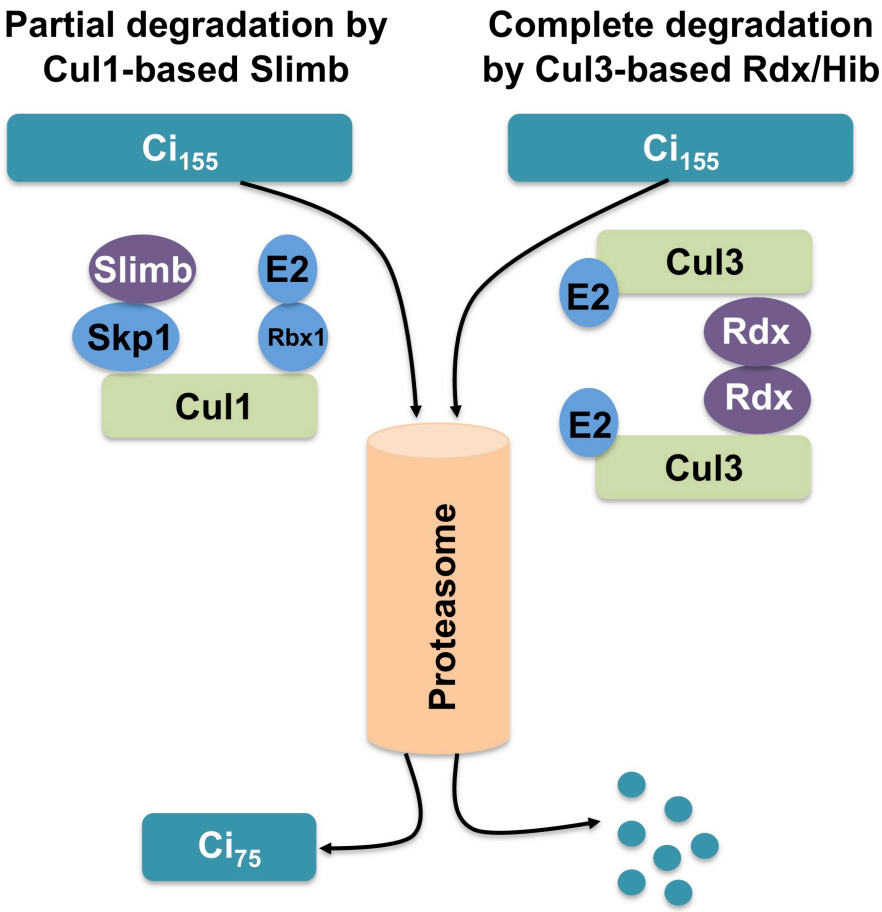

Figure 1.7: Dual regulation of Ci_{155} by ubiquitylation. In the absence of Hh ligand, Ci_{155} is ubiquitylated by the Cul1-based Slimb E3 ligase complex, resulting in its partial proteolytic processing to a truncated Ci_{75} repressor protein via the 26S proteasome (left). In the presence of Hh ligand, the Cul3-based Rdx/Hib E3 ligase complex regulates Hh pathway activity by ubiquitylating Ci_{155} and targeting it for complete degradation via the 26S proteasome (right).

1.2.4 Ci: Nuclear translocation, Hh target gene transcription, and degradation

In the presence of Hh ligand, the activation of Smo and downstream signaling events prevent the phosphorylation and proteolytic processing of Ci, which in turn permits the translocation of full-length Ci to the nucleus to activate transcription of Hh target genes (**Figure 1.6**). Ci is tethered to the cytosolic HSC through its interaction with the scaffold protein Cos2, which retains Ci in the cytoplasm and mediates interactions with both its positive and negative regulators (Robbins et al. 1997; W. Zhang et al. 2005). As a result, Cos2 is itself a negative regulator of Ci, in addition to the kinases that promote hyperphosphorylation and subsequent proteoytic processing of Ci (PKA, CKIα, and GSK3β). In addition, the cytoplasmic protein SuFu also binds Ci and prevents its translocation to the nucleus (Farzan et al. 2008). Conversely, Ci is positively regulated by the kinase Fu. Following Hh binding to Ptc, the stabilization and dimerisation of phosphorylated Smo at the plasma membrane results in the recruitment of the HSC to the Smo cytoplasmic tail, and the autoactivation of Fu, which is thought to involve dimerisation. Once activated, Fu phosphorylates Cos2, which results in the release of full-length Ci from the HSC (Ruel et al. 2007; Shi et al. 2011; Y. Zhang et al. 2011). Fu is also thought to antagonize SuFu, although the mechanism is unclear and does not appear to involve phosphorylation by Fu (Q. Zhou & Kalderon 2011). Instead, it has been suggested that Fu and other proteins may modify Ci directly to prevent its interaction with SuFu (Briscoe & Thérond 2013). Once full length Ci (Ci_{155}) is released from Cos2 and SuFu, it translocates to the nucleus and activates gene expression. There are many tissue specific Ci target genes, but the most ubiquitously expressed target gene is *ptc* (Ohlmeyer & Kalderon 1998). Another Ci target gene is *rdx/hib*, which encodes the Cul3-based E3 ubiquitin ligase Roadkill (Rdx)/ Hh-induced MATH and BTB domain-containing protein (Hib) (*Hs* Speckle-type PPZ; SPOP), and ubiquitylates Ci_{155} to target it for complete degradation via the 26S proteasome (**Figure 1.7**) (Q. Zhang et al. 2009; Kent et al. 2006; Q. Zhang et al. 2006). Both

expression of *ptc* and ubiquitylation of Ci_{155} by Rdx/Hib, as a result of nuclear accumulation of Ci_{155}, therefore confer negative feedback to the pathway.

1.2.5 Function of Hh signaling in Drosophila Eye development

1.2.5.1 Eye Development in *Drosophila*

Drosophila lends itself to studying eye development as flies can be genetically manipulated in a relatively simple and quick way. In addition, the fly eye-antennal (EA) imaginal disc (**Figure 1.8**) allows the simultaneous visualisation of spatial and temporal gene expression during the course of development, making it the ideal model organism for studying signalling pathways that contribute to the development of complex tissues. Furthermore defective adult eyes do not significantly impair the animals' viability.

The *Drosophila* adult compound eye is a highly organised lattice structure consisting of up to 800 independent subunits known as ommatidia. Each ommatidium is composed of 20 specialized cells, which include eight photoreceptor (PR) neurons, six pigment cells, 4 cone cells, and two mechanosensory bristles. The photoreceptors (PRs) form the core of the ommatidium and are further subdivided into six outer (R1-R6) and two inner PRs (R7 and R8) (Ready et al. 1976).

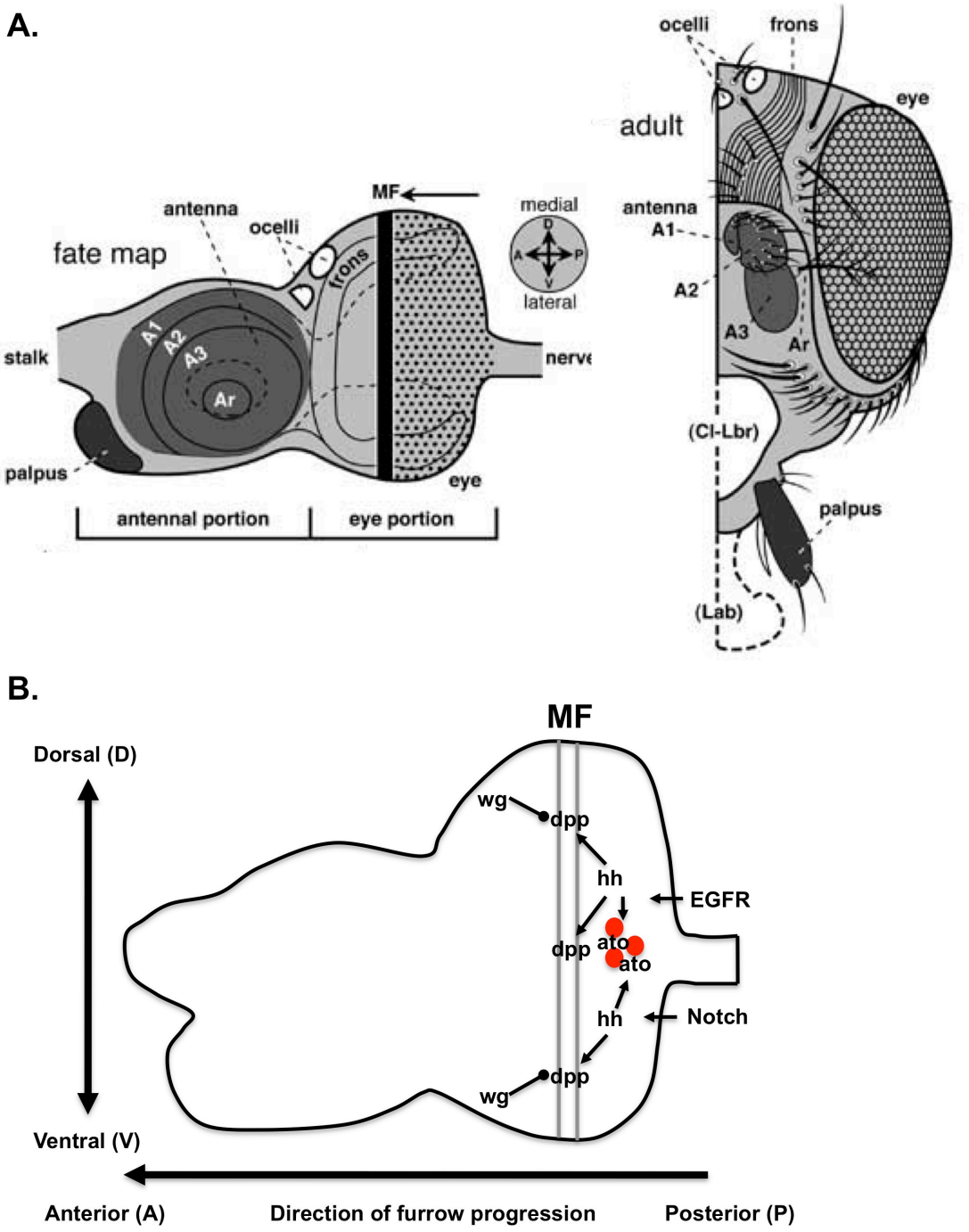

Figure 1.8: Development of the adult Drosophila eye and head from the larval eye-antennal (EA) imaginal disc. (**A**) Distinct regions of the EA disc give rise to specific structures that make up the adult head and retina. Figure taken from **(Held 2005)**. (**B**) Expression of growth factors and morphogens that contribute to photoreceptor differentiation as the MF moves from the posterior to the anterior of the EA disc. A1-A3 (antennal segments 1-3), Ar (arista), Fr (frons; parallel grooves ≈ a

human fingerprint), MF (morphogenetic furrow), n (nerve = optic stalk), Oc (ocelli; oval = lateral ocellus; half-oval = median ocellus), Palp (palpus).

During larval development, a monolayered epithelium called the eye-antennal disc gives rise to all ommatidial cells, and eventually the adult compound eye, head and antennae (**Figure 1.8 A**), as a result of various stages of patterning, determination and differentiation. The disc is derived from a cluster of 20 cells (Garcia-Bellido & Merriam 1969) and is subdivided into distinct anterior and posterior regions early on during embryogenesis, which will eventually give rise to the antenna, and the retina, the vertex and the ocelli, respectively (**Figure 1.8 A**) (Tsachaki & Sprecher 2012). Following initial proliferation, eye disc cells are sequentially committed to becoming PRs or support cells during a wave of differentiation that is marked by a visible trough known as the morphogenetic furrow (MF). The MF moves across the disc from posterior to anterior, leaving differentiated cells behind it (i.e. posterior to the MF) (**Figure 1.8 B**) (Ready et al. 1976; Wolff & Ready 1991). During embryogenesis, all cells destined to give rise to the eye-antennal disc are marked by expression of the transcription factors Eyeless (Ey) and Twin of eyeless (Toy). During the early second instar larval stage, the disc begins to be separated into the posterior region, which mainly expresses Ey, and the anterior region, which mainly expresses the homeodomain transcription factor Cut (Kenyon et al. 2003). The subdivision of the disc also involves two major signaling pathways: the Epidermal Growth Factor Receptor (EGFR) pathway, which results in the activation of the Ras/Raf/MEK/ERK signalling cascade, and the Notch (N) pathways, which continue to play diverse roles throughout subsequent stages of eye development (J. P. Kumar & Moses 2001a; Dominguez et al. 2004; Kenyon et al. 2003).

In order to generate a sufficient number of cells that will follow a retinal fate, controlled cell proliferation has to take place during the initial growth phase of the disc, and this is mainly regulated by Notch signaling (Domínguez & de Celis 1998). Notch signaling in turn activates the Janus tyrosine kinase/signal transducer and activator of transcription (JAK/STAT) pathway (Chao et al. 2004; Ekas et al. 2006;

Reynolds-Kenneally & Mlodzik 2005; Tsai & Y. H. Sun 2004), which is initiated by the cytokine-like ligand Unpaired (Upd) (Harrison et al. 1998).

Once sufficient proliferation has taken place and the region of the eye-antennal disc that will give rise to the eye field has been determined, undifferentiated precursor cells are sequentially committed to adopt a retinal fate as a result of a wave of differentiation starting at the posterior edge and ending within the anterior region of the disc. This wave of differentiation is associated with the MF, which moves across the disc over a two-day period (Tsachaki & Sprecher 2012). The MF is visible as a narrow channel resembling a trough, its morphological appearance being the result of cellular contraction. Several signaling pathways, including the Notch, EGFR, Wingless (Wg), Hh and Dpp signaling pathways, work in concert to initiate the MF at the posterior margin of the eye disc early during the third larval instar stage (J. P. Kumar & Moses 2001b). As the MF moves towards the anterior region of the disc, it causes cells to arrest at the G1 phase of the cell cycle, marking the onset of differentiation, and this requires both Hh and Dpp signaling (Escudero & Freeman 2007; Firth & Baker 2005).

The first PR to be specified at the centre of each ommatidium is the R8 PR, which then recruits the remaining PRs in a stereotypic pattern (Tomlinson & Ready 1987). The first PRs to join PR8 are R2 and R5, followed by R3 and R4, and finally R1 and R6, and R7. The R8 PR expresses the EGFR ligand Spitz, which activates the Ras pathway and specifies the fate of the recruited PRs (Freeman 1994). Once all PRs have been specified, they undergo terminal differentiation, which involves the choice to express a specific rhodopsin gene, encoding photosensitive GPCRs, which are sensitive to a certain wavelength of light (Terakita 2005). Finally, ommatidial development is completed during the pupal stage, where pigment cells and mechanosensory bristles are added at the periphery of the ommatidia.

1.2.5.2 The Role of Hh and other signalling pathways in Drosophila eye development

Hh is the main signal that directs differentiation during the movement of the MF across the eye disc. Hh is secreted by cells posterior to the furrow (**Figure 1.9, panel a**), and signals to cells anterior to the MF, prompting them to withdraw from the cell cycle. As a result, ectopic expression of Hh anterior to the MF results in the generation of ectopic furrows (C. Ma et al. 1993). Some functions of Hh signaling during retinal differentiaton are direct, whereas others are indirect and a result of Hh-mediated expression of Dpp ligand (**Figure 1.8 B**) and subsequent stimulation of Dpp signalling (Heberlein et al. 1993). Hh initiates the expression of the proneural transcription factor Atonal (Ato) in a transient strip anterior to the MF (**Figure 1.8 B**) (Jarman et al. 1994). Ato is required for the specificiation of the R8 PR, the first PR that differentiates and forms the centre of the ommatidium. This in turn results in the activation of EGFR/Ras signalling, which directs the recruitment and differentiation of the remaining PRs (Roignant & Treisman 2009). Ato mutants are defective in the specification of eye disc cells, and, as a result, lack eyes completely (Jarman et al. 1995). EGFR/Ras signalling also ensures that the Hh pathway is no longer active in differentiated cells by promoting the expression of Rdx/Hib (Baker et al. 2009). Rdx/Hib is only expressed in the posterior region of the disc (**Figure 1.9, panels e and g**), and ubiquitylates full-length Ci_{155}, targeting it for degradation by the proteasome (Ou et al. 2002).

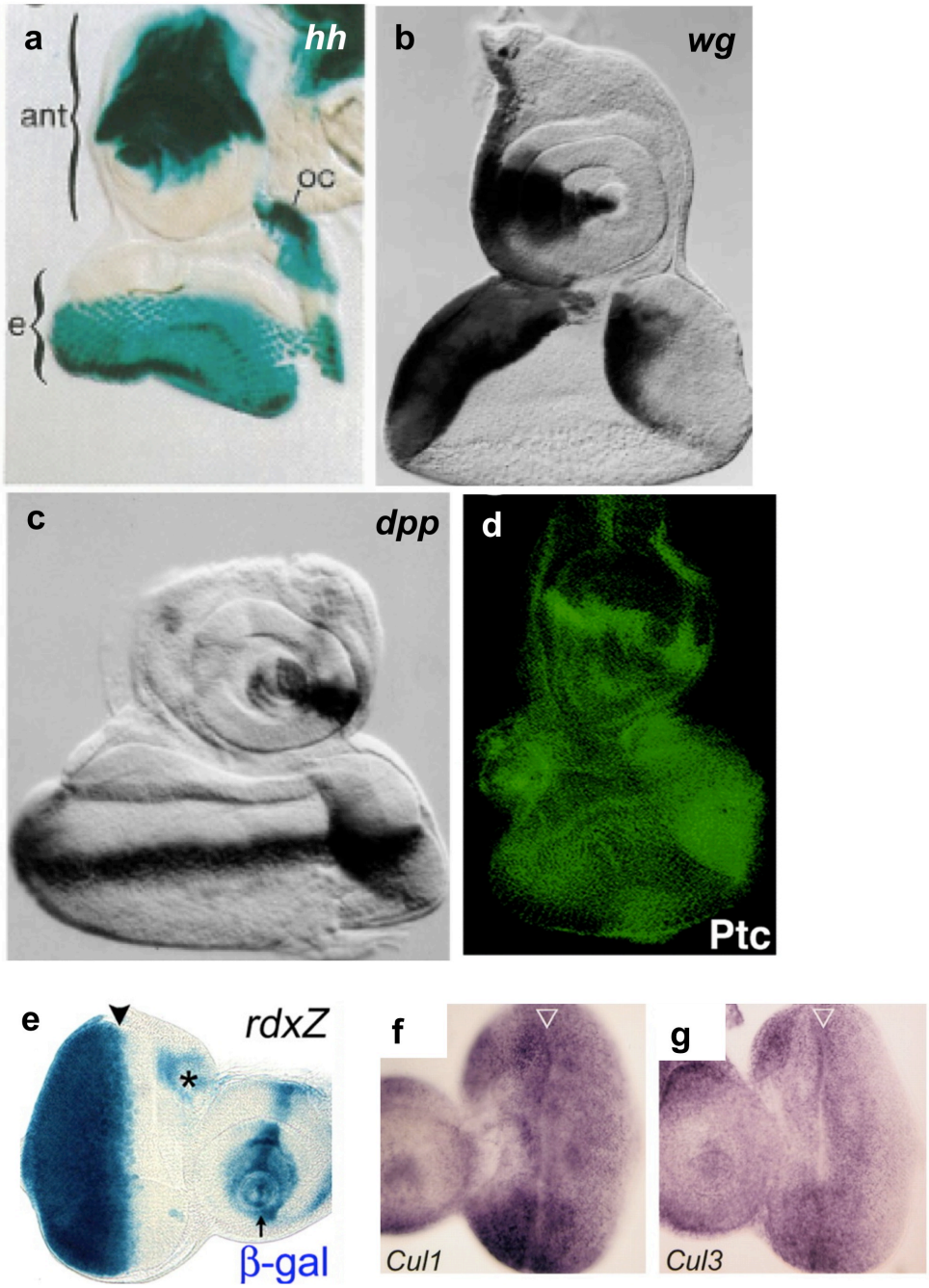

Figure 1.9: Morphogen and Hh pathway component expression patterns in L3 EA discs. (**a**) X-gal staining of β-gal expression from a *hh* enhancer trap (hh^{P30}), indicating the expression pattern of *hh* in the EA disc **(J. J. Lee et al. 1992)**. (**b**) and (**c**) X-gal staining of β-gal expression from *wg* (**b**) and *dpp* (**c**) *lacZ* reporters **(A. Mukherjee et al. 2000)**. (**d**) Immunofluorescence image of Ptc antibody staining, indicating Ptc protein expression **(Shyamala & Bhat 2002)**. (**e**) X-gal staining of β-gal expression from an *rdx lacZ* reporter, indicating *rdx/hib* expression **(Kent et al. 2006)**. (**f**) and (**g**) Expression patterns of *slimb/cul1* (**f**) and *rdx/cul3* (**g**) as determined by *in situ* hybridization with antisense probes of Cul1 and Cul3, respectively **(Ou et al. 2002)**.

Antagonising Hh-regulated events, Wg signalling acts to suppress progression of the MF. During the third larval instar, Wg is expressed in the anterior-lateral margins of the disc (**Figure 1.9, panel b**), where it acts to promote head capsule development and inhibit retinal differentiation (Legent & Treisman 2008).

1.2.6 Hh signalling in cancer

Although Hh signalling plays a vital role during embryogenesis and development, it also occurs in the adult, mostly associated with stem/progenitor cell populations, at a few specialized sites, such as CNS neural stem cells and the gut epithelium, where it is required for tissue maintenance and repair (L. L. Rubin & de Sauvage 2006; Scales & de Sauvage 2009). Unsurprisingly, inappropriate activation of Hh signalling in humans is linked to cancer. Aberrant Hedgehog signalling encompasses both activating mutations in Hh pathway components, as well as mis-expression of Hh ligand that leads to activation of the Hh pathway in the same (autocrine) and/or neighbouring cells (paracrine or juxtacrine) (Scales & de Sauvage 2009). Regardless of method, activation of the Hh pathway has various outcomes which are context and/or cell type-dependent (Scales & de Sauvage 2009), but include upregulation of: cyclins and cyclin-dependent kinases, resulting in proliferation (Duman-Scheel et al. 2002; Yoon et al. 2002); anti-apoptotic proteins such as B-cell lymphoma 2 (Bcl2), promoting cell survival (Bigelow et al. 2004; Regl et al. 2004); vascular endothelial growth factor (VEGF) and angiopoietins, which promote angiogenesis (Pola et al. 2001); and the Zinc finger protein SNAI1 (also known as SNAIL), which initiates the epithelial-mesenchyme transition during tumour metastasis (Feldmann et al. 2007). All of these Hh –associated outcomes contribute to tumourigenesis through driving cell proliferation, resistance to cell death and metastasis.

Three models, known as Type I to III/IIIb, have been proposed for Hh pathway activity in human cancers (**Figure 1.8A**) (L. L. Rubin & de Sauvage 2006). Type I cancers are Hh ligand independent and harbour activating mutations in Hh pathway

components, such as Ptc. By contrast, type II and type III cancers are Hh ligand dependent and are chracterised by mis-expression of Hh ligand by cancer cells. Hh ligand secreted by the tumour epithelium either signals to the same (autocrine) or neighbouring cells (juxtacrine) in type II tumours, or to more distant stromal cells (paracrine) surrounding the tumour. Type III tumours respond to Hh stimulation by secreting other extracellular signalling molecules that, in turn, signal back to the tumour cell to promote its growth and survival (L. L. Rubin & de Sauvage 2006).

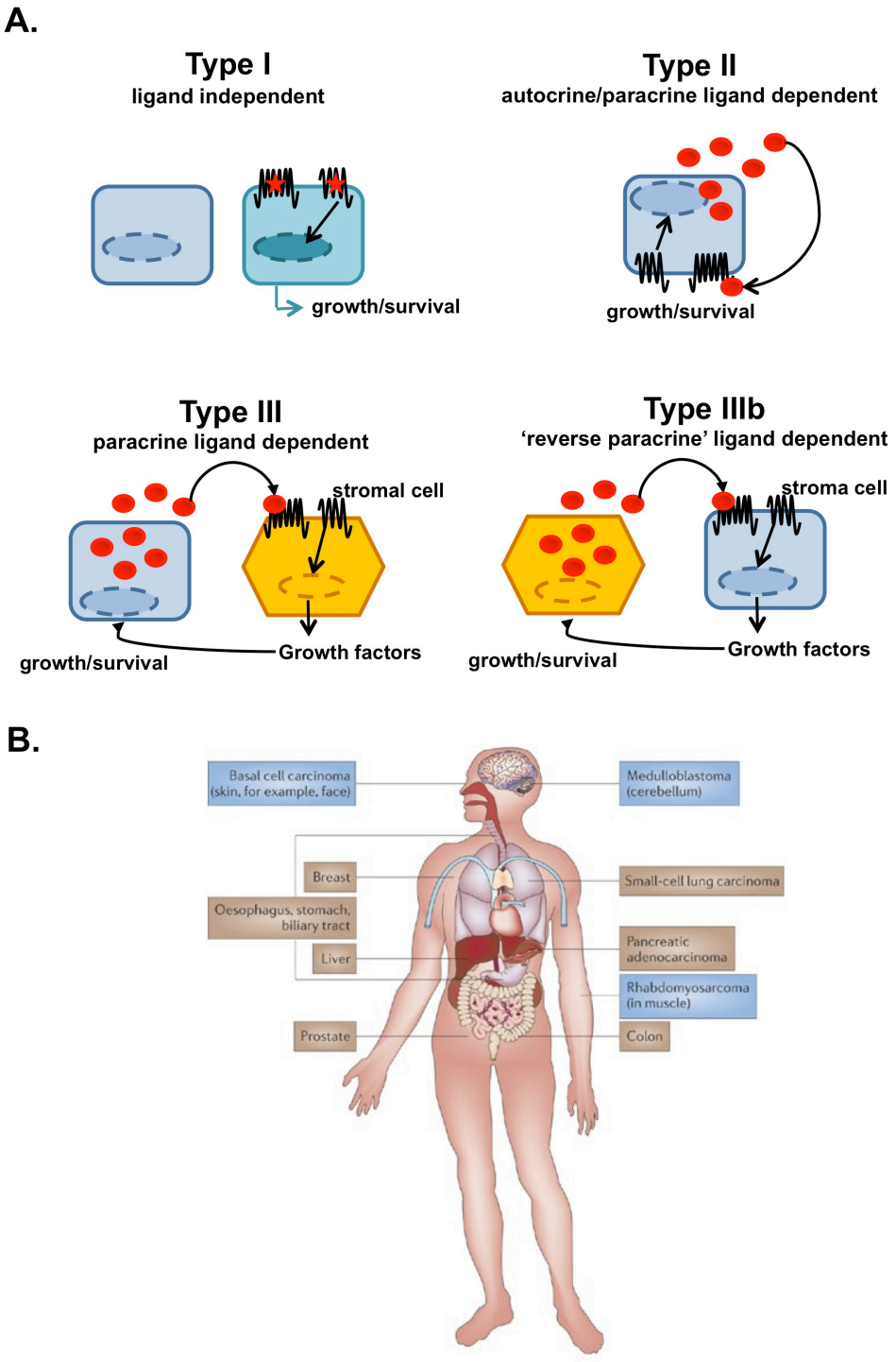

Figure 1.10: Hh signalling in human cancer. (**A**) Three models of Hh signal activation that promote tumour growth and survival. (**B**) Hh signalling is de-regulated in human cancer. Cancers with mutations in the Hh signal transduction pathway (e.g. Ptc and Smo), leading to constitutive activation of the pathway, are shown in blue boxes. Cancers with an autocrine requirement for Hh ligand are shown in brown boxes. (L. L. Rubin & de Sauvage 2006)

1.2.6.1 Type I tumours

The first indication that aberrant Hh signalling plays a role in cancer came with the discovery that the rare genetic condition called Gorlin syndrome (also known as basal cell nevus syndrome) is caused by inactivating mutations in PTCH1 (Hahn et al. 1996; R. L. Johnson et al. 1996). This leads to constitutive activation of the Hh pathway even in the absence of Hh ligand (**Figure 1.10**). Gorlin patients are therefore predisposed to numerous types of cancer, and develop basal cell carcinomas (BCCs), a skin tumour of keratinocytes, in addition to medulloblastomas (cancer of the cerebellum) and rhabdomyosarcomas (a rare form of muscle cancer) during the early stages of their lives (L. L. Rubin & de Sauvage 2006; Scales & de Sauvage 2009).

In addition, the majority (>85%) of sporadically occurring BCCs also harbour inactivating mutations of PTCH1 or loss of heterozygosity, and in some cases contain activating mutations in SMO that prevent its inhibition by PTCH1 (Unden et al. 1996; Gailani et al. 1996; Reifenberger et al. 1998; Reifenberger et al. 2005; Xie et al. 1997). In all cases, this leads to increased Hh signaling in the tumour cells. Rhabdomyosarcoma and medulloblastoma are mainly paediatric cancers that are associated with loss of heterozygosity or mutations in the negative Hh pathway regulators PTCH1 or SUFU (Raffel et al. 1997; Pietsch et al. 1997; Vorechovsky et al. 1997; M. D. Taylor et al. 2002; Tostar et al. 2006). Although cell autonomous activation of the Hh pathway activity is well established in these tumours, there is little evidence that suggests this particular mechanism occurs in other tumour types (L. L. Rubin & de Sauvage 2006).

1.2.6.2 Type II tumours

In type II tumours, the tumour cells mis-express and secrete Hh ligand, which then signals to the same cells or neighbouring tumour cells to stimulate their proliferation

and/or survival (**Figure 1.10**), ultimately leading to tumour growth (Scales & de Sauvage 2009). Hh over-expression as a tumour promoting factor was first identified in small cell lung cancer (SCLC) (Watkins et al. 2003). Since then several tumours that over-express Hh have been identified, including non-small cell lung cancer (nSCLC) (Yuan et al. 2007), pancreatic cancer (Thayer et al. 2003; Berman et al. 2003), upper gastrointestinal tract cancer (Berman et al. 2003; X. Ma et al. 2006), colorectal cancer (Qualtrough et al. 2004), prostate cancer (Karhadkar et al. 2004; Sanchez et al. 2004), breast cancer (S. Mukherjee et al. 2006) and melanoma (Stecca et al. 2007) tumours. Although there is much evidence for Hh over-expression occurring in tumour biopsies and cancer cells in culture, type II Hh signaling has not yet been conclusively demonstrated *in vivo* (L. L. Rubin & de Sauvage 2006).

1.2.6.3 Type III tumours

In contrast to autocrine/juxtacrine Hh signaling observed in type II tumours, type III tumours involve paracrine Hh signaling between the tumour and the surrounding stromal cells (**Figure 1.10**), which includes fibroblasts, endothelial cells and immune cells (Scales & de Sauvage 2009). Human prostate, pancreatic and metastatic colon tumours express Hh in the tumour epithelium, which results in increased GLI1 expression (i.e. Hh pathway activation) in the surrounding stromal cells (Fan et al. 2004; Bailey et al. 2008; H. Tian et al. 2009). The stromal cells in turn send growth and/or survival signals back to the tumour, creating a favourable microenvironment for tumour growth (Scales & de Sauvage 2009). In addition, a 'reverse paracrine' model (Type IIIb) has been proposed, in which Hh is secreted by stromal cells instead and signals to tumour cells. However, this has only been observed in B-cell lymphoma, multiple myeloma and leukemia so far, where Hh secreted from the bone marrow stroma appears to be essential for the survival of cancer cells *in vitro* (Dierks et al. 2007; Hegde et al. 2008).

1.2.6.4 Therapeutics

Hh pathway inhibitors (HPIs) that block Hh signaling at or below the level of Smo could theoretically be used to treat both Hh ligand independent (type I) and Hh ligand dependent (type II and III) cancers. Ptch1+/- heterozygous mice develop spontaneous medulloblastomas and are often used as a model system for testing HPIs (Romer et al. 2004; Sanchez & Ruiz i Altaba 2005). Cyclopamine and jervine were the first HPIs to be identified and were originally isolated from corn lilies (Bryden et al. 1971). Both inhibit the Hh pathway by binding to SMO, which is thought to involve a conformational change in the SMO protein (Cooper et al. 1998; J. K. Chen, Taipale, Cooper, et al. 2002a). However, several factors, such as their low binding affinity, poor oral bioavailability and unfavourable pharmacokinetics (Lipinski et al. 2008), led to the generation of more potent and/or soluble derivatives of cyclopamine (J. K. Chen, Taipale, Young, et al. 2002b; Tremblay et al. 2008). In addition, several screens identified novel synthetic HPIs, including HhAntag (Frank-Kamenetsky et al. 2002), SANT1–SANT4 (J. K. Chen, Taipale, Young, et al. 2002b), Cur-61414 (Williams et al. 2003) and GDC-0449 (Scales & de Sauvage 2009). Some HPIs also act upstream of SMO by blocking the interaction of Hh with Ptc, and examples of these include the Hh-blocking antibody 5E1 (Ericson et al. 1996) and the small molecule inhibitor robotnikinin (Stanton et al. 2009). Notably, although several drugs and antibodies that inhibit Hh binding to Ptc are being developed, no compounds are known to exist that inhibit Hh over-expression at the source, which is the underlying cause of tumour growth in the more common type II and type III Hh ligand dependent cancers (Scales & de Sauvage 2009).

Only HPIs inhibiting SMO have been tested in humans so far. Cyclopamine, applied topically in a cream formulation, resulted in the regression of BCC tumours (Tabs & Avci 2004), and the orally available SMO inhibitor GDC-0449 (Genentech and Curis) promoted tumour regression in phase I clinical trials with patients that had various metastatic or advanced tumours. As a result, GDC0449 has since entered

phase II trials for several cancers. Finally, the HPIs IPI-926 (Infinity Pharmaceuticals) and BMS-833923 (also known as XL139; Bristol Myers Squibb and Exelixis) are also currently used in phase I clinical trials (Scales & de Sauvage 2009).

1.3 The Wg/Wnt Pathway and its regulation by the kinase Shaggy(Sgg)/GSK3β

Wg/Wnt signalling plays an important role in cellular proliferation and differentiation during development (van Amerongen & Nusse 2009). The *wingless (wg)* gene was originally identified as a regulator of segment polarity during larval development in *Drosophila* (Nüsslein-Volhard & Wieschaus 1980). Its mammalian homologue *Wnt* (Rijsewijk et al. 1987), which is expressed by one of 19 different genes in humans, is a proto-oncogene that produces a secreted, cysteine-rich protein (Tanaka et al. 2002). Wnt proteins are lipid modified (Willert et al. 2003), which is a requirement for Wnt signalling and is thought to be important for Wnt secretion (Franch-Marro et al. 2008; Kurayoshi et al. 2007; Willert et al. 2003). Although Wnts are often thought of as classical morphogens, forming a gradient that determines cell fate in a concentration-dependent manner over relatively large distances (endocrine signalling) as seen in the *Drosophila* wing imaginal disc (Zecca et al. 1996), they mediate juxtacrine (contact-dependent) or paracrine (short-range) signalling over a short distance in most tissues (Clevers & Nusse 2012).

1.3.1 Wg/Wnt activates the Wg/Wnt pathway in target cells

Wnt proteins activate the Wnt signaling pathway by binding to a heterodimeric receptor complex on target cells (**Figure 1.11**). The Wnt receptor complex contains the seven-transmembrane (7TM) receptor Frizzled, which interacts directly with Wnt

proteins through its large extracellular amino terminus (Bhanot et al. 1996; Dann et al. 2001; Janda et al. 2012), and the single-pass transmembrane protein LRP5/6, which is also known as Arrow in *Drosophila* (Pinson et al. 2000; Tamai et al. 2000; Wehrli et al. 2000).

Binding of Wg/Wnt ligand to the Frizzled-LRP6 receptor complex induces a conformational change of the latter, resulting in phosphorylation of its cytoplasmic tail by the kinases GSK3β and CK1γ (X. He et al. 2004; Tamai et al. 2004). This results in the recruitment of the Wg/Wnt pathway protein Axin, which interacts with LRP6 (Mao et al. 2001). However, relatively little is known on how GSK3β and CK1γ are recruited and/or activated as a result of Wg/Wnt pathway activation, and the role of the Frizzled receptor component in pathway transduction remains unclear. Frizzled interacts with the cytoplasmic protein Dishevelled (Dsh) (W. Chen et al. 2003), which is thought to promote the interaction between Axin and the LRP tail.

The major molecular outcome of Wg/Wnt pathway transduction is the regulation of the stability of the transcriptional effector protein β-catenin by the APC/Axin destruction complex. The destruction complex consists of β-catenin, the tumour suppressor protein APC, the serine-threonine kinases GSK3β and CK1γ, and the scaffold protein Axin, which also interacts with the LRP tail (**Figure 1.11**) (reviewed in (Clevers & Nusse 2012)). In the absence of Wg/Wnt ligand binding to the Frizzled-LRP6 receptor, CK1γ and GSK3β sequentially phosphorylate β-catenin at multiple serine and threonine residues. The phosphorylated β-catenin is subsequently recognized by the F box/WD repeat protein Slimb/β-TrCP, which forms part of a multi-subunit E3 ubiquitin ligase complex, leading to ubiquitylation and degradation of β-catenin via the proteasome (Aberle et al. 1997). Phosphorylated β-catenin dissociates from the APC/Axin/GSK3β/CK1γ complex and is bound by cytoplasmic β-TrCP to be degraded by the proteasome. Conversely, Wg/Wnt pathway activation promotes the association of Axin with the LRP6 tail, resulting in the dissociation of

the complex and releasing β-catenin, which translocates to the nucleus to activate transcription of Wg/Wnt pathway target genes (**Figure 1.11**).

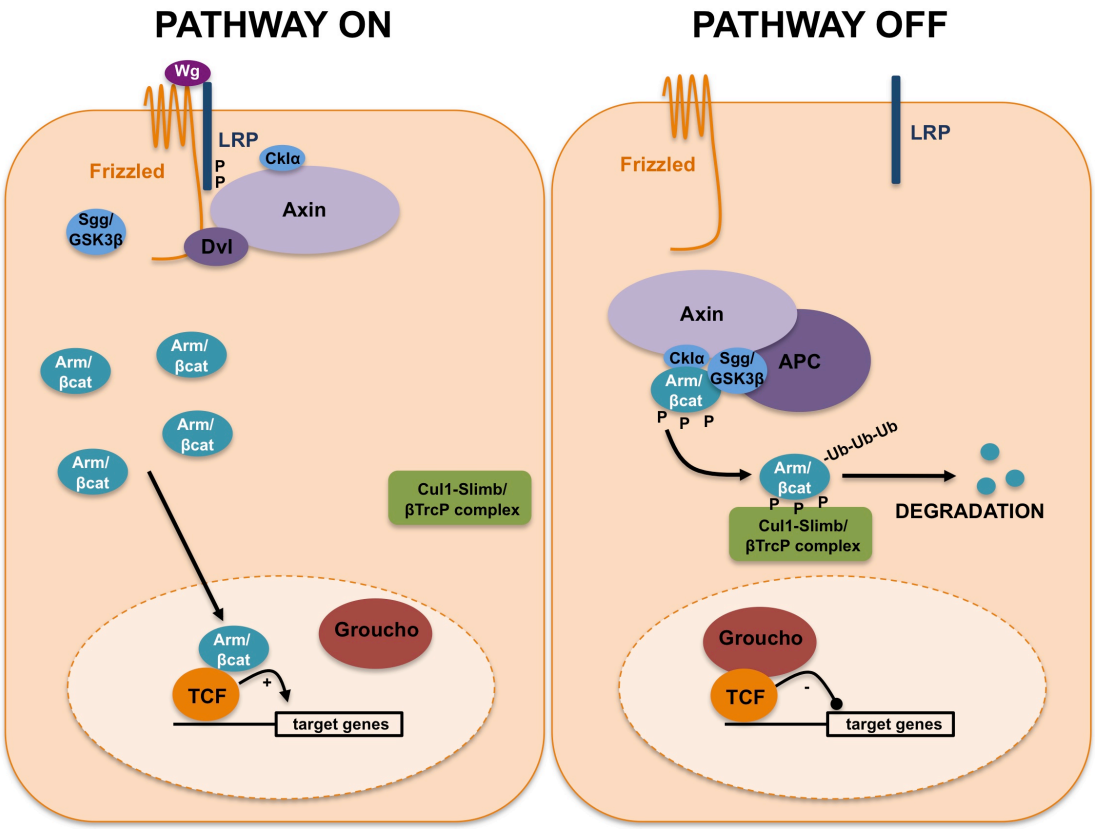

Figure 1.11: The Wg/Wnt signalling pathway. (**left panel**) Wg binding to target cells results in the heterodimerisation of the Frizzled and LRP/Arrow receptors. This results in LRP/Arrow phosphorylation and subsequent sequestration of Axin and Dishevelled (Dvl). Cytoplasmic Armadillo (Arm)/β-catenin (βcat) translocates to the nucleus and binds DNA-bound T cell factor (TCF) transcription factors to activate target gene transcription. (**right panel**) In the absence of Wg ligand, the Frizzled and LRP/Arrow receptors dissociate, and Axin forms a multi-protein complex with APC, Arm/βcat, and the kinases CKI and Sgg/GSK3β. CKI and Sgg/GSK3β phosphorylate Arm/βcat at multiple sites, which results in its recognition and ubiquitylation by the Cul1-based E3 ligase Slimb/βTrcP, and its subsequent degradation via the proteasome. Target gene transcription is repressed by the binding of the co-repressor protein Groucho (Gro) to TCF transcription factors. Adapted from (Clevers & Nusse 2012).

Once in the nucleus, β-catenin interacts with DNA-bound T cell factor (TCF) transcription factors, also known as Pangolin in *Drosophila*, to initiate Wnt/Wg target gene transcription (**Figure 1.11**) (Behrens et al. 1996; Molenaar et al. 1996).

TCF transcription factors recognize the highly conserved consensus motif AGATCAAAGG in both vertebrates and *Drosophila* (van de Wetering et al. 1997). The pTOPflash Wnt/TCF reporter, which contains various repeats of the consensus sequence, is a widely used experimental tool, which exploits the high affinity of TCF for this motif (Korinek et al. 1997). Two other proteins, Bcl9/Legless and Pygopus, which were first identified in *Drosophila*, are also thought to associate with the β-catenin/TCF complex to activate gene transcription, although their exact roles in the process are less clear (Kramps et al. 2002; Parker et al. 2002; Thompson et al. 2002). In the absence of Wg/Wnt pathway activation, and thus the absence of nuclear β-catenin, the transcription of Wg/Wnt target genes is prevented as a result of the interaction of TCF with the transcriptional repressor protein Groucho (**Figure 1.11**) (Cavallo et al. 1998; Roose et al. 1998). Many Wg/Wnt target genes exist, including the well-known Wnt target gene *AXIN2* (Lustig et al. 2002), however most are tissue and/or developmental stage specific (Clevers & Nusse 2012).

1.3.2 Wg/Wnt Signaling in Cancer

Human tumours frequently harbour Wnt pathway mutations. Notably, the vast majority of colorectal cancers contain mutations in the *APC* tumour suppressor gene (Wood et al. 2007). Loss of APC leads to stabilization of β-catenin and constitutive activation of Wnt target genes (Korinek et al. 1997). *APC* gene mutations can be inherited, causing a hereditary cancer syndrome known as familiar adenomatous polyposis (FAP) (Kinzler et al. 1991; Nishisho et al. 1991). FAP is caused by heterozygous APC mutation, which promotes the growth of benign colon adenomas and polyps. However, the additional mutation of the second APC allele (Kinzler & Vogelstein 1996), or other genes such as *KRAS*, *P53*, and *SMAD4*, results in malignant tumour formation. In rare cases of colorectal cancer where APC is not mutated, loss-of-function mutations in Axin (W. Liu et al. 2000), as well as activating point mutations in β-catenin (Morin et al. 1997) have been reported. In addition, similar mutations have also been identified in hepatocellular carcinomas

and melanomas, as well as other tumours (Rubinfeld et al. 1997; Reya & Clevers 2005).

1.3.3 The multiple cellular functions and regulation of the kinase GSK3β

1.3.3.1 Cellular functions of GSK3β

Although glycogen synthase kinase 3 β (GSK3β) was originally identified as a key enzyme involved in glycogen metabolism, many other functions for this versatile serine/threonine kinase have since come to light, including its involvement in various signalling pathways, such as insulin, growth factor, Wg/WNT and Hh/SHH pathways, as well as the control of the cell cycle, apoptosis and microtubule function (reviewed in (Cohen & Frame 2001)).

GSK3β is a negative regulator of both glycogen and protein synthesis. GSK3β phosphorylates and thereby inactivates the enzyme glycogen synthase, which catalyses the final step in glycogen synthesis, and the eukaryotic initiation factor 2B (eIF2B). Insulin-induced signaling results in the activation of protein kinase B, which in turn phosphorylates and inhibits GSK3β (Cross et al. 1995), resulting in the desphosphorylation and activation of glycogen synthase and eIF2B (Hughes et al. 1992; Welsh & Proud 1993). GSK3β is also thought to negatively regulate cell cycle entry and cellular proliferation by phosphorylating cyclin D1 (Alt et al. 2000; Diehl et al. 1998) and c-myc (Sears et al. 2000), promoting their subsequent ubiquitylation and degradation via the proteasome. Growth factor signalling results in the inhibition of GSK3β and therefore promotes stabilization of cyclin D and c-myc and cell growth and proliferation.

Interestingly, GSK3β also plays a key role in morphogen signalling, including the Wg/WNT and Hh/SHH pathways. Within WNT signalling, GSK3β has dual, switchable roles: (i) in the presence of WNT it promotes pathway activation at the receptor level by phosphorylating the LRP6 cytoplasmic tail and; (ii) in the absence of WNT ligand it negatively regulates pathway activity by phosphorylating the transcriptional effector β-catenin and promoting its proteasomal degradation (Clevers & Nusse 2012).

In *Drosophila*, the Wg pathway is crucial in the determination of the pattern of segment polarity during larval development, which is characterized by alternating rows of bristles, and regions lacking bristles called naked cuticles. Loss of function (LOF) mutations in the *wg* gene result in the loss of naked cuticle, whereas LOF mutations in the fly homologue of GSK3β, Shaggy (Sgg)/zeste-white 3 (zw3), completely reversed this phenotype, leading to the loss of bristles, suggesting that Sgg negatively regulates the Wg pathway (Siegfried et al. 1992). Sgg/GSK3β negatively regulates Arm/β-catenin by phosphorylating it, which leads to its recognition and ubiquitylation by the Cul-1 based E3 ligase Slimb/βTrcP, and subsequent degradation (**Figure 1.11**) (Aberle et al. 1997). Similarly, Sgg/GSK3β negatively regulates Hh pathway activity by phosphorylating Ci_{155}, leading to Ci ubiquitylation by Slimb/βTrcP and subsequent partial proteolytic processing to a transcriptional repressor form, Ci_{75} (**Figure 1.5**) (J. Jia et al. 2002).

1.3.3.2 Substrate specificity and regulation of GSK3 activity

GSK3β's substrate specificity is defined by the requirement for a 'priming phosphorylation' on many of its substrates as a prerequisite to recognition and phosphorylation. GSK3β typically phosphorylates a substrate containing a priming phosphate on a serine/threonine residue located four residues carboxy terminal to another serine/threonine (**Figure 1.12 A**) (Fiol et al. 1987). For example, the

phosphorylation of Armadillo/β-catenin in the Wg/Wnt pathway by SGG/GSK3β requires a priming phosphorylation by casein kinase 1 (CK1) (C. Liu et al. 2002; Yanagawa et al. 2002).

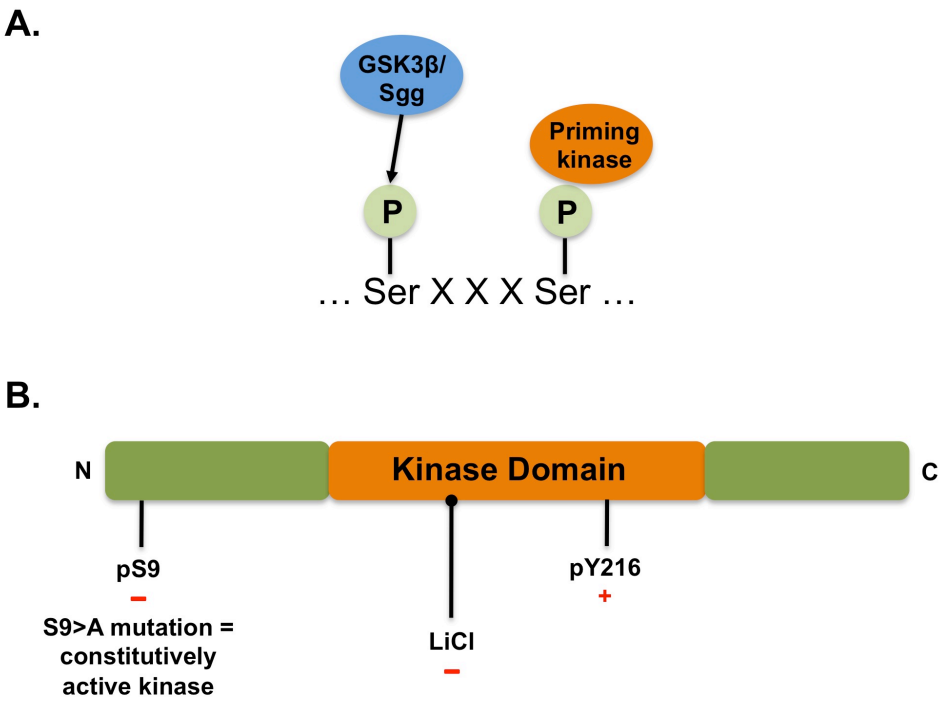

Figure 1.12: GSK3β substrate specificity and regulation. (**A**) GSK3β recognises a priming phosphate four residues carboxy terminal of its phosphorylation target site. (**B**) GSK3β activity is negatively (-) regulated by phosphorylation on Ser9 and treatment with LiCl, and positively (+) regulated by phosphorylation on Tyr216 (Tyr 214 for Sgg). Mutation of Ser9 to Ala generates a constitutively active kinase mutant.

GSK3β is itself regulated by phosphorylation (**Figure 1.12 B**). GSK3β is considered to be constitutively active as a result of high levels of phosphorylation on a tyrosine residue present in the activation loop (Tyr214), which is incidentally equivalent to the mechanism of activation seen in MAPKs (Hughes et al. 1993). However, unlike MAPKs, an additional requirement for full GSK3β activation is the induction of the active kinase conformation through binding of the priming phosphate.

Phosphorylation of a serine residue at the extreme amino terminal of GSK3β (Ser9) is also used to negatively regulate its activity. The phosphorylation results in the recognition of this phosphoserine as a 'pseudosubstrate' by the GSK3β binding pocket that normally binds the priming phosphate on target substrates. This effectively prevents substrates from binding GSK3β, as well as sterically blocking access to the catalytic site (Frame et al. 2001). This serine residue is phopshorylated by different kinases in response to different stimuli, such as by PKB/AKT in response to insulin signalling (Cross et al. 1995). Finally, lithium ions were also shown to specifically inhibit GSK3β activity (Klein & Melton 1996; Stambolic et al. 1996).

Importantly, in the Wg/Wnt pathway, Sgg/GSK3β is not regulated via phosphorylation on Ser9 or Tyr214/216. Wg pathway transduction does not alter inhibitory Ser9 or activating Tyr214 phosphorylation levels of Sgg (Papadopoulou et al. 2004). In the Wg/Wnt pathway, Sgg/GSK3β is sequestered into the APC/Axin/β-catenin destruction complex rather than diffusing freely in the cytoplasm. The inhibition of Sgg/GSK3β activity following Wg/Wnt pathway activation is thought to involve the disruption of the interaction of GSK3β with Axin by another protein complex. This protein complex is believed to contain at least two proteins, including Dishevelled and FRAT (frequently rearranged in advanced T- cell lymphomas) (L. Li et al. 1999), the mammalian homologue of the GSK3-binding protein (GBP) first identified in Xenopus (Yost et al. 1998). Additionally, recent findings have led to the proposal of two new models of GSK3β regulation in Wnt signalling (Metcalfe & Bienz 2011). One involves the negative regulation of GSK3β activity following phophorylation of a serine residue in the LRP receptor cytoplasmic tail, which acts as a 'pseudosubstrate' and binds to the GSK3β binding pocket, preventing the interaction with β-catenin. Another model proposes that Wnt pathway activation triggers the uptake of GSK3β into multivesicular bodies (MVBs), thus physically sequestering GSK3β and preventing phosphorylation of β-catenin (Metcalfe & Bienz 2011).

1.3.4 Wingless signaling in *Drosophila* eye development

Wg plays a crucial role in *Drosophila* eye development by defining head tissue and retinal tissue boundaries, as well as regulating eye disc growth (reviewed in (Legent & Treisman 2008)). The eye antennal disc gives rise to both the retina and he surrounding head tissue (see **Section 1.2.5** and **Figure 1.8 A**). Wg is mainly expressed in the anterior lateral margins of the eye disc (**Figure 1.9, panel b**), which will eventually give rise to the head capsule, where it acts to promote head capsule differentiation and restrict eye development (Treisman & G. M. Rubin 1995; Heslip et al. 1997; C. Ma & Moses 1995; Royet & Finkelstein 1996). Additionally, Wg contributes to the subdivision of the two tissue types by antagonizing the action of posteriorly expressed signalling molecules including Hh and Dpp, and thus defines the boundaries of the retinal field. As would be expected, inhibition of Wg activity using a temperature-sensitive allele or removal of the downstream signalling effector Dishevelled (Dsh) results in invasion of the eye field into the lateral regions of the dorsal head tissue (C. Ma & Moses 1995; Royet & Finkelstein 1996; Heslip et al. 1997). Conversely, loss of negative regulators of Wg signaling, such as Shaggy (Sgg) or Axin (Axn), results in the expansion of head tissue at the expense of the retinal field (Treisman & G. M. Rubin 1995; Heslip et al. 1997; Baonza & Freeman 2002; J. D. Lee & Treisman 2001). Finally, Wg is also a regulator of eye disc growth, as clones over-expressing Wg or lacking the negative regulator Axin cause dramatic overgrowth of the eye disc (Treisman & G. M. Rubin 1995; Baonza & Freeman 2002; J. D. Lee & Treisman 2001).

1.4 Hyperplastic Discs (Hyd) and its mammalian orthologues

Hyperplastic Discs (Hyd) is a *Drosophila* HECT-domain bearing E3 ubiquitin ligase protein (Callaghan et al. 1998). The *hyd* gene was first identified in a genetic screen for temperature sensitive mutations, which caused overgrowth of imaginal discs in mutant *hyd* larvae raised at restrictive temperatures (Martin et al. 1977). Further genetic evidence identified Hyd as a tumour suppressor following the isolation of twenty new mutant *hyd* alleles in a screen for mutations causing imaginal disc overgrowth (Mansfield et al. 1994). Homozygous mutation of the *hyd* gene is generally lethal, with most alleles causing lethality between the second larval instar and the pupal stages, although the null phenotype is predicted to be lethal at or before the second larval instar. In most cases, any temperature sensitive alleles of *hyd* that give rise to viable adults at permissive temperatures result in sterility, defects in germ tissue morphology and reduced lifespan (Mansfield et al. 1994). In agreement with this observation, *hyd* mutants display various spermatogenesis defects, including defects in chromosome condensation, spindle attachment and centrosome behaviour during meiosis (Pertceva et al. 2010).

Mosaic genetic screens using homozygous mutant *hyd* clones in the eye imaginal disc later implicated Hyd in the regulation of Hh signalling (J. D. Lee et al. 2002). In developing *Drosophila* larvae, anterior eye disc clonal cells containing homozygous mutations of the *hyd* gene mis-express the morphogens *hedgehog* (*hh*) and *decapentaplegic* (*dpp*). This results in non-autonomous premature photoreceptor differentiation and ectopic proliferation of surrounding wild type tissue, giving rise to overgrown (i.e hyperplastic) and/or deformed eyes in adult flies (**Figure 1.13 A**) (J. D. Lee et al. 2002).

Furthermore, Hyd negatively regulates *hh* gene expression and Hh pathway activity through independent mechanisms (**Figure 1.13 B**), as these findings show that (i) Hyd regulates *dpp* expression downstream of *hh* expression, as well as (ii) regulating *hh* expression independently of Ci.

dpp is transcribed in response to Hh pathway activation at the morphogenetic furrow (MF) (Penton et al. 1997). However, in *hyd* and *hh* double mutant clones, *dpp* is still mis-expressed, suggesting that ectopic *dpp* expression was not a consequence of Hh pathway activation, and that Hyd regulates *dpp* expression independently of its regulatory effects on *hh* expression. Additionally, loss of *hyd* in *hyd* and *hh* double mutant clones also caused full-length Ci_{155} to accumulate in anterior clones, suggesting that Hyd reduces Ci_{155} levels independently of Hh pathway activity, and that Hyd regulates Hh pathway activity upstream or at the level of Ci (**Figure 1.13 B**).

On the other hand, over-expression of a ci_{75} transgene, encoding the Ci_{75} transcriptional repressor, in *hyd* mutant clones blocked *dpp* expression, but not *hh* expression. Ci_{75} normally represses the transcription of *dpp*, and also represses the transcription of *hh* in anterior cells in the wing disc (see **Section 1.2.1.1**) (Domínguez et al. 1996; Méthot & Basler 1999). However, these findings suggest that, in the eye disc, Hyd regulates *hh* expression independently of Ci_{75}.

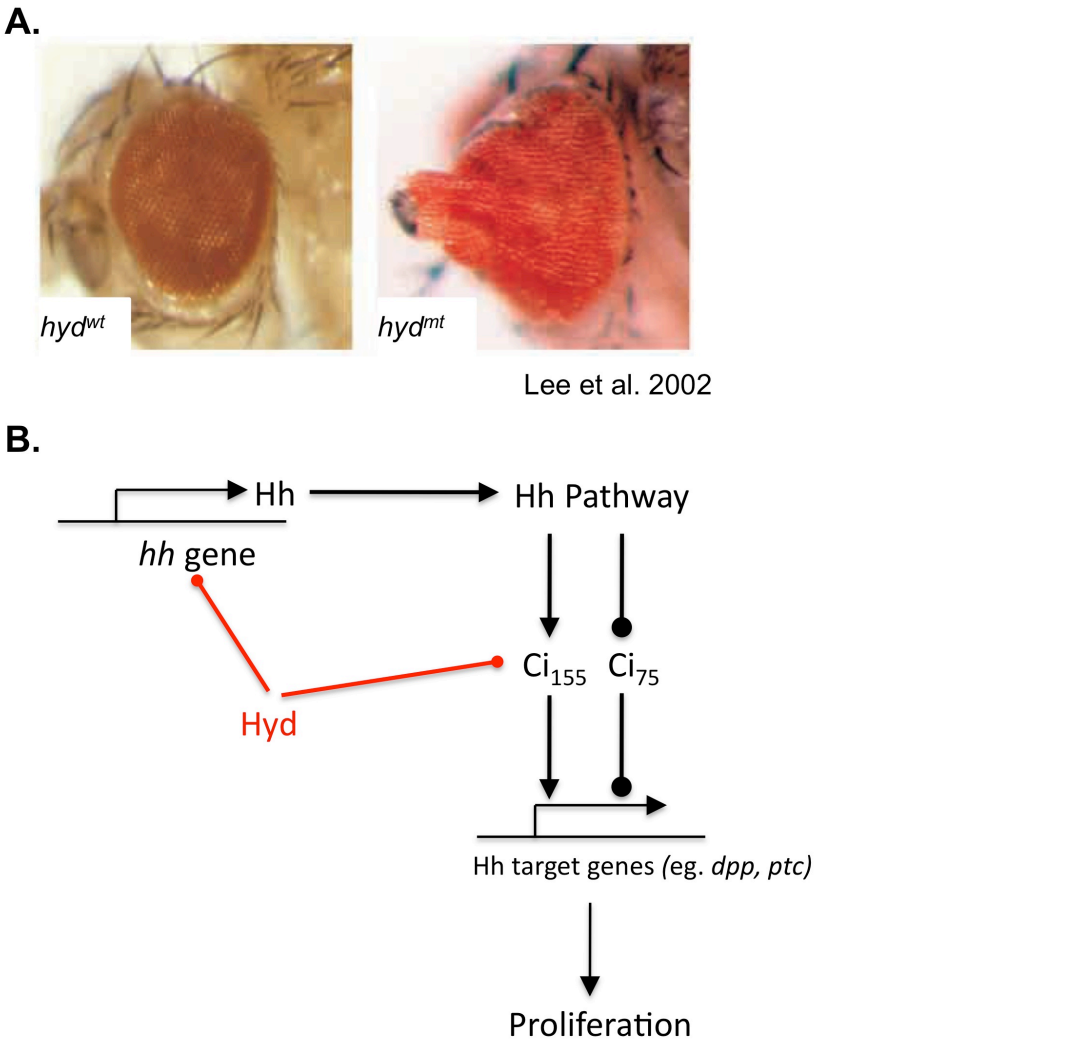

Figure 1.13: *hyd* mutant phenotype, role in Hh signalling and domain structure. (**A**) *hyd*^{mt} clones in the eye disc cause non-autonomous overgrowth of eye tissue and hyperplasia in adult eyes. **(J. D. Lee et al. 2002)** (**B**) Hyd regulates Hh signalling via two independent mechanisms. (**C**) Hyd domain structure. Hyd contains five functional domains: the ubiquitin-associated (UBA) domain, the regulator of chromatin condensation (RCC) domain, the UBR-type zinc finger domain, the poly(A)-binding protein C-terminal (PABC) domain, and the catalytic E6AP-type E3 ubiquitin-protein ligase (HECT) catalytic domain.

Although genetic evidence implicates Hyd in the regulation of Hh signaling and morphogen gene expression, the molecular mechanism underlying its role in these processes is unknown.

The Hyd protein was found to be both cytoplasmic and nuclear, whereas its potential localization in the plasma membrane was excluded (Mansfield et al. 1994). At the time of commencing this project, there was only one potential interaction for the Hyd protein described in the literature. Lewis et al. performed a mass spectrometry co-purification experiment on fractionated *Drosophila* embryo extracts, which demonstrated the existence of a large, multi-protein complex, the Myb-MuvB/dREAM complex, which is involved in regulating DNA replication and gene transcription during development. In this experiment, Hyd was co-purified with two of the core complex components, Mip120 and Mip130 (Lewis et al. 2004). The Myb-MuvB/dREAM complex was shown to epigenetically regulate gene transcription *in vivo*, in particular the expression of *polo kinase 1 (PLK1*), a regulator of spindle pole assembly, and components of the spindle assembly checkpoint (SAC) (Wen et al. 2008). An interaction with the Myb-MuvB/dream complex would therefore implicate Hyd in the regulation of the cell cycle and mitosis. Since then, large-scale co-affinity purification mass spectrometry screens with *Drosophila* proteins have produced a wealth of protein-protein interaction data (Guruharsha et al. 2011; Friedman et al. 2011), in which a number of potential Hyd interacting proteins were identified. This data is publicly accessible on the Drosophila Interactions Database (DroID; http://www.droidb.org).

1.4.1 Structure and function of the Hyd protein

A vital source of information with regards to the molecular function of the Hyd protein lies in its amino acid sequence. Hyd is a relatively large protein (319 kDa) and contains five distinct domains, as well as two nuclear localization signals (**Figure 1.13 C**). Hyd shares up to 40% sequence identity with its mammalian homologues UBR5 (*Mus musculus*) (Saunders et al. 2004) and E3 in Differential Display (EDD) (*Homo sapiens*) (Callaghan et al. 1998). Remarkably, sequence identity between the three homologues rises up to 90% across individual domains, suggesting that they may also share evolutionarily conserved functions (**Figure 1.14)**.

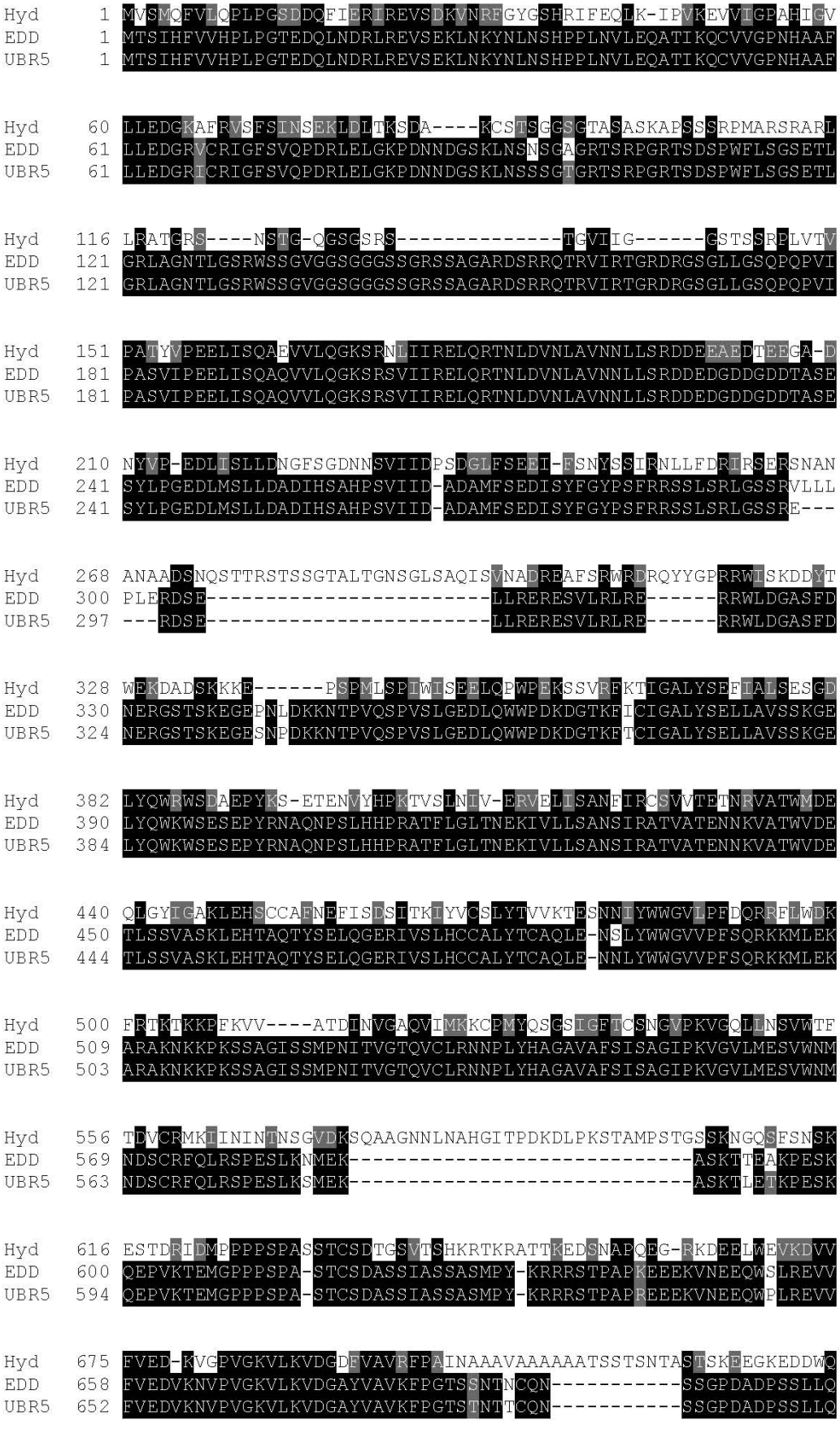
Hyd 1 MVSMQFVLQPLPGSDDQFIERIREVSDKVNRFGYGSHRIFEQLK-IPVKEVVIGPAHIGV
EDD 1 MTSIHFVVHPLPGTEDQLNDRLREVSEKLNKYNLNSHPPLNVLEQATIKQCVVGPNHAAF
UBR5 1 MTSIHFVVHPLPGTEDQLNDRLREVSEKLNKYNLNSHPPLNVLEQATIKQCVVGPNHAAF
Hyd 60 LLEDGKAFRVSFSINSEKLDLTKSDA----KCSTSGGSGTASASKAPSSSRPMARSRARL
EDD 61 LLEDGRVCRIGFSVQPDRLELGKPDNNDGSKLNSNSGAGRTSRPGRTSDSPWFLSGSETL
UBR5 61 LLEDGRICRIGFSVQPDRLELGKPDNNDGSKLNSSSGTGRTSRPGRTSDSPWFLSGSETL
Hyd 116 LRATGRS----NSTG-QGSGSRS--------------TGVIIG------GSTSSRPLVTV
EDD 121 GRLAGNTLGSRWSSGVGGSGGGSSGRSSAGARDSRRQTRVIRTGRDRGSGLLGSQPQPVI
UBR5 121 GRLAGNTLGSRWSSGVGGSGGGSSGRSSAGARDSRRQTRVIRTGRDRGSGLLGSQPQPVI
Hyd 151 PATYVPEELISQAEVVLQGKSRNLIIRELQRTNLDVNLAVNNLLSRDDEEAEDTEEGA-D
EDD 181 PASVIPEELISQAQVVLQGKSRSVIIRELQRTNLDVNLAVNNLLSRDDEDGDDGDDTASE
UBR5 181 PASVIPEELISQAQVVLQGKSRSVIIRELQRTNLDVNLAVNNLLSRDDEDGDDGDDTASE
Hyd 210 NYVP-EDLISLLDNGFSGDNNSVIIDPSDGLFSEEI-FSNYSSIRNLLFDRIRSERSNAN
EDD 241 SYLPGEDLMSLLDADIHSAHPSVIID-ADAMFSEDISYFGYPSFRRSSLSRLGSSRVLLL
UBR5 241 SYLPGEDLMSLLDADIHSAHPSVIID-ADAMFSEDISYFGYPSFRRSSLSRLGSSRE---
Hyd 268 ANAADSNQSTTRSTSSGTALTGNSGLSAQISVNADREAFSRWRDRQYYGPRRWISKDDYT
EDD 300 PLERDSE------------------------LLRERESVLRLRE------RRWLDGASFD
UBR5 297 ---RDSE------------------------LLRERESVLRLRE------RRWLDGASFD
Hyd 328 WEKDADSKKKE------PSPMLSPIWISEELQPWPEKSSVRFKTIGALYSEFIALSESGD
EDD 330 NERGSTSKEGEPNLDKKNTPVQSPVSLGEDLQWWPDKDGTKFICIGALYSELLAVSSKGE
UBR5 324 NERGSTSKEGESNPDKKNTPVQSPVSLGEDLQWWPDKDGTKFTCIGALYSELLAVSSKGE
Hyd 382 LYQWRWSDAEPYKS-ETENVYHPKTVSLNIV-ERVELISANFIRCSVVTETNRVATWMDE
EDD 390 LYQWKWSESEPYRNAQNPSLHHPRATFLGLTNEKIVLLSANSIRATVATENNKVATWVDE
UBR5 384 LYQWKWSESEPYRNAQNPSLHHPRATFLGLTNEKIVLLSANSIRATVATENNKVATWVDE
Hyd 440 QLGYIGAKLEHSCCAFNEFISDSITKIYVCSLYTVVKTESNNIYWWGVLPFDQRRFLWDK
EDD 450 TLSSVASKLEHTAQTYSELQGERIVSLHCCALYTCAQLE-NSLYWWGVVPFSQRKKMLEK
UBR5 444 TLSSVASKLEHTAQTYSELQGERIVSLHCCALYTCAQLE-NNLYWWGVVPFSQRKKMLEK
Hyd 500 FRTKTKKPFKVV----ATDINVGAQVIMKKCPMYQSGSIGFTCSNGVPKVGQLLNSVWTF
EDD 509 ARAKNKKPKSSAGISSMPNITVGTQVCLRNNPLYHAGAVAFSISAGIPKVGVLMESVWNM
UBR5 503 ARAKNKKPKSSAGISSMPNITVGTQVCLRNNPLYHAGAVAFSISAGIPKVGVLMESVWNM
Hyd 556 TDVCRMKTININTNSGVDKSQAAGNNLNAHGITPDKDLPKSTAMPSTGSSKNGQSFSNSK
EDD 569 NDSCRFQLRSPESLKNMEK----------ASKTTEAKPESK
UBR5 563 NDSCRFQLRSPESLKSMEK----------ASKTLETKPESK
Hyd 616 ESTDRIDMPPPPSPASSTCSDTGSVTSHKRTKRATTKEDSNAPQEG-RKDEELWEVKDVV
EDD 600 QEPVKTEMGPPPSPA-STCSDASSIASSASMPY-KRRRSTPAPKEEEKVNEEQWSLREVV
UBR5 594 QEPVKTEMGPPPSPA-STCSDASSIASSASMPY-KRRRSTPAPREEEKVNEEQWPLREVV
Hyd 675 FVED-KVGPVGKVLKVDGDFVAVRFPAINAAAVAAAAAATSSTSNTASTSKEEGKEDDWQ
EDD 658 FVEDVKNVPVGKVLKVDGAYVAVKFPGTSSNTNCQN----------SSGPDADPSSLLQ
UBR5 652 FVEDVKNVPVGKVLKVDGAYVAVKFPGTSTNTTCQN----------SSGPDADPSSLLQ

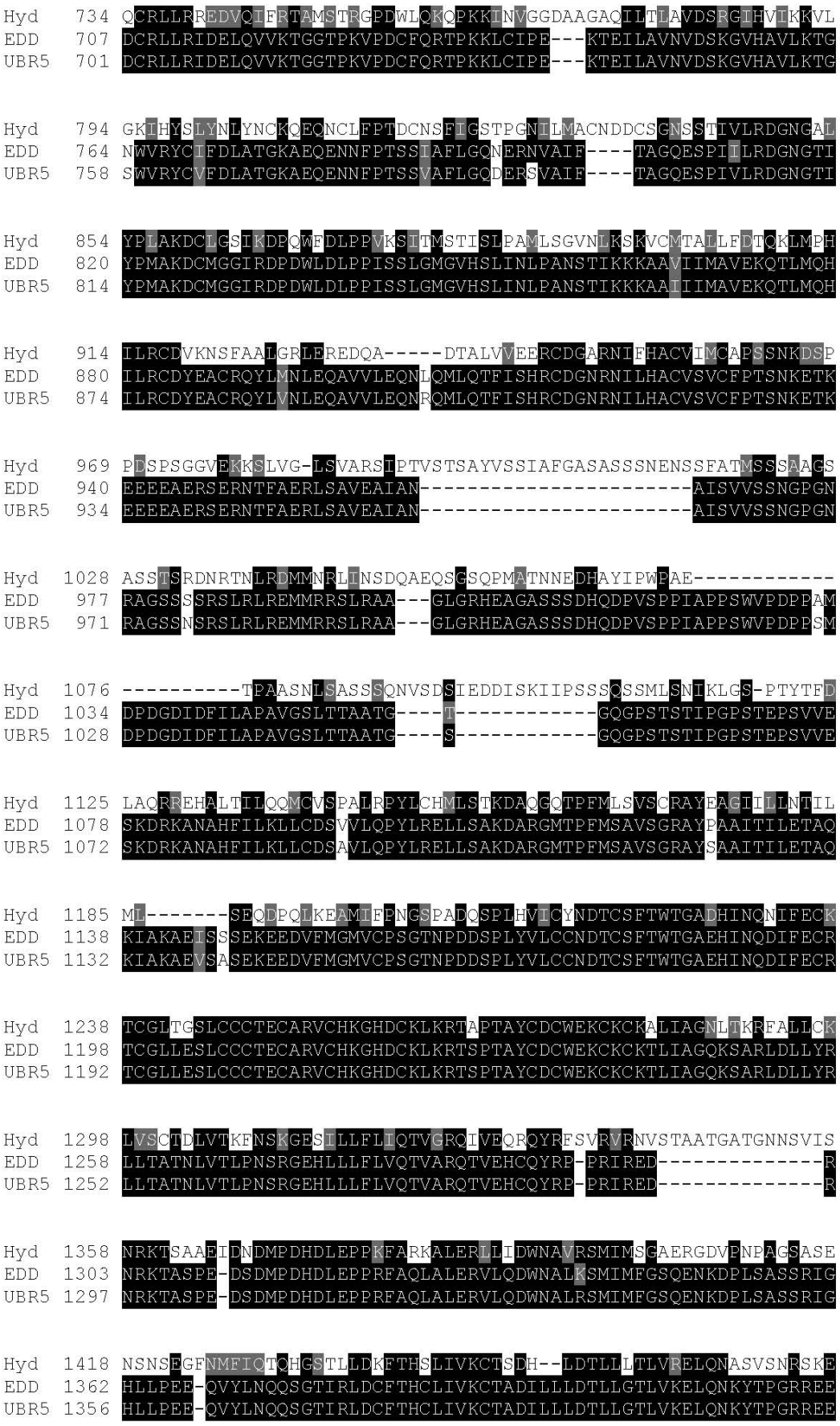
Hyd 734 QCRLLRREDVQIFRTAMSTRGPDWLQKQPKKINVGGDAAGAQILTLAVDSRGIHVIKKVL
EDD 707 DCRLLRIDELQVVKTGGTPKVPDCFQRTPKKLCIPE---KTEILAVNVDSKGVHAVLKTG
UBR5 701 DCRLLRIDELQVVKTGGTPKVPDCFQRTPKKLCIPE---KTEILAVNVDSKGVHAVLKTG
Hyd 794 GKIHYSLYNLYNCKQEQNCLFPTDCNSFIGSTPGNILMACNDDCSGNSSTIVLRDGNGAL
EDD 764 NWVRYCIFDLATGKAEQENNFPTSSIAFLGQNERNVAIF----TAGQESPIILRDGNGTI
UBR5 758 SWVRYCVFDLATGKAEQENNFPTSSVAFLGQDERSVAIF----TAGQESPIVLRDGNGTI
Hyd 854 YPLAKDCLGSIKDPQWFDLPPVKSITMSTISLPAMLSGVNLKSKVCMTALLFDTQKLMPH
EDD 820 YPMAKDCMGGIRDPDWLDLPPISSLGMGVHSLINLPANSTIKKKAAVIIMAVEKQTLMQH
UBR5 814 YPMAKDCMGGIRDPDWLDLPPISSLGMGVHSLINLPANSTIKKKAAIIIMAVEKQTLMQH
Hyd 914 ILRCDVKNSFAALGRLEREDQA-----DTALVVEERCDGARNIEHACVIMCAPSSNKDSP
EDD 880 ILRCDYEACRQYLMNLEQAVVLEQNLQMLQTFISHRCDGNRNILHACVSVCFPTSNKETK
UBR5 874 ILRCDYEACRQYLVNLEQAVVLEQNRQMLQTFISHRCDGNRNILHACVSVCFPTSNKETK
Hyd 969 PDSPSGGVEKKSLVG-LSVARSIPTVSTSAYVSSIAFGASASSSNENSSFATMSSSAAGS
EDD 940 EEEEAERSERNTFAERLSAVEAIAN----------AISVVSSNGPGN
UBR5 934 EEEEAERSERNTFAERLSAVEAIAN----------AISVVSSNGPGN
Hyd 1028 ASSTSRDNRTNLRDMMNRLINSDQAEQSGSQPMATNNEDHAYIPWPAE----------
EDD 977 RAGSSSSRSLRLREMMRRSLRAA---GLGRHEAGASSSDHQDPVSPPIAPPSWVPDPPAM
UBR5 971 RAGSSNSRSLRLREMMRRSLRAA---GLGRHEAGASSSDHQDPVSPPIAPPSWVPDPPSM
Hyd 1076 ----------TPAASNLSASSSQNVSDSIEDDISKIIPSSSQSSMLSNIKLGS-PTYTFD
EDD 1034 DPDGDIDFILAPAVGSLTTAATG----T----------GQGPSTSTIPGPSTEPSVVE
UBR5 1028 DPDGDIDFILAPAVGSLTTAATG----S----------GQGPSTSTIPGPSTEPSVVE
Hyd 1125 LAQRREHALTILQQMCVSPALRPYLCHMLSTKDAQGQTPFMLSVSCRAYEAGILLLNTIL
EDD 1078 SKDRKANAHFILKLLCDSVVLQPYLRELLSAKDARGMTPFMSAVSGRAYPAAITILETAQ
UBR5 1072 SKDRKANAHFILKLLCDSAVLQPYLRELLSAKDARGMTPFMSAVSGRAYSAAITILETAQ
Hyd 1185 ML-------SEQDPQLKEAMIFPNGSPADQSPLHVICYNDTCSFTWTGADHINQNIFECK
EDD 1138 KIAKAEISSSEKEEDVFMGMVCPSGTNPDDSPLYVLCCNDTCSFTWTGAEHINQDIFECR
UBR5 1132 KIAKAEVSASEKEEDVFMGMVCPSGTNPDDSPLYVLCCNDTCSFTWTGAEHINQDIFECR
Hyd 1238 TCGLTGSLCCCTECARVCHKGHDCKLKRTAPTAYCDCWEKCKCKALIAGNLTKRFALLCK
EDD 1198 TCGLLESLCCCTECARVCHKGHDCKLKRTSPTAYCDCWEKCKCKTLIAGQKSARLDLLYR
UBR5 1192 TCGLLESLCCCTECARVCHKGHDCKLKRTSPTAYCDCWEKCKCKTLIAGQKSARLDLLYR
Hyd 1298 LVSCTDLVTKENSKGESILLFLIQTVGRQIVEQRQYRFSVRVRNVSTAATGATGNNSVIS
EDD 1258 LLTATNLVTLPNSRGEHLLLFLVQTVARQTVEHCQYRP-PRIRED----------R
UBR5 1252 LLTATNLVTLPNSRGEHLLLFLVQTVARQTVEHCQYRP-PRIRED----------R
Hyd 1358 NRKTSAAEIDNDMPDHDLEPPKFARKALERLLIDWNAVRSMIMSGAERGDVPNPAGSASE
EDD 1303 NRKTASPE-DSDMPDHDLEPPRFAQLALERVLQDWNALKSMIMFGSQENKDPLSASSRIG
UBR5 1297 NRKTASPE-DSDMPDHDLEPPRFAQLALERVLQDWNALRSMIMFGSQENKDPLSASSRIG
Hyd 1418 NSNSEGFNMFIQTQHGSTLLDKFTHSLIVKCTSDH--LDTLLLTLVRELQNASVSNRSKE
EDD 1362 HLLPEE-QVYLNQQSGTIRLDCFTHCLIVKCTADILLLDTLLGTLVKELQNKYTPGRREE
UBR5 1356 HLLPEE-QVYLNQQSGTIRLDCFTHCLIVKCTADILLLDTLLGTLVKELQNKYTPGRREE

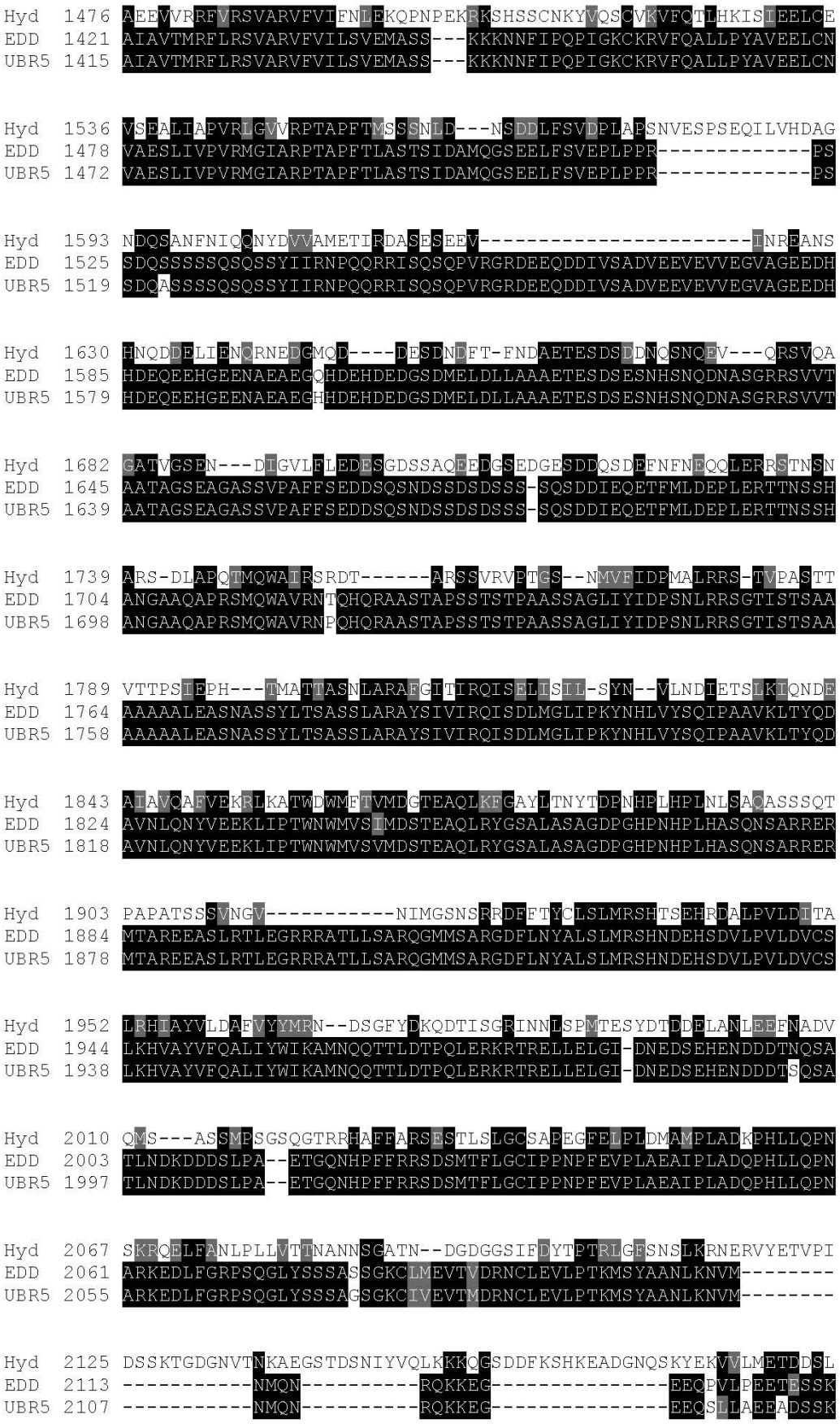
Hyd 1476 AEEVVRRFVRSVARVFVIFNLEKQPNPEKRKSHSSCNKYVQSCVKVFQTLHKISIEELCE
EDD 1421 AIAVTMRFLRSVARVFVILSVEMASS---KKKNNFIPQPIGKCKRVFQALLPYAVEELCN
UBR5 1415 AIAVTMRFLRSVARVFVILSVEMASS---KKKNNFIPQPIGKCKRVFQALLPYAVEELCN
Hyd 1536 VSEALIAPVRLGVVRPTAPFTMSSSNLD---NSDDLFSVDPLAPSNVESPSEQILVHDAG
EDD 1478 VAESLIVPVRMGIARPTAPFTLASTSIDAMQGSEELFSVEPLPPR----------PS
UBR5 1472 VAESLIVPVRMGIARPTAPFTLASTSIDAMQGSEELFSVEPLPPR----------PS
Hyd 1593 NDQSANFNIQQNYDVVAMETIRDASESEEV----------INREANS
EDD 1525 SDQSSSSSQSQSSYIIRNPQQRRISQSQPVRGRDEEQDDIVSADVEEVEVVEGVAGEEDH
UBR5 1519 SDQASSSSQSQSSYIIRNPQQRRISQSQPVRGRDEEQDDIVSADVEEVEVVEGVAGEEDH
Hyd 1630 HNQDDELIFNQRNEDGMQD----DESDNDFT-FNDAETESDSDDNQSNQEV---QRSVQA
EDD 1585 HDEQEEHGEENAEAEGQHDEHDEDGSDMELDLLAAAETESDSESNHSNQDNASGRRSVVT
UBR5 1579 HDEQEEHGEENAEAEGHHDEHDEDGSDMELDLLAAAETESDSESNHSNQDNASGRRSVVT
Hyd 1682 GATVGSEN---DIGVLFLEDESGDSSAQEEDGSEDGESDDQSDEFNFNEQQLERRSTNSN
EDD 1645 AATAGSEAGASSVPAFFSEDDSQSNDSSDSDSSS-SQSDDIEQETFMLDEPLERTTNSSH
UBR5 1639 AATAGSEAGASSVPAFFSEDDSQSNDSSDSDSSS-SQSDDIEQETFMLDEPLERTTNSSH
Hyd 1739 ARS-DLAPQTMQWAIRSRDT------ARSSVRVPTGS--NMVFIDPMALRRS-TVPASTT
EDD 1704 ANGAAQAPRSMQWAVRNTQHQRAASTAPSSTSTPAASSAGLIYIDPSNLRRSGTISTSAA
UBR5 1698 ANGAAQAPRSMQWAVRNPQHQRAASTAPSSTSTPAASSAGLIYIDPSNLRRSGTISTSAA
Hyd 1789 VTTPSIEPH---TMATTASNLARAFGITIRQISELISIL-SYN--VLNDIETSLKIQNDE
EDD 1764 AAAAALEASNASSYLTSASSLARAYSIVIRQISDLMGLIPKYNHLVYSQIPAAVKLTYQD
UBR5 1758 AAAAALEASNASSYLTSASSLARAYSIVIRQISDLMGLIPKYNHLVYSQIPAAVKLTYQD
Hyd 1843 AIAVQAFVEKRLKATWDWMFTVMDGTEAQLKFGAYLTNYTDPNHPLHPLNLSAQASSSQT
EDD 1824 AVNLQNYVEEKLIPTWNWMVSIMDSTEAQLRYGSALASAGDPGHPNHPLHASQNSARRER
UBR5 1818 AVNLQNYVEEKLIPTWNWMVSVMDSTEAQLRYGSALASAGDPGHPNHPLHASQNSARRER
Hyd 1903 PAPATSSSVNGV----------NIMGSNSRRDEFTYCLSLMRSHTSEHRDALPVLDITA
EDD 1884 MTAREEASLRTLEGRRRATLLSARQGMMSARGDFLNYALSLMRSHNDEHSDVLPVLDVCS
UBR5 1878 MTAREEASLRTLEGRRRATLLSARQGMMSARGDFLNYALSLMRSHNDEHSDVLPVLDVCS
Hyd 1952 LRHIAYVLDAEVYYMRN--DSGFYDKQDTISGRINNLSPMTESYDTDDELANLEEFNADV
EDD 1944 LKHVAYVFQALIYWIKAMNQQTTLDTPQLERKRTRELLELGI-DNEDSEHENDDDTNQSA
UBR5 1938 LKHVAYVFQALIYWIKAMNQQTTLDTPQLERKRTRELLELGI-DNEDSEHENDDDTSQSA
Hyd 2010 QMS---ASSMPSGSQGTRRHAFFARSESTLSLGCSAPEGFELPLDMAMPLADKPHLLQPN
EDD 2003 TLNDKDDDSLPA--ETGQNHPFFRRSDSMTFLGCIPPNPFEVPLAEAIPLADQPHLLQPN
UBR5 1997 TLNDKDDDSLPA--ETGQNHPFFRRSDSMTFLGCIPPNPFEVPLAEAIPLADQPHLLQPN
Hyd 2067 SKRQELFANLPLLVTTNANNSGATN--DGDGGSIFDYTPTRLGFSNSLKRNERVYETVPI
EDD 2061 ARKEDLFGRPSQGLYSSSASSGKCLMEVTVDRNCLEVLPTKMSYAANLKNVM--------
UBR5 2055 ARKEDLFGRPSQGLYSSSAGSGKCIVEVTMDRNCLEVLPTKMSYAANLKNVM--------
Hyd 2125 DSSKTGDGNVTNKAEGSTDSNIYVQLKKKQGSDDFKSHKEADGNQSKYEKVVLMETDDSL
EDD 2113 -----------NMQN----------RQKKEG---------------EEQPVLPEETESSK
UBR5 2107 -----------NMQN----------RQKKEG---------------EEQSLLAEEADSSK

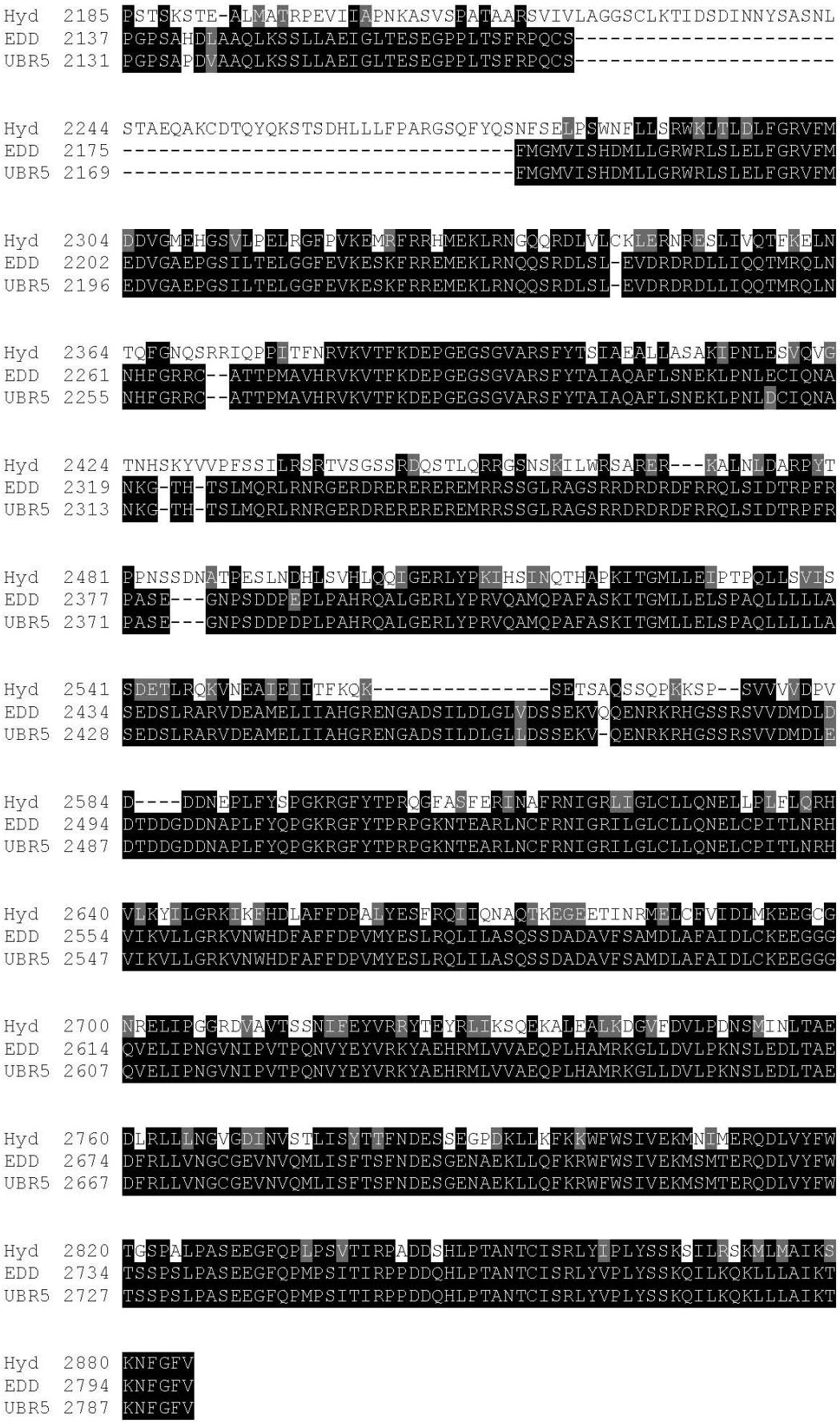
Hyd 2185 PSTSKSTE-ALMATRPEVITAPNKASVSPATAARSVIVLAGGSCLKTIDSDINNYSASNL
EDD 2137 PGPSAHDLAAQLKSSLLAEIGLTESEGPPLTSFRPQCS----------
UBR5 2131 PGPSAPDVAAQLKSSLLAEIGLTESEGPPLTSFRPQCS----------
Hyd 2244 STAEQAKCDTQYQKSTSDHLLLFPARGSQFYQSNFSELPSWNFLLSRWKLTLDLFGRVFM
EDD 2175 ----------FMGMVISHDMLLGRWRLSLELFGRVFM
UBR5 2169 ----------FMGMVISHDMLLGRWRLSLELFGRVFM
Hyd 2304 DDVGMEHGSVLPELRGFPVKEMRFRRHMEKLRNGQQRDLVLCKLERNRESLIVQTFKELN
EDD 2202 EDVGAEPGSILTELGGFEVKESKFRREMEKLRNQQSRDLSL-EVDRDRDLLIQQTMRQLN
UBR5 2196 EDVGAEPGSILTELGGFEVKESKFRREMEKLRNQQSRDLSL-EVDRDRDLLIQQTMRQLN
Hyd 2364 TQFGNQSRRIQPPITFNRVKVTFKDEPGEGSGVARSFYTSIAEALLASAKIPNLESVQVG
EDD 2261 NHFGRRC--ATTPMAVHRVKVTFKDEPGEGSGVARSFYTAIAQAFLSNEKLPNLECIQNA
UBR5 2255 NHFGRRC--ATTPMAVHRVKVTFKDEPGEGSGVARSFYTAIAQAFLSNEKLPNLDCIQNA
Hyd 2424 TNHSKYVVPFSSILRSRTVSGSSRDQSTLQRRGSNSKILWRSARER---KALNLDARPYT
EDD 2319 NKG-TH-TSLMQRLRNRGERDRERERERMRRSSGLRAGSRRDRDRDFRRQLSIDTRPFR
UBR5 2313 NKG-TH-TSLMQRLRNRGERDRERERERMRRSSGLRAGSRRDRDRDFRRQLSIDTRPFR
Hyd 2481 PPNSSDNATPESLNDHLSVHLQQIGERLYPKIHSINQTHAPKITGMLLEIPTPQLLSVIS
EDD 2377 PASE---GNPSDDPEPLPAHRQALGERLYPRVQAMQPAFASKITGMLLELSPAQLLLLLA
UBR5 2371 PASE---GNPSDDPDPLPAHRQALGERLYPRVQAMQPAFASKITGMLLELSPAQLLLLLA
Hyd 2541 SDETLRQKVNEAIEIITFKQK----------SETSAQSSQPKKSP--SVVVVDPV
EDD 2434 SEDSLRARVDEAMELIIAHGRENGADSILDLGLVDSSEKVQQENRKRHGSSRSVVDMDLD
UBR5 2428 SEDSLRARVDEAMELIIAHGRENGADSILDLGLLDSSEKV-QENRKRHGSSRSVVDMDLE
Hyd 2584 D----DDNEPLFYSPGKRGFYTPRQGFASFERINAFRNIGRLIGLCLLQNELLPLFLQRH
EDD 2494 DTDDGDDNAPLFYQPGKRGFYTPRPGKNTEARLNCFRNIGRILGLCLLQNELCPITLNRH
UBR5 2487 DTDDGDDNAPLFYQPGKRGFYTPRPGKNTEARLNCFRNIGRILGLCLLQNELCPITLNRH
Hyd 2640 VLKYILGRKIKFHDLAFFDPALYESFRQIIQNAQTKEGEETINRMELCFVIDLMKEEGCG
EDD 2554 VIKVLLGRKVNWHDFAFFDPVMYESLRQLILASQSSDADAVFSAMDLAFAIDLCKEEGGG
UBR5 2547 VIKVLLGRKVNWHDFAFFDPVMYESLRQLILASQSSDADAVFSAMDLAFAIDLCKEEGGG
Hyd 2700 NRELIPGGRDVAVTSSNIFEYVRRYTEYRLIKSQEKALEALKDGVFDVLPDNSMINLTAE
EDD 2614 QVELIPNGVNIPVTPQNVYEYVRKYAEHRMLVVAEQPLHAMRKGLLDVLPKNSLEDLTAE
UBR5 2607 QVELIPNGVNIPVTPQNVYEYVRKYAEHRMLVVAEQPLHAMRKGLLDVLPKNSLEDLTAE
Hyd 2760 DLRLLLNGVGDINVSTLISYTTFNDESSEGPDKLLKFKKWFWSIVEKMNIMERQDLVYFW
EDD 2674 DFRLLVNGCGEVNVQMLISFTSFNDESGENAEKLLQFKRWFWSIVEKMSMTERQDLVYFW
UBR5 2667 DFRLLVNGCGEVNVQMLISFTSFNDESGENAEKLLQFKRWFWSIVEKMSMTERQDLVYFW
Hyd 2820 TGSPALPASEEGFQPLPSVTIRPADDSHLPTANTCISRLYIPLYSSKSILRSKMLMAIKS
EDD 2734 TSSPSLPASEEGFQPMPSITIRPPDDQHLPTANTCISRLYVPLYSSKQILKQKLLLAIKT
UBR5 2727 TSSPSLPASEEGFQPMPSITIRPPDDQHLPTANTCISRLYVPLYSSKQILKQKLLLAIKT
Hyd 2880 KNFGFV
EDD 2794 KNFGFV
UBR5 2787 KNFGFV

Figure 1.14: ClustalW Alignment of Hyd (*D melanogaster*), EDD (*H sapiens*) and UBR5 (*M musculus*) protein sequences. Hyd shares high sequence identity with EDD and UBR5 across individual domains: UBA (aa 154-196), UBR (aa 1217-1285), PABC (aa 2484-2561), and HECT (aa 2782-2885).

1.4.1.1 Homologous to E6-AP C-terminus (HECT) Domain

The presence of the homologous to the E6-AP carboxyl terminus (HECT) catalytic domain at its carboxyl terminus classifies Hyd as a HECT family E3 ubiquitin ligase (Huibregtse et al. 1995), and suggests its involvement in the ubiquitylation of its target proteins. The HECT domain defines a family of E3 ubiquitin protein ligases in which a conserved cysteine residue accepts ubiquitin from an E2 ubiquitin-conjugating enzyme in the form of a thioester and then directly catalyses the transfer of ubiqitin to target substrates (Huibregtse et al. 1995). EDD reversibly binds ubiquitin *in vitro* via the conserved cysteine residue (C2768) in its HECT domain, as substitution of this residue completely abrogated the ability to bind ubiquitin (Callaghan et al. 1998). Accordingly, EDD ubiquitylates a number of substrates, including katanin (Maddika & J. Chen 2009), TopBP1 (Honda et al. 2002), and β-catenin (Hay-Koren et al. 2011) (see **Section 1.4.2** below). Taken together with the fact that Hyd's HECT domain shares high sequence identity with the EDD HECT domain, this suggests that Hyd most likely also functions as an E3 ubiquitin ligase.

1.4.1.2 Poly(A)-binding Protein C-terminal (PABC) Domain

Immediately adjacent to the carboxy terminal HECT domain, Hyd contains a highly conserved protein-protein binding domain, termed the Poly(A)-binding Protein C-terminal (PABC) domain. Interestingly, the PABC domain is found exclusively in only Hyd (and its homologues), and in the poly(A)-binding protein (PABP) (Deo et al. 2001). PABP plays a key role in eukaryotic protein synthesis and mRNA stability. It recognizes the 3' poly(A) mRNA tail and recruits several translation and mRNA

processing factors to the mRNA pol(A) tail via its PABC domain(Deo et al. 2001; Kozlov et al. 2004).

The EDD and human PABP PABC domains share 56% sequence identity over the most highly conserved 60 amino acid region (Deo et al. 2001). The structures of both PABC domains from EDD and human PABP have been determined, revealing several structural similarities, as well as a conserved binding surface (Deo et al. 2001; Kozlov et al. 2004). The PABC domain recognizes a conserved sequence motif of 12-15 amino acids, known as PAM2 (PABP-interacting motif 2) (Kozlov et al. 2001; Kozlov et al. 2004), which is present in several known binding partners of human PABP, including the PABP-interacting proteins Paip1 and Paip2, as well as eRF3 (Craig et al. 1998; Khaleghpour et al. 2001; Hoshino et al. 1999). Site-directed mutagenesis of conserved PABC domain residues revealed essential residues required for peptide recognition. Substitution of a conserved phenylalanine residue in the human PABP PABC domain (F22) to alanine completely abrogated the binding to Paip1 and Paip2, whereas mutation of an additional conserved leucine residue (F22A, L40A) prevented the binding of eRF3 (Kozlov et al. 2004).

The high conservation between the PABP and EDD PABC domains suggests that they may share one or more interaction partners. As expected, the EDD PABC domain also binds PAM2 peptides with high affinity (Lim et al. 2006), and EDD interacts with full-length Paip1 (Deo et al. 2001) and the anti-proliferative protein transducer of ErbB2 (Tob2) (Lim et al. 2006). Tob2 belongs to the BTG/Tob family of proteins, which share a conserved amino terminal B Cell Translocation Gene (BTG)/Tob homology domain, and have known functions in cell cycle control (Raburn et al. 1995), differentiation (Rodier et al. 1999), and transcriptional regulation (Okochi et al. 2005). Additionally, bioinformatics-based sequence analysis has identified several PAM2 containing proteins, representing putative EDD binding partners, which include ataxin-2, USP10, dNF-x1, TPRD/TTC3 and dMAP205

(Albrecht & Lengauer 2004). Hence EDD/Hyd's PABC domain may be involved in substrate recognition and recruitment prior to EDD/Hyd-mediated substrate ubiquitylation. Taken together with the high conservation of the PABC domain, this makes it an interesting domain to investigate in order to shed light on Hyd/EDD's mechanism of action in the cell.

1.4.1.3 UBR-type Zinc Finger Domain

The UBR box motif is a zinc finger fold that is found in a unique family of E3 ubiquitin ligases that target substrates as part of the N-end rule pathway(Tasaki et al. 2005). It consists of two conserved zinc finger motifs: a Cys2 His2 motif containing a zinc ion, and a Cys6 His1 motif containing two zinc ions. The N-end rule relates the half-life of a cellular protein to the identity of its amino terminal residue (reviewed in (Tasaki et al. 2012). In the N-end rule pathway, a subset of proteins containing degradation signals in the form of destabilizing amino terminal residues, known as N-degrons, are targeted for ubiquitylation and subsequent degradation by a unique class of E3 ubiquitin ligases termed N-recognins, which include Hyd/UBR5/EDD. N-degrons are generated by several mechanisms, including proteolytic cleavage and posttranslational modification of proteins by conjugation (e.g. arginylation, phenylalanylation, etc.), the latter being the major mechanism of generating N-degrons in eukaryotes. Conjugation of destabilizing amino terminal residues is carried out by evolutionary conserved aminoacyl-tRNA transferases.

UBR5/EDD was classed as a member of the UBR box family of N-recognins, along with UBR1, UBR2 and UBR4, in a study that employed an affinity assay for proteins that bind to destabilizing amino terminal residues (Tasaki et al. 2005). Beads conjugated with Type 1 (Arg) or Type 2 (Phe) N-degron-containing peptides were used to pull down endogenous N-recognins from mouse tissue extracts. This revealed that UBR5/EDD, unlike UBR1, UBR2 and UBR4, bound exclusively to Type 1

(Arg) N-degron beads (Tasaki et al. 2005). Interestingly, Hyd's isolated UBR domain also interacts with cleaved, Arg-bearing *Drosophila* Inhibitor of Apoptosis 1 (DIAP1) (Ditzel et al. 2008). This experiment was successfully replicated in the *Drosophila melanogaster* cell line D.Mel-2, suggesting that both UBR5/EDD and Hyd share a conserved N-recognin function and specifically recognize Type 1 (Arg) N-degrons in putative substrate proteins (Tasaki et al. 2005).

1.4.1.4 Regulator of Chromatin Condensation (RCC) Domain

The RCC domain is found in the cell cycle regulator protein RCC1, a guanine nucleotide-exchange factor for the nuclear Ras homologue Ran (Bischoff & Ponstingl 1991). The crystal structure of RCC1 has been solved and reveals a seven-bladed propeller, which may also bind to DNA (Renault et al. 1998). Hyd and EDD both contain an N-terminal RCC1-like domain, two putative nuclear localization signals (Callaghan et al. 1998; Dingwall & Laskey 1991), and both proteins are localized predominately in the nucleus (Mansfield et al. 1994; Hay-Koren et al. 2011), suggesting that they may translocate to the nucleus to bind DNA directly via the RCC-like domain.

1.4.1.5 Ubiquitin-Associated (UBA) Domain

UBA domains are frequently found in proteins that are involved in ubiquitin-mediated degradation and regulatory pathways (Hofmann & Bucher 1996). Although sequence similarity between UBA domains is relatively low, they generally contain structurally conserved surface patches of hydrophobic residues, which form a binding platform for protein-protein interactions. Most UBA domains bind ubiquitin and proteins containing ubiquitin-like (UBL) folds (Mueller & Feigon 2002).

The structure of the EDD UBA domain, which shares 90% sequence identity with the Hyd UBA domain, has been solved in complex with ubiquitin (Kozlov et al. 2007). Several techniques, including isothermal titration calorimetry (ITC), NMR, and pull down assays, were used to assess the binding affinity of the EDD UBA domain for various ubiquitin linkages. This revealed that, although the EDD UBA domain can bind both mono-and poly-ubiquitin molecules, it has a higher binding affinity for monoubiquitin (Kozlov et al. 2007). Interestingly, this is in contrast to other UBA domains, which generally bind polyubiquitin chains with a higher affinity (Raasi et al. 2005; Trempe et al. 2005). While EDD was able to bind both K48- and K63-linked ubiquitin chains, it displayed a relatively higher affinity for K63-linked chains (Kozlov et al. 2007), suggesting that the ubiquitylation of target proteins by EDD may have predominantly nonproteolytic functions (see **Section 1.1.5**). Finally, site-directed mutagenesis was used to assess the functional importance of conserved residues involved in ubiquitin binding. A fully folded double point mutant, in which two conserved hydrophobic EDD UBA domain residues (Val196 and Leu224) were substituted with a hydrophilic residue (Lys), failed to bind both mono- and polyubiquitin (Kozlov et al. 2007), indicating that these residues are also likely to be crucial for ubiquitin binding in the Hyd UBA domain.

1.4.2 Molecular functions of conserved mammalian Hyd orthologues

The Hyd protein is highly conserved in mammalian cells, and shares a large proportion of sequence identity and functional domains with its human and murine counterparts EDD and UBR5, respectively (**Figure 1.14**). Over the last few years elucidation of EDD's molecular mechanism has implicated it in diverse roles in cancer, cell cycle control, DNA damage repair pathways, gene transcription, Wnt signaling, miRNA-mediated gene regulation, mRNA translation, glucose metabolism, and viral infection (discussed below). Importantly, EDD's mode of

action in these diverse processes could provide clues on Hyd and EDD's putative molecular function in Hh signalling.

1.4.2.1 UBR5$^{-/-}$ mice display severe developmental defects

Analogous to the effects of Hyd deficiency in flies, UBR5 deficient (UBR5$^{-/-}$) mice display severe developmental defects and embryonic lethality at mid-gestation (Saunders et al. 2004). Although heterozygous UBR5$^{+/-}$ mice developed normally and were fertile, UBR$^{-/-}$ embryos died at or before E10.5. In addition, UBR$^{-/-}$ embryos between gestational stages E8.5 and E10.5 were developmentally retarded, displaying growth defects and defective yolk sac and allantoic vascular development, resulting in defective chorioallantoic fusion and embryonic death (Saunders et al. 2004). Interestingly, Indian Hedgehog (Ihh) has been reported to play a critical role in yolk sac vasculogenesis (Byrd et al. 2002), which suggests that UBR5 and other mammalian Hyd orthologues like EDD are likely to play a key role in development through regulation of Hh signalling.

1.4.2.2 EDD is frequently over-expressed in human cancers

The human homologue of Hyd, EDD, was first isolated in a screen for progestin-regulated genes in human breast cancer cells (Callaghan et al. 1998). The *EDD* gene is localized to chromosome *8q22*, a locus that is subject to allelic imbalance in several human cancers. The *EDD* locus is most frequently amplified in ovarian cancer (Clancy et al. 2003), which correlates with high EDD expression in tumours and is associated with a two-fold increased risk of cancer relapse and death in ovarian cancer patients who initially responded to chemotherapy (O'Brien et al. 2008). Amplification of the *EDD* gene has also been reported in breast cancer, hepatocellular carcinoma, squamous carcinoma of the tongue, and metastatic

melanoma, and EDD was overexpressed in breast cancer tumours and cell lines (Clancy et al. 2003). Interestingly, these findings support an oncogenic role for EDD in human cancers, as opposed to the tumour suppressor role for Hyd reported in *Drosophila* imaginal discs (J. D. Lee et al. 2002).

1.4.2.3 EDD plays a role in DNA damage signalling pathways

In order to maintain genomic and cellular integrity, the cellular response to DNA damage usually involves the arrest of the cell cycle in G1, S or G2 phases, followed by DNA repair and/or cell death. This mechanism prevents the replication of damaged DNA, and defects in the associated signalling pathways can lead to uncontrolled proliferation and genomic instability, both of which contribute to tumourigenesis. DNA damage events lead to the activation of the ATM-CHK2/ATR-CHK1 kinase signaling networks, which in turn orchestrate cell cycle arrest, DNA repair and/or cell death by phosphorylating a number of target proteins (Munoz et al. 2007).

Several reports implicate EDD in DNA damage signaling. EDD interacts with PMS1 and PMS2 during mismatch repair, binds calcium- and integrin-binding protein (CIB)/DNA-dependent protein kinase-interacting protein, which is potentially involved in the DNA damage response (Henderson et al. 2002), and ubiquitinates topoisomerase II-binding protein (TopBP1) *in vitro* (Honda et al. 2002).

EDD coordinates the action of TopBP1 in the DNA damage response by targeting it for proteasomal degradation (Honda et al. 2002). TopBP1 is usually degraded by the proteasome, but the introduction of DNA damage events by radiation inhibits the ubiquitylation of TopBP1 by EDD and results in TopBP1 activation by phosphorylation, and subsequent colocalisation with Gamma-H2AX nuclear foci at

sites of DNA damage. EDD interacts with the BRCA1 domain containing carboxy terminus of TopBP1, a domain commonly found in DNA damage checkpoint proteins and cell cycle regulators (Honda et al. 2002).

EDD also interacts with and modulates the activity of the DNA damage checkpoint kinase CHK2 (Henderson et al. 2006). EDD acts upstream of CHK2 in the DNA damage signaling pathway by promoting the activating phophorylation of CHK2 in response to DNA damage. The interaction between EDD and CHK2 is itself dependent on EDD phosphorylation, although EDD is not a target of CHK2 phosphorylation(Henderson et al. 2006). The mechanism of EDD mediated CHK2 activation may involve non-proteolytic ubiquitination as a trigger for subsequent CHK2 phosphorylation, however this remains to be investigated.

In accordance with EDD's role in modulating CHK2 activity, EDD is required for G1/S and intra S phase DNA damage checkpoint activation, and for the maintenance of G2/M arrest after DNA damage (Munoz et al. 2007). EDD deficient cells displayed radiation-resistant DNA synthesis, premature entry into mitosis, accumulation of polyploidy cells, and cell death via mitotic catastrophe, as well as altered expression of the cell cycle mediators Cdc25A/C and E2F1 (Munoz et al. 2007). Taken together, these findings suggest that EDD plays a significant role in the DNA damage response and thus the maintenance of genomic stability, which could in part explain the link between dysregulated EDD and cancer.

1.4.2.4 EDD, cell cycle control and proliferation

EDD interacts with Dual specificity tyrosine-phosphorylation-regulated kinase 2 (DYRK2), which results in the formation of an E3 ubiquitin ligase complex that directs the ubiquitylation and degradation of the mitotic regulator katanin p60

(Maddika & J. Chen 2009). DYRK2's name is derived from the unique self-activation mechanism employed by DYRK kinases. DYRK2 autophosphorylates a tyrosine residue within its activation loop during protein sysnthesis, which simultaneously results in a loss of its tyrosinekinase activity and activation of its function as a serine/threonine kinase. A limited number of DYRK2 substrates have been identified, although interestingly these include the Hh pathway transcriptional effector protein GLI2 (Varjosalo et al. 2008), suggesting that, analogous to previous findings in *Drosophila*, EDD may be indirectly involved in GLI and Hh pathway regulation.

Surprisingly, the Dyrk2 kinase acts as an essential scaffold protein for the formation of the E3 ligase complex containing EDD as the catalytic subunit, as well as the DDB1 and VPRBP proteins (EDVP-Dyrk2 complex). DDB1 (DNA-damage binding protein 1) and VPRBP (also known as CAF1) are adaptor and substrate recognition subunits, respectively, of the Cul4-Roc1 E3 ligase complex. However, the EDVP-Dyrk2 complex appears to be unique as it does not contain Cul4 and Roc1.

Although Dyrk2 kinase activity is not required for EDVP-Dyrk2 complex formation, the phosphorylation of katanin by Dyrk2 is a priming event for subsequent polyubiquitination and degradation of katanin by EDD and the proteasomal system. Katanin is a microtubule AAA-ATPase and plays an important role during mitosis, as it severs microtubules at the mitotic spindles, allowing the disassembly of microtubules and the segregation of sister chromatids to proceed during anaphase. This suggests that EDD is an important regulator of mitotic transition through its effects on katanin protein levels (Maddika & J. Chen 2009).

The regulation of katanin levels is dependent on EDD's ubiquitylation activity. However, a recent report proposes an E3 ligase-independent function of EDD during

cell cycle progression (Ling & W.-C. Lin 2011). EDD interacts with the tumour suppressor p53, a critical regulator regulator of cell cycle progression during the G1/S phase transition. Phosphorylation of p53 by ATM stabilizes p53 and leads to cell cycle arrest and apoptosis, however, the interaction with EDD inhibits the phosphorylation of p53 by ATM. Interestingly, it was determined that the catalytic activity of EDD was not required for the suppression of p53 activity (Ling & W.-C. Lin 2011). This suggests that EDD has additional functions in the regulation of cell cycle progression that are not dependent on its ubiquitylation activity.

In addition to its role in mitotic progression, there is evidence that EDD is involved in other pathways controlling cellular proliferation. EDD interacts with the anti-proliferative protein Tob2 via its PABC domain (Lim et al. 2006). Tob2 inhibits cellular proliferation by negatively regulating cyclin D1 expression, whereas Tob2 itself is subject to negative regulation through ERK1- and ERK2-mediated phosphorylation. Interestingly, both EDD (Eblen et al. 2003) and Tob2 (Suzuki et al. 2002) are substrates for the ERK2 kinase. The extracellular signal-regulated kinase (ERK) pathway (also known as the mitogen-activated protein kinase (MAPK)1 pathway) regulates several important cellular processes, including proliferation, differentiation, gene transcription, and cellular migration. Binding of the mitogen epidermal growth factor (EGF) to the membrane epidermal growth factor recetpr (EGFR) results in activation of the oncogenic Ras GTPase, and subsequent activation of the Raf protein kinases. The Raf kinases phosphorylate and activate MAPK kinase or ERK kinases (MEK) 1 and 2, which in turn phosphorylate and activate the ERK1 and ERK2 kinases, prompting these to migrate to various cellular locations to phosphorylate specific effector proteins (Eblen et al. 2003). Interestingly, ERK2 is ubiquitylated by MEK Kinase 1 (MEKK) via its RING finger-like plant homeodomain (PHD), which negatively regulates ERK2 activity (Lu et al. 2002).

ERK2 phosphorylation on EDD is thought to occur mainly on serine residues, although some threonine phosphorylation was also observed (Eblen et al. 2003). Several novel EDD phosphorylation sites on EDD have already been identified by mass spectrometry, including Ser1018, which was also found to be phosphorylated in UBR5, and is predicted to be a putative ERK2 phoshorylation site (Bethard et al. 2011). Phosphorylation of EDD by ERK2 may affect EDD's ubiquitylation activity, which in turn may be involved in positively regulating ERK2 activity, and opposing the negative regulation of ERK2 by MEKK ubiquitylation (Lu et al. 2002).

1.4.2.5 EDD function in the Wnt signaling pathway

Wnt signalling plays a crucial role in cellular proliferation and differentiation, and its de-regulation is linked to a number of human cancers (see **Section 1.3**). EDD interacts with a number of Wnt pathway's components, yet conflicting evidence identifies it as both a positive and negative regulator of the Wnt signaling pathway. EDD directly interacts with GSK3β, which in turn mediates the indirect interaction of EDD with β-catenin (Hay-Koren et al. 2011). Over-expression of EDD promoted β-catenin K29- and K11-linked poly-ubiquitylation by EDD, and subsequent up-regulation of β-catenin stability, its nuclear accumulation and activity. Potentially paralleling GSK3β-directed Ci ubiquitylation, EDD-mediated β-catenin ubiquitylation is GSK3β dependent. Therefore, GSK3β may mediate phosphorylation of β-catenin prior to ubiquitylation by EDD. Interestingly, EDD does not appear to ubiquitylate GSK3β, but EDD itself is a putative substrate for GSK3β phosphorylation on Thr1736 (Bethard et al. 2011). These results suggest that, through its interaction with GSK3β, EDD positively regulates the Wnt signaling pathway and functions as a putative colorectal oncogene. In addition, this implies that GSK3β can act as both a negative and positive regulator of β-catenin, and subsequent Wnt pathway activity.

However, a different study also identified EDD as a negative regulator of Wnt signaling and a potential colorectal tumour suppressor protein (Ohshima et al. 2007). EDD co-localised with and up-regulated APC in the cytoplasm, resulting in down-regulation of β-catenin by the APC/Axin/GSK3β destruction complex(Ohshima et al. 2007). This is in contrast to previous work, which demonstrated nuclear EDD staining, and co-localisation of EDD with β-catenin but not cytoplasmic GSK3β (Hay-Koren et al. 2011). The discrepancy between these conflicting results could be due to the use of different cell lines and experimental conditions, but could also indicate a dual role for EDD in both the positive and negative regulation of the Wnt pathway, which is perhaps dependent on other factors such as cellular localization, cell type or the phosphorylation state of EDD.

1.4.2.6 EDD function in gene expression

In addition to its role in post-translational regulation, EDD also regulates gene expression at the transcriptional, post-transcriptional and translational stages. Hyd and EDD have a putative role in the transcription of Hh/SHH and Wg/WNT pathway target genes, as they interact with the respective transcriptional effector proteins Ci (Wang et al. 2014) and β-catenin (Hay-Koren et al. 2011). EDD also affects transcription of progestin-mediated genes by acting as a transcriptional coactivator for the nuclear steroid progesterone receptor (PR). EDD interacts with PR in response to ligand binding and enhances its transcriptional activity (Henderson et al. 2002). EDD has also been reported to interact with the CDK9 kinase subunit of positive transcripton elongation factor b (P-TEFb). RNA polymerase II (RNAPII) is regulated by several factors, including transcription factor IIS (TFIIS) and P-TEFb during elongation of transcription. EDD positively regulates this process by binding to bothTFIIS and P-TEFb, resulting in the polyubiquitination of the PTEF-b CDK9 subunit, which enhances its activity rather than leading to its degradation (Cojocaru et al. 2011).

These findings indicate that EDD can regulate gene transcription directly at the DNA level. However, the reported interaction between EDD and DYRK2 also suggests that EDD may be involved in epigenetic gene regulation. In *Drosophila*, the DYRK2 homologues dDyrk2 and Minibrain interact with the chromatin remodeling factors SNR1 and TRX (Kinstrie et al. 2006), which function in establishing open and repressive chromatin states to regulate transcription. SNR1 is a major subunit of the Drosophila Brm (Brahma) ATP-dependent chromating remodeling complex, whereas TRX is a highly conserved epigenetic regulator involved in maintaining homeotic gene expression in association with the Polycomb group genes (Kinstrie et al. 2006).

In addition to regulating gene expression at the transcriptional level, EDD is also involved in regulating the translation of transcribed gene products by modulating the levels of the translational regulatory molecule Paip2 (Yoshida et al. 2006). Paip2 inhibits translation by displacing PABP from the mRNA. Both PABP and EDD compete for binding of Paip2 via their PABC domains. Binding of EDD to Paip2 results in Paip2 ubiquitylation and subsequent degradation (Yoshida et al. 2006). This indicates that EDD is a positive regulator of translation.

Finally, EDD appears to regulate gene expression at the mRNA level, as both Hyd (R. Zhou et al. 2008) and EDD (H. Su et al. 2011a) are implicated in the miRNA silencing pathway. A genetic screen in mouse embryonic stem (ES) cells identified EDD as a key component of the miRNA silencing pathway, where EDD deficiency results in impaired miRNA function and growth defects (H. Su et al. 2011a). MicroRNAs (miRNAs) suppress gene expression by destabilising and preventing the translation of their mRNA targets. During miRNA biogenesis, the ribonucleases Drosha and Dicer process long stem-loop primary RNA transcripts to generate miRNA duplexes, which are then loaded onto Argonaute (Ago) proteins to form the miRNA-induced silencing effector complexes (miRISCs). miRNAs are partially

complementary to their mRNA targets and thus recruit the miRISC to initiate silencing of specific mRNAs (H. Su et al. 2011a).

EDD interacts with Ago-miRNA complexes through a PAM2 motif in the GW182 protein TNRC6A. The interaction between EDD and TNRC6A is mediated through both the PABC domain and heterodimersiation of the UBA domains present in both EDD and TNRC6A. Interestingly, the PABC domain of EDD was shown to be essential for its role in miRNA silencing, whereas its E3 ubiquitin ligase activity was not required. Once associated with miRISCs, EDD recruits downstream effectors, such as Paip2, ATXN2, eRF3a, eRF3b and Tob1/2, via its PABC domain. For example, Tob1/2 recruits CCR4-CAF1 complexes which promote the target mRNA deadenylation, destabilization and subsequent decoupling from translation (H. Su et al. 2011a).

1.4.2.7 Other reported functions of EDD

In addition to its diverse functions in DNA damage signalling, cell cycle control, Wnt signaling and gene expression, EDD also regulates cellular metabolism. EDD ubiquitylates the metabolic enzyme phosphoenolpyruvate carboxykinase (PEPCK1), which leads to its subsequent degradation via the proteasome (W. Jiang et al. 2011). PEPCK1 catalyzes the first committing and rate-limiting step of gluconeogenesis, and plays a central role in maintaining glucose homeostasis. It has been linked with type II diabetes as increased levels of PEPCK1 elevate blood glucose levels. Normally, high glucose levels stimulate the acetylation of PEPCK1 by the P300 acetyltransferase, which destabilizes PEPCK1 by promoting the interacton with EDD, resulting in ubiquitylation and degradation of PEPCK1. Interestingly, inhibition of EDD activity results in increased glucose production, suggesting that loss of EDD may also be linked to type II diabetes (W. Jiang et al. 2011).

Finally, a role for EDD in the cellular response to viral infection was proposed as EDD was shown to regulate the Human Papillomavirus Type 18 E6/E6AP Ubiquitin Ligase Complex(Tomaic et al. 2011). Human papillomaviruses (HPVs) are small double-stranded DNA viruses that cause hyperproliferative lesions in epithelial tissues, and infection with high-risk HPV types, such as 16 and 18, has been linked to tumourigenesis, especially in cervical cancer. Viral oncoproteins, such as the E3 ligases E6 and E7, interact with cellular proteins that are involved in the cell cycle and apoptosis, such as p53, and induce their proteasomal degradation, effectively leading to cellular immortalization and transformation. EDD interacts with the viral E3 ligase complex containing E6 and E6AP, and regulates its expression level. Increased EDD expression led to down-regulation of E6/E6AP expression and activity, suggesting that EDD acts as a tumour suppressor in the context of HPV-18-induced cervical cancer(Tomaic et al. 2011).

1.5 Aims

Based on previous findings in *Drosophila*, and its close similarity to EDD, as discussed above, Hyd regulates *hh* gene expression, Hh pathway activity and potentially Wg pathway activity. However, the molecular mechanisms behind Hyd-mediated regulation of these processes, and how they may involve Hyd's ubiquitylation activity, are unknown.

The principal aims of this project were to understand the molecular mechanisms Hyd employs to regulate (i) *hh* gene expression, (ii) Ci levels and/or activity and (iii) Wg pathway activity.

In order to achieve this, the following questions were addressed:

1. What are Hyd's protein binding partners, and are they also ubiquitylated substrates of Hyd?

2. Do these Hyd interactors have a role in the regulation of *hh* expression, Hh pathway activity, or other morphogen pathways, such as the Wg pathway?

3. To what degree are the proteins, complexes and/or molecular pathways that Hyd is associated with conserved across species/phyla (e.g. mammals)?

Experimentally, this involved the mass spectrometric and biochemical identification of novel binding partners and ubiquitylated substrates of Hyd, and their subsequent placement in the context of putative signal transduction pathways regulating morphogen expression, using bioinformatics and *Drosophila* genetics.

The detailed molecular analysis of Hyd's role in morphogen regulatory pathways, and their molecular components, is an important step in the development of more efficacious treatments for Hh ligand dependent cancers. Evolutionary analysis of Hyd, its closely related human orthologue EDD, and newly identified pathway components, would significantly further the development of therapeutic compounds that could target morphogen regulatory pathways and correct morphogen mis-expression in humans. Increased knowledge of morphogen regulatory pathways would also improve screening for associated diagnostic markers, which would allow determination of the appropriate treatment regime in cancer patients.

Chapter 2: Materials and methods

2.1 Bacterial methods

2.1.1 Generation of competent bacteria

DH5alpha cells from a frozen glycerol stock were streaked onto an LB agar plate without antibiotics and grown at 37°C overnight. A single colony was inoculated into 20 mL Super Optimal Broth with Catabolite repression (SOC) medium [2% (w/v) tryptone, 0.5% (w/v) yeast extract, 10 mM NaCl, 2.5 mM KCl, 10 mM $MgCl_2$, 20 mM glucose] in a 250 mL conical flask and grown overnight in a 37°C shaker at 200 rpm. 5 mL of the culture was split and diluted into two 1 L conical flasks, containing 250 mL 2xYT medium (16 g/L tryptone, 10 g/L yeast extract, 5 g/L NaCl) each, and grown in a 37°C shaker until an OD600 of 0.5 was reached. The bacteria were pelleted in a Sorvall centrifuge at 5,000 rpm (4°C) for 10 minutes. All subsequent steps were carried out in a cold room at 4°C. The supernatant was removed and each pellet was resuspended in 83 mL Buffer RF1 [166 mL total; 100 mM RbCl, 50 mM $MnCl_2$, 30 mM CH_3CO_2K, 10 mM $CaCl_2$, 15% (w/v) glycerol, pH 5.8] until no clumps were visible. The cell suspension was incubated on wet ice for 1 hour, before being spun at 5,000 rpm (4°C) for 10 minutes. The supernatant was removed, and each pellet was resuspended in 20 mL Buffer RF2 [40 mL total; 10 mM MOPS, 10 mM RbCl, 75 mM $CaCl_2$, 15% (w/v) glycerol] until no clumps were visible. The cell suspension was incubated on wet ice for 15 minutes, and aliquoted (200 µL) into eppendorff microcentrifuge tubes on dry ice. The aliquots of competent DH5alpha cells were submerged in liquid nitrogen in a Dewar flask, and stored at -80°C.

2.1.2 Bacterial transformation

0.1-1 µg DNA was added to 80 µL competent bacterial cells and incubated on ice for 30 minutes. The bacteria were heat-shocked at 42°C for 1 minute and cooled on ice for 10 minutes. 1 mL of Lysogeny Broth (LB; 10 g/L tryptone, 5 g/L yeast extract, 10 g/L NaCl) without antibiotics was added, and the bacteria were incubated at 37°C

with shaking for 1 hour. The cells were then pelleted at 3,000 rpm for 2 minutes in a microcentrifuge. Most of the supernatant (~1 mL) was removed, and the remaining mixture was resuspended and spread onto an LB agar plate containing the appropriate antibiotic (ampicillin or kanamycin at a final concentration of 50 μg/mL). The plate was incubated overnight at 37°C or 32°C (for large plasmids and/or plasmids prone to recombination).

2.1.3 Bacterial culture conditions

Bacteria were generally grown in LB or 2xYT medium containing the appropriate antibiotic (ampicillin or kanamycin at a final concentration of 50μg/ml) in a shaking incubator at 37°C and 200 rpm.

2.1.3.1 Isolation of plasmid DNA

For small-scale DNA preparations, a single colony was inoculated into 6 mL LB containing the appropriate antibiotic and grown in a shaker at 37°C or 32°C overnight. The cells were pelleted in a large tabletop centrifuge at 4,000 rpm for 10 minutes, and the DNA was isolated using the QIAprep Spin Miniprep Kit (QIAGEN, Cat. No. 27104) and resuspended in 30-40 μL dH_2O.

For large-scale, transfection quality DNA preparations, a single colony was inoculated into 200-500 mL LB containing the appropriate antibiotics and grown in a shaker at 37°C or 32°C overnight. The cells were pelleted in a Sorvall centrifuge at 4,500 rpm for 15 minutes. The DNA was isolated using the QIAGEN Plasmid Midi or Maxi Kit (QIAGEN Cat. No. 12143, 12162), and resuspended in 0.1-1 mL dH_2O, depending on the amount of DNA.

2.1.3.2 Production of recombinant protein

BL21(DE3) competent cells (Novagen/Merck Millipore, Cat. No. 69450) were transformed with pGEX vector expression constructs (**Table 2.1**) and grown

overnight at 37°C on an LB/Ampicillin agar plate. A single colony was inoculated into 50 mL LB containing ampicillin, and grown in a shaker at 37°C overnight. The culture was diluted 10-fold and incubated at 37°C with shaking until an OD_{600} of 0.6 was reached. The culture was then moved to an 18°C shaking incubator and protein expression was induced with 1 mM Isopropyl β-D-1-thiogalactopyranoside (IPTG) overnight. The cells were pelleted in a Sorvall centrifuge at 4,500 rpm (4°C) for 10 minutes prior to lysis and isolation of the recombinant protein (see 2.4.4).

Table 2.1: pGEX vector expression constructs allow expression of Glutathione S-transferase (GST) tagged recombinant proteins in bacterial cells.

Name of construct	Description	Antibiotic resistance
Dm FL Hyd pGEX 6P-1	Bacterial expression of recombinant full-length *Drosophila* Hyd protein containing an amino terminal GST tag (expected MW ~347 kDa)	Ampicillin
Dm Hyd large HECT pGEX 6P-1	Bacterial expression of recombinant partial carboxy-terminal region of the *Drosophila* Hyd protein, consisting of the PABC and HECT domains, and containing an amino terminal GST tag (expected MW ~92 kDa)	Ampicillin

2.2 Molecular biology

2.2.1 General cloning procedure

2.2.1.1 Cloning Strategy

An amino terminally (NT) HA-Strep (HSP)-tagged Hyd pMT expression construct had previously been cloned in the lab. In order to facilitate the generation of S2 cells stably expressing HSP-Hyd and HSP-Hyd C>A, the inserts were sub-cloned into the pMT-PURO vector, which contains an integrated puromycin resistance gene (Iwaki & Castellino 2008), in a two-step process. First, the HSP fragment was lifted out of

the original vector and ligated into pMT-PURO using the KpnI-EcoRV sites flanking the tag. Following the successful generation of an NT HSP pMT-PURO vector, the Hyd inserts were sub-cloned using the NotI sites flanking the inserts, generating the following constructs: *Dm* NT HSP-Hyd pMT-PURO and *Dm* NT HSP Hyd C>A pMT-PURO.

Potential Hyd binding partners were cloned into a pMT vector containing a carboxy terminal (CT) FLAG-V5 (F/V) tag. Cloning primers were generally designed to include at least one pair of restriction sites that cut only once within the multiple cloning site of the destination vector, as well as being absent from the open reading frame (ORF) sequence of the gene in question. In addition, a Kozak consensus sequence (AAA CAC ACA), which plays an important role in the process of translation initiation (De Angioletti et al. 2004), prior to the ATG start codon was included, whereas the stop codon at the end of the ORF was omitted to allow expression of the CT F/V tag.

2.2.1.2 Polymerase Chain reaction

DNA containing the coding sequence of the gene of interest was amplified by polymerase chain reaction (PCR) from cDNA clones or expressed sequence tags (ESTs), purchased from the Drosophila Genomics Resource Centre (DGRC), and using the relevant primers (**Table 2.2**).

Table 2.2: Cloning of potential Hyd binding partners from DGRC consructs.

Protein Name	PCR template construct (DGRC)	Forward (F) and reverse (R) primers used	Final destination vector	Restriction sites used for sub-cloning
APP-BP1	AT09990 in pOTB7	F: GAATTCAAACACACAA TGTCCTCGCCAGCCCCCAAATC G R: GCGGCCGCGCTAGCTT CAATGTGACACTTTCTGTGG	pMT CT V/F	EcoRI-NotI
Real-time	GH05975	F: GGTACCAAACACACAA TGGTGCAAAAATTCCAGTCACC	pMT CT	KpnI-NotI

Protein Name	PCR template construct (DGRC)	Forward (F) and reverse (R) primers used	Final destination vector	Restriction sites used for sub-cloning
		CGTTCG R: GCGGCCGCGCTCGACT CTGCACCGAGCTGGCCGCCGAC GAGTTCGATGAGAATG	V/F	
PERQ	RH02748	F: GAATTCAAACACACAA TGACAGATTCAATGAAATTTGG CCCGG R: GCGGCCGCGCTCTTATT CTTTTTAATCTTTTTTTTTTGTTC TTGCTGTCGGC	pMT CT V/F	EcoRI-NotI
Akirin	LD26817 in pOT2	F: GAATTCAAACACACAA TGGCCTGTGCAACCCTGAAACG R: GCGGCCGCGCCGACAG GTAGCTAGGCGCTGCCTCGTAG	pMT CT V/F	EcoRI-NotI
Tcp-1	RE70560	F: GGTACCAAACACACA ATGTCGACCCTGGCCTCTCCTC TGTC R: GCGGCCGCGCACCGTC CAGCTCGCCGGCAGCGCATGCA TCGGCGTAACTCTG	pMT CT V/F	KpnI-NotI
Sgg	FMO02659 in pDNR-Dual	F: GGTACCAAACACACAA TGAGCGGTCGTCCAAGAACTTC CTCCTTCG R: GCGGCCGCGCTGAATC TGTTACATTGGCGCCGCCGGCA TTAGTCG	pMT CT V/F	KpnI-NotI
Tob	LD04013 in pBS SK(-)	F: GAATTCAAACACACAA TGCATATTGAAATCCAGGTCGC R: GCGGCCGCGCGTTGGC AACCAATAGTTGCTGATACG	pMT CT V/F	EcoRI-NotI
Dyrk3	RE60792 in pFlc-1	F: GGTACCAAACACACAA TGGTCGGTTCTCAAGAAAAAAA AAACAATCATATCG R: GCGGCCGCGCCATATC CTTCGATTGTACTTTTAATTTAT TCGTATGAAGAGAC	pMT CT V/F	KpnI-NotI

PCR reactions were carried out using the KOD Hot Start DNA Polymerase kit (Novagen/Merck Millipore, Cat. No. 71086), and reaction components and cycling conditions are summarized in **Table 2.3**. Following PCR amplification using the KOD polymerase, 1 µL Taq DNA Polymerase (Sigma, Cat. No. D1806) and 1 µL dNTPs (2mM each, from KOD kit) were added directly to the PCR reaction, and an additional extension step (93°C for 2 minutes, 72°C for 10 minutes) was carried out. Since the KOD DNA polymerase produces blunt-ended DNA products, this additional extension step, which adds T or A overhangs to the DNA ends, is necessary to allow subsequent cloning into the pGEM® T-Easy Vector (Promega, Cat. No. A1360).

Table 2.3: KOD Hot Start Polymerase PCR reaction set-up and cycling conditions.

PCR Reaction Setup		**Cycling Conditions**		
Reaction Component	**Amount**	**Step**	**Temperature (°C)**	**Time**
10X Reaction Buffer	5µl	1	95	2 min
25mM $MgSO_4$	3µl	2	95	20 sec
dNTPs (2mM each)	5µl	3	Tm-5°C (Tm based on primer sequence identical to target sequence only)	10 sec
DNA template	10ng	4	70	Variable*
Forward primer (10µM)	1.5µl	5	Go to step (2) for 6 cycles	
Reverse primer (10µM)	1.5µl	6	95	20 sec
KOD polymerase	1µl	7	Tm-5°C (Tm based on entire primer sequence)	10 sec
dH_2O	Xµl	8	70	Variable*
TOTAL	50µl	9	Go to step (6) for 30 cycles	

*Depends on size of amplified fragment - see manufacturer's protocol.

2.2.1.3 Agarose gel electrophoresis and gel extraction

DNA was separated on a 0.8% or 1% (w/v) agarose gel, prepared in Tris/Borate/EDTA (TBE) buffer (89 mM Tris, 89 mM boric acid, 2 mM EDTA) and containing 0.5 μg/mL Ethidium bromide, alongside a 1 kb DNA ladder (Hyperladder I, Biogene, Cat. No. BIO-33053). Bands were visualized by ultraviolet (UV) radiation and excised using a scalpel. DNA was extracted from the agarose chunks using the QIAquick Gel Extraction Kit (QIAGEN. Cat. No. 28704), and purified DNA was eluted in 30 μL dH_2O.

2.2.1.4 pGEM T-Easy cloning

Purified DNA fragments were ligated into the pGEM® T-Easy Vector using the pGEM® T-Easy Vector System I kit (Promega, Cat. No. A1360). A molar ratio of 3 parts of insert DNA to 1 part of vector DNA was maintained, according to the formula: [(Amount vector DNA (ng) x size of insert (kb)) / size of vector (kb)] x 3 = Amount of insert DNA. The reactions were set up according to the manufacturer's protocol and incubated at 18°C overnight. The ligation reaction was then transformed in competent DH5alpha cells, and DNA from at least 4 independent colonies was prepared (miniprep) for restriction digest and sequencing, confirming the integrity of the construct prior to sub-cloning into an expression vector.

2.2.1.5 Sequencing

Sequencing of miniprep DNA was carried out by the MRC HGU Human Genetics Unit sequencing service (Edinburgh) using the standard T7 and Sp6 primers for the pGEM® T-Easy Vector, as well as a number of custom gene specific sequencing primers that were designed to cover the entire region of the inserted sequence in 500 bp increments.

2.2.1.6 Restriction digest and alkaline phosphatase treatment

Once the sequence integrity of a particular construct and miniprep was confirmed, the insert was lifted out of pGEM® T-Easy by restriction digest, using the restriction sites flanking the insert as designed in the original cloning primers (see **Table 2.2**). The destination vector (e.g. CT F/V pMT) was also digested with the same enzymes, ready to receive the insert. Briefly, 0.5 µL of each enzyme (various from New England BioLabs and Roche), 0.5 µL BSA (New England BioLabs), and 2 µL of the appropriate 10X reaction buffer (New England BioLabs 10X reaction buffers 1-4; refer to New England BioLabs website for enzyme compatibility) were combined with 1 µg DNA and dH_2O to a final volume of 20 µL. The reaction was incubated at 37°C for 1 hour. To minimize re-ligation of the destination vector, 1 µL Alkaline Phosphatase (AP) and 2 µL 10X AP reaction buffer (New England BioLabs, Cat. No. M0371S) were added directly to the restriction digest mix and incubated for a further 20 minutes at 37°C. The restriction digests for both insert and vector were then separated on an agarose gel, and the relevant DNA fragments were excised and purified using the QIAquick Gel Extraction Kit (QIAGEN. Cat. No. 28704).

2.2.1.7 Ligation

The insert DNA was ligated into the destination vector using the T4 DNA Ligase enzyme. 1 µL of 10X T4 Ligation Buffer and 1 µL T4 DNA Ligase (both New England BioLabs, Cat. No. M0202S) were combined with the purified insert and vector DNA, and dH_2O to a total volume of 10 µL. A molar ratio of 3 parts of insert DNA to 1 part of vector DNA was maintained (see 2.2.1.4). The reaction was incubated at 18°C overnight, transformed, and DNA from at least 4 independent colonies was prepared (miniprep) for restriction digest, confirming the integrity of the construct prior to preparation of a transfection quality DNA master stock (maxiprep).

2.2.2 Site-directed mutagenesis

Site-directed mutagenesis (SDM) was used to introduce up to two missense amino acid mutations into a given construct. SDM was carried out using custom designed primers, containing the desired coding sequence base pair mutation flanked by regions complementary to the template DNA, to amplify the mutagenised plasmid by PCR. The non-mutagenised template plasmid is removed via DpnI restriction enzyme treatment prior to purification of the mutagenised plasmid DNA. The DpnI restriction enzyme recognizes methylated adenine in plasmids purified from bacteria expressing the Deoxyadenosine (Dam) methyltransferase (J. Tian et al. 2010). Briefly, the PCR reaction mix was set up as detailed in **Table 2.3**, and cycling conditions were identical to steps 1 to 4 as outlined in (New England BioLabs, Cat. No.) , which were repeated for 16 cycles. 2 µL of DpnI enzyme (New England BioLabs, Cat. No.) was then added directly to the PCR reaction mix, and incubated for 2 hours at 37°C. The mutagenised plasmid DNA was purified using the QIAquick PCR Purification Kit (QIAGEN, Cat. No. 28104), and eluted in 30 µL dH_2O. 10 µL of the purified plasmid DNA was used to transform competent DH5aplha cells for the preparation of miniprep DNA and sequencing. Once satisfactory incorporation of the desired mutation was confirmed by sequencing, a large-scale, transfection quality master stock of the plasmid DNA was prepared (maxiprep). All mutagenised constructs and the relevant SDM primers used are summarized in **Table 2.4**.

Table 2.4: Use of site-directed mutagenesis to generate plasmids expressing mutagenised proteins.

Construct name	Amino acid mutation (s)	Coding sequence (CDS) nucleotide mutation(s)	Parent template	SDM forward (F) and reverse (R) primers
HSP Hyd HECT point mutant (PM)	C2854>A	Had already been generated in the lab (Mark Ditzel).		
HSP Hyd PABC double	Y2509>A	tac>gcc	NT HSP	F1: CAAATTGGGGAACGTCTT

Construct name	Amino acid mutation (s)	Coding sequence (CDS) nucleotide mutation(s)	Parent template	SDM forward (F) and reverse (R) primers
PM	L2527>A	@7525 ctg>gcg @7579	Hyd pMT	[GC]CCCGAAGATCCATTCG R1: CGAATGGATCTTCGGG[GC]AAGACGTTCCCCAATTTG F2: CGAAGATAACAGGAATG[GC]GCTGGAGATACCCACTCCGC R2: GCGGAGTGGGTATCTCCAGC[GC]CATTCCTGTTATCTTCG
HSP Hyd UBA PM	V166>K	gtt>aag @496	NT HSP Hyd pMT	F: GCTCATATCCCAAGCAGAGGTG[AAG]CTACAGGGCAAGAGC R: GCTCTTGCCCTGTAG[CTT]CACCTCTGCTTGGGATATGAGC

2.2.3 dsRNA production

dsRNA was produced for RNAi treatment of endogenous mRNAs, resulting in knock down of target gene expression, in *Drosophila* Schneider (S2) cells and/or transfection of other *Drosophila* cultured cells. dsRNAs were synthesized by amplifying a DNA template encoding a T7 RNA polymerase consensus site from cDNA using primers specific for EGFP (RNAi control), Hyd, and the 3'UTR region of the *hyd* gene. The MEGAscript® T7 Transciption Kit (Life Technologies, Cat. No. AM1333) was then used to synthesize ssRNA from the DNA templates for 6 hours at 37°C, following to the manufacturer's protocol. RNA was precipitated by adding 2 µL 3M sodium acetate ($C_2H_3NaO_2$) and 40 µL ethanol pre-cooled to -20°C to the reaction mix. The tubes were then spun at 13,000 rpm for 5 minutes, and the RNA pellets were air dried for 5 minutes before being resuspended in 40 µL RNAse

free dH_2O. ssRNA was annealed by heating at 65°C for 5 minutes, and left to cool slowly overnight. dsRNA was stored at -20°C .

Table 2.5: Primers used to generate dsRNA DNA templates by PCR.

dsRNA DNA template	Parent DNA template (plasmid)	Forward (F) and reverse (R) primers
T7 EGFP DNA	pEGFP (Clontech)	F: GAATTAATACGACTCACTATAGGGAGA acgtaaacggccacaagttc R: GAATTAATACGACTCACTATAGGGAGA tgctcaggtagtggttgtcg
T7 Hyd @7950 DNA	NT HSP Hyd pMT	F: GAATTAATACGACTCACTATAGGGAGA gttccacgacttggcatttttcg R: GAATTAATACGACTCACTATAGGGAGA ccggtccagaagtaaaccaaatcc
T7 Hyd 3'UTR DNA	Hyd 3'UTR pMT	F: GAATTAATACGACTCACTATAGGGAGA gcgattggaagtctttcccatc R: GAATTAATACGACTCACTATAGGGAGA tggccgttttattggttacaatgg
T7 Sgg DNA	Sgg CT F/V pMT	F: GAATTAATACGACTCACTATAGGG AGAGTTTGGCCTACATCCACTCG R: GAATTAATACGACTCACTATAGGG AGAATACGATACATTCGGCTCGC

2.2.4 Isolation of genomic DNA from *Drosophila*

Single flies were frozen individually in eppendorff tubes at -20°C. Flies were mashed in 50 µL "Squishing Buffer" (10 mM Tris HCl pH 8.2, 1 mM EDTA, 25 mM NaCl, 200 µg/mL Proteinase K) and incubated at 37°C for 30 minutes, before Proteinase K activity was inactivated by heating to 95°C for 2 minutes. The crude genomic DNA was stored at 4°C and was used at a 1 in 10 dilution in PCR reactions.

2.2.4.1 Sequencing of mutant *hyd* strains

The following fly tocks were used for sequencing *hyd* mutant alleles:

FRT^{82B}, $hyd^{K7.19}$/TM6B

FRT^{82B}, $hyd^{K3.5}$/TM6B

hyd^{15}/TM6B GFP

FRT^{82B}, hyd^{WC461}/TM6B

Sb/TM3 GFP (*hyd^{WT}* control)

Heterozygous adult flies were collected and genomic DNA was extracted as described in Section 2.2.4. 1 µL of the crude genomic DNA extract, diluted 1 in 10, was used in PCR reactions (see section 2.2.1.2 for general PCR reaction set up) to amplify the *hyd* gene region prior to sequencing. Due to the size of the *hyd* extended gene region, the *hyd* gene region was amplified in two parts, designated "*hyd* front end" and "*hyd* back end", using specifically designed primers (see **Table 2.6**). PCR reactions were separated on a 0.8% agarose gel, and the generated fragments were excised and purified using the QIAquick Gel Extraction Kit (QIAGEN. Cat. No. 28704). Purified DNA was eluted in 30 µL dH_2O and pooled for each *hyd* allele, before being sent to The GenePool Sequencing facility (University of Edinburgh, Edinburgh), along with a set of custom *hyd* sequencing primers designed to cover the *hyd* front and back ends in 500-800 bp overlapping increments (see **Table 2.6**). Mutations were identified by scanning for the presence of a double trace in the chromatogram (i.e. DNA extracted from heterozygote animals).

Table 2.6: Primers used for amplification and sequencing of *hyd* alleles.

Primer Name	Sequence	Target	Intended use
5' NotI/SmaI FL Hyd (+ATG)	GCGGCCGCCCCGGGAGATGgtttccatgcaatttgttttgcaacc	*hyd* front end	PCR and sequencing

Primer Name	Sequence	Target	Intended use
5' *hyd* genomic @2580	CGAAAGAAGCTTGCAGAAGTCCATGC	*hyd* front end	Sequencing
5' *hyd* genomic @3104	CTTGACTTGACCAAATCAGACGC	*hyd* front end	Sequencing
5' *hyd* genomic @3627	CGTGCCCGAAGACCTTATCTCCCTGCTGG	*hyd* front end	Sequencing
5' *hyd* genomic @4156	GGATATCTGAAGAATTGCAGC	*hyd* front end	Sequencing
5' *hyd* genomic @4680	CGCCGCTTCTTGTGGGACAAATTCCGG	*hyd* front end	Sequencing
5' *hyd* genomic @5211	GTGAAGGACGTGGTGTTTGTCG	*hyd* front end	Sequencing
5' *hyd* genomic @5736	GTGCTTCGTGATGGCAATGGAGC	*hyd* front end	Sequencing
5' *hyd* genomic @6255	GCAACTATGAGTTCATCCGCTGCCGG	*hyd* front end	Sequencing
5' *hyd* genomic @6779	GCTAAAGGAGGCCATGATTTTCCCG	*hyd* front end	Sequencing
5' *hyd* genomic @7302	GATAATGATATGCCGGACCATGATCTGGAGC	*hyd* front end	Sequencing
3'seq *hyd*@4536	aacacagctctgcacgtatttgttgc	*hyd* front end	PCR and sequencing
5'*hyd* @3000	CTCGACAAGCGCTTACGTTAG	*hyd* back end	PCR and sequencing
5' *hyd* genomic @6779	GCTAAAGGAGGCCATGATTTTCCCG	*hyd* back end	Sequencing
5' *hyd* genomic	GATAATGATATGCCGGACCATGATCTGGAGC	*hyd* back end	Sequencing

Primer Name	Sequence	Target	Intended use
@7302			
5' *hyd* genomic @7775	GCTGCACAAGATATCCATCGAGG	*hyd* back end	Sequencing
5' *hyd* genomic @8309	GGACGGCATGCAAGATGACGAGAGC	*hyd* back end	Sequencing
5' *hyd* genomic @8839	CGACAACGGCCAGCAACTTGGC	*hyd* back end	Sequencing
5' *hyd* genomic @9384	GCTCACACACCTCTGAGCACCGAGACG	*hyd* back end	Sequencing
5' *hyd* genomic @9955	CGATTCTAGTAAGACGGGTGATGG	*hyd* back end	Sequencing
5' *hyd* genomic @10505	GCCGCTGGAAGCTAACTCTGG	*hyd* back end	Sequencing
5' *hyd* genomic @11029	CGTTCGGCCCGTGAGAGGAAGG	*hyd* back end	Sequencing
5' *hyd* genomic @11570	GCCAAGGCTTTGCATCATTCGAGCG	*hyd* back end	Sequencing
5' *hyd* genomic @12088	GGAGGTATGGGCAAATATTGCG	*hyd* back end	Sequencing
5' *hyd* genomic @12548	CGACTGCGAATACTTGTATCTCTCGG	*hyd* back end	Sequencing
Rev T7 Hyd 3'UTR	gaattaatacgactcactatagggagaTGGCCGTTTTATTGGTTACAATGG	*hyd* back end	PCR and sequencing

2.3 Cell culture and cell biology methods

2.3.1 Mammalian tissue culture conditions

HEK293 cells were maintained at 37°C with 5% CO_2 in Dulbecco's Modified Eagle's Medium (DMEM; Life Technologies) containing 10% heat inactivated fetal bovine serum (FBS; Life Technologies).

2.3.2 *Drosophila* tissue culture conditions

S2 cells were grown at room temperature in Schneider's Drosophila Medium (Lonza) containing 10% heat inactivated fetal bovine serum (FBS; Life Technologies). Clone 8 (Cl8+) cells were grown at room temperature in M3 medium (Sigma) supplemented with 0.05% $KHCO_3$ (Sigma), 2.5% fly extract (see 2.3.2.1 below), 5 μg/ml insulin (Sigma), and 2% fetal bovine serum (FBS; Life Technologies).

2.3.2.1 Generation of fly extract

Adult flies of any genotype were collected in 50 mL tubes and frozen at -20°C for 45 minutes. Frozen flies were weighed and transferred to a glass homogeniser on ice. 6.8 mL M3 medium supplemented with 0.05% $KHCO_3$ was added per 1 g of flies. Flies were homogenised thoroughly on ice until completely mashed. The mixture was then transferred to a centrifuge tube and spun at 1,500 x g at 4°C for 15 minutes. The resulting supernatant was transferred to a fresh tube and incubated at 60°C in a waterbath for 5 minutes. Finally, the extract was spun at 1,500 x g at 4°C for 90 minutes. The resulting supernatant is the fly extract, which was filter sterilized through a 0.2 μM filter, aliquoted, and stored at -20°C.

2.3.3 Transfection of tissue culture cells

Cells were seeded the day before transfection. Transfections were performed using Effectene Transfection reagent (QIAGEN, Cat. No. 301425) according to the manufacturer's protocol. Optimised transfection conditions are summarised in **Table 2.7**. Briefly, the required amount of DNA was diluted in Buffer EC. Enhancer was added and the transfection mix was incubated for 5 minutes at room temperature, before Effectene was added and the mix was incubated for a further 10 minutes at room temperature. The transfection mix was then added directly to cultured cells in a drop-wise manner, and the plates were gently rocked to mix. If necessary, protein expression was induced in *Drosophila* cells by adding 5 µL 140 mM $CuSO_4$ to the cell culture medium 12 hours post-transfection. Cells were incubated for 48 hours prior to lysis and/or analyis.

Table 2.7: Optimised Transfection Conditions for HEK293, S2 and Cl8+ cells.

Cell type	HEK293	S2/Cl8+	S2/Cl8+ (Luciferase assays)
Plate format	10 cm (10 mL)	6-well plate (6 x 2 mL)	96 well plate (100 µL per well)
Seeding density (1 day before transfection)	3 x 10^6	~50-60% confluency	~50-60% confluency
Total amount of DNA per well/plate	2 µg	0.4 µg	0.1 µg (+ 200 ng dsRNA – optional)
Total volume of EC buffer used to dilute DNA	300 µL per plate	100 µL per well	50 µL per well
Volume of Enhancer to add per well/plate	16 µL per plate	3.2 µL per well	0.8 µL per well
Volume of Effectene to add per well/plate	60 µL per plate	10 µL per well	2.5 µL per well

2.3.3.1 dsRNA treatment of S2 cells

S2 cells were seeded into 6-well plates at ~50-60% confluency the day before dsRNA treatment in complete growth medium. On the day of dsRNA treatment, the complete medium was removed and cells were washed gently in serum-free medium (no FBS). dsRNA was added to the cells suspended in serum-free medium at 15 µg per well. The cells were incubated for 1 hour with the dsRNA in serum-free medium, before an additional 2 mL of complete growth medium was added. Cells were incubated for 24 to 48 hours prior to lysis and/or analysis.

2.3.3.2 Generation of stably transfected S2 cells

S2 cells were transfected with NT HSP pMT-PURO expression constructs. Alternatively, S2 cells were transfected with the expression construct of choice and a separate puromycin resistance plasmid at a 7 to 1 molar ratio. 48 hours post-transfection, cells were harvested carefully and spun down at 1,200 rpm for 3 minutes. The cells were then resuspended in 5 mL of complete medium containing 6 µg/mL puromycin, and transferred to a T25 tissue culture flask. Cells were observed regularly to monitor cell death. Stably transfected cells were maintained in complete growth medium containing 6 µg/mL puromycin.

2.3.4 Luciferase assays with S2 and Cl8+ cells

S2 or Cl8+ cells were seeded into 96-well plates at ~50 to 60% confluency and transfected in triplicate with 200 ng dsRNA against EGFP or Hyd,10 ng Renilla Luciferase, 50 ng ptcΔ136-luciferase or ptcΔ136-mutant, and 40 ng Hh-N DNA per well (see **Table 2.7**). Cells were harvested after 5 days, and luciferase activity was measured using the Dual-Luciferase® Reporter Assay System (Promega, Cat. No. E1910) following the manufacturer's protocol.

2.3.5 Immunofluorescence with cultured cells

Cells were seeded and transfected in plates containing sterile, round glass cover slips. Transfected cells were washed gently in Phosphate Buffered Saline (PBS) and fixed with 4% paraformaldehyde (PFA) in PBS for 15 minutes at room temperature. The cells were washed again in PBS before being permeabilised with 0.1% Triton X-100 in PBS for 5 minutes at room temperature. The cells were then washed in PBS and the slides blocked in blocking solution [1% (w/v) BSA, 1% (v/v) FBS, PBS] for 30 minutes at room temperature. The primary antibody was diluted in blocking solution and was generally used at a dilution 10-fold more concentrated than if used for Western blotting. 50 µL of the primary antibody solution per cover slip was dispensed onto a sheet of parafilm, and cover slips were carefully placed face down onto the solution using tweezers. The cover slips were incubated with the primary antibody for 1 hour at room temperature in a damp incubation chamber. Following the primary antibody incubation period, the cover slips were washed twice briefly in PBS pre-dispensed onto parafilm sheets, before being incubated with 50 µL (per cover slip) of the secondary antibody diluted in blocking buffer on a fresh parafilm sheet for 1 hour at room temperature in a dark incubation chamber. The cover slips were then washed briefly twice, and again for 10 minutes in PBS, before being mounted cell-side down onto glass microscope slides using 5-10 µL mounting medium (Vectashield Mounting Medium with DAPI, Vector Laboratories, Cat. No. H-1200). Images were captured on a Nikon A1R confocal microscope at 100X magnification.

2.4 Protein methods

2.4.1 Cell lysis

Cells were harvested 48 hours post-transfection, washed once in ice-cold PBS, and lysed with approximately 10 pellet volumes of Triton lysis buffer (50 mM Tris pH

7.5, 100 mM NaCl, 2 mM EDTA, 1% Triton X-100, 1X Roche protease inhibitor mix, 1X Roche phosphatase inhibitor mix). The lysates were clarified by centrifugation at 13,000 rpm for 15 minutes at 4°C.

2.4.2 Co-immunoprecipitation and pulldown assays

HA-Strep (HSP)-tagged Hyd/EDD was pulled down using StrepTactin sepharose (GE Healthcare) for 1 hour at 4°C with rotation. Samples were washed three times with Triton lysis buffer, and protein complexes were eluted with one bead volume of 1X NuPAGE LDS Sample Buffer (Life Technologies, Cat. No. NP0008) containing 100 mM dithiothreitol (DTT). To immunoprecipitate endogenous Hyd protein, 5 µL anti-M19 antibody (200 µg/mL; Santa Cruz) was added to the lysate and incubated at 4°C with rotation for 2 hours, followed by Protein A-Agarose (Sigma, Cat. No. P2545) for 30 minutes with rotation at 4°C. Samples were washed and eluted as described.

2.4.3 Tandem affinity purification (TAP) for mass spectrometry analysis

Stable S2 cells expressing HSP-Hyd, HSP-Hyd C>A or HSP only were lysed as described in Section 2.4.1. HA-Strep (HSP)-tagged Hyd was pulled down using StrepTactin sepharose (GE Healthcare) for 1 hour at 4°C with rotation. Samples were washed four times with Triton lysis buffer, and protein complexes were eluted with five bead volumes of Desthiobiotin Elution Buffer (50 mM Tris pH 7.5, 100 mM NaCl, 2 mM EDTA, 1% Triton X-100, 2.5 M *d*-Desthiobiotin) for 30 minutes at 4°C with rotation. The eluted HSP-Hyd complexes were then immunoprecipitated using anti-HA antibody conjugated agarose for 1 hour at 4°C with rotation. Samples were washed four times with Triton lysis buffer, and a further two times with lysis buffer lacking Triton X-100 detergent. The protein complexes were then eluted with two bead volumes of 8 M Urea. Samples were run on pre-cast 4-12% Bis-Tris gels (Life

Technologies) until the samples had completely entered the gel (i.e. advanced 1-2 cm from the well). Gels were fixed and stained with Coomassie, and gel sections containing the eluted proteins were excised. The following procedure was performed by Flavia Alves at the Rappsilber Lab, University of Edinburgh: Coomassie stained gel sections containing the eluted proteins were reduced in 10 mM DTT for 30 minutes at 37°C, alkylated in 55 mM iodoacetamide for 20 minutes at room temperature in the dark, and digested overnight at 37°C with 12.5 ng/µL trypsin (Proteomics Grade, Sigma T6567). The solution was then acidified to 0.1% Trifluoroacetic acid (TFA) and spun onto StageTips, before peptides were eluted in 20 µL of 80% acetonitrile in 0.1% TFA and concentrated to 4 µL using Eppendorf concentrators. The eluted peptide sample was then diluted to 5 µL using 0.1% TFA for LC-MS/MS analysis in a Velos LTQ-Orbitrap mass spectrometer (Thermo Fisher Scientific) coupled to a Waters Nano AQUITY UPLC (Waters). Mascot searches were conducted against a database containing *Drosophila melanogaster* sequences, and the search parameters were as follows: MS accuracy, 6 ppm; MS/MS accuracy, 0.6 Da; enzyme, trypsin; allowed number of missed cleavages, 2; fixed modification, carbamidomethylation on cysteine; variable modifications, oxidation on methionine and double glycine (GlyGly) fragment on lysine.

2.4.4 Purification of recombinant proteins from bacterial cells

Bacterial cells expressing the protein of interest were grown and harvested as described in Section 2.1.3.2. Harvested cells were resuspended in 10 mL ice cold Bacterial Lysis Buffer (1X PBS, 300 mM NaCl, 1 mM DTT, 1X Roche protease inhibitor mix) and sonicated five times for 10 seconds. Lysates were cleared by spinning at 4,500 – 10,000 rpm at 4°C for 30 minutes. Lysates were then incubated with Glutathione Sepharose (GE Healthcare) for 1 hour at 4°C with rotation. Samples were washed three times with 10 mL cold Tris-buffered saline (TBS; 50 mM Tris, 150 mM NaCl, pH 7.6), and recombinant GST-tagged proteins were eluted with two bead volumes of Glutathione (GSH) Elution Buffer (50 mM Tris-HCl pH 8, 12.5 mM GSH) for 30 minutes at room temperature with occasional agitation. Eluted

proteins were dialysed overnight at 4°C against Dialysis Exchange Buffer (50 mM Tris pH 8, 100 mM NaCl, 1 mM EDTA, 0.02% Triton X-100, 5% glycerol), and stored in 50% glycerol at -80°C.

2.4.4.1 Peptide ELISA

Peptide array slides were blocked in 3 mL of 5% BSA/TBS-T [5% BSA (w/v), 50 mM Tris pH 7.5, 150 mM NaCl, 0.05% Tween 20] for 1 hour at room temperature. Slides were rinsed twice in TBS-T (50mM Tris pH 7.5, 150mM NaCl, 0.05% Tween 20), and incubated with the recombinant protein (1-2 μM per slide), diluted in 0.5% BSA/TBS-T [0.5% BSA (w/v), 50 mM Tris pH 7.5, 150 mM NaCl, 0.05% Tween 20], overnight at 4°C. Slides were washed three times for 10 minutes each, before being incubated with the primary antibody (anti-EDD M19, 1:1,000; Santa Cruz) diluted in 1% BSA/TBS-T [1% BSA (w/v), 50 mM Tris pH 7.5, 150 mM NaCl, 0.05% Tween 20] for 3 hours at room temperature. The slides were then washed twice for 5 minutes each and incubated with the secondary antibody (anti-goat HRP; 1:10,000; Abcam) diluted in 1% BSA/TBS-T for 1 hour at room temperature. Finally, the slides were washed three times for 10 minutes each, before being treated with ECL substrate reagent and being exposed to autoradiography film (Amersham).

2.4.5 Ubiquitylation assays

S2 or HEK293 cells were transfected with His-tagged Ubiquitin, SGG-FLAG and dsRNA/RNAi against EGFP or Hyd/EDD. Cells were harvested after 48 h, washed once in ice-cold PBS, and lysed in 6 M Guanidinium HCl (GnHCl) Buffer I (6 M GnHCl, 0.01 M Tris HCl pH 8, 0.1 M Na_2HPO_4, 0.1 M NaH_2PO_4, 5 mM Imidazole, 10 mM β-Mercaptoethanol). Lysates were sonicated briefly, cleared by centrifugation at 4,500 rpm at 4°C for 15 minutes, and incubated with Ni-NTA agarose beads (QIAGEN) at room temperature for 3 hours. The beads were washed sequentially in the following buffers: GnHCl Buffer II (6 M GnHCl, 0.01 M Tris HCl pH 8, 0.1 M Na_2HPO_4, 0.1 M NaH_2PO_4, 10 mM β-Mercaptoethanol), Wash

Buffer A (8 M Urea, 0.01 M Tris HCl pH 8, 0.1 M Na_2HPO_4, 0.1 M NaH_2PO_4, 10 mM β-Mercaptoethanol), Wash buffer B (8 M Urea, 0.01 M Tris HCl pH 6.3, 0.1 M Na_2HPO_4, 0.1 M NaH_2PO_4, 10 mM β-Mercaptoethanol, 0.2% Triton X-100), Wash Buffer C (8 M Urea, 0.01 M Tris HCl pH 6.3, 0.1 M Na_2HPO_4, 0.1 M NaH_2PO_4, 10 mM β-Mercaptoethanol), and Wash Buffer D (8 M Urea, 0.01 M Tris HCl pH 6.3, 0.1 M Na_2HPO_4, 0.1 M NaH_2PO_4, 10 mM β-Mercaptoethanol, 0.1% Triton X-100). His-ubiquitin protein complexes were eluted with one bead volume of His Elution Buffer (0.15 M Tris HCl pH 6.7, 30% glycerol, 5% SDS, 200 mM Imidazole, 0.72 M β-Mercaptoethanol).

2.4.6 SDS-PAGE gel electrophoresis

The protein concentration in cell lysates was measured using the Bradford Protein Assay Kit (Thermo Fisher Scientific, Cat. No. 23200) according to the manufacturer's instructions. 15-25 μg of protein per well was prepared for sodium dodecyl sulphate polyacrylamide gel electrophoresis (SDS-PAGE) by adding 1X NuPAGE LDS Sample Buffer (Life Technologies, Cat. No. NP0008) and DTT to a final concentration of 100 mM. The samples were heated at 70°C for 10 minutes before loading onto 4-12% Bis-Tris or 3-8% Tris-Acetate gels (Life Technologies), and running at 200V for 1-2 hours in 1X MOPS buffer (Life Technologies).

2.4.7 Western blotting

Proteins separated on SDS-PAGE gels were transferred onto Polyvinylidene fluoride (PVDF) membranes using a wet transfer system. Gels, filter paper, and PVDF membranes were equilibrated in Transfer Buffer (0.25 M Tris, 1.9 M glycine, 10% (v/v) methanol) and transfers were performed overnight in transfer buffer at 30 V at 4 ºC. Membranes were blocked in 5% Milk/PBS [5% (w/v) dried milk powder, 1X

PBS] or 5% BSA/PBS [5% BSA (w/v), 1X PBS] for 1 hour at room temperature with agitation. The membrane was then incubated with the primary antibody, diluted in either 5% Milk/PBS-T [5% (w/v) dried milk powder, 1X PBS, 0.05% Tween 20] or 3-5% BSA/PBS-T [3-5% BSA (w/v), 1X PBS, 0.05% Tween 20] for 3 hours at room temperature, or overnight at 4°C, with agitation. Membranes were washed several times (3 x 10 minutes) in wash buffer [1X PBS, 0.05% Tween 20] and incubated with a secondary horseradish peroxidase (HRP)-linked antibody, diluted 1:10,000 – 1:30,000 in either 5% Milk PBS-T or 3-5% BSA/PBS-T, as above, for 1 hour at room temperature with agitation. Following a final wash step with wash buffer (3 x 5 minutes), before being treated with ECL substrate reagent and being exposed to autoradiography film (Amersham). Primary antibodies used were goat EDD M-19 (1:1,000; Santa Cruz), mouse HA (1:2,000; Cell Signaling), rabbit FLAG (1:2,000; Cell Signaling), mouse Sgg (1:5,000; Euromedex), rabbit GSK3β (1:2,000; Cell Signaling), rat Ci 2A1 [1:100; Developmental Studies Hybridoma Bank (DSHB)], mouse Armadillo (1:100; DSHB), and mouse tubulin (1:30,000; Cell Signaling).

2.4.8 Coomassie blue and silver staining

SDS-PAGE gels were stained with SimplyBlue™ SafeStain (Life Technologies, Cat. No. LC6060) or the Silver Quest™ Silver Staining Kit (Life Technologies, Cat. No. LC6070), following the manufacturer's protocol.

2.5 *Drosophila* methods

2.5.1 *Drosophila melanogaster* stocks

These alleles are described in Flybase: $hyd^{K7.19}$, $sgg^{S9A.Scer\UAS}$, $sgg^{HMS01751}$ (RNAi). w^{1118}; *UAS-*sgg^{S9A} (5255) and y^{1} sc^{*} v^{1}; sgg^{RNAi} (38293) stocks were obtained from

the Bloomington *Drosophila* Stock Center. *hyd*$^{K7.19}$ stocks were obtained from Jessica Treismann (NYU School of Medicine, New York, NY, USA). *Sp//SM6-TM6* was obtained from Marcos Vidal (Beatson Institute for Cancer Research, Glasgow, UK). Flies were maintained on standard medium at 18°C or 25°C.

2.5.2 Mosaic Analysis with a repressible cell marker (MARCM)

The MARCM technique (Lee and Luo, 2001) was used to generate GFP-expressing *hyd*$^{K7.19}$ *hh-lacZ* clones. Clones were induced by expression of *ey-flp*$^{3.6}$. Crosses were maintained at 25°C. Two- to three-hour timed L3 larvae collections were made prior to dissections of eye discs. The following stocks were used for clonal analysis:

yw ey-flp$^{3.6}$*; act>y+>GAL4, UAS-GFP; FRT*^{82B}*, tubGAL80//SM6-TM6*

FRT^{82B}*, hh-lacZ/TM6B*

FRT^{82B}*, hyd*$^{K7.19}$ *hh-lacZ/TM6B*

UAS-sgg^{S9A}*; FRT*^{82B}*, hyd*$^{K7.19}$ *hh-lacZ//SM6-TM6*

UAS-sgg^{S9A}*; FRT*^{82B}*, hh-lacZ//SM6-TM6*

sgg^{RNAi}*; FRT*^{82B}*, hyd*$^{K7.19}$ *hh-lacZ//SM6-TM6*

sgg^{RNAi}*; FRT*^{82B}*, hh-lacZ//SM6-TM6*

2.5.3 Wholemount immunofluorescence of eye-antennal imaginal discs

Eye-antennal imaginal discs were dissected from L3 stage larvae in PBS as previously described (Legent & Treisman 2008) and fixed in 4% paraformaldehyde for 30 minutes. The discs were washed three times 5 minutes in PBST [1X PBS,

0.1% (v/v) Triton X-100], placed in blocking solution [2% (w/v) BSA, 1X PBS, 0.1% (v/v) Triton X-100] for 30 minutes, and incubated with primary antibodies diluted in blocking solution overnight at 4°C. Discs were washed as described and incubated with secondary antibodies diluted in blocking solution for 2 hours at room temperature, followed by washing and mounting in Vectashield mounting medium containing 4',6-diamidino-2-phenylindole (DAPI) (Vector Laboratories Inc.). Primary antibodies used were mouse β-galactosidase (1:100; DSHB), rabbit Hh (1:400; a gift from Pascal Thérond), rat Ci 2A1 (1:10; DSHB), mouse Ptc (1:10; DSHB), and mouse Wg (1:10; DSHB). Secondary antibodies used were Alexa 594 and Cy5 (1:500; Life Technologies). Images were captured on a Nikon A1R confocal microscope at 20X magnification.

2.5.4 Xgal staining of eye-antennal imaginal discs

Eye-antennal imaginal discs were dissected and fixed as described in 2.5.3. The discs were washed two times 10 minutes in PBST [1X PBS, 0.1% (v/v) Triton X-100], and incubated in pre-warmed Xgal Staining Solution {0.2% (w/v) Xgal, 7.2 mM Na_2HPO_4, 2.8 mM NaH_2PO_4, 150 mM NaCl, 1 mM $MgCl_2$, 3 mM $K_3[Fe(CN)_6]$, 3 mM $K_4[Fe(CN)_6]$} overnight at 37°C. Discs were washed briefly in 1X PBS and imaged on a light microscope at 10X magnification.

Chapter 3: Proteomics approaches to identify novel Hyd binding partners

3.1 Introduction

Although Hyd has been functionally implicated in the negative regulation of *hh* gene expression and Hh pathway activity (J. D. Lee et al. 2002), no protein binding partners for Hyd had been reported at the time of starting this project in 2010. This greatly complicated the task of elucidating the molecular mechanism by which Hyd regulates morphogen signalling. In order to facilitate this task, a key objective of this project was to identify novel Hyd binding partners, especially those that are already known to be involved in morphogen signaling and/or gene expression.

To increase the chances of identifying *bona fide* Hyd binding proteins, I employed several complementary approaches/techniques. As several binding partners have been published for Hyd's human orthologue EDD, I firstly employed a literature-based approach and selected EDD binding partners that may be involved in Hh signaling. Secondly, I performed mass spectrometry on a Hyd pulldown from cultured *Drosophila* cells to identify binding partners, which were then subjected to bioinformatics analysis to identify any associations to morphogen signaling. Results from both of these approaches were finally subjected to biochemical verification of any potential interactions. Lastly, I performed a peptide ELISA to identify specific peptide sequences that bind to Hyd with a high affinity, and used this data as an alternative approach to identify novel Hyd binding partners.

3.2 Hyd does not interact with members of the DYRK2 kinase family

A number of proteins bind to Hyd's human orthologue, EDD, implicating it in a diverse range of pathways and processes (see **Chapter 1, Section 1.4.2**). However, prior to 2014 Hyd had no published binding partners. Therefore, in a biased and

literature-guided approach, I selected known EDD binding partners based on their potential involvement in pathways regulating morphogen signaling.

EDD interacts with the kinase DYRK2. DYRK2 forms a complex with EDD, and members of the Cul4-Roc1 E3 ligase complex DDB1 and VPRBP (Maddika & J. Chen 2009). DYRK2 is involved in a number of cellular processes, notably including its role in the mammalian SHH pathway, where it contributes to the phosphorylation and destabilization of the major transcriptional effector protein GLI2 (Varjosalo et al. 2008).

Interestingly, the *Drosophila* DYRK2 homologue, also known as smell-impaired (smi35A), interacts with the chromatin remodelling factors SNR1 and TRX (Kinstrie et al. 2006), which regulate *hh* gene transcription (Chanas & Maschat 2005; Terriente-Félix et al. 2011). In addition to directly regulating Hh pathway activity through affecting Ci processing, a physical interaction between smi35A and Hyd could also epigenetically influence *hh* gene expression. However, both these hypotheses rely on the conservation of function between human and *Drosophila*.

3.2.1 Hyd does not interact with smi35A

Assuming that the function of DYRK2 is conserved between humans and *Drosophila*, I first tested whether Hyd can interact with DYRK2 in HEK293 cells. An N-terminally Haemaglutinin (HA)- and Streptavidin (Strep)-tagged Hyd construct, containing a Precission cleavage site to enable enzymatic removal of the tag (collectively termed HSP), had previously been cloned in the lab (Mark Ditzel). This epitope tagged construct will be referred to subsequently as HSP-Hyd. In addition, a similar HSP-EDD construct, and a DYRK2-FLAG construct had also been cloned previously (Mark Ditzel), and were used as a positive binding control.

To verify an interaction, HEK293 cells were co-transfected with HSP-Hyd, DYRK2-FLAG, and HSP-EDD, and Hyd and EDD were pulled down using StrepTactin sepharose beads. Additionally, a catalytically inactive Hyd mutant (HSP-Hyd C>A) was also included in the binding assay to test whether Hyd's ubiquitylation activity could be required for a potential interaction to take place. Hyd-mediated ubiquitylation of DYRK2 could be a prerequisite for the interaction to take place, resulting in the generation of a new binding surface, or a conformational change in the DYRK2 protein that allows binding of Hyd. In this case, the wild-type Hyd protein, but not the C>A mutant Hyd protein would be expected to bind. Alternatively, if Hyd normally ubiquitylates and degrades DYRK2, then using this mutant in the binding assay would increase the chance of detecting an interaction. In the C>A mutant, the catalytic cysteine residue in the HECT domain has been replaced with an alanine residue, which prevents both the binding of ubiquitin at the active site, and subsequent transfer of ubiquitin to substrates (see **Chapter 1, Sections 1.1.2.1 and 1.4.1.1**).

As expected, DYRK2-FLAG was successfully pulled down with HSP-EDD (**Figure 3.1 A**), confirming the published result (Maddika & J. Chen 2009), and ascertaining that the epitope tags do not interfere and that the assay is capable of detecting the interaction. However, DYRK2-FLAG failed to interact with Hyd (**Figure 3.1 A**). If the potential interaction between DYRK2 and Hyd is not binary, an intermediate binding partner could be required for the complex to form. Further to this, if this intermediate binding partner is either not conserved between *Drosophila* and humans, or is simply not present in HEK293 cells, this could explain the negative binding result. Of course, another possibility is that DYRK2 significantly differs in sequence and or structure to smi35 and is therefore unable to bind Hyd (**Figure 3.2 A**).

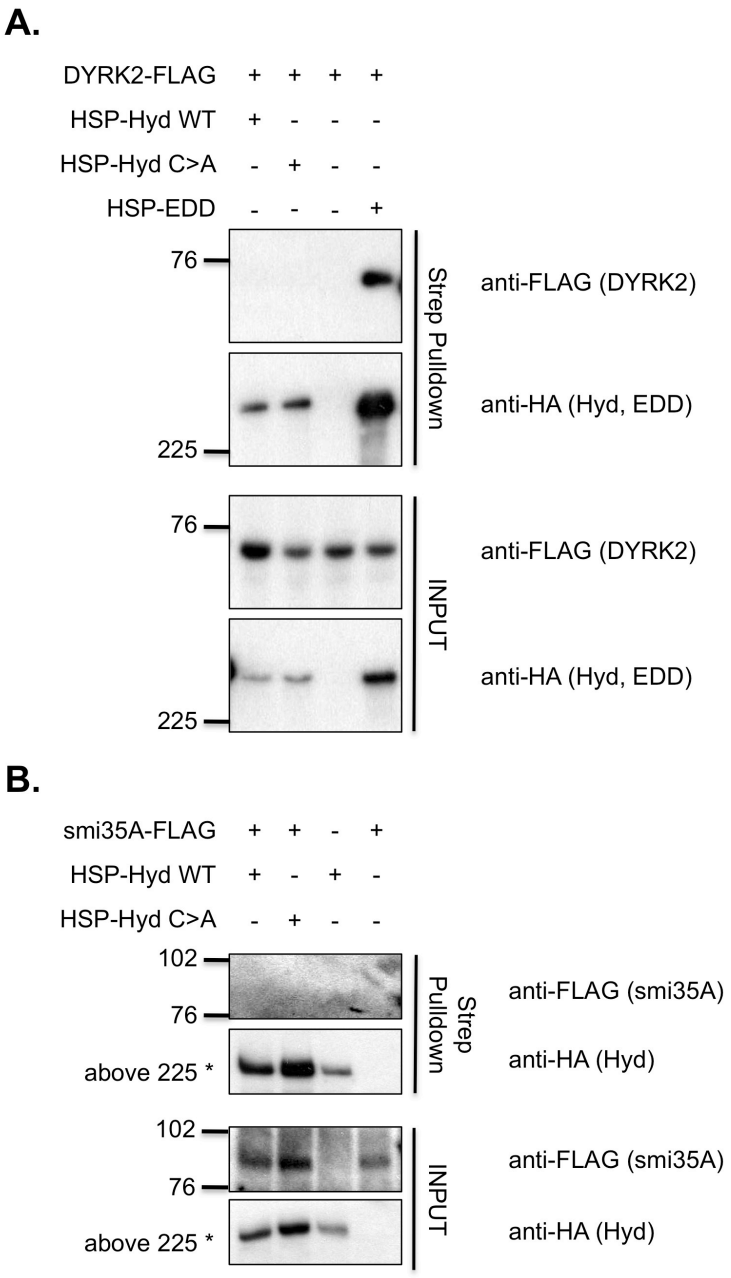
A.
DYRK2-FLAG + + + +
HSP-Hyd WT + - - -
HSP-Hyd C>A - + - -
HSP-EDD - - - +
76
225
Strep Pulldown
anti-FLAG (DYRK2)
anti-HA (Hyd, EDD)
76
225
INPUT
anti-FLAG (DYRK2)
anti-HA (Hyd, EDD)
B.
smi35A-FLAG + + - +
HSP-Hyd WT + - + -
HSP-Hyd C>A - + - -
102
76
above 225 *
Strep Pulldown
anti-FLAG (smi35A)
anti-HA (Hyd)
102
76
above 225 *
INPUT
anti-FLAG (smi35A)
anti-HA (Hyd)

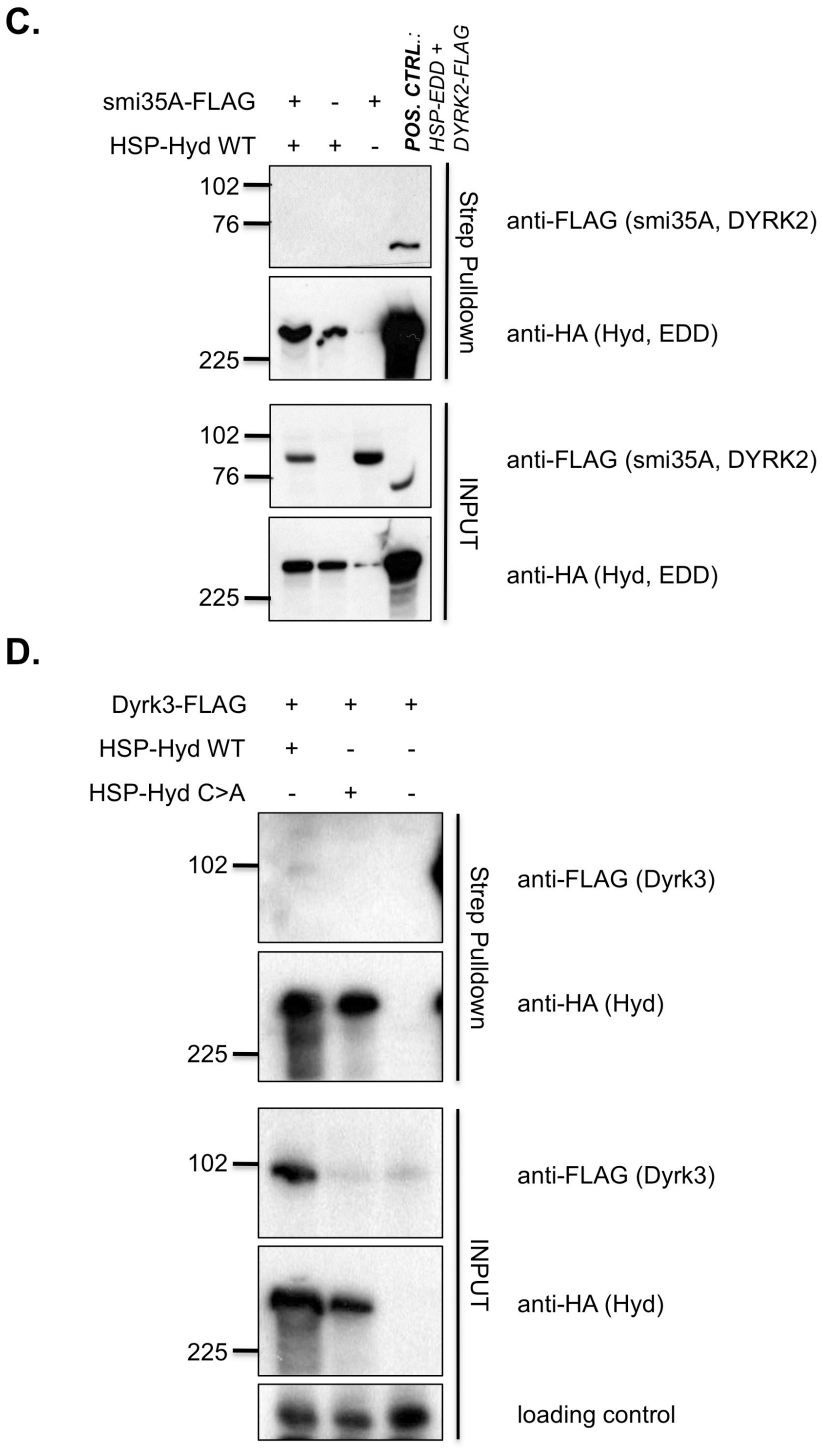

Figure 3.1: Hyd and EDD interactions with DYRK2 and its homologues. (**A**) StrepTactin pulldown in HEK293 cells. HEK293 cells were transfected with HSP-Hyd WT, HSP-Hyd C>A, HSP-EDD and DYRK2-FLAG constructs. (**B**) StrepTactin pulldown in S2 cells. S2 cells were transfected with HSP-Hyd WT, HSP-Hyd C>A and smi35A-FLAG constructs. (**C**) StrepTactin pulldown in HEK293 cells. HEK293 cells were transfected with HSP-Hyd WT and smi35A-FLAG constructs.

HSP-EDD and DYRK2-FLAG were used as a positive binding control (POS. CTRL.). (**D**) StrepTactin pulldown in S2 cells. S2 cells were transfected with HSP-Hyd WT, HSP-Hyd C>A, and Dyrk3-FLAG constructs.

With this in mind, I cloned the *Drosophila* orthologue of DYRK2, known as smell-impaired (smi35A). The smi35A construct contains a C-terminal FLAG tag, and was cloned into both *Drosophila* and mammalian expression vectors. Schneider 2 (S2) cells, which were originally derived from *Drosophila* embryos (Schneider 1972) and are one of the most commonly used *Drosophila* cell lines, were co-transfected with smi35A-FLAG and HSP-Hyd, and subjected to a StrepTactin pulldown. Unfortunately, the expression levels of the smi35A-FLAG construct were sub-optimal and no binding was detected in S2 cells (**Figure 3.1 B**). I therefore tried to detect a possible interaction in HEK293 cells, as these are known to easily produce large amounts of over-expressed proteins, and are therefore ideal for binding assays. Smi35A-FLAG and HSP-Hyd were co-transfected into HEK293 cells, followed by a StrepTactin pulldown of HSP-Hyd. However, no interaction was detected between smi35A-FLAG and HSP-Hyd WT or HSP-Hyd C>A (**Figure 3.1 C**). This was despite the fact that the binding conditions allowed binding of DYRK2-FLAG to HSP-EDD in the positive control (**Figure 3.1 C**).

3.2.2 Hyd may interact with *Dm* Dyrk3 and increase its expression level

From the previous binding assay results, it appeared that smi35A did not bind Hyd, even though DYRK2 readily interacts with EDD. However, the low expression levels of smi35A in S2 cells could also account for the lack of an observed reaction. Alternatively, this could be due to the divergence of sequence conservation between *Drosophila* DYRK2 homologues and DYRK2. Closer investigation of all existing *Drosophila* homologues of DYRK2 using protein BLAST revealed that smi35A only shared 47% sequence identity with DYRK2 (**Figure 3.2 B**). It also revealed that another *Drosophila* DYRK2 homologue, Dyrk3, is in fact more closely related to

DYRK2, sharing a significant 72% sequence identity (**Figure 3.2 B**).

A.

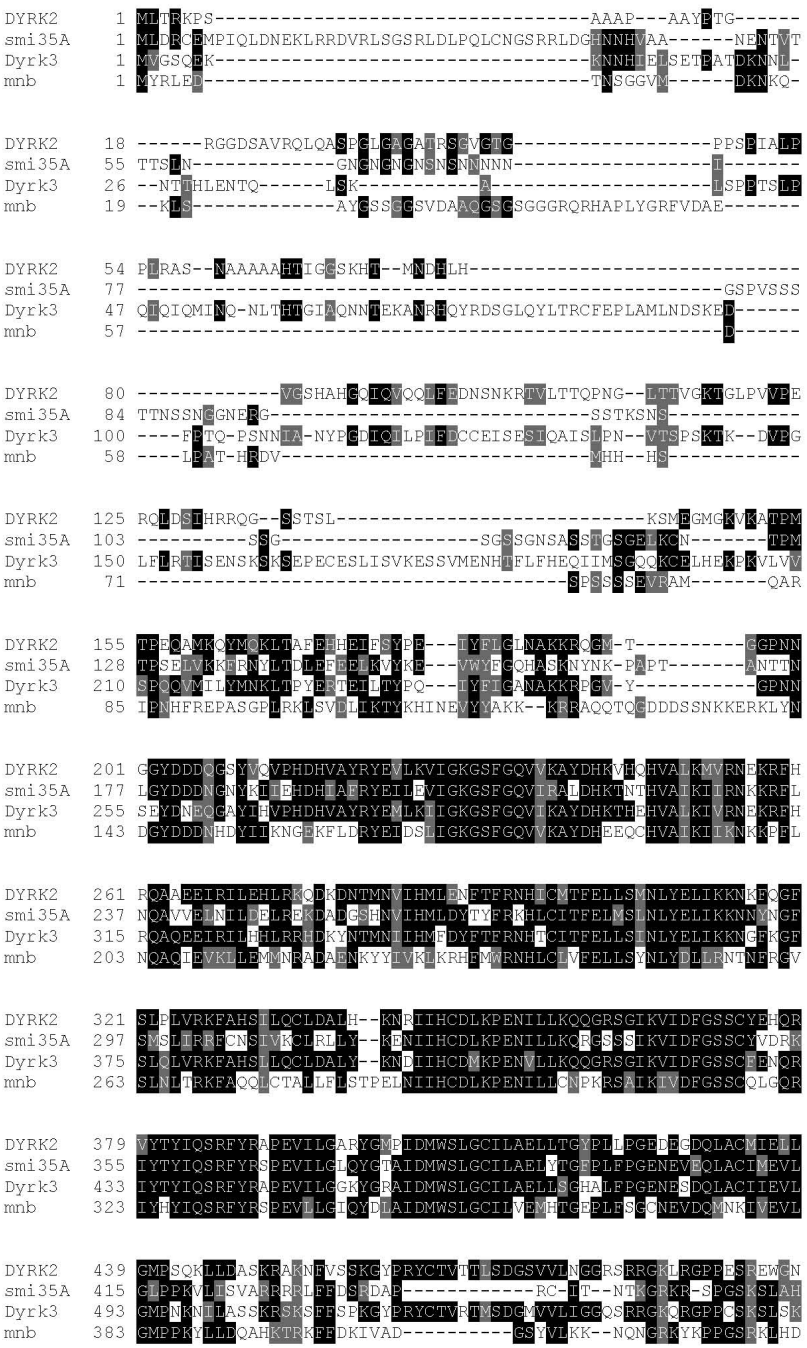

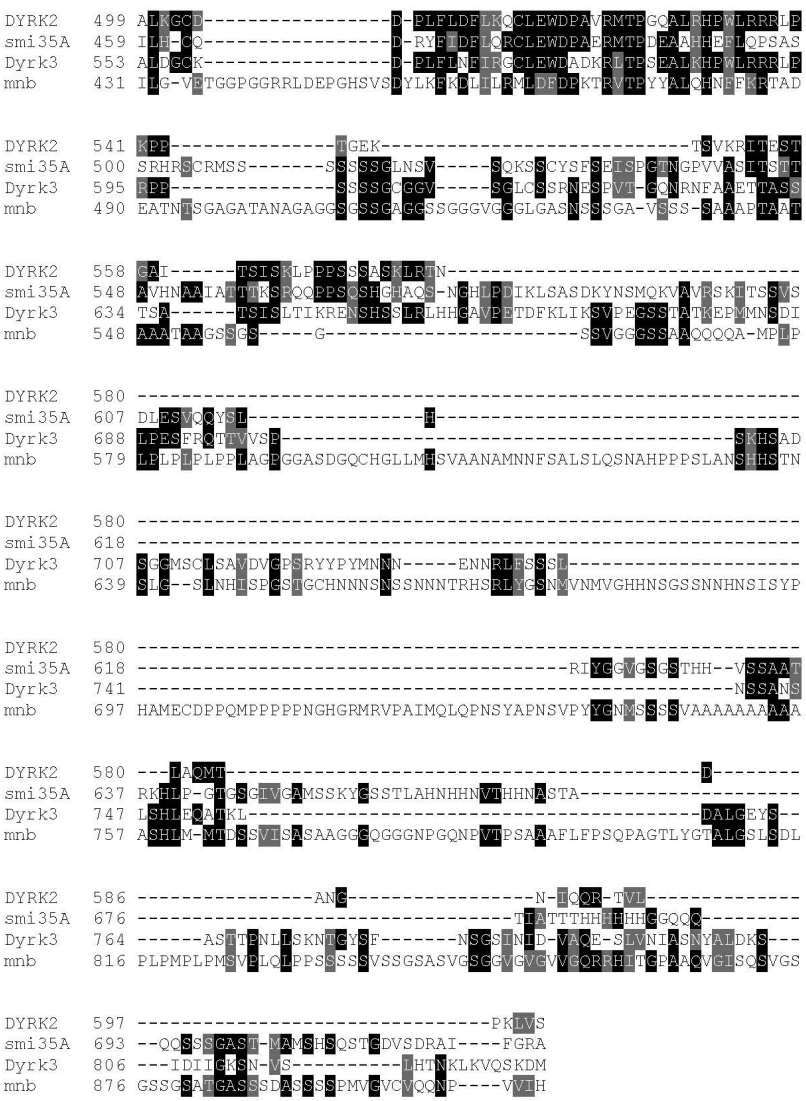

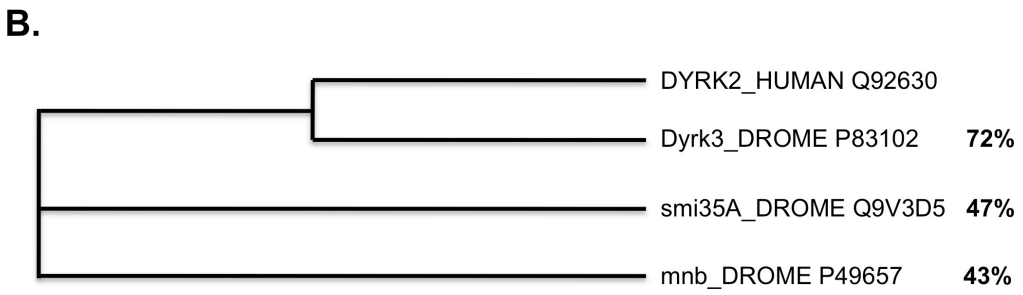

Figure 3.2: Sequence identity between DYRK2 and its *Drosophila* homologues. (**A**) Amino acid sequence alignment of DYRK2, smi35A, Dyrk3 and minibrain (mnb). (**B**) Schematic summarising protein BLAST alignment results of DYRK2 and its closest homologues in *Drosophila* based on sequence conservation. Percentages indicate sequence identity with respect to DYRK2.

I therefore reasoned that Dyrk3 may be a better candidate to interact with Hyd and cloned a Dyrk3-FLAG construct to test the binding to Hyd. S2 cells were co-transfected with Dyrk3-FLAG, HSP-Hyd WT and HSP-Hyd C>A, and a binding assay was performed using StrepTactin beads. Dyrk3-FLAG did not appear to interact with either Hyd WT or Hyd C>A, although a very weak signal was detected in the Dyrk3 and Hyd WT binding sample (**Figure 3.1 D**; upper panel). Interestingly, the expression of Dyrk3 was significantly higher in the presence of Hyd WT, compared to in the presence of Hyd C>A or when expressed on its own (**Fig. 3.1 D**; third panel from top). This could explain why a small amount of Dyrk3 could have been pulled down with Hyd WT.

3.2.3 Summary

In conclusion, I was unable to establish a positive interactive pairing between Hyd and the DYRK kinases. Hyd does not appear to interact with DYRK2 or smi35A, but may interact with Dyrk3. The latter result also suggests that Hyd may be involved in positively regulating Dyrk3 protein levels through its ubiquitylation activity. However, this hypothesis would have to be investigated further. Firstly, the binding assay would have to be repeated using a larger amount of transfected S2 cell lysate and/or a more sensitive Western blotting detection reagent, such as SuperSignal West Femto Chemiluminescent Substrate (Thermo Fisher Scientic Inc.). In addition, I would perform a ubiquitylation assay with Hyd and Dyrk3 in S2 cells, to assess whether Hyd affects Dyrk3 ubiquitylation levels. Finally, to determine whether Hyd regulates Dyrk3 protein levels and by what mechanism, I would assess the effects of the presence and absence of Hyd protein in S2 cells (e.g. over-expression and RNAi) on Dyrk3 protein levels in the presence of the proteasome inhibitor MG132 and/or the protein synthesis inhibitor cycloheximide.

3.3 Optimisation of Tandem Affinity Purification (TAP) of Hyd for Mass Spectrometry (MS)

One of the key objectives of this project is to identify novel Hyd protein binding partners and/or ubiquitylated substrates. In an unbiased proteomics-based approach, I employed a specific tandem affinity purification (TAP) protocol in combination with mass spectrometry (Gingras et al. 2007) to purify and analyse Hyd complexes from *Drosophila* S2 cells.

The TAP procedure involves a sequential pulldown of Hyd, and its associated binding partners, using a StrepTactin affinity resin, followed by elution with desthiobiotin, and immunoprecipitation with an anti-HA antibody-conjugated resin (**Figure 3.3**, steps 1 and 2) (Gingras et al. 2007). The Strep-tag fused to Hyd is a synthetic peptide that binds with high affinity to StrepTactin, a specifically engineered Streptavidin (Schmidt & Skerra 2007). TAP enables the elimination of many non-specific contaminants that may bind to the resins, and may otherwise be detected as false positives in the final elution (**Figure 3.3**, step 3).

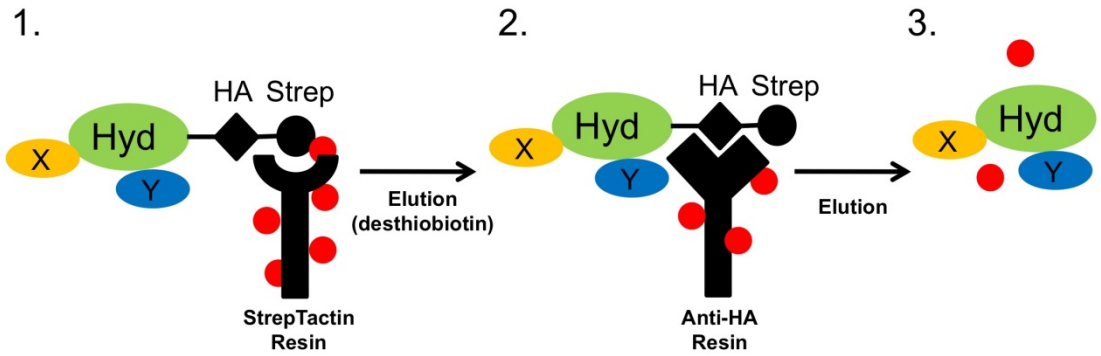

Figure 3.3: HA-Strep Hyd Tandem Affinity Purification (TAP). S2 cells expressing HSP-tagged contructs are lysed and are subjected to a two-step purification procedure. First, HSP-Hyd, and associated binding partners (e.g. X, Y) are purified using Strep-Tactin sepharose beads (step 1). HSP-tagged comlexes are then eluted using desthiobiotin and purified using anti-HA-conjugated agarose

beads (step 2). Finally, proteins are eluted from the anti-HA beads for analysis by mass spectrometry (step 3). This eliminates most contaminants (red circles) that bind non-specifically to the sepharose or agarose resins.

S2 cells were chosen as they endogenously express Hyd (modENCODE project, (Celniker et al. 2009), suggesting that they also contain Hyd protein binding partners. In addition, S2 cells are easily cultured and express a relatively high amount of protein when transfected. In order to produce quality protein material for affinity purification, S2 cell lines stably expressing HSP-Hyd constructs were generated (**Figure 3.4 A**). S2 cells were transfected with HSP-Hyd constructs that were cloned into the pMT-PURO expression vector, which allows inducible expression of Hyd and contains a puromycin resistance gene (Iwaki & Castellino 2008). S2 cells were then subjected to puromycin-based selection to obtain cells stably expressing HSP-Hyd constructs.

Hyd is an E3 ubiquitin ligase, meaning that it may coordinate the ubiquitylation and degradation of its binding partners. This would effectively minimize the detection of some endogenous binding partners following affinity purification of HSP-Hyd. To circumvent this issue, an S2 cell line stably expressing the catalytically inactive mutant HSP-Hyd C>A was also generated (**Figure 3.4 A**). In addition to this, an S2 cell line expressing the HSP tag only was generated as a negative binding control (**Figure 3.4 A**). Any proteins interacting with the HSP tag would therefore be subtracted from those identified as HSP-Hyd interacting proteins.

Next, TAP of Hyd complexes from stable S2 cell lysates was optimized to yield a high quality sample for analysis by mass spectrometry (MS). The procedure was initially carried out as described previously (Gingras et al. 2007) on lysates from stable HSP-Hyd WT cells and normal S2 cell lysates. A silver stain of the final elution of this pilot experiment revealed that, in addition to exogenous Hyd, there

were several unique bands in the Hyd WT elution sample (**Figure 3.4 B**). The complexes were eluted using a denaturing buffer containing 4% SDS, which would also denature and detach the heavy and light chains of the HA antibodies conjugated to the anti-HA resin. This explains the large background band present in both the experimental and control elutions, which is likely to represent the heavy chain of the HA antibody (**Figure 3.4 B**).

In an attempt to obtain a cleaner and higher quality final elution for subsequent mass spectrometric analysis, I optimized the final elution step of the procedure. I compared three different elution methods: 4% SDS buffer, HA peptide, and 8M Urea. In this experiment, both the HA peptide and 8M Urea elutions were cleaner than the SDS elutions (**Figure 3.4 C**). However, in the HSP control sample eluted with HA peptide, there was an inexplicably high amount of background. Further to this, HA peptide elution would require the removal of the HA peptide prior to mass spectrometric analysis of the sample to reduce interference. I therefore chose to proceed with the 8M Urea elution method.

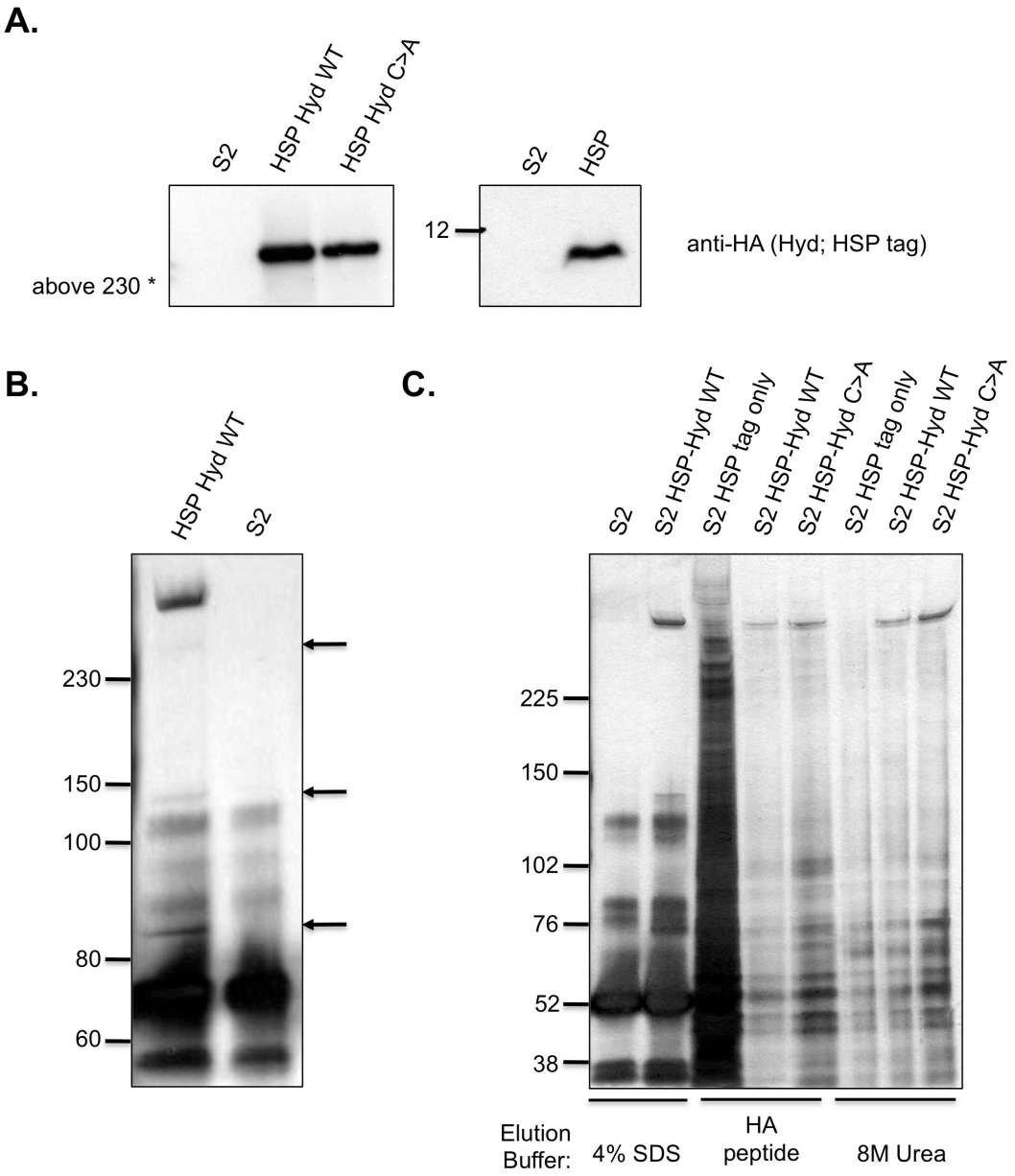

Figure 3.4: Generation of tools and Optimisation of TAP procedure for identification of Hyd binding partners. (**A**) Expression of WT HSP-Hyd and C>A HSP-Hyd (left panel), and the HSP epitope tag (right panel) in stably transfected S2 cell lines. Lysates of non-transfected S2 cells were included as a negative control. (**B**) Silver stain analysis of TAP samples. Non-transfected S2 cells (negative control) and S2 cells staby expressing HSP-Hyd WT were lysed and subjected to TAP, prior to elution with 4% SDS. Unique bands in the HSP-Hyd eluted fraction are indicated by arrows. (**C**) Silver stain assessment of different elution buffers used for the final elution of the TAP procedure. Eluted samples following TAP from non-transfected S2 cells or S2 cells stably expressing the HSP tag only (negative controls) were run alongside samples from S2 cells stably expressing HSP-Hyd WT and HSP-Hyd C>A. The final elution was performed with either 4% SDS, HA peptide, or 8M Urea.

3.4 Mass Spectrometry identifies potential novel Hyd binding partners

In an attempt to identify novel Hyd binding partners, I used S2 cells stably expressing HSP alone, HSP-Hyd WT and HSP-Hyd C>A to purify complexes as described in Section 3.3. The 8M urea-eluted fractions were subsequently loaded into individual wells of a pre-cast SDS-PAGE gel, and allowed to run 1-2 cm into the gel. Following Coomassie staining, this portion of the gel was then excised in its entirety, effectively containing Hyd and all of the complexed material, irrespective of molecular weight. The gel fraction was trypsinized, and the sample was analysed by mass spectrometry using the search engine Mascot to generate a list of identified proteins from the raw peptide mass fingerprint data (carried out by Flavia Alves, Rappsilber Lab, Institute of Cell Biology, University of Edinburgh, see **Materials and Methods, Section 2.4.3** for details of sample preparation, processing and analysis).

3.4.1 Mass spectrometry results

All identified proteins also present in the HSP-tag only control were eliminated, and the combined results from five independent experiments are summarised in **Table 3.1**. From all five experiments, over 100 protein hits were identified. However, a large proportion of these hits were proteins, which were unlikely to be involved in signalling pathways with Hyd, such as actin, tubulin, and heat shock proteins. The simplified list presented in **Table 3.1** contains a total of 26 potential novel Hyd binding partners chosen from the combined dataset on the basis of their likelihood to be involved in processes related to known Hyd/EDD functions (see **Section 1.4.2**). Several proteins were identified that appear to exclusively interact with either Hyd WT or Hyd C>A, with the exception of Tcp1 and Gustatory Receptor 97a. This

suggests that Hyd's ubiquitylation activity could be essential for binding to some of its binding partners. Unfortunately, most proteins were identified based on the presence of a single peptide, with the highest peptide count per protein being five. This suggests that the quality of the mass spectrometry data is relatively poor and could be due to several factors, including significant protein loss during the relatively complex TAP procedure, or insufficient trypsinization of proteins contained within the gel chunk. Although I attempted to optimise the experiment during 4 additional runs, I was unable to improve the peptide count. However, some protein hits, although identified by as little as one peptide, had a good peptide coverage over multile experiments. For example, Armadillo, Shab and Copia were identified by single, but different, peptides in multiple, independent experiments, which increases the confidence level and indicates that these may be genuine Hyd binding partners.

3.4.2 Bioinformatics analysis of mass spectrometry hits

With the intention of identifying novel Hyd binding partners involved in morphogen signalling and/or expression, my original plan was to use bioinformatics to narrow down a potentially large list of protein hits. Since the list in **Table 3.1** is shorter than expected, I decided to use a combination of bioinformatics and biochemical verification to sift out proteins that are genuine Hyd binding partners and are likely to be functionally involved in morphogen pathways.

The Uniprot database is a central repository of information on protein sequence and function. In addition, it integrates the Basic Local Alignment Search Tool (BLAST) algorithms, which I used to identify homologous proteins and infer information on uncharacterised *Drosophila* proteins. I identified the closest human orthologue and the relevant percentage of sequence identity between the *Drosophila* and human proteins for each MS hit (**Table 3.1**). This revealed that most of the hits showed very close (i.e. >40% sequence identity) sequence homology to a human protein. This is important, because the extent of co-evolution among Hyd/EDD binding partners

between organisms is a crucial factor in the discovery of conserved biological processes in mice and humans, ultimately aiding translational research

Interestingly, analysis of the individual protein hits revealed Armadillo, the *Drosophila* homologue of β-catenin, to be a potential Hyd binding partner (**Table 3.1**). Armadillo/β-catenin is the key transcriptional effector in the Wg/Wnt pathway (see **Chapter 1, Section 1.3.1**), suggesting that Hyd may also be involved in regulating Wg morphogen signaling.

Table 3.1: Combined TAP Mass Spectrometry Results. Proteins identified in a total of 5 independent pulldown experiments with both WT HSP-Hyd and C>A HSP-Hyd are listed.

Protein Name/Uniprot ID	Experiment Number	No. of peptides identified (HSP-Hyd WT pulldown)	Protein Score	No. of peptides identified (HSP-Hyd C>A pulldown)	Protein Score	Closest human orthologue (% identity) and predicted function
Hyperplastic discs (Hyd) **P51592**	1	18	**766**	132	**13,459**	EDD (38%) O95071: Putative E3 ligase involved in negatively regulating Hh signalling.
	2	123	**8,742**	177	**14,009**	
	3	103	**4,029**	191	**13,726**	
	4	106	**9,377**	64	**4,233**	
	5	83	**1,633**	-	-	
Tcp1 (T-cp1) **P12613**	2	-	-	1	**48**	TCP1 (73%) P17987: Molecular chaperone
	4	-	-	5	**179**	
	5	1	**30**	-	-	
Pyruvate kinase (PyK) **O62619**	5	4	**42**	-	-	PyK PKM (65%) P14618: Regulation of glucose metabolism
Copia (GIP) **P04146**	4	1	**47**	-	-	Retrotransposon; encodes a retroviral-like protease
	5	3	**32**	-	-	
Eukaryotic translation initiation factor 2 (EiF-2) **Q24208**	4	3	**46**	-	-	EiF2 (81%) P41091: Protein synthesis
Akirin **Q9VS59**	4	-	-	2	**26**	Akirin-2 (40%) Q53H80: Embryonic development; Effector of immune deficiency pathway

Protein Name/Uniprot ID	Experiment Number	No. of peptides identified (HSP-Hyd WT pulldown)	Protein Score	No. of peptides identified (HSP-Hyd C>A pulldown)	Protein Score	Closest human orthologue (% identity) and predicted function
Shab **P17970**	3	-	-	2	**27**	Potassium voltage-gated channel (70%) Q14721: Voltage-dependent potassium ion permeability
	4	-	-	1	**27**	
ATP synthase subunit alpha (blw) **P35381**	4	1	**38**	-	-	ATP synthase subunit alpha (81%) P25705: ATP production
	5	2	**29**	-	-	
Rpn7 **Q9V3G7**	4	2	**92**	-	-	26S proteasome non-ATPase regulatory subunit 6 (70%) Q15008: Regulatory subunit of the 26S proteasome
Protein similar (sima) **Q24167**	1	-	-	1	**27**	Hypoxia-inducible factor 1-alpha (31%) Q16665: Possible DNA-binding transcriptional activator
Bangles and beads (bnb) **P29746**	2	-	-	1	**25**	Neurofilament heavy polypeptide (25%) P12036: May play an important role during development
Fibroblast growth factor receptor homolog 1 (htl) **Q07407**	2	-	-	1	**28**	Fibroblast growth factor receptor 3 (40%) P22607: May be required for patterning of muscle precursor cells
Tudor (tud) **P25823**	3	-	-	1	**33**	Tudor domain-containing protein 6 (20%) O60522: Formation of primordial germ cells

Protein Name/Uniprot ID	Experiment Number	No. of peptides identified (HSP-Hyd WT pulldown)	Protein Score	No. of peptides identified (HSP-Hyd C>A pulldown)	Protein Score	Closest human orthologue (% identity) and predicted function
Gustatory receptor 97a (Gr97a) **Q8IMQ6**	2	1	28	-	-	Probable role in the gustatory response
	3	-	-	1	**26**	
Glycogen Phosphorylase (GlyP) **Q9XTL9**	3	-	-	1	**41**	Glycogen phosphorylase (73%) P11217: Carbohydrate metabolism
Dystrophin (Dys) **Q9VDW6**	4	1	**38**	1	**26**	Dystrophin (42%) P11532: Anchors the extracellular matrix to the cytoskeleton in muscle cells
Real-time (retm) **Q9VMD6**	4	-	-	1	**34**	SEC14-like protein 1 (44%) Q92503: Unknown function
APP-BP1 **Q9VTE9**	4	-	-	1	**32**	NEDD8-activating enzyme E1 regulatory subunit (45%) Q13564: Regulatory subunit of the dimeric Uba3-Ula1 E1 enzyme
Armadillo (arm) **P18824**	1	1	**59**	-	-	Catenin beta-1 (68%) P35222: Transcriptional effector protein in the Wg/Wnt pathway
	2	1	**97**	-	-	
	4	1	**110**	1	**102**	
Ran **Q9VZ23**	3	1	**67**	-	-	GTP-binding nuclear protein Ran (87%) P62826: GTP-binding protein involved in nucleo-cytoplasmic transport
Cryptochrome 1	4	1	**43**	-	-	Cryptochrome-1 (41%) Q16526: Regulation

Protein Name/Uniprot ID	Experiment Number	No. of peptides identified (HSP-Hyd WT pulldown)	Protein Score	No. of peptides identified (HSP-Hyd C>A pulldown)	Protein Score	Closest human orthologue (% identity) and predicted function
(cry) **O77059**						of circadian feedback loop
Cytochrome B (Mt:Cyt-b) **P18935**	4	1	**47**	-	-	ATP synthesis
Flightin (fln) **P35554**	4	1	**39**	-	-	Possibly involved in the regulation of flight muscle contraction
PERQ **Q7KQM6**	4	1	**33**	-	-	GIGYF2 (26%) Q6Y7W6: Unknown function
Rpn2 **Q9V3P6**	4	1	**26**	-	-	26S proteasome non-ATPase regulatory subunit (62%) Q99460: Regulatory subunit of the 26S proteasome
Cysteine desulfurase **Q9VKD3**	5	1	**58**	-	-	Cysteine desulfurase, mitochondrial (78%) Q9Y697: Removal of elemental sulfur from cysteine to produce alanine
ATP synthase subunit beta (ATP-syn beta) **Q05825**	5	1	**34**	-	-	ATP synthase subunit beta (89%) P06576: ATP production

To gain more insight into potential molecular and/or functional relationships between the MS hits, I used additional bioinformatics databases, aiming to identify any shared functions and pathway-related interrelationships between the potential binding partners. The protein interaction database IntAct was used to identify any shared binding partners between the identified proteins, with the aim of identifying potential 'nodes' with shared roles in particular cellular processes. The cytoscape program was then used to visualize the network as a node and edge diagram from the list of binding partners resulting from the IntAct database query (**Figure 3.5**). This revealed that Ran and Pyruvase kinase interact and may therefore exist in a complex with Hyd. Furthermore, the IntAct analysis showed that there are several shared binding partners between the potential Hyd binding proteins, which appear to be involved in a diverse array of cellular processes (**Figure 3.5** and **Table 3.2**).

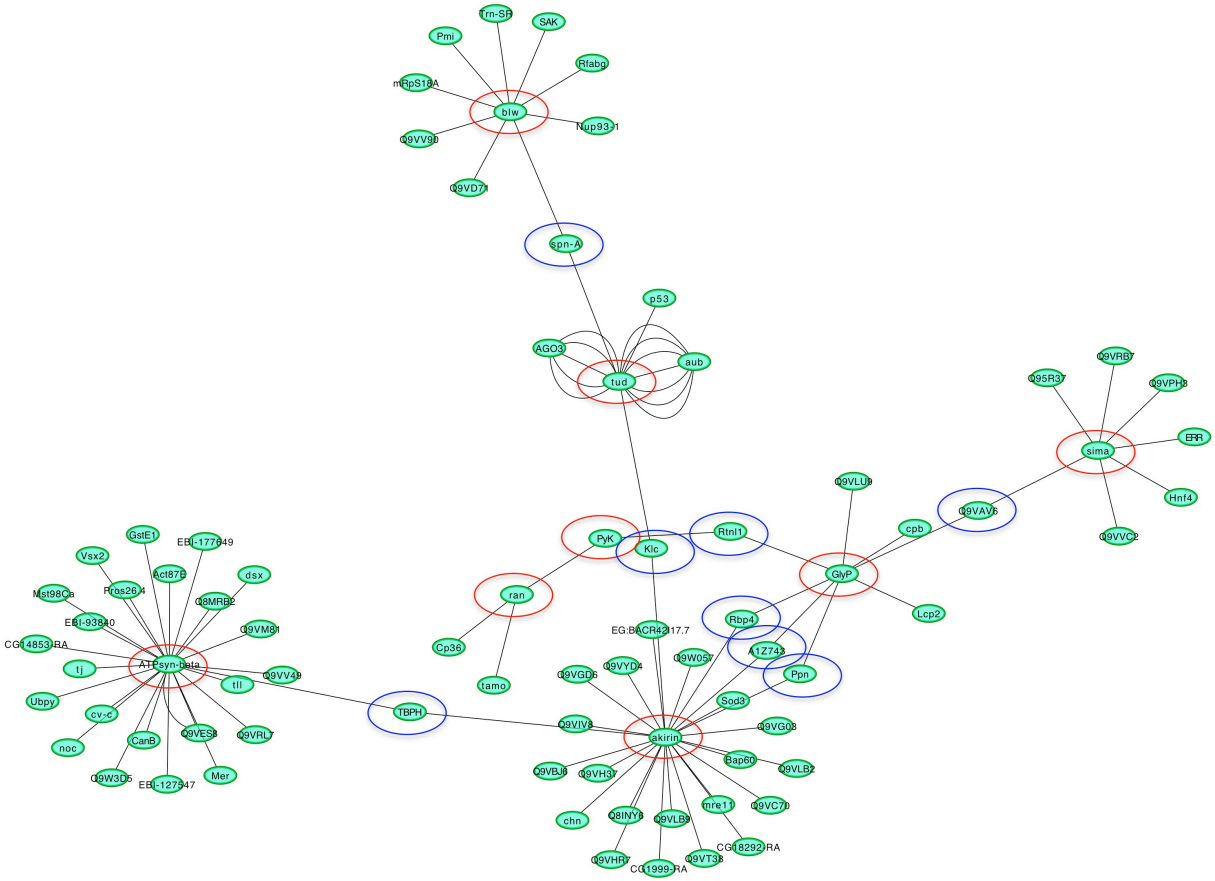
Trn-SR
SAK
Pmi
Rfabg
mRpS18A
blw
Nup93-1
Q9VV96
Q9VD71
spn-A
p53
AGO3
aub
tud
Q95R37
Q9VRB7
Q9VPH8
sima
EHR
Hnf4
Q9VVC2
Q9VAV6
Q9VLU9
cpb
PyK
Klc
Rtnl1
GlyP
Lcp2
ran
Cp36
tamo
Rbp4
EG:BACR42I17.7
A1Z743
Ppn
Q9W05X
Q9VYD4
Q9VGD6
Sod3
TBPH
Q9VIV8
akirin
Q9VGG8
Bap60
Q9VLB2
Q9VBJ0
Q9VH37
mre11
Q9VC70
chn
Q8INY1
Q9VLB9
CG18292-RA
Q9VHR7
CG11999-RA
Q9VT38
GstE1
EBI-177849
Vsx2
Act87E
dsx
Mst98Ca
Fras264
Q8MRB2
EBI-938840
Q9VM81
CG14853-RA
tj
ATPsyn-beta
tll
Q9VV49
Ubpv
cv-c
CanB
Q9VES8
Q9VRL7
noc
Q9W3D5
EBI-127547
Mer

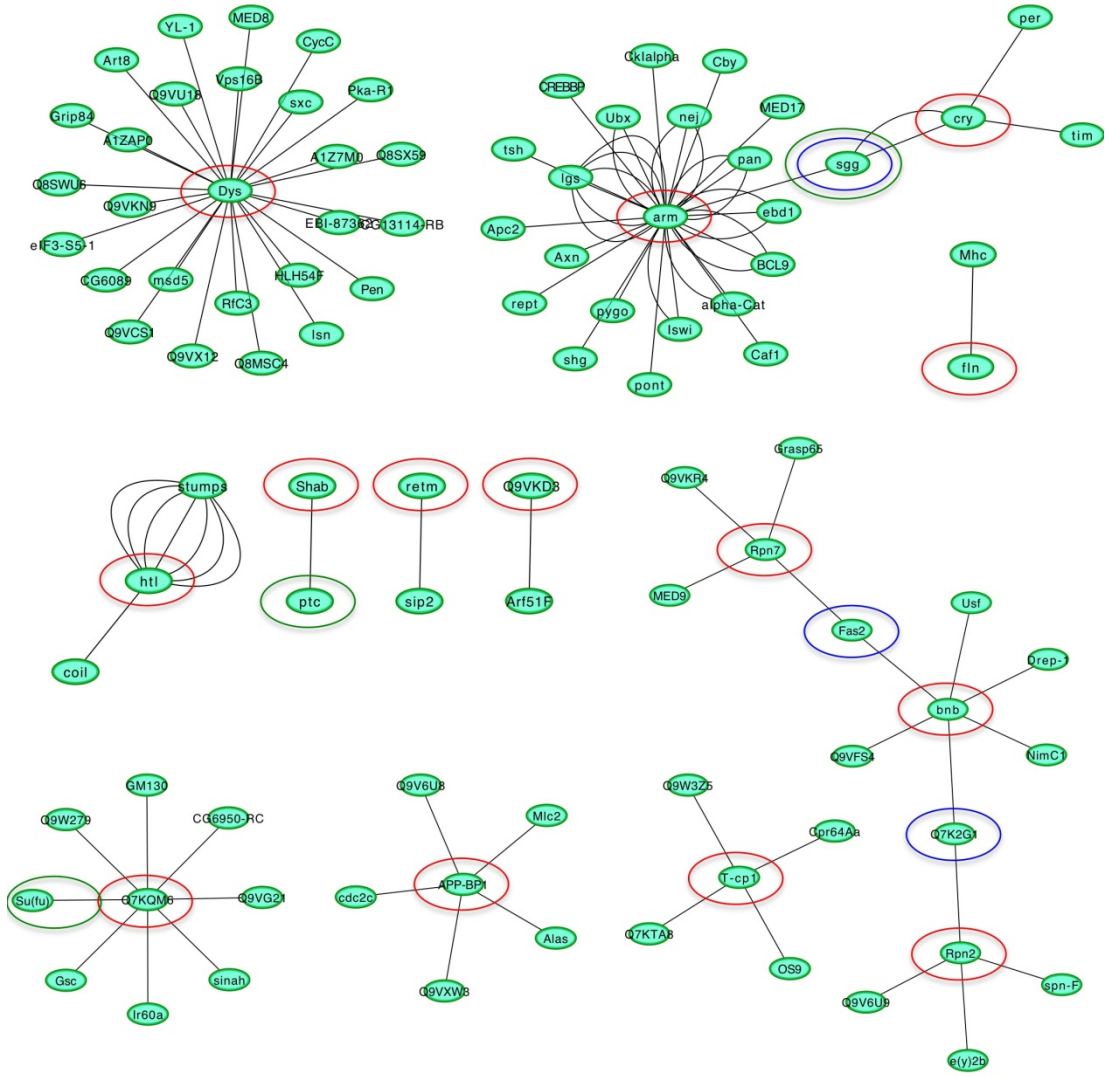

Figure 3.5: Analysis of mass spectrometry data using bioinformatics databases. Protein Network Analysis using the IntAct database. Proteins that have been identified as potential Hyd binding partners by mass spectrometry are in red circles; shared binding partners are in blue circles; proteins involved in Hh signaling are in green circles.

Table 3.2: Shared binding partners between mass spectrometry hits. Analysis of the mass spectrometry list of potential Hyd binding partners using the IntAct database reveals several shared binding partners.

Protein Name	Short name/ Uniprot ID	Binding partners	Closest human orthologue (% identity)	Function
Shaggy	Sgg P18431	arm cry	Glycogen synthase kinase 3-beta (74%) P49841	Negative regulator of the Hh and Wg pathways
Fasciclin-2	Fas2 P34082	Rpn7 bnb	Proteasomal ubiquitin receptor ADRM1 (43%) Q16186	Neuronal recognition molecule for the MP1 axon pathway
ADRM1 homolog	Q7K2G1	bnb Rpn2	Neural cell adhesion molecule 2 (28%) O15394	May function as a proteasomal ubiquitin receptor. May promote the deubiquitinating activity associated with the 26S proteasome
Rad51 homolog	Spn-A Q27297	blw tud	DNA repair protein RAD51 homolog 1 (68%) Q06609	Binds to single and double-stranded DNA and exhibits DNA-dependent ATPase activity. Underwinds duplex DNA.
Kinesin	Klc P46824	tud akirin	Kinesin light chain 1 (69%) Q07866	Microtubule-associated force-producing protein that may play a role in organelle transport
TBPH	TBPH Q8SXP8	ATP-syn beta akirin	TAR DNA-binding protein 43 (46%) Q13148	Unknown. Inferred function from homology: DNA and RNA-binding protein which regulates transcription and splicing.
RNA-binding protein 4	Rbp4 Q9VFT3	akirin GlyP	Heterogeneous nuclear ribonucleoprotein A1 (39%) P09651	Unknown. Inferred function from homology: involved in mRNA splicing.
A1Z743	A1Z743	akirin GlyP	Protein FAM46C (61%) Q5VWP2	Unknown. Inferred function from homology: enhances replication of some viruses in response to type I interferon.
Papilin	Ppn Q868Z9	akirin GlyP	Papilin (40%) O95428	Essential extracellular matrix (ECM) protein that influences cell rearrangements. May act by modulating metalloproteinases action during organogenesis.
Reticulon-like protein	Rtnl1 Q9VMV9	GlyP PyK	Reticulon-4 (38%) Q9NQC3	Unknown. Inferred function from homology: Developmental neurite growth regulatory factor with a role as a negative regulator of axon-axon adhesion and growth, and as a facilitator of neurite branching.
Q9VAV6	Q9VAV6	GlyP sima	Histone acetyltransferase KAT8 (44%) Q9H7Z6	Unknown. Inferred function from homology: Histone acetyltransferase which may be involved in transcriptional activation.

Importantly, some binding partners and/or shared binding partners were identified that are known to be directly involved in Hh signaling. For example, the potassium voltage-gated channel, Shab, interacts with Patched (Ptc), the receptor for the Hh ligand on Hh receiving cells (Nakano et al. 1989). Further to this, the protein with Uniprot identifier Q7KQM6, also known as PERQ, which has no known function as yet, interacts with Suppressor of Fused [Su(fu)]. Su(fu) regulates Ci activity by sequestering active Ci_{155} in the cytoplasm (Méthot & Basler 2000), thus preventing translocation to the nucleus and transcription of Hh target genes. This intriguing link could support the idea that Hyd negatively regulates Hh pathway activity, whereby Hyd exists in a complex with PERQ and Su(fu) and negatively regulates Ci activity. Since the function of PERQ is, as of yet, unknown, there is no reason to exclude its involvement in the Hh pathway. Finally, the kinase Shaggy (Sgg) is a shared binding partner between Cryptochrome (Cry) and Armadillo (Arm). Notably, Sgg plays a key regulatory role in both the Hh and Wg pathways, where it negatively regulates the respective transcriptional effector proteins and subsequent target gene expression (J. Jia et al. 2002; Peifer et al. 1994; Aberle et al. 1997).

In conclusion, the mass spectrometry-based screen for novel Hyd binding partners returned several potential binding partners. Although none of the hits are known to be directly involved in Hh signaling, bioinformatics analysis revealed a number of interesting links to key Hh and Wg pathway components, which in turn provides a starting point for further investigation into the molecular mechanism of Hyd-mediated Hh pathway regulation.

3.5 Biochemical verification of mass spectrometry hits

The TAP of Hyd and subsequent mass spectrometry analysis yielded a list of 26 potential novel Hyd binding partners. Although bioinformatics analysis of the dataset revealed some interesting connections of the binding partners to both Hh and Wg

signaling pathway components, there are some limitations to the mass spectrometry data that must nonetheless be considered, especially considering the relatively poor quality of the mass spectrometry data. No physiological interaction can be inferred from mass spectrometry identification alone. Therefore, experimental verification of any interaction must be performed, either in cultured cells or *in vivo*. Importantly, the low peptide count obtained for the protein hits complicates the confident selection of potential binding partners for further analysis *in vivo*. Therefore, a screening approach was taken to sift out *bona fide* Hyd binding partners from the generated MS hits, whereby expression constructs for each MS hit were either obtained or cloned for binding assays in S2 cells.

3.5.1 Binding assays using stable HSP-Hyd S2 cells and recombinant substrate expression constructs

Due to time constraints and the limited availability of resources, cloning 27 different expression constructs from scratch would have been too ambitious. Fortunately, the majority of constructs were available from the Drosophila Genetic Research Consortium (DGRC), either as sequence-verified DNA clones that were used for sub-cloning, or as HA-FLAG tagged expression constructs in a pMK33 vector containing an inducible metallothionein promoter. Obtained cDNA clones were subcloned by PCR amplification and ligation into the pGEM vector, followed by sub-cloning into a pMT Drosophila expression vector containing a carboxy-terminal V5-FLAG epitope tag. Cloning and/or expression testing of the constructs proved very time-consuming, hence the complete cloning of some expression constructs was not completed within the time-scale of the project. All expression constructs and their current status are summarized in **Table 3.3** below.

Table 3.3: Expression construct library for MS hits.

Expression construct	Size (kDa)	Status
GlyP HA-FLAG pMK33	98	Expression construct obtained; ***stable cell line generated***
Tudor HA-FLAG pMK33	110	Expression construct obtained; ***stable cell line generated***
FGFR1 HA-FLAG pMK33	84	Expression construct obtained; Difficulties with expression
Ran HA-FLAG pMK33	25	Expression construct obtained; Expression tested
ATPsynB HA-FLAG pMK33	54	Expression construct obtained; Expression tested
blw HA-FLAG pMK33	59	Expression construct obtained; Expression tested
Arm HA-FLAG pMK33	92	Expression construct obtained; ***stable cell line generated***
bnb HA-FLAG pMK33	46	Expression construct obtained; Expresses but wrong size (kDa)
Cry HA-FLAG pMK33	63	Expression construct obtained; Difficulties with expression
Flightin HA-FLAG pMK33	21	Expression construct obtained; Difficulties with expression
APP-BP1 V5-FLAG pMT	59	cDNA clone obtained; cloning into pMT V5-FLAG successful; ***stable cell line generated***
Tcp1 V5-FLAG pMT	60	cDNA clone obtained; cloning into pMT V5-FLAG successful; ***stable cell line generated***
Akirin V5-FLAG pMT	23	cDNA clone obtained; cloning into pMT V5-FLAG successful
Real-time V5-FLAG pMT	76	cDNA clone obtained; cloning into pMT V5-FLAG successful
PERQ V5-FLAG pMT	170	cDNA clone obtained; cloning into pMT V5-FLAG unsuccessful
Copia	163	cDNA obtained

Following a series of initial expression tests in S2 cells (Data not shown), a sub-set of the candidate proteins were screened for their ability to interact with HSP-Hyd. A Streptactin pulldown method was chosen for these binding assays, as it most closely resembles the TAP procedure used to generate the MS data. The Streptactin

pulldown method was chosen over HA immunoprecipitation as most of the expression constructs also contained an HA epitope tag. This involved transfection of the FLAG-tagged expression constructs into S2 cells stably expressing WT or C>A HA-Strep-tagged Hyd. Pulldown assays were performed with Streptactin-sepharose and in the same buffer used for the TAP-MS purification, in an attempt to reproduce the original binding conditions. This method yielded negative binding results for ATP synthase β, Ran, FGFR1, Armadillo, Glycogen Phosphorylase, and Tudor (Data not shown).

As an alternative approach, I therefore also employed the reciprocal co-immunoprecipitation conditions, whereby the candidate binding protein is immunoprecipitated using an anti-FLAG agarose resin. Binding to Hyd was then assessed by detection of HSP-Hyd (anti-HA antibody) in the immunoprecipitated fraction. An example of an experiment performed using this method is shown in **Figure 3.6 A**, where FLAG-tagged GlyP, Tudor, FGFR1, and Flightin were transfected into S2 cells stably expressing HA-Hyd, and immunoprecipitated using anti-FLAG beads. Unfortunately, this approach also proved uninformative due to a high level of background HA-Hyd binding to the anti-FLAG agarose resin (**Figure 3.6 A**). In addition, the expression levels of some candidate proteins were poor (e.g. FGFR1 and Flightin in **Figure 3.6 A**) and generally non-reproducible between experiments (Data not shown). In summary, difficulties with expression levels, as well as lack of reproducibility, represented the biggest obstacles to performing binding assays. Therefore, I decided to generate S2 cells stably expressing the candidate proteins to try and eliminate this variable.

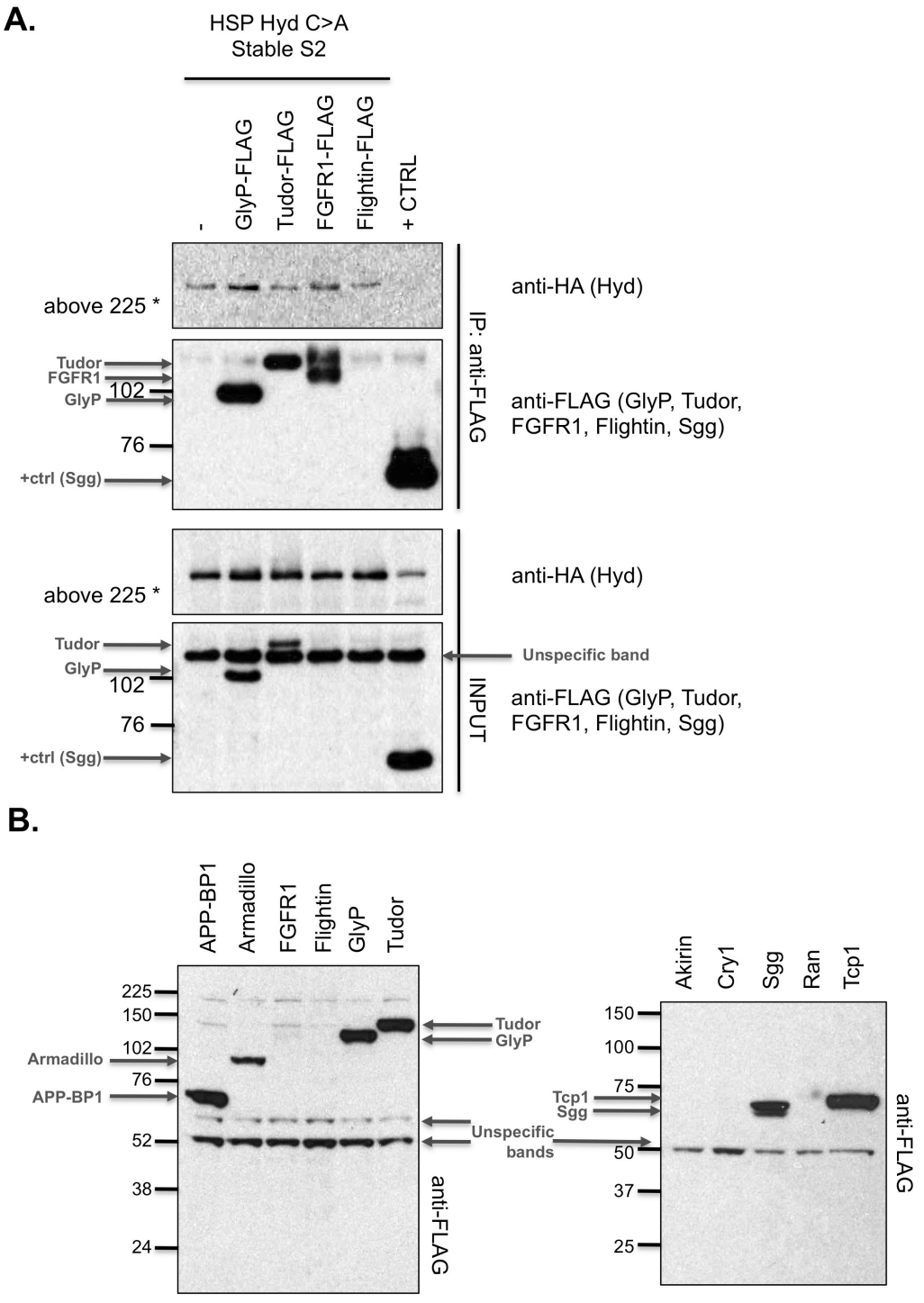

Figure 3.6: Biochemical verification of mass spectrometry protein hits. (**A**) anti-FLAG immunoprecipitation in S2 cells stably expressing HSP-Hyd C>A. Stable HSP-Hyd C>A S2 cells were transfected with GlyP-FLAG, Tudor-FLAG, FGFR1-FLAG, and Flightin-FLAG. Positive control: Sgg-FLAG. (**B**) Expression test of S2 cells stably expressing APP-BP1-FLAG, Arm-FLAG,

FGFR1-FLAG, Flightin-FLAG, GlyP-FLAG, Tudor-FLAG, Akirin-FLAG, Cry1-FLAG, Sgg-FLAG, Ran-FLAG, Tcp1-FLAG.

3.5.2 Generation of stable S2 cells expressing potential Hyd binding partners for use in binding assays

S2 cells stably expressing the candidate proteins were generated by transfecting S2 cells with the relevant expression construct and a vector containing a puromycin resistance gene in a 7:1 molar ratio. The purpose of the 7:1 ratio was to generate a population of cells that are more likely to have received the expression construct and the puromycin resistance gene, or the expression construct alone, rather than the puromycin resistance gene alone. The latter would give rise to unwanted puromycin-resistant cells, which are not expressing the construct of interest.

With some constructs, I was repeatedly unsuccessful in obtaining a surviving cell population following puromycin treatment. However, the remaining puromycin-resistant cell lines were expression tested (**Figure 3.6 B**). This revealed that only about half of the surviving cell lines were expressing the constructs of interest at detectable levels. As a result, S2 cells stably expressing FLAG-tagged APP-BP1, Armadillo, GlyP, Tudor, and Tcp1 were successfully generated, whereas the generation of stable FGFR1, Flightin, Akirin, Cry1, and Ran cell lines was deemed unsuccessful (**Figure 3.6 B**).

3.5.3 Hyd interacts with Armadillo

The successfully generated S2 stable cells expressing a subset of the Hyd MS hits were subsequently used in binding assays in a further attempt to verify a physical interaction with Hyd. To maximize expression levels of the candidate binding partners, binding assays were performed by combining lysates of HSP-Hyd WT

stable cells with lysates of S2 cells stably expressing FLAG-tagged APP-BP1, Armadillo, GlyP, Tudor and Tcp1. The lysates were then subjected to a Streptactin pulldown, and the eluted material was probed for the candidate binding proteins (anti-FLAG) (**Figure 3.7 A**). As a negative control, lysates expressing the FLAG-tagged proteins were also incubated with Streptactin resin and S2 cell lysates lacking HSP-Hyd. To confirm that the assay conditions were capable of detecting a Hyd interaction I used two potential positive binding controls inferred from published EDD interactants: Sgg (Hay-Koren et al. 2011) and Tob (Lim et al. 2006). Although some background issues were encountered, both Tob and Sgg signals were increased upon HSP-Hyd purification (**Figure 3.7 A**). The expression levels of all candidate proteins in the lysate input control (lower panel, **Figure 3.7 A**) was sufficient, except for GlyP, which failed to express. One explanation for this is that the S2 stable cells have expelled the GlyP expression construct following generation of the cell line, resulting in S2 cells that are resistant to puromycin but no longer express the protein of interest. In the StrepTactin Pulldown (upper panel, **Figure 3.7 A**), HSP-Hyd was successfully pulled down, but no binding was observed with GlyP and Tudor, although the negative binding result with GlyP is almost certainly due to lack of its expression. Both APP-BP1 and Tcp1 were detected in the HSP-Hyd pulldown fraction, however a high level of background binding to the Streptactin resin in the negative S2 control (upper panel, **Figure 3.7 A**) suggests that both of these binding results are also negative. However, Armadillo was found to bind to Hyd at a level that was significantly above a small background binding level in the negative control, suggesting that Armadillo may be a *bona fide* Hyd binding partner (upper panel, **Figure 3.7 A**). These results therefore indicate that Hyd does not appear to interact with APP-BP1, Tcp1, whereas binding to GlyP could not be determined in this experiment.

In order to verify the Armadillo:Hyd interaction in an independent experiment, I performed an endogenous immunoprecipitation experiment in *Drosophila* Clone 8 (Cl8+) cells. Cl8+ cells were originally derived from wing imaginal discs (Currie et al. 1988), and, unlike S2 cells, are capable of transducing both the Hh and Wg

pathways (Lum et al. 2003; DasGupta et al. 2005). Hyd was successfully immunoprecipitated using the anti-EDD M-19 antibody (**Figure 3.7 B**). This antibody was raised against the HECT domain of EDD, but due to high sequence conservation between the Hyd and EDD HECT domains, the antibody is also capable of recognising Hyd. Both the anti-Hyd and the negative control (IgG) immunoprecipitated fractions were probed with an anti-Armadillo antibody, confirming the endogenous interaction between Armadillo and Hyd (**Figure 3.7 B**). In summary, these experiments strongly suggest that Hyd interacts with Armadillo, and may therefore also play a role in the Wg pathway.

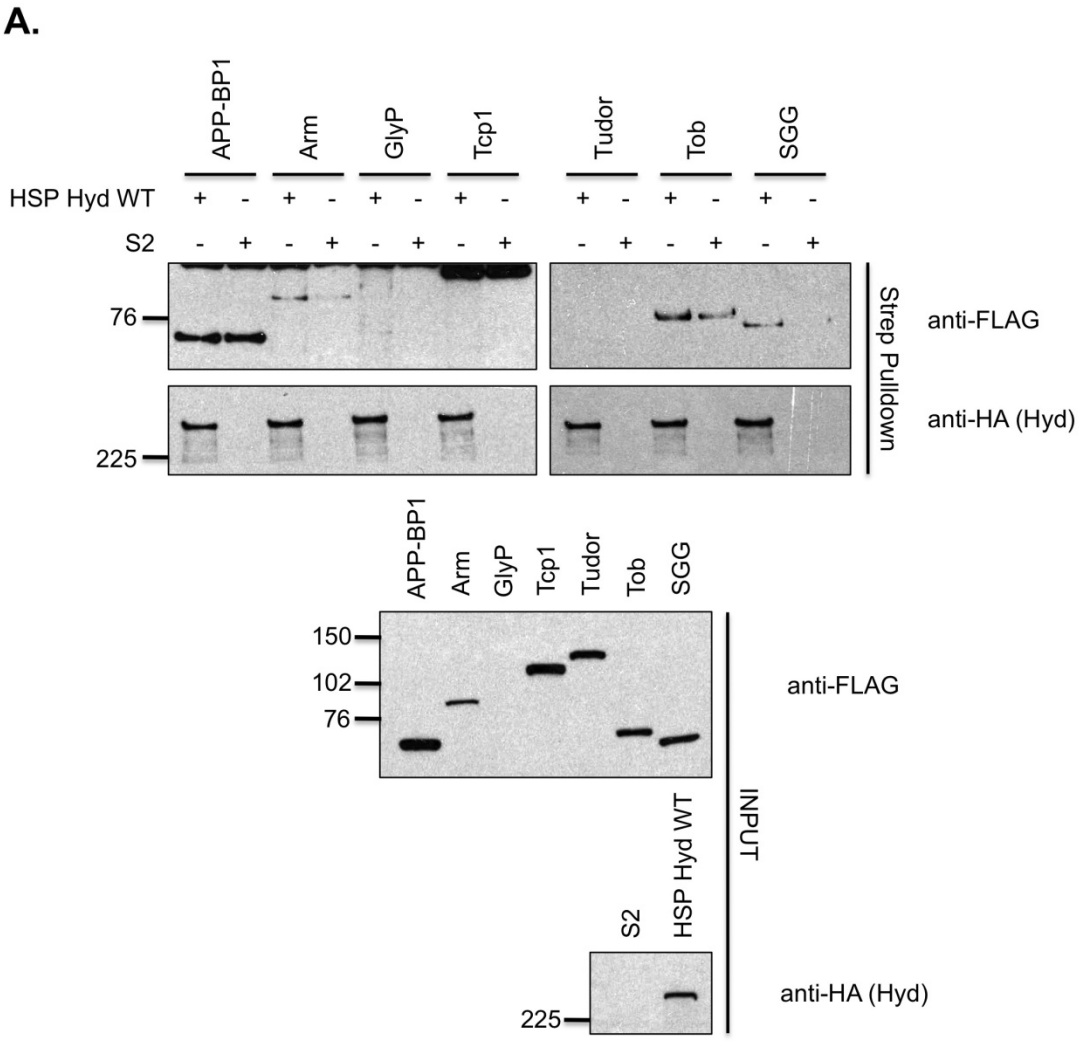

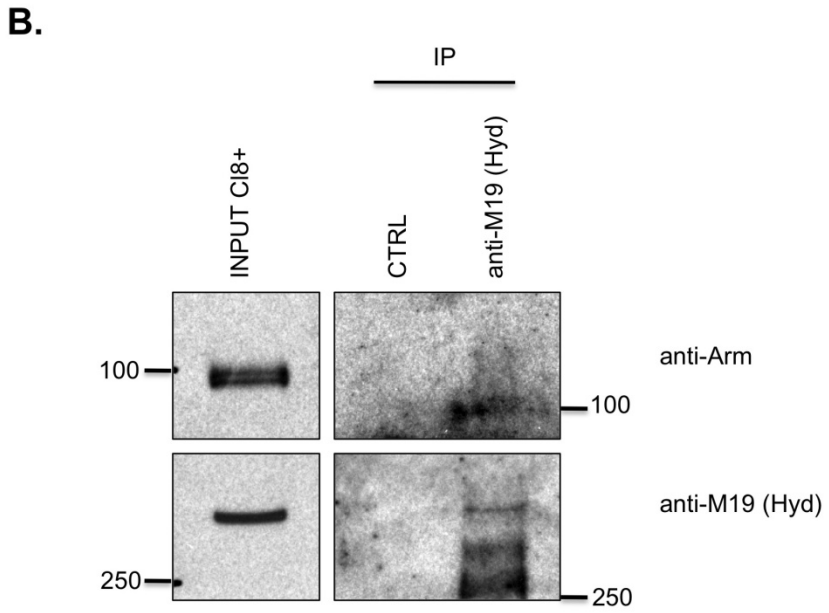

Figure 3.7: Hyd interacts with Armadillo. (**A**) StrepTactin pulldown in S2 cells. S2 cells were transfected with APP-BP1-FLAG, Arm-FLAG, GlyP-FLAG, Tcp1-FLAG, Tudor-FLAG, Tob-FLAG, and Sgg-FLAG, and lysed after 48 hours. S2 cells stably expressing HSP-Hyd were lysed separately (non-transfected S2 cells were also lysed separately and used as a negative control). Each S2 lysate containing an over-expressed FLAG-tagged protein was combined 1:1 with the HSP-Hyd cell lysate, or the negative control lysate, and combined lysates were subjected to a StrepTactin pulldown. (**B**) anti-Hyd (M19) immunoprecipitation in S2 cells. Endogenous Hyd was immunoprecipitated with antti-M19, followed by Protein A agarose. Negative control = IgG.

3.6 Phage Display approach to identify Hyd binding partners

As an alternative, as well as complementary, approach to identify novel Hyd binding partners, a phage display screen using recombinant protein encoding the Hyd HECT domain as the bait had been carried out previously in the laboratory (Mark Ditzel). This yielded 50 12-mer peptides that represented potential Hyd-HECT binding peptides (**Table 3.4**).

The phage display method utilises genetically modified bacteriophages - viruses that infect bacteria. A gene encoding the protein or peptide of interest (e.g. a cDNA or peptide library) is inserted into a phage coat protein gene (Smith 1985). The

bacteriophage is then allowed to infect bacteria (e.g. *E. coli*), which results in its multiplication and the subsequent lysis of the bacteria. Importantly, the new bacteriophage particles now "display" the protein of interest as a coat protein (Smith 1985). These phage particles, displaying a mixture of proteins from a cDNA/peptide library, can then be screened against a recombinant protein immobilised on a slide, which in this case was the recombinant Hyd-HECT fragment, containing the PABC and HECT domains. Unbound bacteriophages are washed off and bound bacteriophages are sequenced to identify the binding peptides/proteins (Kehoe & Kay 2005).

To confirm the binding of these peptides to Hyd, I performed an ELISA in which the peptides, along with mutagenised versions of the parent peptides, were immobilised onto glass slides and assessed for their ability to bind recombinant Hyd protein. The aim of the peptide verification ELISA was to identify peptide sequences that have a high binding affinity for Hyd, and subsequently use bioinformatics to match these peptide sequences to potential novel Hyd binding partners and/or the MS hits. The presence of a binding peptide sequence in an existing MS hit would not only increase the confidence of the hit, but also provide valuable information on the location and nature of the interaction between Hyd and the protein of interest.

Table 3.4: Phage Display Synthetic Peptide Sequences.

Peptide identifier	Amino Acid Sequence	Mutagenised peptide sequences & identifiers
1	AFHTSSMIFPSH	-
2	AFTHTSSMIFPSH	AFTHTSAAIFPSH (83) AFTHTSSMAAPSH (84) AFTHTSSMIFASH (85)
3	DNYVPSVTGDRW	-
4	ESFWPQLDVGLS	ESFWPQLDAALS (61) ESFWPQLDAAAA (63) ESAAPQLDVGLS (146) ESFWAALDVGLS (147) ESFWPQAAVGLS (148) ESFWPQLDAGLS (149)
5	FFTSLIARSH	AATSLIARSH (143) FFAALIARSH (144) FFTSAAARSH (145)

Peptide identifier	Amino Acid Sequence	Mutagenised peptide sequences & identifiers
6	FGKNIPNPTLV	FGKNAANPTLV (119) FGKNIPAATLV (120) FGKNIPNPAAV (121)
7	FQGEKIIIAILL	-
8	GGYSMPHAECSV	-
9	GLKIWSFPPHHG	AAKIWSFPPHHG (86) GLAAWSFPPHHG (87) GLKIAAFPPHHG (88) GLKIWSAAPHHG (89) GLKIWSFAAHHG (90) GLKIWSFPPAAG (91) GLKIWSFPPHHA (92)
10	GLKVPSSPLWDG	AAKVPSSPLWDG (93) GLAAPSSPLWDG (94) GLKVAASPLWDG (95) GLKVPSAALWDG (96)
11	GLRLSLMDDAYR	GLRAALMDDAYR (132) GLRLSAADDAYR (133) GLRLSLMAAAYR (134)
12	GLYFGVCRRFCG	-
13	HESLGYVPHQKL	AASLGYVPHQKL (53) HEAAGYVPHQKL (54) HESLAAVPHQKL (55) HESLGYAPHQKL (56)
14	HETLHYLEHRSW	AATLHYLEHRSW (57) HEAAHYLEHRSW (58) HETLAALEHRSW (59) HETLHYAEHRSW (60)
15	HFSRSLYVGASA	HFSRSLYAAASA (62) HFSRSLYVGAAA (64) HAARSLYVGASA (150) HFSAALYVGASA (151) HFSRSAAVGASA (152) HFSRSLYAGASA (153)
16	HHASHAYIDSQP	-
17	HHGHSPTSPQFG	AAGHSPTSPQFG (122) HHAASPTSPQFG (123) HHGHAATSPQFG (124) HHGHSPAAPQFG (125) HHGHSPTSAAFG (126)
18	HHGHSPTSPQVR	AAGHSPTSPQVR (127) HHAASPTSPQVR (128) HHGHAATSPQVR (129) HHGHSPAAPQVR (130) HHGHSPTSAAVR (131)
19	HHIIVLRLLRFG	HHIIVLRAARFG (77) HHIIVLRLLAAG (78) HHIIVLRLLRFA (79)
20	HNHMHYNQGPKT	HAAMHYNQGPKT (65) HNHAAYNQGPKT (66) HNHMHANQGPKT (67) HNHMHYNAAPKT (139) HNHMHYNQGAAT (140)
21	HVKKLYRNPPRA	-

Peptide identifier	Amino Acid Sequence	Mutagenised peptide sequences & identifiers
22	KIFIRRGILLV	-
23	KIWQGHLYVHDQ	AAWQGHLYVHDQ (100) KIAAGHLYVHDQ (101) KIWQAALYVHDQ (102) KIWQGHAYVHDQ (103)
24	KIWQGHPSPHNM	AAWQGHPSPHNM (104) KIAAGHPSPHNM (105) KIWQAAPSPHNM (106) KIWQGHASPHNM (107)
25	KIWQGLLVRIIC	AAWQGLLVRIIC (108) KIAAGLLVRIIC (109) KIWQAALVRIIC (110) KIWQGLAVRIIC (111)
26	KIWQGLPLFPPI	AAWQGLPLFPPI (112) KIAAGLPLFPPI (113) KIWQAAPLFPPI (114) KIWQGLALFPPI (115)
27	KVFLLPNPPLPT	KVFLAANPPLPT (116) KVFLLPAAPLPT (117) KVFLLPNPAAPT (118)
28	LIRGMRRGSFRF	-
29	LLHYQFILLRF	-
30	LLYIHASFIANG	-
31	LPFLHNTPPSFW	-
32	LYTALSGPKA	LYTALAAPKA (141) LYTALSGAAA (142)
33	NATSQRPVHIAQ	-
34	NLFISFHPVRA	-
35	PYNRYPSLLRFG	PYNRYPSAARFG (80) PYNRYPSLLAAG (81) PYNRYPSLLRFA (82)
36	QHANHQAWNNLR	-
37	QSAHSKIRSYD	QSAHAAIRSYD (71) QSAHSKAASYD (72) QSAHSKIRAYD (73)
38	RTLMYAKVVSE	RTLAAAKVVSE (137) RTLMYAAVVSE (138)
39	SFDNRASMIRSR	SFDNRAAAIRSR (74) SFDNRASMAASR (75) SFDNRASMIRAR (76)
40	SHLHYHVHPGLK	AALHYHVHPGLK (68) SHAAYHVHPGLK (69) SHLHAHVHPGLK (70)
41	SSHHQKILPPPS	-
42	SVSMYMKPSPRP	SVSAAMKPSPRP (135) SVSMYAAPSPRP (136)
43	TGRNDAAPSPIG	-
44	TQYDKRLPPHHG	TQYDKRLAAHHG (97) TQYDKRLPPAAG (98) TQYDKRLPPHHA (99)
45	TVKSVQSLKHRL	-
46	WDPSHGISSRDG	-
47	FSHELSWKPRKA	-

Peptide identifier	Amino Acid Sequence	Mutagenised peptide sequences & identifiers
48	AFGPDSTTPPEP	-
49	ALHPLTNRYHAT	-
50	SNFTTQMTFYTG	-

3.6.1 Purification of recombinant Hyd from bacterial cells

The ELISA verification assay requires the use of purified recombinant protein at a concentration of 1-2 μM. The original phase display screen was carried out using the recombinant Hyd HECT domain, comprising of a large portion of the carboxy terminal of the protein (aa 2315-2885), which includes both the PABC and HECT domains. However, recombinant full length Hyd can also be used for binding in the ELISA, and this may even enhance the interaction with some peptides if other regions of Hyd are also involved in peptide recognition.

In order to produce recombinant Hyd HECT and FL Hyd proteins, the corresponding GST-tagged constructs, which had already been cloned in the lab, were transformed into bacterial cells. Protein expression was induced using IPTG, cells were lysed, and the lysates were clarified by centrifugation prior to purification of the GST-tagged recombinant proteins using GSH sepharose (see Materials and Methods). The large Hyd HECT domain was detected at the expected weight of ~100 kDa in all fractions following IPTG induction on a silver stained gel (**Figure 3.8 A**). The purified fraction contained a relatively large amount of Hyd HECT domain, and was mostly free of contaminating proteins apart from a few proteins running below the Hyd HECT band (**Figure 3.8 A**). However, these bands could represent degradation products of the recombinant Hyd HECT protein, which retain the amino terminal GST tag and are therefore present in the GSH pulldown fraction. This could be due to the presence of contaminating proteases, or alternatively the spontaneous hydrolysis of the protein. Contrary to the Hyd HECT domain, full-length

recombinant Hyd protein was not detected by silver staining (**Figure 3.8 A**). The samples were therefore probed with the anti-M19 Hyd antibody on a Western blot, which is an even more sensitive detection method compared to silver staining. This revealed that GST-FL Hyd was successfully expressed and purified from bacterial cells, albeit at very low levels (**Figure 3.8 B**). At 319 kDa, Hyd is a very large protein, and it is therefore not surprising that its expression and purification from bacterial cells results in low protein yields. The low expression level could be due to misfolding and subsequent degradation of FL Hyd during and/or after protein expression. The expression of high levels of recombinant protein in *E. coli*, especially large proteins, commonly leads to the formation of insoluble particles called inclusion bodies, which consist of partially folded aggregates of the protein of interest. There are several methods, which could potentially increase the solubility and thus yield of full-length recombinant Hyd by promoting correct protein folding, including expression as a fusion protein, co-expression with molecular chaperones, and the use of multiple constructs for each protein (Peleg & Unger 2012).

3.6.2 Verification of binding by peptide ELISA

As full length Hyd was poorly expressed and produced low yields, the extended Hyd HECT domain, which had a much better yield, was subsequently used in the ELISA. To assess binding of the recombinant Hyd HECT domain to the phage display peptides, the relevant synthetic peptides were spotted onto glass slides (**Figure 3.8 C**), along with mutagenised versions of some of the peptides, in which selected residues were replaced with alanine (Ala, A) (**Table 3.3**). The glass slides were incubated with the purified recombinant Hyd HECT protein and subsequently washed off. Retained peptide-bound Hyd HECT was detected by Western blotting. Two identical slides were processed in duplicate, and the binding results are shown in **Figure 3.8 D**. Binding intensity wad judged by eye, whereby white spots indicate no binding, black spots indicate strong binding, and varying levels of grey represent a scale of weak to medium binding affinity. Following visual assessment of all spots on both slides, and taking into account both the parent and respective mutagenised

peptides, five peptides in particular were found to interact with Hyd to varying degrees. These peptides and the accompanying mutagenised sequences are boxed and colour coded in **Figure 3.8 C** and **D**, and the relevant peptides numbers are 10, 14, 23, 26 and 27 (**Table 3.3**). Interestingly, mutation of any of the residues in peptide 14 results in complete abrogation of the strong binding observed with the parent peptide, suggesting that this peptide sequence may represent a highly conserved Hyd binding motif (**Figure 3.8 D; yellow boxes**). On the other hand, some of the peptides that bound the Hyd HECT protein with a medium affinity appeared to have a higher binding affinity towards the protein following mutation of certain residues (peptides 23, 26 and 27; **Figure 3.8 D;** green, red and purple boxes, respectively). A comparative analysis was performed between the relevant binding level of the parent peptide and the mutagenised peptides (i.e. comparable, stronger, weaker or no binding) to determine the relative importance of individual residues for effective binding to the Hyd HECT domain protein. The combined results of this analysis are summarized in **Table 3.4**, where residues coloured in grey are less important for binding, and residues highlighted in bold are indispensable for binding.

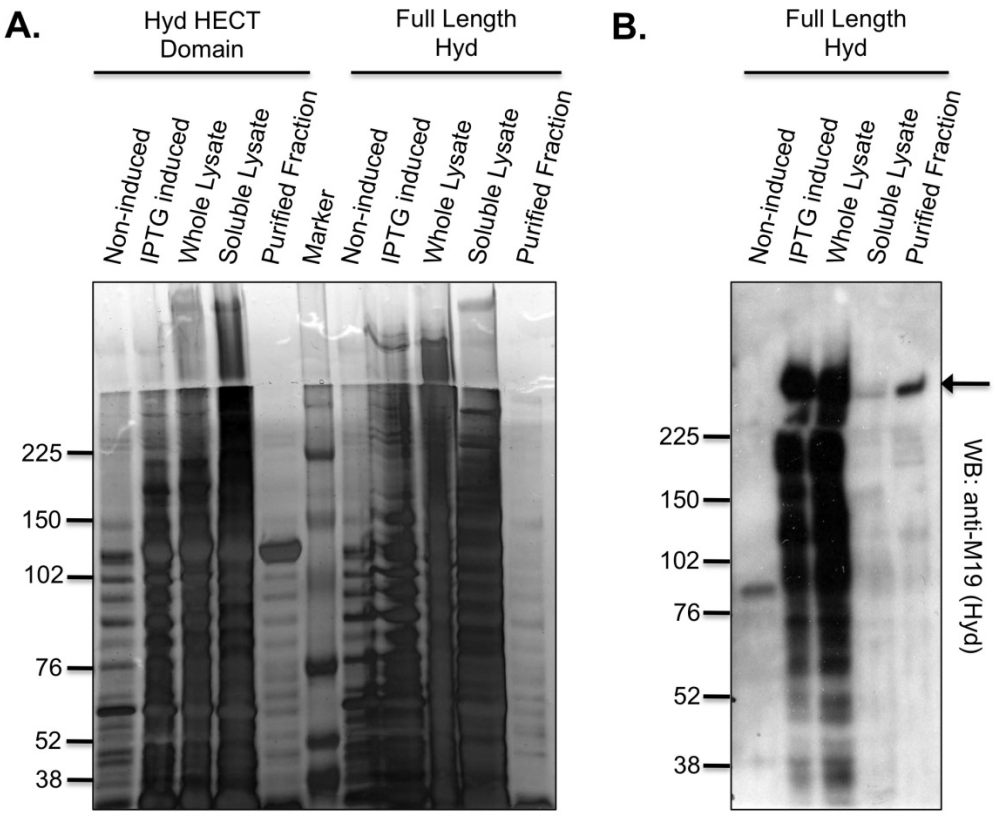
A.
Hyd HECT Domain
Full Length Hyd
Non-induced
IPTG induced
Whole Lysate
Soluble Lysate
Purified Fraction
Marker
Non-induced
IPTG induced
Whole Lysate
Soluble Lysate
Purified Fraction
225
150
102
76
52
38
B.
Full Length Hyd
Non-induced
IPTG induced
Whole Lysate
Soluble Lysate
Purified Fraction
225
150
102
76
52
38
WB: anti-M19 (Hyd)

C.

•	•	•	•	•	•	•	•	•	•	•	•	•	•	•	•	•	•	•	•	•	•
•	1	2	3	4	5	6	7	8	9	10	11	12	13	14	15	16	17	18	19	20	•
•	1	2	3	4	5	6	7	8	9	10	11	12	13	14	15	16	17	18	19	20	•
•	21	22	23	24	25	26	27	28	29	30	31	32	33	34	35	36	37	38	39	40	•
•	21	22	23	24	25	26	27	28	29	30	31	32	33	34	35	36	37	38	39	40	•
•	41	42	43	44	45	46	47	48	49	50	51	52	53	54	55	56	57	58	59	60	•
•	41	42	43	44	45	46	47	48	49	50	51	52	53	54	55	56	57	58	59	60	•
•	61	62	63	64	65	66	67	68	69	70	71	72	73	74	75	76	77	78	79	80	•
•	61	62	63	64	65	66	67	68	69	70	71	72	73	74	75	76	77	78	79	80	•
•	81	82	83	84	85	86	87	88	89	90	91	92	93	94	95	96	97	98	99	100	•
•	81	82	83	84	85	86	87	88	89	90	91	92	93	94	95	96	97	98	99	100	•
•	101	102	103	104	105	106	107	108	109	110	111	112	113	114	115	116	117	118	119	120	•
•	101	102	103	104	105	106	107	108	109	110	111	112	113	114	115	116	117	118	119	120	•
•	121	122	123	124	125	126	127	128	129	130	131	132	133	134	135	136	137	138	139	140	•
•	121	122	123	124	125	126	127	128	129	130	131	132	133	134	135	136	137	138	139	140	•
•	141	142	143	144	145	146	147	148	149	150	151	152	153								•
•	141	142	143	144	145	146	147	148	149	150	151	152	153								•
•	•	•	•	•	•	•	•	•	•	•	•	•	•	•	•	•	•	•	•	•	•

D.

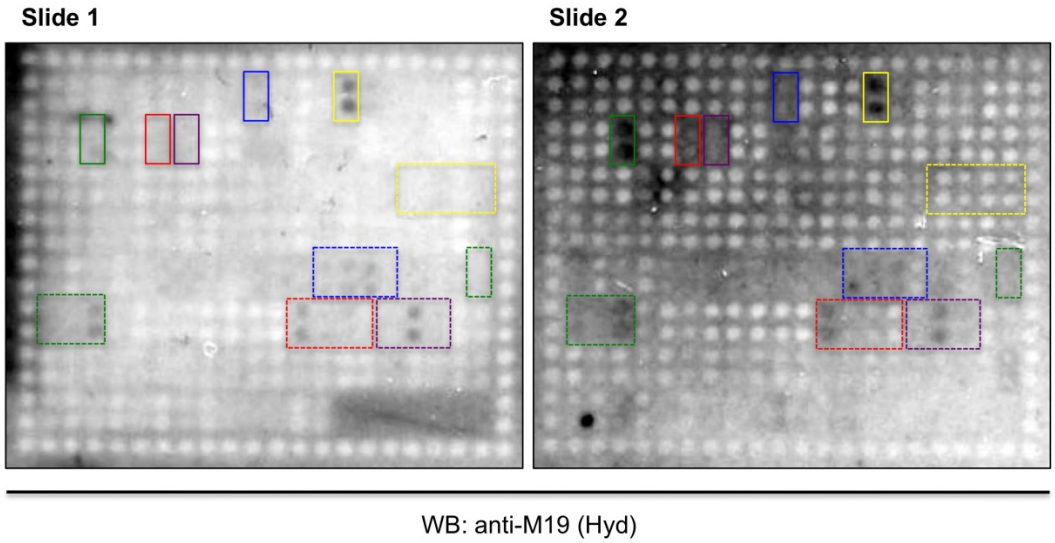

Figure 3.8: Verification of Hyd HECT domain binding peptides. (**A**) Silver stain analysis of recombinant production of GST-Hyd HECT domain and full-length (FL) GST-Hyd in E.coli. GST-tagged proteins were purified and eluted using reduced glutathione (GSH) agarose and GSH, respectively. (**B**) Immunoblot analysis of recombinant production and purification of FL GST-Hyd in E.coli. Black arrow indicates position of GST-Hyd. (**C**) GRID layout of peptide slides. Refer to Table 3.3 for sequence information. (**D**) Immunoblot analysis of ELISA assay showing successful binding of recombinant Hyd HECT domain to peptides indicated by coloured boxes – refer to panel C for petide number and Table 3.3 for sequence information). Lower panel of slide corresponds to mutagenised peptides (corresponding wild type peptides in colour-coded boxes). Slides containing immobilised peptides were incubated with recombinant Hyd-HECT protein. Slides were washed to remove excess

protein, and probed with anti-M19 (Hyd) antibody to detect bound Hyd-HECT. Each spots represents one peptide identity, and each peptide was spotted in duplicate.

3.6.3 Analysis of binding peptides using the protein BLAST algorithm

In order to identify potential novel Hyd binding partners and/or any of the existing MS protein hits that may contain parts of the binding peptide sequences, the NCBI proteinBLAST algorithm was used to align the identified peptide sequences to the *D. melanogaster* proteome. Interestingly, this led to the identification of two of the MS hits, as well as several other proteins directly related to both Hh and Wg signaling (**Table 3.5**). The sequences of peptides 23 and 27 were part aligned with the Tudor and Cry-1 amino acid sequences, respectively (**Table 3.5**). This result increases the confidence level for these MS hits to be bona fide Hyd binding partners. Additionally, Dyrk2/smi35A, Ci, and Roadkill, which are all involved in the Hh pathway, were also identified (**Table 3.5**). Roadkill forms a key part of the E3 ligase complex responsible for degrading the transcriptional effector protein Ci (see **Chapter 1, Section 1.2.4**), and an interaction between Hyd and these proteins could indicate a potential regulatory mechanism by which Hyd negatively regulates the Hh pathway. Finally, the key eye-specific transcription factor Atonal (see **Chapter 1, Section 1.2.5.2**), as well as the Wg pathway proteins Frizzled and Axin (see **Chapter 1, Section 1.3.1**) were also identified (**Table 3.5**), supporting the hypothesis that Hyd plays an important role in the development of the *Drosophila* eye by regulating more than one morphogen pathway.

Table 3.5: Peptide ELISA Results. A selection of potentially relevant protein hits from the pBLAST analysis using phage display peptides.

Peptide identifier	Sequence	Protein hits (Uniprot identifier)	pBLAST alignment peptide vs. protein hit (a.a. coordinates)	E-value
10	GLKVPS**SP**LWDG	Protein roadkill (Q9VFP2.2)	4 VPSSPL 9 VPS PL 461 VPSPPL 466	**94**
14	**HETLHYL**EHRSW	General odorant-binding protein 57b (Q8MKJ4.1)	1 HETLHYL 7 HETL YL 56 HETLDYL 62	**5**
		Protein atonal (P48987.2)	1 HETLH 5 HETL+ 294 HETLQ 298	**169**
23	KIWQGHLYVHDQ	Frizzled-4 (Q9NBW1.2)	6 HLYV 9 HLYV 203 HLYV 206	**126**
		Maternal protein tudor (P25823.2)	5 GHLY 8 GHLY 470 GHLY 473	**169**
26	KIWQGL**P**LFPPI	Cubitus interruptus (P19538.2)	8 LFPP 11 LFPP 1297 LFPP 1300	**169**
			5 GLPL 8 GLPL 615 GLPL 618	**169**
		Dyrk2 (Q9V3D5.1)	5 GLPLFP 10 G PLFP 394 GFPLFP 399	**70**
27	KVFLLPNPPLPT	Protein roadkill (Q9VFP2.2)	6 PNPPLP 11 P PPLP 462 PSPPLP 467	**22**
		Cryptochrome-1 (O77059.1)	3 FLLPNPPLP 11 F LPN LP 249FYLPNQALP257	**70**
			8 PPLPT 12 PP PT 171 PPRPT 175	**2380**
		Axin (Q9V407.1)	5 LPN—PPLP 11 LP PPLP 652LPHQPPPLP 660	**70**

3.7 Discussion

In an effort to identify novel Hyd binding partners that form part of a potential molecular mechanism in the negative regulation of Hh pathway activity and/or *hh* gene expression, I employed several complementary experimental and bioinformatic approaches. Firstly, in a literature-based approach, I tested the binding of Hyd to the EDD binding protein Dyrk2, a kinase involved in the mammalian Shh pathway. This revealed that, although Hyd does not interact with Dyrk2, it may interact with the close Dyrk2 homologue Dyrk3. Secondly, I performed a tandem affinity pulldown of Hyd from *Drosophila* S2 cells in conjunction with mass spectrometry, which identified 26 potential novel Hyd binding partners. Although subsequent bioinformatics, biochemical and peptide ELISA approaches generated some interesting data which identifies several potential Hyd binding partners, some of which are also involved in morphogen signaling, the only successfully verified interaction was shown between Hyd and the Wg pathway transcriptional effector Armadillo.

3.7.1 Hyd and DYRK2 family kinases

My results indicate that *Hs* Dyrk2 and *Dm* Dyrk2 (smi35) do not interact with Hyd, even though I was able to replicate the previously published interaction between EDD and *Hs* Dyrk2 (Maddika & J. Chen 2009). *Hs* Dyrk2 negatively regulates the Shh pathway by phosphorylating and negatively regulating Gli protein stability, indicating that phosphorylation of Gli proteins by Dyrk2 contributes to the ubiquitylation and proteolytic processing of Gli proteins (Varjosalo et al. 2008). In addition, it was shown to act as a scaffold protein, which is required for the formation of an E3 ubiquitin ligase complex, containing the Cul4-Roc1 family members DDB1 and VPRBP, and EDD. This E3 ligase complex appears to regulate mitotic transition by promoting the phosphorylation (requiring Dyrk2) and subsequent ubiquitylation (requiring EDD) and proteasomal degradation of the microtubule-severing enzyme katanin (Maddika & J. Chen 2009). Because the

expression levels of transfected *Dm* Dyrk2-FLAG were suboptimal in S2 cells, I used human HEK293 cells to test the interaction between *Dm* Dyrk2 and Hyd instead. This experiment suggested that no interaction between the two proteins takes place. However, if the interaction is not binary, and both proteins interact as part of an E3 ligase complex, requiring the presence of DDB1 and VPRBP, this may explain the negative binding result. DDB1 and VPRBP both have homologues in *Drosophila melanogaster*. As determined by the protein BLAST algorithm, the Dm DDB1 homologue (Uniprot identifier Q9XYZ5) shares 61% sequence homology with the human protein, whereas the Dm VPRBP homolog, also known as protein mahjong (Uniprot identifier Q9W2F2), shares only 38% sequence identity with its human counterpart. As a result, the experiment may be improved by over-expressing Dm DDB1 and Dm mahjong together with Hyd and *Dm* Dyrk2 in HEK293 cells to assess whether they act as intermediate proteins required for a potential interaction between Hyd and *Dm* Dyrk2. Importantly, it is not known whether the phosphorylation of Gli2 by *Hs* Dyrk2 also requires E3 ligase complex formation, including EDD, DDB1 and VPRBP. This would indicate that EDD contributes to the ubiquitylation and processing of Gli proteins in addition to the known E3 ligase protein targeting Gli, βTrcP (Bhatia et al. 2006). Conversely, if Dyrk2 does not act as part of an E3 ligase complex to phosphorylate Gli2, this would indicate that EDD is not involved in this process. These hypotheses could be tested using a suitable cell based assay, such as a luciferase reporter assay in a cell line that is capable of transducing the Hh pathway (e.g the Drosophila wing disc-derived cell line Clone 8), in combination with RNAi, to assess whether Dyrk2 regulates the Hh pathway in *Drosophila*, and whether this requires Hyd, DDB1, and mahjong.

Intriguingly, the negative binding result between Hyd and *Dm* Dyrk2 prompted me to investigate the existence of other *Drosophila* Dyrk2 homologues, and led to the discovery that *Dm* Dyrk3 is in fact more closely related to *Hs* Dyrk2 than *Dm* Dyrk2 (smi35) based on sequence identity. Although a binding assay with *Dm* Dyrk3 and Hyd in S2 cells proved inconclusive, the result suggested that the presence of WT Hyd, but not catalytic inactive Hyd (C>A), increases *Dm* Dyrk3 protein levels. The

increase in *Dm* Dyrk3 activity could be due to an increase in expression levels and/or increased protein stability, and appears to be dependent on Hyd's E3 ligase activity. This raises the possibility that Hyd could increase *Dm* Dyrk3 protein stability through non-degradative ubiquitylation, analogous to the stabilization of β-catenin as a result of EDD ubiquitylation (Hay-Koren et al. 2011). In order to test this hypothesis, a ubiquitylation assay could be used to test wether Hyd can ubiquitylate Dyrk3, as well as assessing *Dm* Dyrk3 protein levels by inhibiting protein synthesis using cycloheximide, and testing the effect of Hyd over-expression and/or knockdown on Dyrk3 protein turn-over.

The complementary phage display peptide ELISA screen yielded some interesting results, including the notion that the large carboxy terminal region of Hyd, including the PABC and HECT domains, binds to the peptide motif GXPLFP. Bioinformatics analysis identified this motif in *Dm* Dyrk2 (GFPLFP, see Table 3.4). Interestingly, a similar motif is found in *Dm* Dyrk3 (GHALFP), and both motifs are located in the respective kinase domains of *Dm* Dyrk2 and *Dm* Dyrk3. If further work were to be dedicated to assessing whether Hyd can interact with either of these proteins, this data would provide valuable hints concerning the positional nature of a possible interaction between Hyd and the Dyrks in *Drosophila*.

3.7.2 Hyd and Glucose Homeostasis

In a separate approach to identifying novel Hyd binding partners, I employed a mass spectrometry screen of endogenously bound proteins complexed to an amino terminally tagged Hyd protein that was stably expressed in S2 cells and subsequently pulled down using a tandem affinity purification (TAP) procedure. Although the peptide scores for individually identified proteins were somewhat disappointing, some interesting potential Hyd binding partners were identified. Among these, pyruvate kinase, which catalyses the last step in gluconeogenesis, and glycogen phosphorylase, which catalyses the first step in glycogenolysis, are both implicated

in glucose metabolism. Both gluconeogenesis (i.e. glucose synthesis) and glycogenolysis (i.e. the breakdown of glycogen into glucose building blocks) are processes that are important in the maintenance of blood glucose levels during starvation (Xiong et al. 2011). Taken together with the fact that EDD was shown to ubiquitylate PEPCK1, the enzyme that regulates the first committed step of gluconeogenesis, in an acetylation-dependent manner, leading to its subsequent degaradation (W. Jiang et al. 2011), suggests that Hyd/EDD is involved in regulating glucose homeostasis and is a target for the treatment of Type II diabetes. Interestingly, pyuvate kinase protein levels were also shown to be regulated by acetylation (Lv et al. 2011), suggesting that it could be a ubiquitylated target of Hyd/EDD similar to PEPCK1.

3.7.3 Other Hyd functions

In addition, several other potential Hyd binding partners were identified in the mass spectrometry screen, including protein synthesis regulator eukaryotic translation initiation factor 2 (EiF-2), the germ cell development protein Tudor, and Ran, a GTP-binding protein thought to be involved in nucleo-cytoplasmic transport. Some of these proteins are linked to previously published work relating to EDD, which is encouraging. For example, it has been proposed that EDD positively regulates translation by ubiquitylating the translational regulator Paip2 (Yoshida et al. 2006), and a possible interaction with EiF-2 could support Hyd/EDD's role as a positive regulator of protein synthesis. Tudor is a large protein that plays an important role in the formation of primordial germ cells. A potential interaction with Hyd could provide insight into the mechanism behind the sterility phenotype seen in many *hyd* mutants (Mansfield et al. 1994). Supporting this notion, Tudor was also one of the proteins found to contain a peptide that bound the carboxy terminal portion of Hyd in the phage display peptide ELISA (**Table 3.4**). Finally, the mass spectrometry data also suggests that Hyd may interact with a protein of unknown function, PERQ. Interestingly, it has been suggested that this protein also interacts with the negative

Ci regulator SuFu (Méthot & Basler 2000). This indicates a potential mechanism in which Hyd could negatively regulate Hh pathway activity.

3.7.4 Hyd and Wg signaling

Perhaps one of the most encouraging findings resulting from the work presented in this chapter is the interaction between Hyd and the Wg pathway transcriptional effector protein Armadillo, also known as β-catenin in humans. This is supported by previously published work, which showed that EDD interacts with, as well as ubiquitylates, β-catenin resulting in its stablilisation and nuclear accumulation (Hay-Koren et al. 2011). This suggests that EDD is a positive regulator of Wg/Wnt pathway activity by promting β-catenin's transcriptional activity. Interestingly, the peptide verification ELISA results also suggested that Hyd could potentially interact with the Wg pathway components Frizzled and Axin (see **Chapter 1, Section 1.3.1**). In light of this interesting result, which suggests that Hyd could be involved in regulating more than one morphogen signaling pathway, I decided to focus my subsequent *in vivo* work on investigating the role of Hyd in regulating both Hh and Wg signaling.

Chapter 4: The role of Hyd in regulating morphogen-expression and -pathway activity

4.1 Introduction

The purpose of performing proteomics-based screens for potential Hyd binding partners and/or substrates was to identify novel regulators of morphogen signalling. More specifically, it was hoped that the function of these candidate proteins could shed light on the molecular mechanisms by which Hyd regulates *hh* expression and/or Hh pathway activity. However, if a protein's function is not known, or its known function does not implicate it in morphogen signalling, it will not be chosen from a proteomics dataset. This represents the paradox of identifying a novel protein function from existing functional data (see **Chapter 3**).

In order to test a given protein's functional role in Hyd-mediated morphogen signalling regulation, a robust functional assay for Hyd was required, which could then be used to assess the functional relevance of Hyd binding partners in morphogen signalling (see **Chapter 5**). In the original work that identified Hyd as a negative regulator of both *hh* expression and Hh pathway activity, Lee et al. generated homozygous *hyd* mutant clones in the *Drosophila* eye-antennal disc (J. D. Lee et al. 2002) (see **Chapter 1, Section 1.4**). This enabled them to assess the expression pattern of *hh* and Hh pathway-related proteins in *hyd* mutant clones and the surrounding wild type cells, and deduce a possible role for Hyd in these processes. To further test the hypothesis that Hyd negatively regulates *hh* expression and Hh pathway activity, and to query what other Hyd binding partners may be involved in facilitating or inhibiting these Hyd-mediated effects, I also used the MARCM system (T. Lee & Luo 2001) to generate *hyd* mutant clones in the eye disc. The MARCM technique allowed me to generate homozygous *hyd* mutant clones that also over-expressed either cDNA for a novel Hyd binding partner, or RNAi to suppress the expression of the latter, thus providing the ideal genetic functional test for a binding partner's involvement in Hyd-mediated *hh* expression or Hh pathway activity. This approach was successfully employed (see **Chapter 5**), however the first step was to confirm whether I could reproduce the previously reported effects on *hh* expression

and Hh pathway activity seen in *hyd*^{mt} clones (J. D. Lee et al. 2002). As a complementary approach, I also wanted to develop a cell-based functional test that could address a protein's involvement in Hyd-mediated regulation of Hh signalling. The main advantage of this system would be its relative ease and speed compared to lengthy genetic crosses.

Finally, the Hh pathway-related effects observed in *hyd*^{mt} clones suggest that Hyd may be acting to directly or indirectly regulate Ci activity (J. D. Lee et al. 2002) (see **Chapter 1, Section 1.4**). Ci activity is regulated by two E3 ubiquitin ligases (reviewed in (J. Jiang 2006) and see **Chapter 1, Section 1.2.3 and 1.2.4**). In the absence of Hh signal, full length Ci_{155} is processed to a truncated repressor form (Ci_{75}) by an SCF ubiquitin ligase complex containing the F box protein Slmb (J. Jiang & Struhl 1998). In the presence of Hh signal, Ci_{155} translocates to the nucleus, where it is degraded by the Cul3-based E3 ubiquitin ligase Hib/Roadkill (Rdx) (Q. Zhang et al. 2006; Kent et al. 2006). I therefore also wanted to investigate whether Hyd can interact with Ci, and whether Hyd can affect Ci protein levels and/or ubiquitylation levels.

4.2 *hyd*$^{K7.19}$ clones encode a severely truncated Hyd protein

In the original mosaic screen for eye differentiation (J. D. Lee et al. 2002), four mutant alleles of *hyd* were discovered: *hyd*$^{K3.5}$, *hyd*$^{K7.19}$, *hyd*^{15}, and *hyd*^{WC461}. However, the molecular nature of the mutations at the DNA and protein level were not known. The molecular characterization of these mutations could provide insight into the function of Hyd in the regulation of morphogen signalling in the hyperplastic phenotype. For example, if a particular domain carried a point mutation or was deleted this could help to decipher a molecular mechanism. Therefore, I wanted to

sequence the region of genomic DNA encoding the *hyd* gene for these four *hyd* mutant strains.

Most mutant *hyd* alleles are homozygous lethal at or before the second instar stage (Mansfield et al. 1994). I therefore collected homozygous mutant *hyd* L1 or L2 larvae to extract genomic DNA for sequencing. A GFP balancer chromosome was used to distinguish homozygous *hyd* mutant larvae from heterozygous animals. To facilitate larvae collection, male and female flies were placed in egg laying chambers containing grape agar plates, and were left to lay eggs in one hour-timed intervals. The plates were then removed and incubated at 25°C until L1 larvae emerged. Larvae that were homozygous for a *hyd* mutation were identified by the absence of a GFP signal under a fluorescence microscope.

A number of L2 larvae were collected for the $hyd^{K7.19}$ and hyd^{WC461} strains, although the ratio of GFP negative larvae to total larvae collected was significantly lower than expected [**Figure 4.2.1**; chi-square test – $hyd^{K7.19}$ X^2 (2, n = 234) = 123.2, $p<0.001$; hyd^{WC461} X^2 (2, n = 104) = 50.7, $p<0.001$]. This is most likely due to some variability in the *hyd* mutant phenotype, where some larvae could experience earlier lethality than others. However, for the $hyd^{K3.5}$ and hyd^{15} strains, no GFP negative L1 or L2 larvae were collected [**Figure 4.2.1**; chi-square test – $hyd^{K3.5}$ X^2 (2, n = 83) = 83, $p<0.001$; hyd^{15} X^2 (2, n = 331) = 331, $p<0.001$], suggesting that the mutations associated with these *hyd* alleles could be more severe and therefore result in even earlier lethality at the embryonic stages. In addition, the variability in total larvae collected for each mutant strain could also be indicative of the effect of heterozygous *hyd* mutation on reproductive health in adults. Sterility has previously been reported as a phenotypic feature in homozygous adult flies with some *hyd* alleles permissible only at certain temperatures (Mansfield et al. 1994). However, the total number of adult flies used to lay eggs was not kept constant between strains during the experiment, and therefore no such assumption can be made.

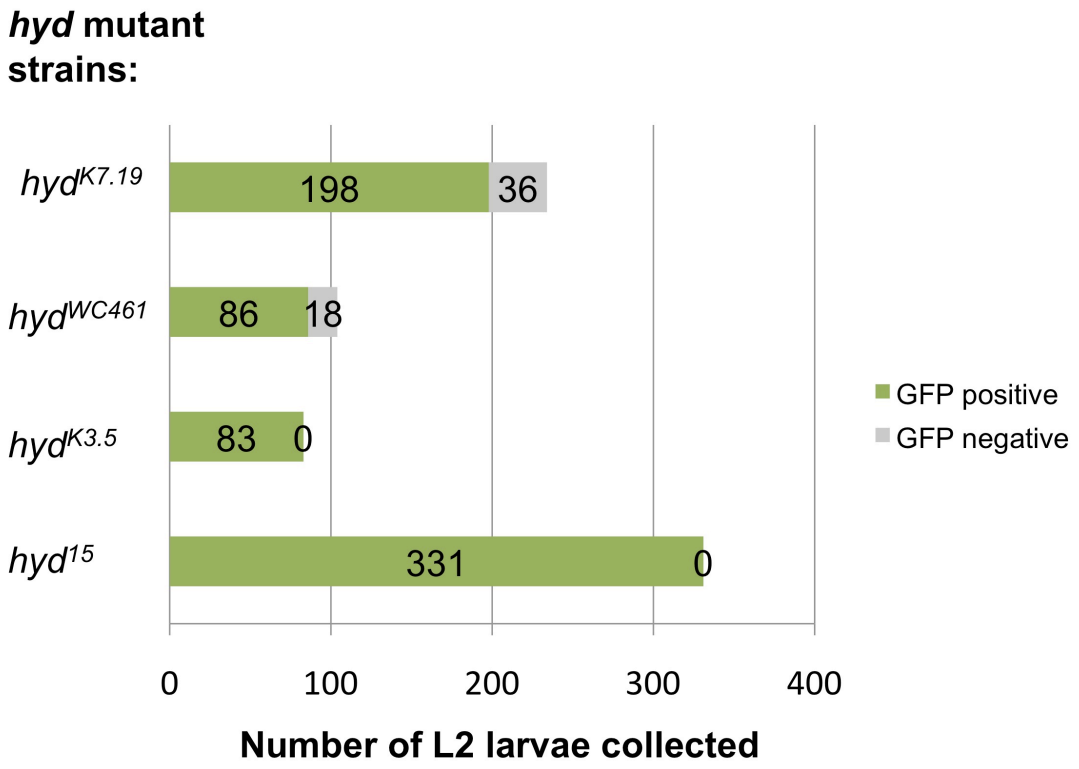

Figure 4.1: Early larval or embryonic lethality of homozygous *hyd* mutant animals. A GFP balancer chromosome was used to distinguish heterozygotes (GFP positive) from homozygotes (GFP negative). Crawling L2 larvae were collected, and analyzed under a fluorescence microscope.

Because I was unable to obtain homozygous $hyd^{K3.5}$ and hyd^{15} larvae, but wanted to sequence the entire set of *hyd* alleles, I opted to sequence the adult heterozygote flies instead. The genotypes used for this sequence analysis are summarized in **Table 4.1**. The genomic DNA was prepared as a crude extract from single female adults. To increase the quality of the sequence data, the *hyd* gene region was amplified by PCR and the purified PCR product was sent for sequence analysis (see Materials and Methods). Some initial optimisation was required to establish a primer pair that would give a clean PCR product from the crude genomic extract. Due to its relatively large size (~13kb), the *hyd* gene was amplified and sequenced in two over-lapping parts: a 5.7kb front region starting at the transcription initiation site (ATG start codon), and a 6.8kb back region, which encompasses a small region of the 3'UTR region (see schematic in **Figure 4.2 A**).

Allele	Genotype
hyd$^{K7.19}$	*FRT82 hyd*$^{K7.19}$ */ TM6B Tb GFP*
hyd$^{K3.5}$	*FRT82 hyd*$^{K3.5}$ */ TM6B Tb GFP*
hyd^{15}	*hyd*^{15} */ TM6B GFP*
hyd^{WC461}	*FRT82 hyd*^{WC461} */ TM6B Tb GFP*

Table 4.1: *hyd* mutant strains used for sequencing analysis.

Mutations were identified in the sequence data by the appearance of an obvious double trace in the chromatogram (**Figure 4.2 B**). Some mutations were confirmed as being known polymorphisms, silent mutations that did not result in a change of amino acid, or were located within intronic regions of the gene. For both the *hyd*$^{K7.19}$ and *hyd*^{15} alleles, nonsense mutations were found early on in the protein coding sequence (**Figure 4.2 B**). The *hyd*$^{K7.19}$ allele contains a C>T nucleotide mutation in exon 4, resulting in an arginine (R) to STOP codon nonsense mutation. This mutation would theoretically produce a severely truncated Hyd protein of 27kDa that would only retain the amino-terminal UBA domain. The *hyd*^{15} allele theoretically produces a slightly less truncated Hyd protein. It contains a G>A nucleotide mutation in exon 7, resulting in a tryptophan (W) to STOP codon nonsense mutation, which would result in a 54kDa Hyd protein that retains the UBA domain and a portion of the RCC domain.

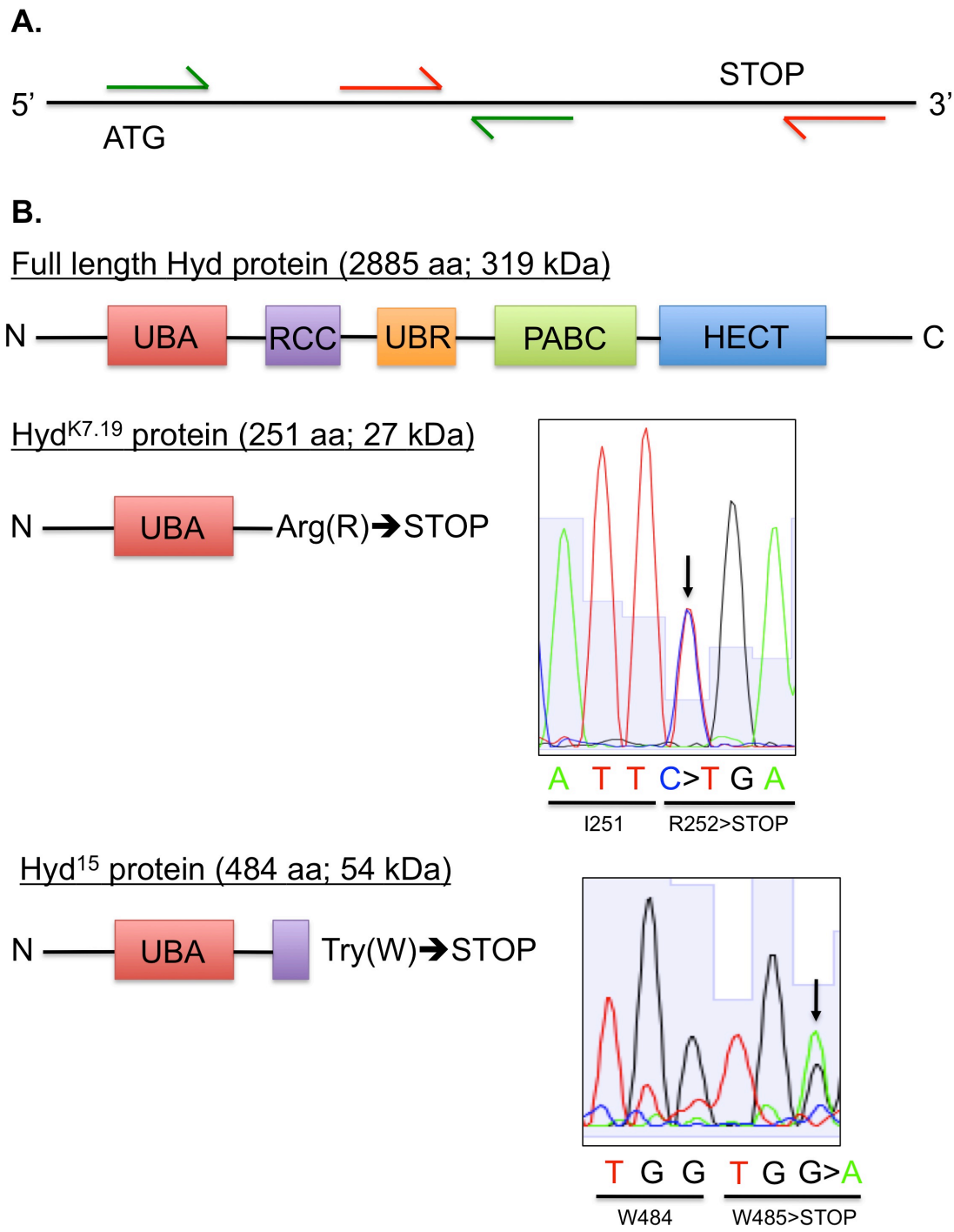

Figure 4.2: Sequencing of heterozygous *hyd* mutant animals. (**A**) Schematic of the *hyd* gene region PCR strategy. (**B**) Sequencing data for $hyd^{K7.19}$ and hyd^{15} alleles. Nucleotide mutations are visible as a double trace in the chromatogram. These nonsense mutations cause the change of the respective amino acid to a STOP codon, resulting in truncated Hyd mutant proteins compared to the full-length wild type Hyd protein.

By contrast, no exonic mutations were found in the $hyd^{K3.5}$ and hyd^{WC461} alleles. A single intronic mutation was found between exon 6 and exon 7 in the $hyd^{K3.5}$ allele, although the mutation is unlikely to affect mRNA splicing as it is not located at either intron/exon junction. However, the aforementioned results indicate that the $hyd^{K3.5}$ allele may result in very premature lethality at the embryonic stages, which suggests that the mutation is even more severe than the hyd^{15} and $hyd^{K7.19}$ mutations. One explanation for the $hyd^{K3.5}$ allele being more severe could be that it produces no Hyd protein in comparison to the truncated Hyd proteins produced by the hyd^{15} and $hyd^{K7.19}$ alleles. Two possible scenarios that could result in very little, or no full-length Hyd protein being made, would be if (1) the mutation is located upstream of the ATG transcription site (e.g. in the promoter region) and negatively affects transcription, or (2) the mutation is located within the extended 3' untranslated (UTR) region not covered by the PCR product and severely affects mRNA stability, preventing translation of the protein. In fact, it is entirely possible that the other alleles could also contain mutations of this nature that were not covered by the sequence data. This would explain why the hyd^{15} allele causes lethality prior to the L2 stage, but is less severe than the $hyd^{K7.19}$ mutation. Finally, a single intronic mutation (G>A) was found in the hyd^{WC461} allele, which results in the change of the splice acceptor site at the intron/exon 13 junction from GG to AG. However, this is unlikely to affect mRNA splicing, as AG is in fact known to be the most favoured splice acceptor nucleotide composition (Moore 2000).

In order to confirm these sequencing results, I would ideally test the presence, absence, or truncation of the Hyd protein by WB on protein extracts of heterozygous flies. However, the Hyd antibody that was routinely used in the lab (M19, Santa Cruz) detects the extreme carboxy terminal region of the protein. There is a Hyd/EDD antibody (N19, Santa Cruz) available that detects the amino terminal of the protein within the UBA domain. This could be used to detect the putative truncated mutant forms of Hyd. Unfortunately, I was not able to detect Hyd protein in fly lysates with either antibody, but this was most likely due to problems with efficient protein extraction from whole flies. Due to time constraints, I was not able

to optimize the use of this antibody and the lysis procedure to detect *Drosophila* Hyd.

4.3 The hyperplastic phenotype

Out of the four *hyd* alleles, only the $hyd^{K3.5}$ and $hyd^{K7.19}$ alleles were used to identify Hyd as a negative regulator of Hh signalling (J. D. Lee et al. 2002). Based on this, and the sequencing data, I chose the $hyd^{K7.19}$ allele for future work, as the molecular nature of the mutation was now known to me.

4.3.1 Generation of hyd^{mt} clones in the eye-antennal (EA) disc using the MARCM technique

Mosaic Analysis with a Repressible Cell Marker (MARCM) is an elegant genetic technique used in *Drosophila* that allows the study of labelled homozygous mutant cells in an otherwise unlabelled heterozygous animal (J. S. Wu & Luo 2006). This is particularly useful when homozygous mutations are developmentally lethal, as is the case with all described *hyd* mutations (Mansfield et al. 1994). A further advantage of the MARCM technique is the ability to express one or more transgenes, encoding either cDNA (protein over-expression) or RNAi (mRNA knockdown), in the labelled mutant clones (J. S. Wu & Luo 2006). This has allowed me to test the ability of a novel Hyd binding partner to modify the $hyd^{K7.19}$ phenotype (see **Chapter 5**).

The technique relies on GAL4-mediated transcription of a positive green fluorescent protein (GFP) marker, as well as an optional transgene of interest, from a UAS promoter element, and GAL80-mediated repression of GAL4 (**Figure 4.3**). GAL4 is a yeast transcription factor that drives transcription from the Upstream Activation Sequence (UAS) (Fischer et al. 1988). As a result, the transcription of any sequence (e.g. cDNA or RNAi) that is cloned downstream of the UAS is mediated by GAL4.

FRT-directed mitotic recombination is used to generate homozygous *hyd* mutant clonal cells in an otherwise heterozygous *hyd* mutant, and therefore viable, animal. FLP-FRT recombination involves Flippase (FLP)-mediated recombination of sequences that are flanked by short Flippase Recognition Target (FRT) sites (Theodosiou & T. Xu 1998). For example, this can be achieved by using an FRT82B strain, which contains FRT sites on chromosome 3 (T. Xu & G. M. Rubin 1993), where the *hyd* gene is also located, for recombination. In order to generate homozygous $hyd^{K7.19}$ clones exclusively in the eye-antennal imaginal disc, we used the *eyeless* promoter to control FLP expression. The *eyeless* gene is expressed early on during eye development, and its expression pattern spans the entire eye region of the EA (eye-antennal) disc, whereas lower expression is detected in the antennal region, and its expression is absent from other imaginal discs (Halder et al. 1998). Another component of the MARCM system is GAL80, a yeast protein that blocks GAL4 activity by binding to its transcriptional activation domain (Suster et al. 2004). Importantly, the hyd^{wt} allele is physically linked to the GAL80 gene, ensuring that, even after FRT-directed recombination, all homozygous or heterozygous hyd^{wt} cells express GAL80. As a result, only homozygous $hyd^{K7.19}$ cells are positively marked by GFP and express the transgene of interest (**Figure 4.3**).

In order to simultaneously investigate *hh* gene expression in hyd^{mt} clones, I also used the β-galactosidase gene (*lacZ*) enhancer trap hh^{P30}, which I will refer to as *hh-lacZ* (J. J. Lee et al. 1992). *hh-lacZ* harbours an insertion of an enhancerless *lacZ* reporter into the 5'UTR of the *hh* gene. Thereby expression of the *lacZ* transgene accurately reflects that of the endogenous *hh* gene. The presence of β-galactosidase (the product of the *lacZ* gene) can be then be visualised in dissected EA imaginal discs using the chromogenic β-galactosidase (βgal) substrate X-gal (Adams & Sekelsky 2002), or by using an antibody specific for βgal and immunofluoresence. To allow clonal analysis of *hh* expression, I used a strain where the *hh-lacZ* enhancer trap had been recombined onto either an FRT82B-bearing chromosome or an FRT82B $hyd^{K7.19}$ chromosome.

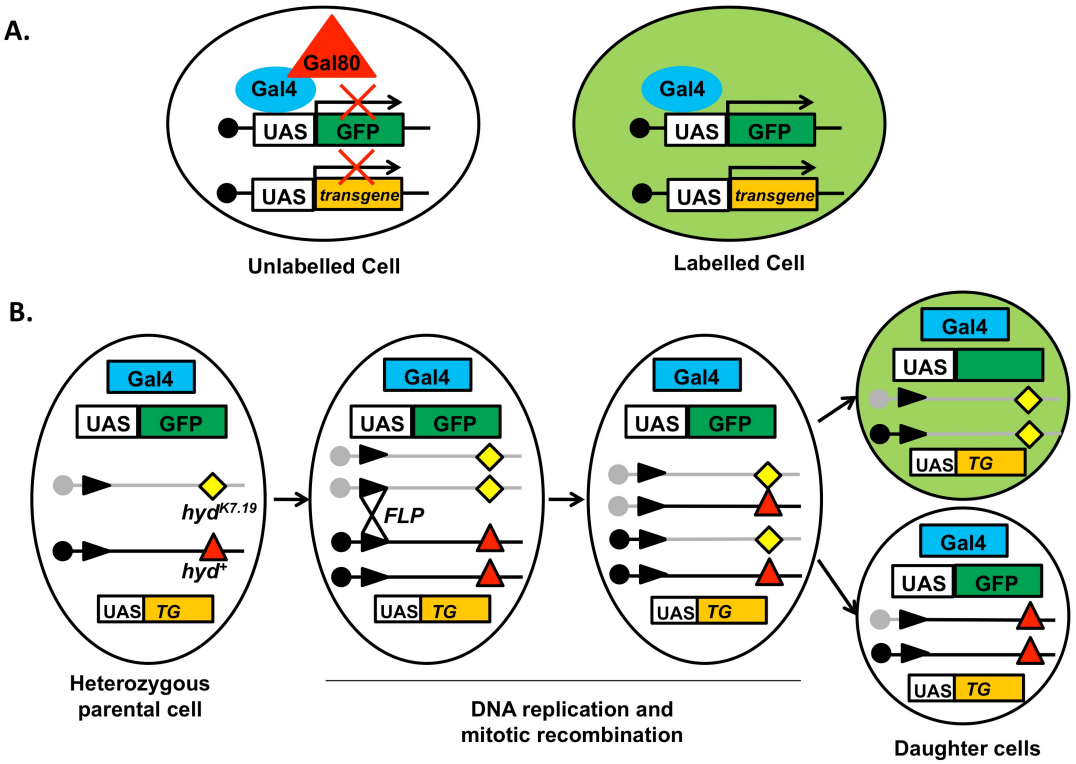

Figure 4.3: Mosaic Analysis with a Repressible Cell Marker (MARCM). (**A**) In cells that contain the GAL80 protein, GAL4-directed expression of both UAS-GFP and UAS-transgene are repressed. In the absence of GAL80, GAL4 can drive the expression of both GFP and the transgene (either cDNA or RNAi) from the UAS element, resulting in green cells. (**B**) Generation of homozygous hydmt clonal cells using MARCM. The parental genotype includes tubulin-GAL4 (resulting in ubiquitous expression of GAL4), UAS-GFP and UAS-transgene on one chromosome (e.g. Chromosome 2). The chromosome containing the *hyd* gene (chromosome 3) is modified by the insertion of FRT sites (black arrowheads) adjacent to the centromere (black circles). One of the heterologous chromosome arms contains the $hyd^{K7.19}$ allele (yellow diamond), whereas the other contains the hyd^{+} allele, adjacent to an inserted GAL80 gene (red triangle). This makes the parent cell heterozygous for the *hyd* mutation. During DNA replication, the chromosomes are duplicated, and site-specific mitotic recombination is directed by the Flippase (FLP) recombination enzyme at FRT sites. This gives rise to two types of homozygous daughter cells. One is homozygous for $hyd^{K7.19}$ and lacks GAL80 expression, therefore allowing expression of the GFP marker and the UAS-transgene by GAL4. The other is homozygous for hyd^{+} and expresses GAL80, which prevents expression of both UAS-GFP and UAS-transgene. Adapted from **(J. S. Wu & Luo 2006)**.

4.3.2 The adult *hyd*$^{K7.19}$ phenotype

The MARCM technique was successfully used to generate FRT82B control clones or FRT82B *hyd*$^{K7.19}$ clones in the eye. *hyd*$^{K7.19}$ mutant clones caused some subtle overgrowth of eye tissue, although the overgrowth was not nearly as pronounced as in adult eyes containing *hyd*$^{K3.5}$ mutant clones (J. D. Lee et al. 2002). Instead, a major feature of the *hyd*$^{K7.19}$ phenotype was the appearance of scars in the eye located at the margin to the head cuticle (**Figure 4.4 A**). There was some variability in the spectrum of mutant eye phenotypes, ranging from at least one scar at the less severe end, and multiple or very large scars in the most severe cases. The scars could be a result of *hyd*$^{K7.19}$ clones being eliminated relatively late in development, or they could also be a result of hyperplastic head tissue invading into the eye area. The eye-antennal imaginal discs give rise to the entire adult head capsule, including the compound eyes, antennae, and head cuticle(Legent & Treisman 2008). Indeed, the head cuticle was extensively overgrown in *hyd*$^{K7.19}$ flies (**Figure 4.4 B**). Eye-to-eye measurements were taken just above the antennae of both control and *hyd*$^{K7.19}$ heads, and *hyd*$^{K7.19}$ heads were found to be significantly wider ($p = 0.004$; **Figure 4.4 B**).

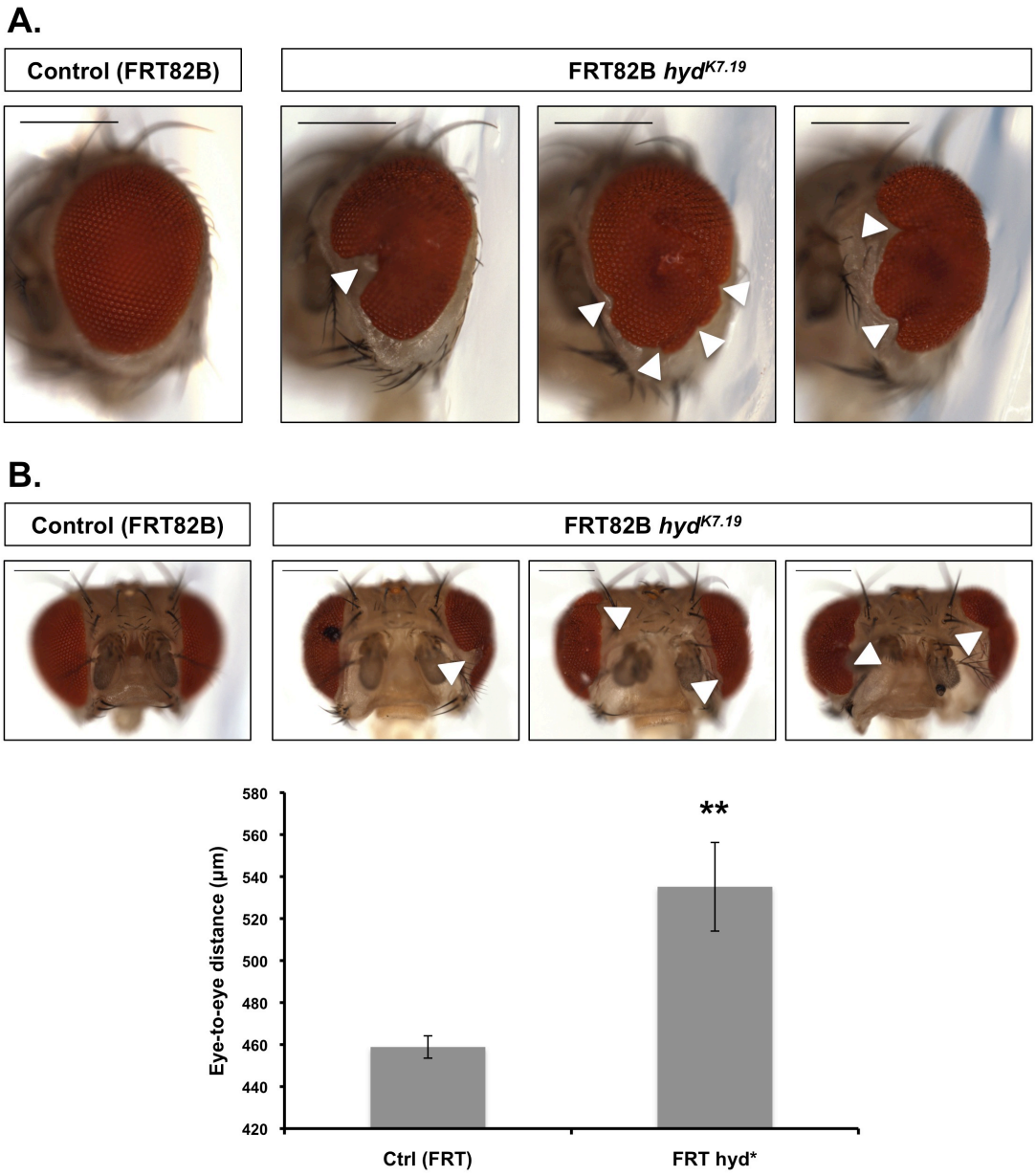

Figure 4.4: The *hyd*$^{K7.19}$ adult phenotype. (**A**) Side view of FRT82B (control) or FRT82B *hyd*$^{K7.19}$ compound eyes. Scale bars are 250µm. Scars are indicated by white triangles. (**B**) Front view of FRT82B (control) or FRT82B *hyd*$^{K7.19}$ heads. Scale bars are 250µm. Scars are indicated by white triangles. Head measurements (µm) were taken from eye-to-eye at a fixed point just above the antennae (n=10), and were significantly wider in FRT82B *hyd*$^{K7.19}$ animals (p = 0.004; t-test).

The interplay between the morphogens Hh and Wg greatly contributes to determining the correct specification and growth of the compound eye and the head cuticle. During the third instar, Wg is exclusively expressed in the lateral margins in

the anterior of the eye disc, where it promotes head capsule formation at the expense of the retinal field by antagonizing the action of Hh and Dpp (Treisman & G. M. Rubin 1995; C. Ma & Moses 1995). On the other hand, Hh and Dpp are expressed in posterior regions and the morphogenetic furrow (MF), and direct photoreceptor differentiation and formation of the compound eye (Royet & Finkelstein 1997). The invasive overgrowth of head tissue, as well scarring of the eyes, observed as a result of the presence of $hyd^{K7.19}$ clones (**Figure 4.4 A**) suggests that retinal cell specification is lost at the expense of head tissue formation, which is promoted by Wg signalling. This suggests that, in addition to its role in Hh signalling, Hyd could also negatively regulate Wg signalling.

4.3.3 $hyd^{K7.19}$ clones cause overgrowth of EA discs

To explain the overgrowth of head tissue and scarring in adult eyes, I proceeded to analyse the behaviour of clones in L3 eye-antennal discs. Indeed, $hyd^{K7.19}$ clones caused non-autonomous overgrowth of eye disc tissue, which was manifested in the folding and distortion of mostly non-clonal disc tissue (**Figure 4.5 A**). This data is in agreement with the non-autonomous overgrowth of wild type or heterozygous tissue surrounding $hyd^{K7.19}$ clones reported previously(J. D. Lee et al. 2002). Individual clusters of $hyd^{K7.19}$ clones had a more "rounded" morphology in some instances (white arrows, **Figure 4.5 A**), which was never observed with control clones. This change in morphology could indicate the premature differentiation of $hyd^{K7.19}$ clones (J. D. Lee et al. 2002). There was no obvious difference in the average number of $hyd^{K7.19}$ clones versus control clones in age-matched third instar discs, however the $hyd^{K7.19}$ clones present in the EA discs did not persist to adulthood in most cases, as visualised by fluorescence microscopy of adult heads and eyes containing or lacking GFP positive $hyd^{K7.19}$ clones (**Figure 4.5 B**). This has been reported previously for $hyd^{K3.5}$ clones (J. D. Lee et al. 2002). $hyd^{K3.5}$ clones generated in a *Minute* genetic background, a mutation that confers a growth disadvantage (Morata & Ripoll 1975), are not eliminated and survive to adulthood, forming compound eyes that are drastically reduced in size, but nonetheless have correctly formed $hyd^{K7.19}$ ommatidia

(J. D. Lee et al. 2002). This suggests that *hyd*$^{K7.19}$ clones may have a growth disadvantage and, as a result, are eliminated by the surrounding non-clonal tissue through cell competition.

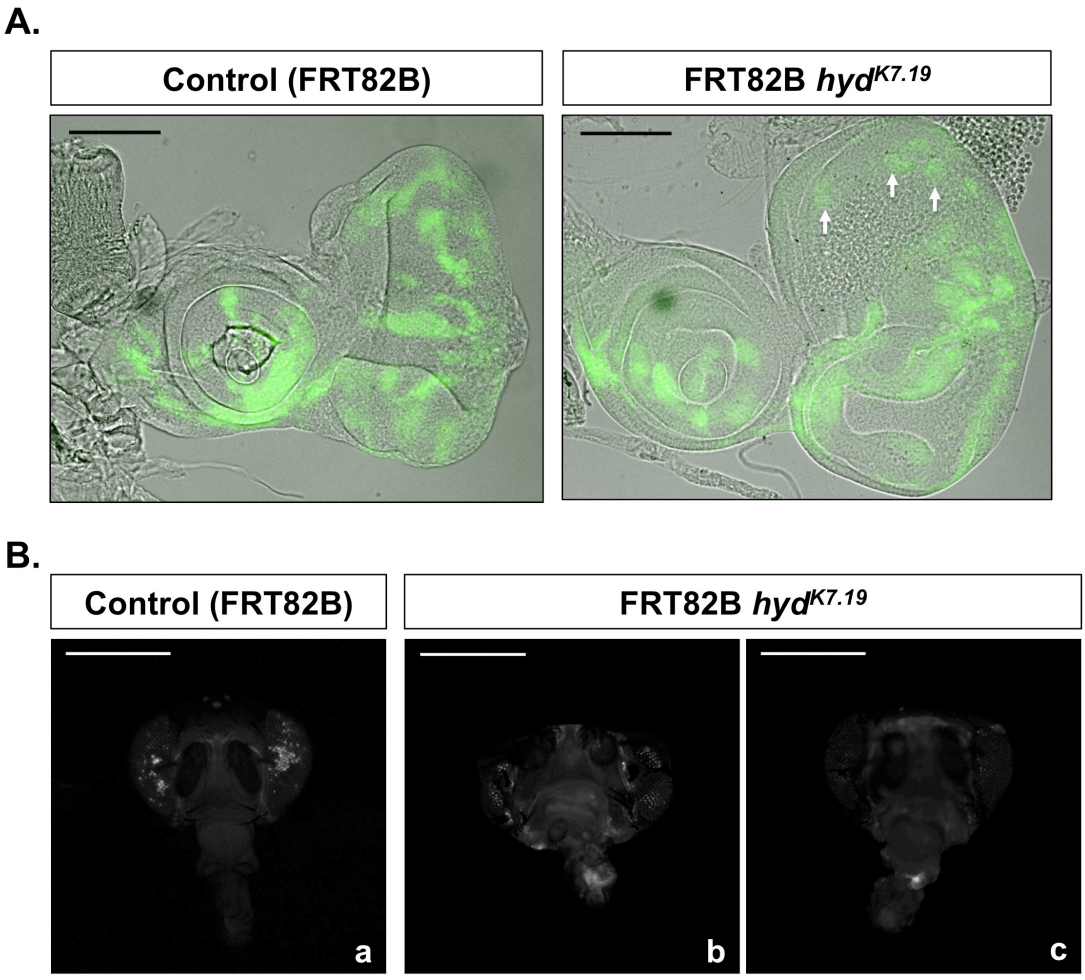

Figure 4.5: Behaviour of *hyd*$^{K7.19}$ clones in L3 EA discs and adult heads. (**A**) Third instar eye-antennal discs containing GFP-positive FRT82B (control) or FRT82B *hyd*$^{K7.19}$ clones. Anterior is to the left, posterior is to the right, dorsal is up, and ventral is down. White arrows indicate rounded morphology of *hyd*$^{K7.19}$ clones. Scale bars are 100µm. (**B**) Front view of FRT82B (control) or FRT82B *hyd*$^{K7.19}$ heads containing GFP-positive clones in the eyes (a only). Scale bars are 500µm.

4.3.4 Over-expression of Hyd, but not a catalytic inactive mutant of Hyd, rescues the *hyd*$^{K7.19}$ phenotype

As discussed above, the *hyd*$^{K7.19}$ mutation results in a severe truncation of the Hyd protein. As a result of a nonsense mutation located immediately after the amino-terminal UBA domain, the putative Hyd$^{K7.19}$ mutant protein is missing the RCC, UBR, PABC, and the catalytic HECT domain. Any one, or a combination, of these domains could therefore be important in the hyperplastic phenotype. Work that had previously been carried out in the lab (**Figure 4.6**; Mark Ditzel) shows that over-expression of a full length Hyd protein in *hyd*$^{K7.19}$ clones results in a nearly complete rescue of the phenotype. The eyes of rescued animals no longer harbour scars, and the head cuticle is reduced to a normal size (**Figure 4.6**). However, overexpression of a catalytic dead Hyd protein (Hyd C>A), in which the catalytic cysteine residue in the HECT domain is mutated, fails to rescue the phenotype. This suggests that Hyd's ubiquitylation activity is required for its function in the hyperplastic phenotype, and for its function as a negative regulator of morphogen signalling.

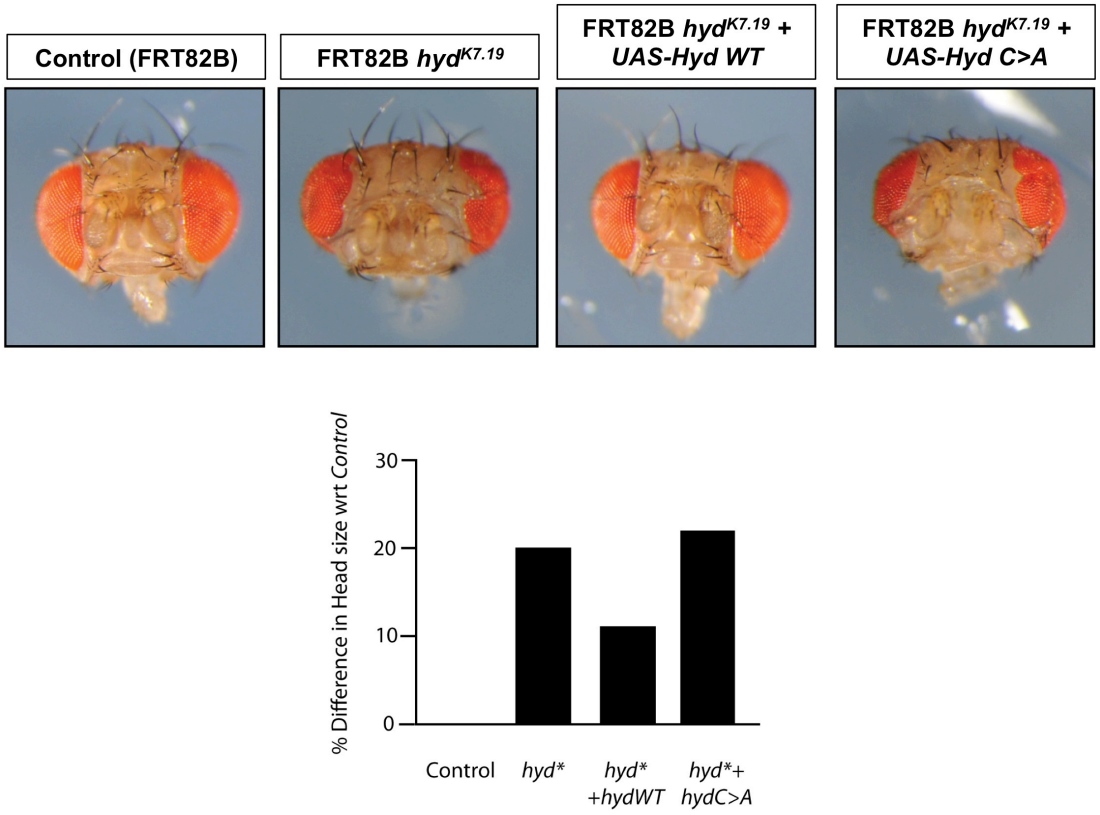

Figure 4.6: Rescue of the adult hyperplastic phenotype using Hyd transgenes. Expression of a UAS-Hyd *wt* transgene in *hyd*$^{K7.19}$ clones rescues the adult phenotype, whereas expression of a UAS-

Hyd C>A transgene fails to rescue. The entire non-eye head area of each fly head shown was measured and is expressed as percentage change in pixel area with respect to the control (n=1). (Experiment performed, and figure provided by Mark Ditzel.)

In order to investigate whether other Hyd domains also play crucial roles in the hyperplastic phenotype, I used site-directed mutagenesis to generate expression constructs encoding HA-tagged Hyd mutants that contained point mutations in the UBA, UBR and PABC domains. The point mutations were chosen on the basis of structural similarity to, and functional significance of the mutation of these domains in other proteins, and are summarized in **Table 4.2**. Briefly, mutation of the (i) UBA domain is expected to abrogate binding to ubiquitin and ubiquitylated proteins (Kozlov et al. 2007), (ii) UBR domain should result in defects in domain folding and thus function (Tasaki et al. 2005), and (iii) PABC domain should impair PAM2-dependent protein-protein interactions (Kozlov et al. 2004) (see **Chapter 1, Section 1.4**). The sequence-verified HA-tagged Hyd mutants were sub-cloned into the *pUAST* vector to allow transgenesis of *Drosophila* embryos, via its integration into the *Drosophila* genome. However, microinjection of embryos with the various *hyd pUAST* constructs (performed by BestGene Inc.) yielded no transformants, or transformants that were not expressing HA-tagged Hyd. Sequencing of the *hyd pUAST* constructs revealed they had undergone extensive recombination following plasmid amplification and purification. This can most probably be attributed to the large size of the constructs, which was in excess of 18kb. If the generation of these transgenic flies were to be attempted once more, I would take extra precautions by using recombination-deficient bacterial strains and incubate the bacteria replicating the constructs at lower temperatures (e.g. 20°C) to reduce recombination, and I would sequence the constructs in full prior to sending them for transformation into flies.

Domain	Amino Acid Point Mutations	Expected Outcome
UBA	V166K L194K	Abrogates binding to mono-and poly-ubiquitin (modeled on EDD UBA-Ub structure)
UBR	C1272A C1274A	Loss of Zn^{2+} coordination and overall UBR fold
PABC	Y2509A L2527A	May abrogate binding to PAM2 containing substrates (e.g. Paip1, Paip2, eRF3, Tob2) (modeled on PABP protein structure)

Table 4.2: Design of UBA, UBR, and PABC Hyd point mutants.

4.4 Ectopic expression of morphogens by *hyd*$^{K7.19}$ clones

Next, I went on to confirm whether *hyd*$^{K7.19}$ clones over-express *hh*, as reported in Lee et al. 2002 (J. D. Lee et al. 2002), and whether this ectopic *hh* expression is also reflected in the Hh protein levels. In light of the overgrowth of head tissue in adult heads containing *hyd*$^{K7.19}$ clones, which, as discussed above, could be indicative of ectopic Wg signalling, I also investigated the effect of *hyd* loss on Wg morphogen expression.

4.4.1 *hh* gene expression and Hh protein levels are elevated in $hyd^{K7.19}$ clones

To investigate the levels of *hh* gene expression in $hyd^{K7.19}$ clones, the *hh-lacZ* enhancer trap was inserted into the chromosome arm containing the *hyd* gene, such that both genetic elements were inserted proximal to the FRT82B site. As a result, all $hyd^{K7.19}$ clones will harbour and express two copies of the *lacZ* gene under the control of the *hh* promoter. The product of *lacZ* gene expression is the β-galactosidase protein, which can be visualized as blue staining using the chromatogenic substrate X-gal. The levels of *lacZ* gene expression in $hyd^{K7.19}$ clones therefore accurately represents the levels of *hh* gene expression.

Third instar EA discs containing control FRT82B *hh*lacZ clones, or FRT82B $hyd^{K7.19}$ *hh*lacZ clones, were stained with X-gal. In control discs, *hh* gene expression was restricted to posterior regions of the eye disc, with the exception of a small area of expression at the lateral dorsal margin in the anterior region of the disc (**Figure 4.7**; panel a). According to previous reports, this is the characteristic *hh* expression pattern in the eye disc during the third larval instar (Cho et al. 2000) (see **Chapter 1, Section 1.2.5**). Loss of *hyd* in $hyd^{K7.19}$ *hhlacZ* clones had both quantitative and spatial consequences on *hh* gene expression. The overall X-gal staining, when examined by eye, appeared increased in posterior regions of *hyd* mutant discs (**Figure 4.7**; panels b-d). Additionally, ectopic *hh* expression was observed in anterior regions of the disc in some instances (**Figure 4.7**; panels b, e, d; arrows). These findings are in agreement with previous work that identifies Hyd as a negative regulator of *hh* expression (J. D. Lee et al. 2002). The expression of *hh* in posterior regions of the eye disc directs photoreceptor differentiation, which progresses as the morphogenetic furrow (MF) moves across the eye disc from posterior to anterior (Royet & Finkelstein 1997). Loss of Hyd was also reported to lead to ectopic *hh* expression in clones anterior to the furrow, which in turn lead to premature photoreceptor differentiation (J. D. Lee et al. 2002).

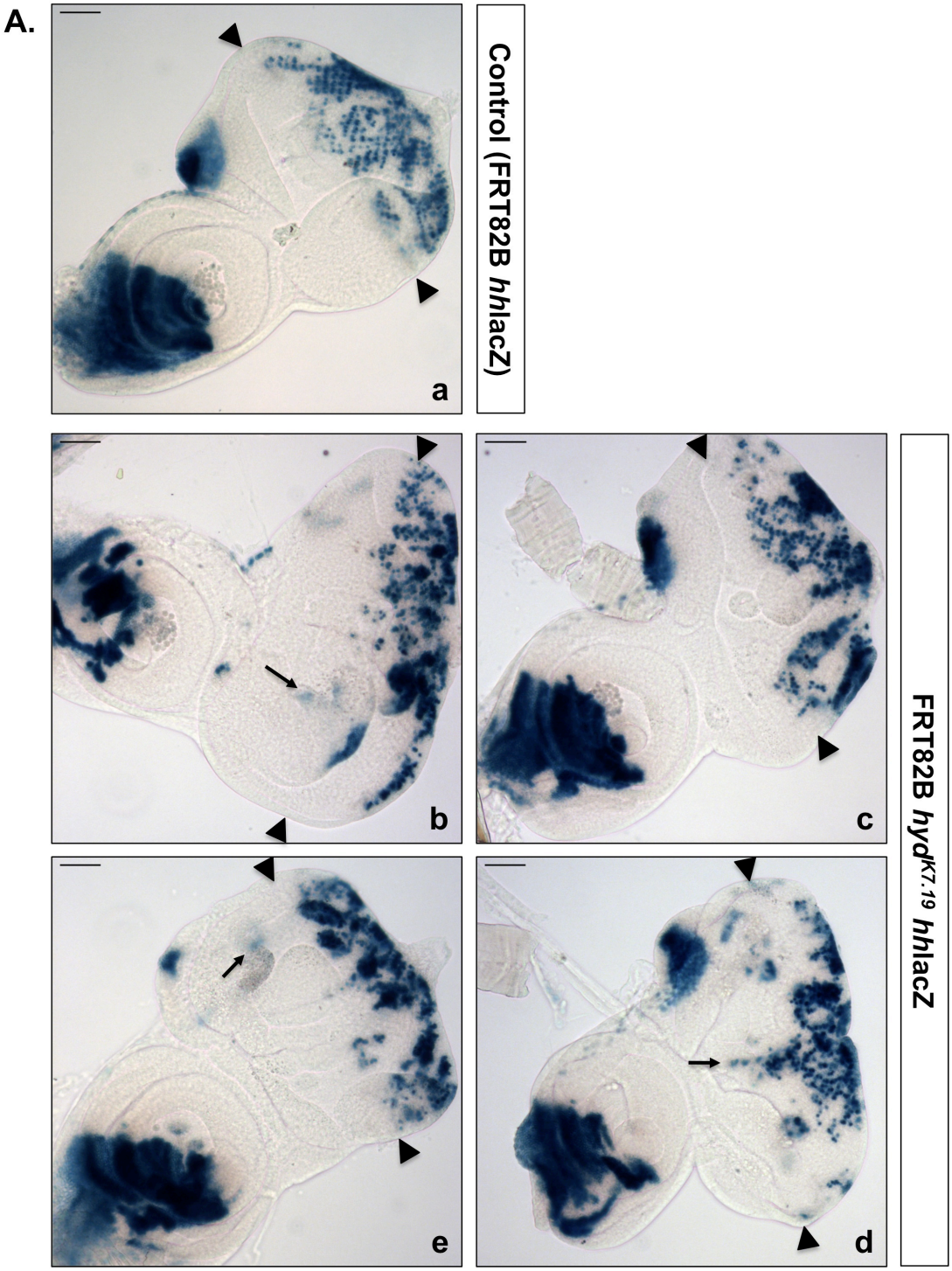
A.
Control (FRT82B hhlacZ)
FRT82B hyd^K7.19 hhlacZ
a
b
c
d
e

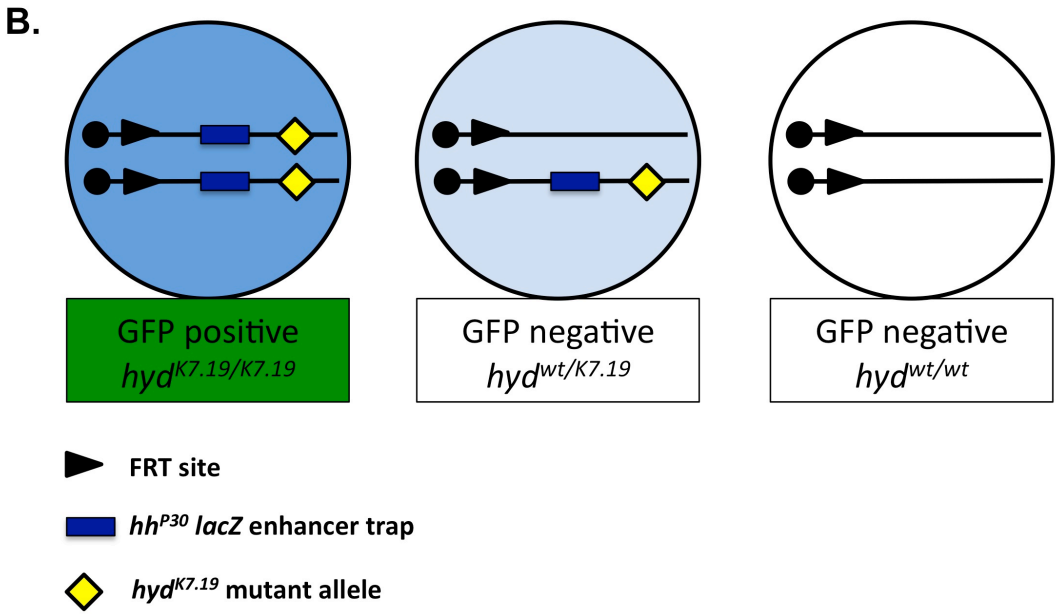

Figure 4.7: *hhlacZ* expression in X-gal-stained L3 EA discs. (A) Third instar eye-antennal discs containing FRT82B *hhlacZ* (control) or FRT82B $hyd^{K7.19}$ *hhlacZ* clones. Anterior is to the left, posterior is to the right, dorsal is up, and ventral is down. Black arrows indicate ectopic *hhlacZ* expression in anterior regions. Scale bars are 100µm. Location of morphogenetic furrow (MF) is indicated by black triangles. **(B)** Schematic of *hhlacZ* expression levels in homozygous $hyd^{K.19}$, heterozygous, and wild type clones. Only homozygous $hyd^{K.19}$clones are also GFP positive. A single copy of hhlacZ in heterozygous $hyd^{K.19}$ clones leads to reduced expression of hhlacZ compared to homozygous $hyd^{K.19}$ clones.

However, one disadvantage of using X-gal staining to assess levels of *hh* gene expression in eye discs containing $hyd^{K7.19}$ clones, is that *hh*-lacZ expression is not exclusively restricted to $hyd^{K7.19}$ clones. The MARCM technique, due to the FLP-FRT-based recombination process, will generate three different types of clones: (i) GFP-positive homozygous control/$hyd^{K7.19}$ clones that receive two copies of *hh*-lacZ; (ii) GFP-negative heterozygous control/$hyd^{K7.19}$ clones that receive one copy of *hh*-lacZ; and (iii) GFP-negative wild-type clones that receive zero copies of *hh*-lacZ (**Figure 4.7 B**). As a result, the blue staining in X-gal-stained MARCM discs is due to *hh*-lacZ expressed by both homozygous and heterozygous control/$hyd^{K7.19}$ clones. Those regions lacking blue stain may either be due to cells (i) expressing *hh* but lack the *hh*-lacZ reporter or (ii) do not express *hh* but do harbour *hh*-lacZ. This is why *hh*-lacZ expression in posterior regions of eye discs containing control clones is not

uniform, as not all cells have received a copy of *hh*-lacZ. This also means that, although *hh*-lacZ expression levels have markedly increased in eye discs containing $hyd^{K7.19}$ clones, it is not clear whether the ectoptic *hh* expression occurs in the homozygous clones or in the remaining heterozygous *hh*-lacZ expressing cells.

In order to get around this caveat, I used immunofluorescence in conjunction with βgal- and Hh-N-specific antibodies to simultaneously visualize *hh* gene expression and Hh protein expression in GFP-labelled homozygous $hyd^{K7.19}$ *hh*-lacZ clones (**Figure 4.8**). In addition, as previous findings relate only to Hyd-mediated regulation of *hh* mRNA levels (J. D. Lee et al. 2002), I wanted to ensure Hh protein levels were also elevated in $hyd^{K7.19}$ clones. As expected, both *hh* gene expression in $hyd^{K7.19}$ clones, and Hh protein expression in eye discs containing $hyd^{K7.19}$ clones was visibly elevated compared to control discs (**Figure 4.8**, A and B). Interestingly, Hh protein expression did not always co-localise with βgal staining or GFP-positive clones. This could be because, unlike β-gal, Hh protein is a diffusible extracellular protein. Furthermore, Hh staining is a cumulative representation of Hh protein produced in *hh* expressing cells – either $hyd^{K7.19}$ or not. Local high concentrations of Hh staining may also reflect physical sequestration of Hh protein by membrane-associated receptors, such as Ptc. Not only did loss of *hyd* function result in elevated Hh protein levels in L3 EA discs, the expression pattern of Hh protein was also notably disrupted, whereby ectopic high levels of Hh protein expression were observed in both posterior and anterior regions of the eye disc (**Figure 4.8**, A and B).

Finally, the relative levels of *hh* gene expression in $hyd^{K7.19}$ clones versus control clones were quantified by measuring the average pixel intensity of the βgal signal in regions of interest (ROI) containing groups of GFP-identifiable clones. This was possible as all images were acquired at the same exposure for the βgal signal. Mean pixel intensity values for βgal staining were measured in groups of GFP postitive clones for each disc using the ImageJ software, and normalised against mean GFP

staining pixel intensities in the same ROI (**Figure 4.8** C). This quantitative analysis revealed that *hh* expression levels were indeed significantly higher ($p = 0.001$) in $hyd^{K7.19}$ clones than in control clones.

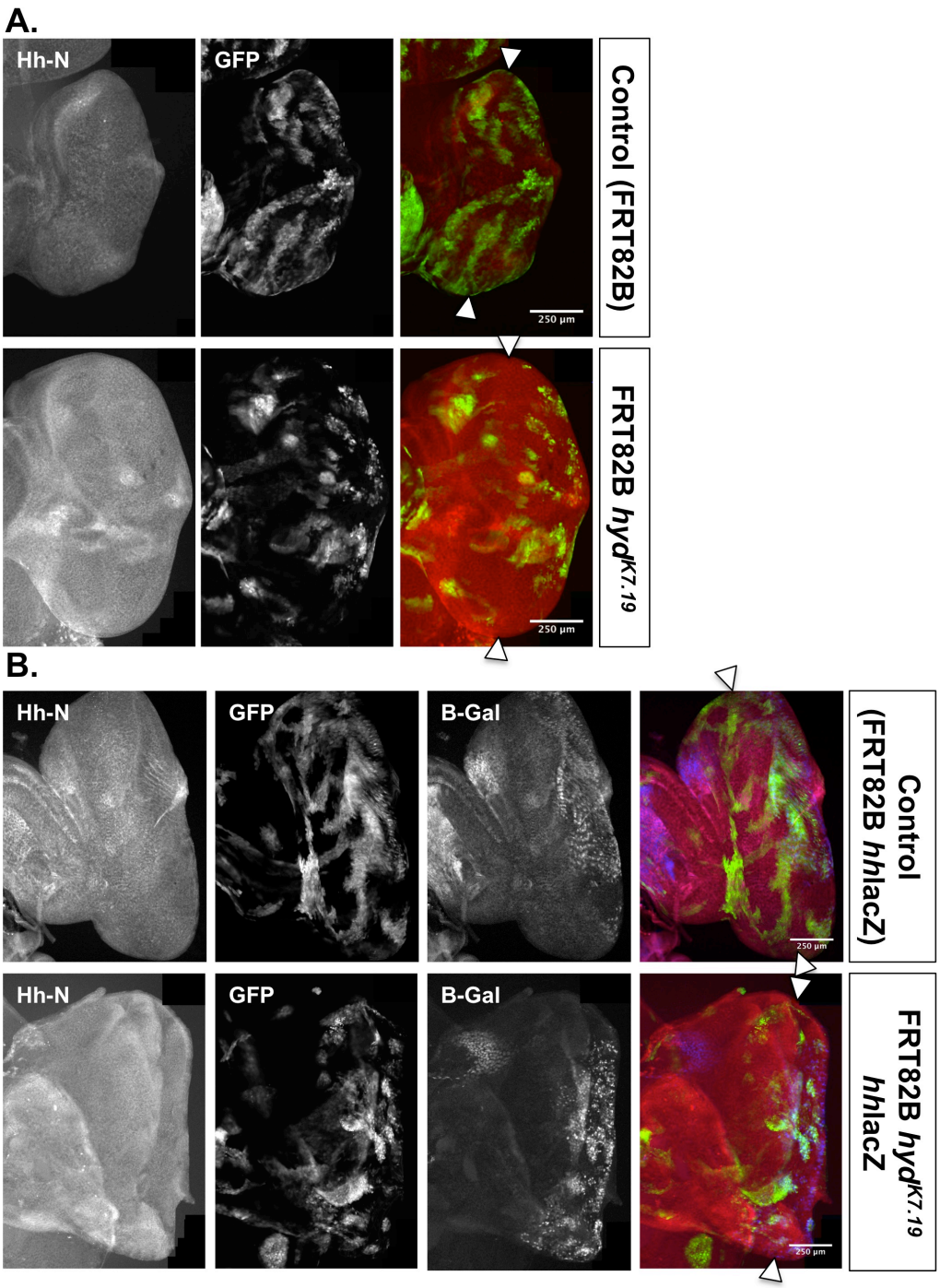

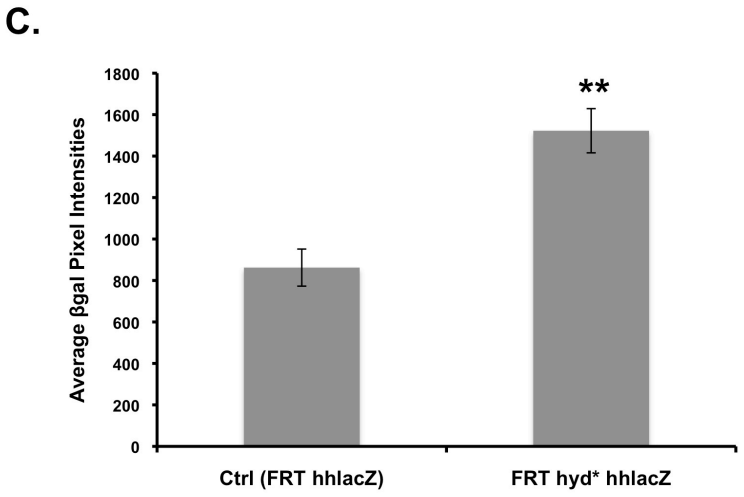

Figure 4.8: *hh*lacZ and Hh expression in *hyd*$^{K7.19}$ mutant L3 EA discs. Anterior is to the left, posterior is to the right, dorsal is up, and ventral is down, and the morphogenetic furrow (MF) is marked by white triangles in all subsequent immunofluorescence (IF) images. (**A**) IF of FRT82B (control) or FRT82B *hyd*$^{K7.19}$ discs containing GFP clones (green), stained for Hh (red). (**B**) IF of FRT82B *hhlacZ* (control) or FRT82B *hyd*$^{K7.19}$ *hhlacZ* discs containing GFP clones (green), stained for Hh (red) and βgal (*hhlacZ*) (magenta). **(C)** Measurements of average pixel intensities in single ROIs containing groups of GFP-positive clones in FRT82B *hhlacZ* (control) discs (n=4) or FRT82B *hyd*$^{K7.19}$ *hhlacZ* (n=6) (p =0.001; t-test). Normalisation was performed by dividing Bgal mean pixel intensites by GFP mean pixel intensities for each ROI.

4.4.2 Loss of *hyd* in clones results in elevated Wg signaling

Whilst the above results and previous reports (J. D. Lee et al. 2002) clearly show that loss of *hyd* in clones results in ectopic expression of Hh morphogen, it is not known whether loss of *hyd* can also affect Wg expression. The specification and growth of the head cuticle, which is normally regulated by Wg signalling (Royet & Finkelstein 1996), is abnormally affected in adult heads containing *hyd*$^{K7.19}$ clones, where loss of *hyd* causes significant overgrowth of head tissue, often at the expense of eye tissue. This indicates elevated Wg signalling as a result of *hyd* loss, and suggests that Hyd could also be a regulator of Wg signaling. Further to this, Hyd protein interacts with Armadillo (see **Chapter 3**), the transcriptional effector of the Wg pathway. I

therefore stained L3 eye discs for Wg protein to address whether loss of *hyd* also affects Wg morphogen expression. Indeed, $hyd^{K7.19}$ clones cause ectopic expression of Wg protein, mainly in anterior regions of the eye disc (**Figure 4.9**), which will eventually give rise to the head cuticle. The Wg protein signal was visibly higher in images of $hyd^{K7.19}$ discs compared to control discs taken at the same exposure. Interestingly, Wg protein levels were highest in cells immediately adjacent to $hyd^{K7.19}$ clones, rather than in the clones themselves. This could reflect increased *wg* expression in $hyd^{K7.19}$ clones, where the secreted Wg ligand then binds and activates the Wg pathway in neighbouring cells. To test this, a *wg*-lacZ reporter could be used, as well as antibody staining for Wg target genes. This would have the potential to uncover another very interesting role for Hyd in the potential negative regulation of Wg signalling. However, due to time constraints, I was not able to pursue this. Instead, I chose to focus on investigating Hyd's function in regulating *hh* expression and Hh pathway activity, as this was the main aim of my project.

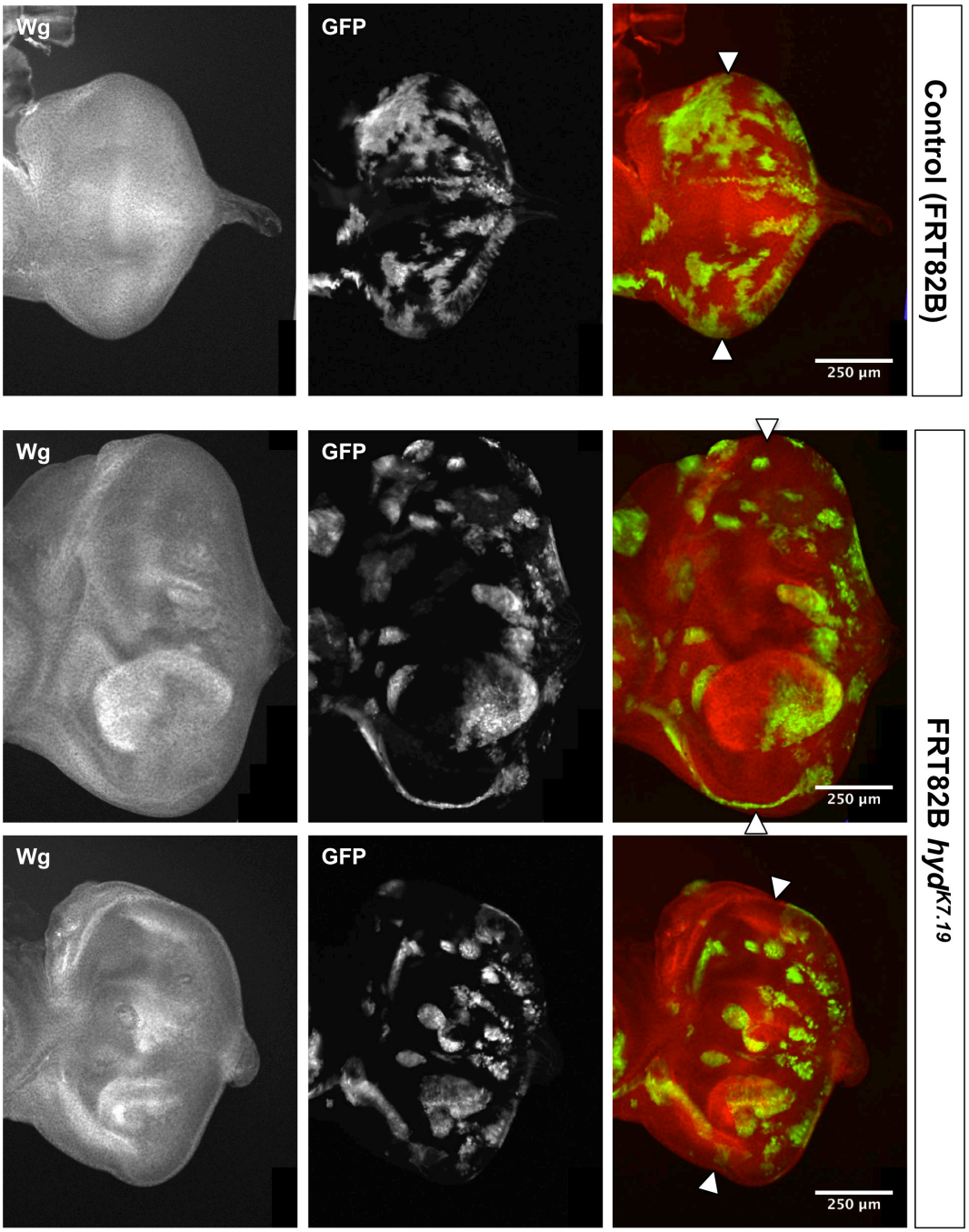

Figure 4.9: Wg expression in *hyd*$^{K7.19}$ mutant L3 EA discs. IF of FRT82B (control) or FRT82B *hyd*$^{K7.19}$ discs containing GFP clones (green), stained for Wg (red). The morphogenetic furrow (MF) is marked by white triangles in all merged images. Scale bars are 250 µm.

4.5 Hh pathway activity in *hyd*$^{K7.19}$ mutant clones

hh gene expression is up-regulated in *hyd*$^{K7.19}$ clones, leading to an increase in Hh protein across the eye disc. As a result of this abundance of Hh protein, one would expect Hh pathway activity to be up-regulated in *hyd*$^{K7.19}$ clones and/or the surrounding cells. Increased levels of Ci_{155}, the full length, active form of the Hh pathway transcriptional effector, had previously been observed in *hyd*$^{K3.5}$ clones anterior to the furrow (J. D. Lee et al. 2002). However, the same effect was also seen in anterior *hyd*$^{K3.5}$ *hh* double mutant clones, suggesting that Hyd normally acts to reduce Ci_{155} levels independently of Hh activity (J. D. Lee et al. 2002).

4.5.1 Loss of *hyd* affects Ci_{155} levels differentially depending on the location of *hyd*$^{K7.19}$ clones

In order to investigate Hh pathway activity, I first stained eye discs containing control or *hyd*$^{K7.19}$ clones with the 2A1 anti-Ci antibody(Motzny & Holmgren 1995). This antibody recognizes the carboxy-terminal region of the full-length Ci_{155} protein, but not the Ci_{75} repressor form, which is lacking the carboxy-terminus due to proteolytic processing. Therefore, all Ci staining is representative of the full length, active form of the Ci_{155} protein only.

The Ci_{155} staining pattern observed in control discs is representative of normal Ci expression in the eye disc at the third larval instar (Baker et al. 2009). Ci_{155} expression levels are kept relatively low throughout the disc, with the exception of a D-V strip of concentrated Ci_{155} staining (**Figure 4.10** A). Differentiated photoreceptors in the posterior half of the eye disc express *hh*, which activates the Hh pathway and leads to *dpp* expression in more anterior cells, thus causing a wave of differentiation across the disc (Royet & Finkelstein 1997). Ci and Dpp are therefore

highly expressed in the MF, a visible indentation that marks the front of differentiation(Penton et al. 1997).

In eye discs containing *hyd*$^{K7.19}$ mutant clones, the dorsal-ventral (D-V) strip of Ci staining, which represents the MF, is visibly disrupted (**Figure 4.10** A). Instead of forming a relatively straight line, the MF takes on an irregular path in the presence of *hyd*$^{K7.19}$ clones. In addition, high levels of Ci staining are no longer restricted to the presumed MF. This suggests that differentiation of photoreceptors from posterior to anterior does not occur at the same speed in different regions of the disc. Loss of *hyd* has previously been reported to cause premature photoreceptor differentiation (J. D. Lee et al. 2002), which could in part explain this result.

Further to this, individual groups of *hyd*$^{K7.19}$ mutant clones have profound autonomous effects on Ci_{155} levels, depending on their location with respect to the MF. Ci_{155} levels are frequently reduced in clones anterior to the D-V stripe of Ci_{155} staining, and sometimes in posterior clones near the MF (**Figure 4.10** A, white arrows). This finding directly contradicts previous reports that loss of *hyd* in *hyd*$^{K3.5}$ clones leads to an increase in Ci_{155} levels in anterior clones(J. D. Lee et al. 2002). On the other hand, elevated Ci_{155} levels were observed only in posterior clones, albeit less frequently (**Figure 4.10** A, yellow arrow). Interestingly, the groups of clones that affect Ci_{155} levels, either positively or negatively, often had a more rounded morphology that was never seen in control discs. The lower Ci_{155} level in anterior clones could indicate that loss of *hyd* results in either the degradation of Ci_{155}, or the processing to the Ci_{75} repressor form, which is not detected by the 2A1 antibody. This suggests that Hyd normally positively regulates full-length Ci_{155} levels in anterior cells, by preventing its degradation, or processing, or both. Conversely, Hyd appears to negatively regulate Ci_{155} levels in posterior cells, which could be due to Hyd promoting Ci_{155} degradation or processing instead.

To investigate whether increased Ci_{155} levels correlated with ectopic *hh* expression in posterior $hyd^{K7.19}$ clones, eye discs containing $hyd^{K7.19}$ *hh*-lacZ clones were double stained with Ci and βgal antibodies (**Figure 4.10** B). Indeed, there was a strong correlation between high levels of Ci_{155} staining and high levels of *hh* expression in posterior clones (**Figure 4.10** B; white arrows), suggesting that the increase in Ci_{155} levels could be a direct result of autonomous Hh pathway activation. This effect was not observed in all eye discs containing mutant clones, which could be due to the variability in the severity of the phenotype already observed in adult eyes. In summary, Hyd appears to prevent expression of full length Ci_{155} ahead of the MF by negatively regulating *hh* expression, whereas it promotes or stabilizes expression of Ci_{155} in cells anterior to the furrow.

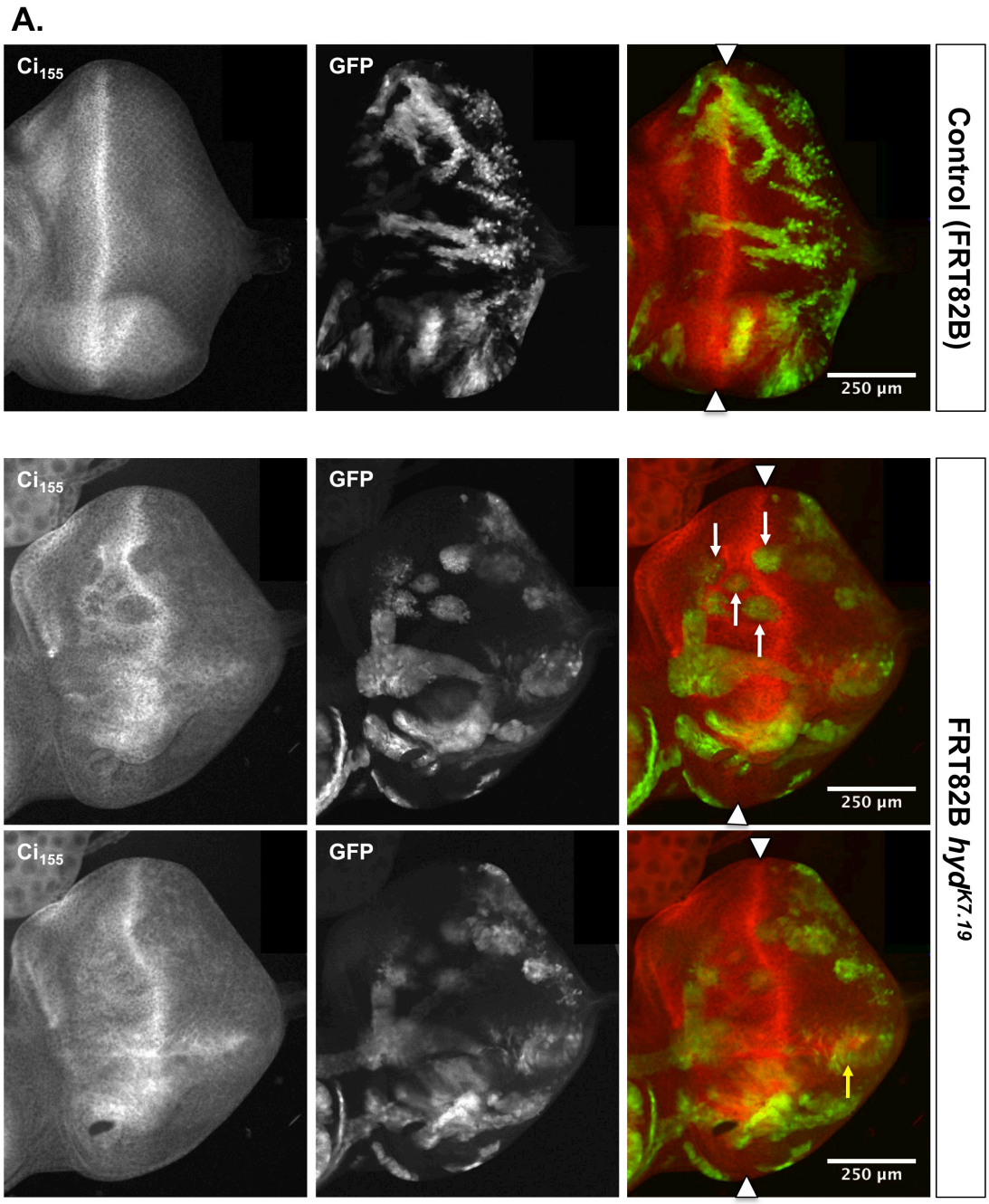
A.
Ci155
GFP
250 µm
Control (FRT82B)
Ci155
GFP
250 µm
Ci155
GFP
250 µm
FRT82B hydK7.19

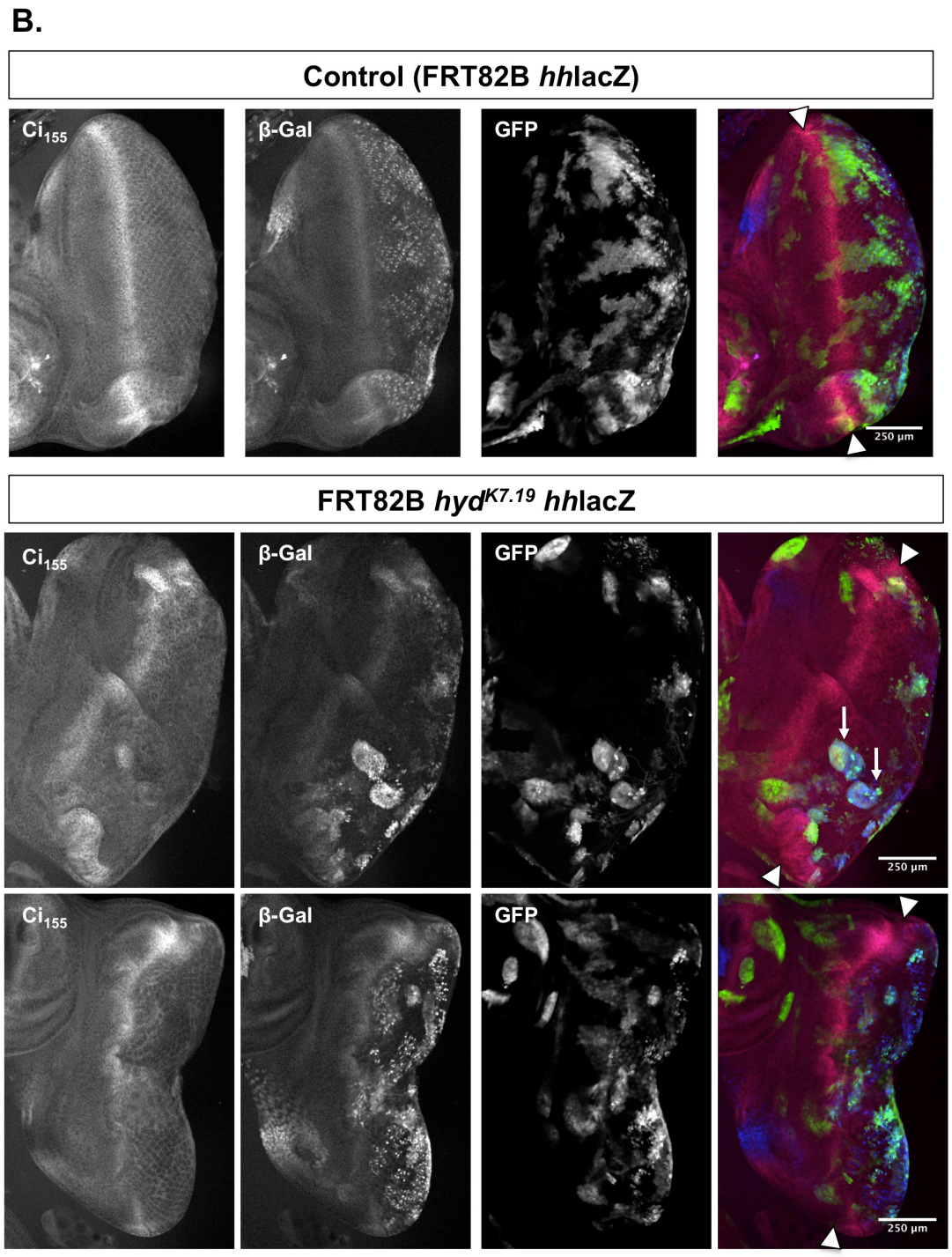

Figure 4.10: Ci_{155} and *hh*lacZ expression in $hyd^{K7.19}$ mutant L3 EA discs. (**A**) IF of FRT82B (control) or FRT82B $hyd^{K7.19}$ discs containing GFP clones (green), stained for Ci_{155} (red). (**B**) IF of FRT82B *hhlacZ* (control) or FRT82B $hyd^{K7.19}$ *hhlacZ* discs containing GFP clones (green), stained for Ci_{155} (red) and βgal (*hhlacZ*) (magenta). The morphogenetic furrow (MF) is marked by white triangles in all merged images. Scale bars are 250 µm.

4.5.2 Loss of *hyd* causes accumulation of Patched (Ptc) in *hyd*$^{K7.19}$ clones and the surrounding tissue

Another indicator of Hh pathway activity is the expression of the transmembrane receptor for Hh ligand, Ptc. Cells expressing Ptc are responsive to Hh ligand and capable of transducing the Hh pathway. When Hh ligand is present and bound to Ptc both can be internalized, removing them from the cell surface (Martín et al. 2001). Importantly, *ptc* is also a Hh pathway target gene, and therefore Ptc expression is a good read-out of Hh pathway activity downstream of Ci_{155}.

Eye discs containing *hyd*$^{K7.19}$ clones were therefore stained for Ptc, which revealed high levels of ectopic Ptc expression in both anterior and posterior regions of the disc. *hyd*$^{K7.19}$ clones caused very pronounced non-autonomous Ptc expression in neighbouring cells, as well as moderate autonomous Ptc expression (**Figure 4.11** A). It therefore appears that loss of *hyd* causes mainly non-autonomous ectopic Hh pathway activity, whilst having autonomous effects on Ci_{155} levels. Indeed, the increased non-autonomous Ptc expression suggests that these cells could have an increased concentration of extracellular Ptc. This could be due to the high levels of Hh protein expression observed in discs containing *hyd*$^{K7.19}$ clones, as well as the diffusible nature of the Hh ligand.

Interestingly, co-staining of eye discs with Ci and Ptc antibodies revealed that both autonomous and non-autonomous expression of Ptc always correlated with high Ci_{155} levels (**Figure 4.11** B). As previously reported (J. D. Lee et al. 2002), my observation of Ci_{155} and Ptc up-regulation support the notion that Hyd negatively regulates Hh pathway activity both by autonomously down-regulating Ci_{155} levels, as well as non-autonomously by suppressing *hh* expression.

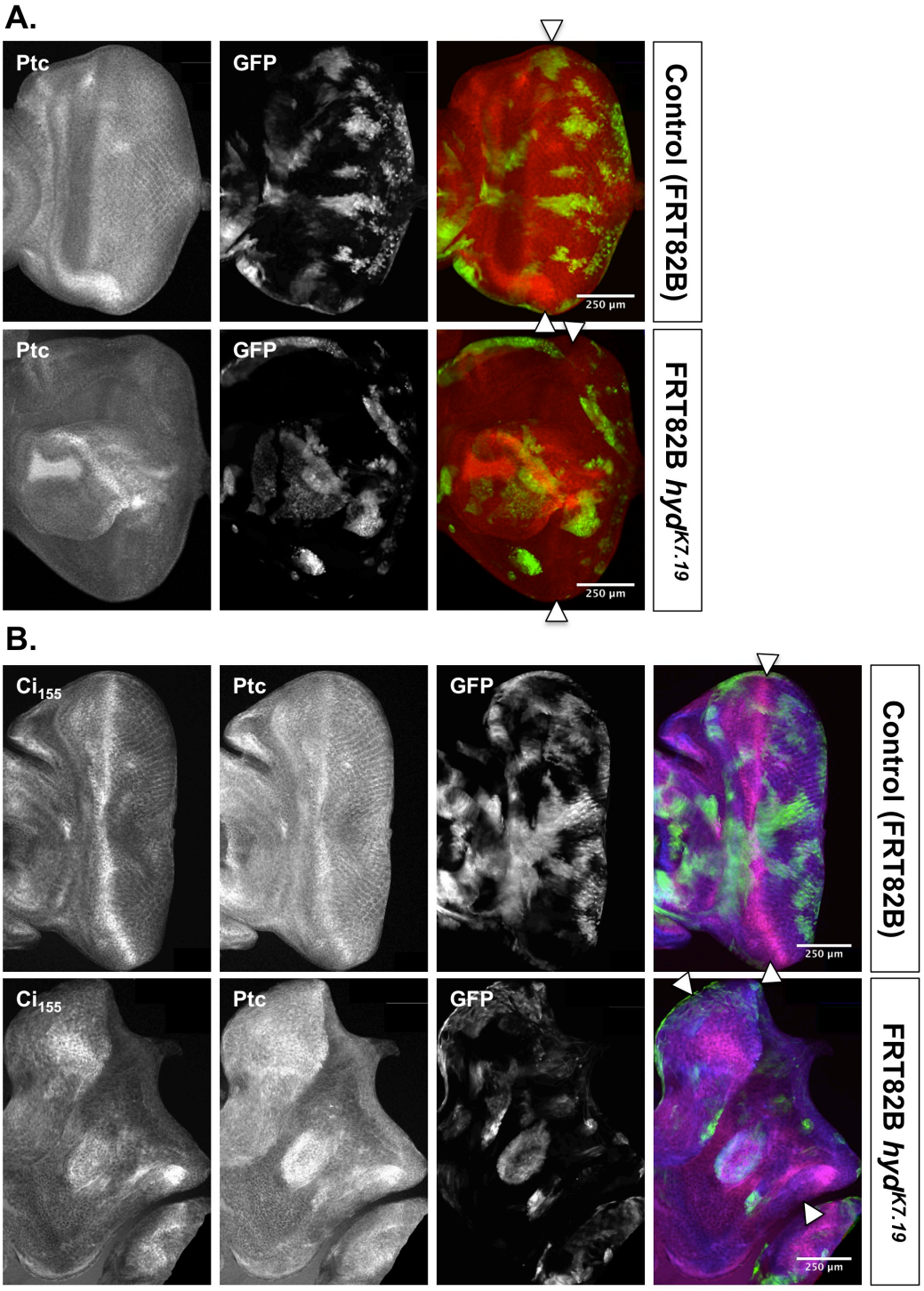

Figure 4.11: Ptc and Ci_{155} expression in $hyd^{K7.19}$ mutant L3 EA discs. (**A**) IF of FRT82B (control) or FRT82B $hyd^{K7.19}$ discs containing GFP clones (green), stained for Ptc (red). (**B**) IF of FRT82B (control) or FRT82B $hyd^{K7.19}$ discs containing GFP clones (green), stained for Ci_{155} (red) and Ptc (magenta). The morphogenetic furrow (MF) is marked by white triangles in all merged images. Scale bars are 250 µm.

4.6 Hyd positively regulates Hh pathway activity in Cl8+ cells

So far, the *in vivo* results suggest that, depending on the location in the EA disc, Hyd regulates Hh pathway activity both positively and negatively. In order to help determine the mechanism(s) by which Hyd can regulate Hh pathway activity and *hh* gene expression, it was necessary to develop a cell culture based model system to reduce the complexity of the *in vivo* system and control for intercellular communication between different cell types. The advantage of an *in vitro* system to study Hyd function in these processes is the reduced complexity compared to *in vivo* studies, eliminating factors such as cell communication between different cell populations within a tissue. Although no *Drosophila* cell lines have been found to date that are capable of producing the Hh ligand (Celniker et al. 2009), most can be used to study the Hh and Wg signaling pathways (Cherbas et al. 2011).

4.6.1 S2 cells transfected with exogenous Ci are capable of transducing the Hh pathway

S2 cells are one of the most commonly used *Drosophila* cell lines. Gene expression studies, however, have revealed that they do not express the relevant components at adequate levels to enable them to transduce the Hh and Wg pathways (Cherbas et al. 2011). For example, S2 cells lack the transmembrane Frizzled2 receptor for the Wg ligand. Similarly, Ci, which is required for Hh target gene expression, is not expressed in S2 cells. When Ci is provided exogenously, however, S2 cells are able to transduce the Hh pathway when stimulated with Hh-N ligand (Fukumoto et al. 2001). I therefore co-transfected S2 cells with Ci and Hh-N ligand, and used a firefly luciferase reporter construct to measure Hh pathway activity. Two patched (ptc)-luciferase reporter constructs were used, ptcΔ136-Luc and ptcΔ136-mut (C. H. Chen et al. 1999), which contained a wild-type or mutant patched promoter, respectively,

driving the expression of firefly luciferase. As expected, transfection of Ci led to reporter activation, which was increased further upon co-transfection with Hh ligand (**Figure 4.12**). The observed signal was significantly higher than in the negative control (ptcΔ126-mut), as well as in the absence of Ci, suggesting that transfection of Ci is absolutely required for the study of the Hh pathway in S2 cells. Although the S2 cell system was optimized and worked well, I thought that the need to transfect Ci, as well as the inability to transduce the Wg pathway in the absence of exogenous Frizzled2 (which was not available in the lab), could complicate things further down the line. So I utilised another *Drosophila* cell line, Cl8+, which does not require exogenous components to transduce the Hh and Wg pathways(Cherbas et al. 2011).

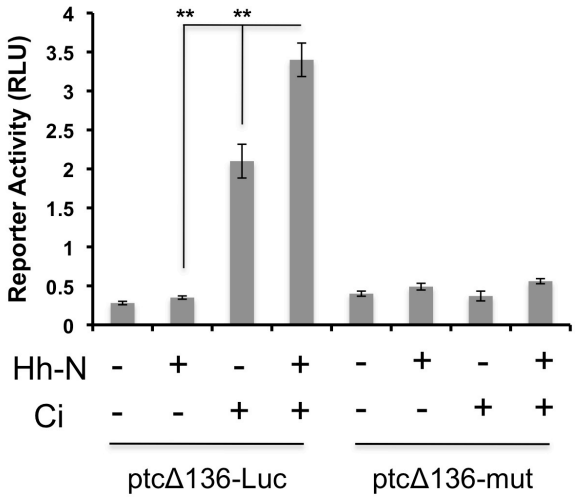

Figure 4.12: Hh pathway activation in S2 cells. S2 cells were transfected with Ci, Hh-N, and the Ptc luciferase reporters ptcΔ136-Luc and ptcΔ136-mut (negative control). Error bars represent standard deviation from three independent transfection replicates (n=3). All luciferase readings were normalized to renilla activity. RLU was significantly (**) enhanced in samples containing ptcΔ136-Luc, Hh-N and Ci, versus ptcΔ136-Luc and Ci only (p = 0.002), and ptcΔ136-Luc and Hh-N only (p = 0.002).

4.6.2 Knock down of Hyd in Cl8+ cells decreases Hh pathway activity

Unlike S2 cells, Cl8+ cells, which are derived from third instar wing discs, express all the necessary components needed to transduce the Hh and Wg pathways (Cherbas et al. 2011). First I investigated whether transfection of Hh-N ligand into Cl8+ cells could also drive ptcΔ136-Luc reporter activity. Stimulation with Hh ligand yielded a strong signal, with minimal background in the absence of Hh and in the negative ptcΔ136-mut control (**Figure 4.13** A). Next, I wanted to investigate what effect removal of Hyd would have on Hh pathway activity. Cl8+ cells were transfected with either dsRNA specific for EGFP (negative control), or dsRNA specific for Hyd (7950) (see **Chapter 2, 2.2.3**). As can be seen in **Figure 4.13** B, the transfection of Hyd 7950 dsRNA results in a very good knockdown of Hyd protein in Cl8+ cells, whereas EGFP dsRNA has no effect on Hyd protein levels.

In the presence of Hh ligand, knockdown of Hyd significantly reduces ptcΔ136-Luc reporter activity compared to the EGFP dsRNA-treated control ($p = 0.007$) (**Figure 4.13** C). This effect was reproduced in an independent experiment, whereby Hyd 7950 dsRNA also decreased Hh pathway activity significantly compared to the EGFP dsRNA-treated control ($p = 0.041$) (**Figure 4.13** D). These results suggest that, in the presence of Hh ligand, Hyd positively regulates Hh pathway activity in Cl8+ cells.

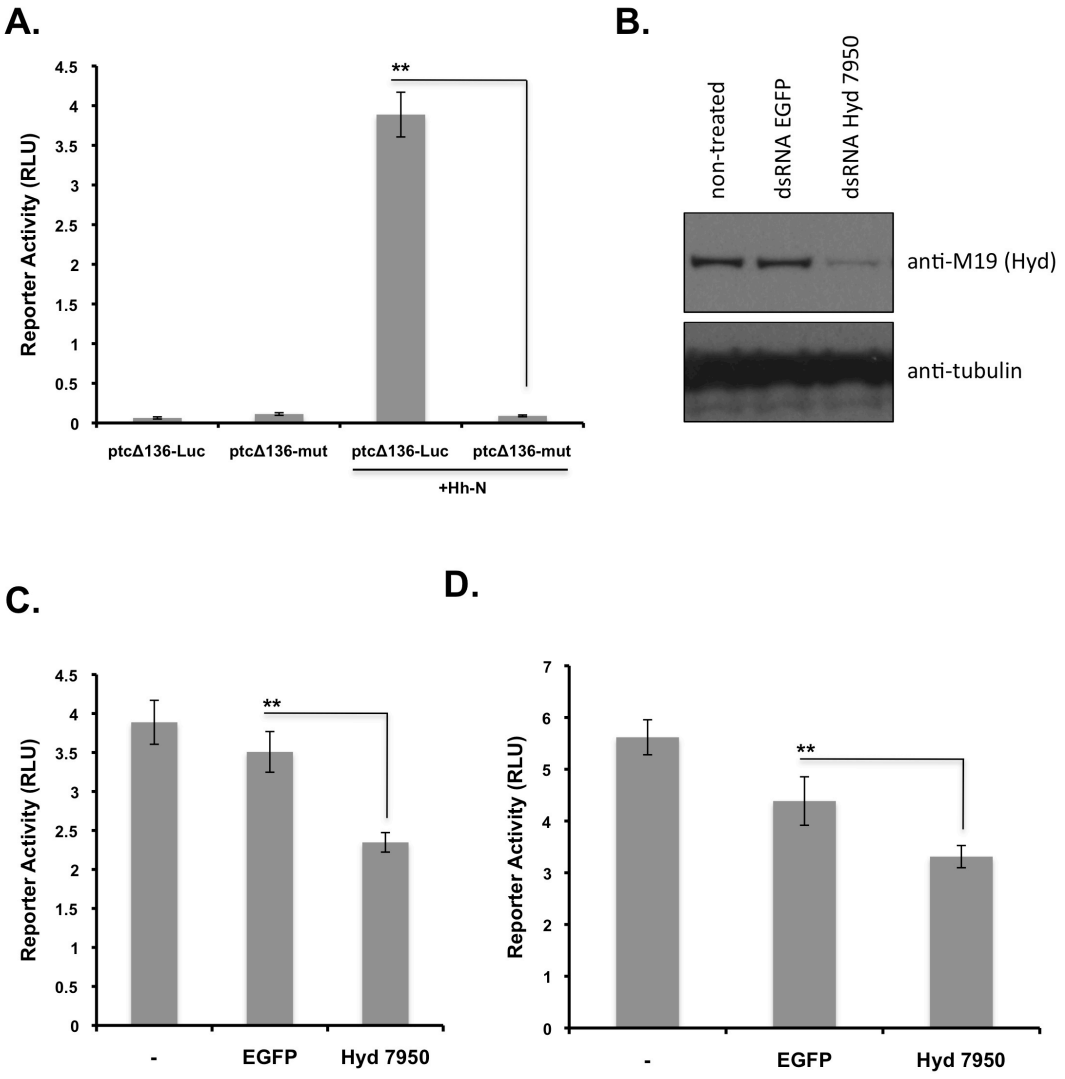

Figure 4.13: Hyd positively regulates Hh pathway activity in Cl8+ cells. (**A**) Hh pathway activation in Cl8+ cells. Cl8+ cells were transfected with Hh-N ligand, and the Ptc luciferase reporters ptcΔ136-Luc and ptcΔ136-mut (negative control). **t-test $p < 0.001$. (**B**) Knockdown of Hyd protein following transfection of Cl8+ cells with dsRNA. (**C**) Treatment with Hyd 7950 dsRNA reduces Hh pathway activity. Cl8+ cells were transfected with dsRNA, Hh-N, and ptcΔ136-Luc reporter. **t-test $p = 0.007$. (**D**) Treatment with Hyd 7950 reduces Hh pathway activity. Cl8+ cells were transfected with dsRNA, Hh-N, and ptcΔ136-Luc reporter. **t-test $p = 0.041$. All error bars represent standard deviation from three independent transfection replicates. All luciferase readings were normalized to Renilla-luciferase activity.

4.6.3 Knockdown of Hyd has no effect on Wg pathway activity in Cl8+ cells

As my data identified Hyd's ability to regulate Wg expression and physically interact with the Wg pathway transcriptional effector, Armadillo, (see **Figure 4.9** and **Chapter 3, Section 3.5.3**), I also wanted to investigate whether Hyd can affect Wg pathway activity in Cl8+ cells. Cl8+ cells were co-transfected with Wg and a luciferase reporter containing 12 repeats of the TCF binding sites (dTF12) (DasGupta et al. 2005; Korinek et al. 1997), which are the binding sites for the Armadillo/TCF transcriptional activator complex controlling target gene expression in the Wg pathway (Behrens et al. 1996; Molenaar et al. 1996). A FOP FLASH reporter, in which these sites are mutated, was included as a negative control. In the absence of Wg ligand, both reporters produced a relatively low-level background signal. Induction with Wg increased the dTF12 signal, and intriguingly, completely ablated the background in the FOP FLASH signal (**Figure 4.14** A). Additionally, the overall intensity of the dTF12 + Wg signal was not as high as in the Hh pathway luciferase assays. This could be due to non-optimal expression of the transfected Wg ligand, which requires $CuSO_4$-mediated induction from a metallothionine promoter. This initial pilot experiment suggests that, under our experimental conditions, the Wg pathway reporter assays is not as robust or reliable as for the Hh pathway reporter assays.

In the presence of Wg ligand, the dTF12 reporter activity did not change significantly in samples treated with Hyd 7950 dsRNA (**Figure 4.14** B). Unfortunately, I did not have time to improve or repeat this assay. Although this experiment was only performed once, the results would suggest that Hyd has no effect on Wg pathway activity in Cl8+ cells. While this could mean that Hyd has no involvement in the Wg pathway in general, it could also suggest that Hyd's function(s) in the Wg pathway are cell/tissue-specific, indicating that Hyd affects Wg signaling in the eye disc, but not in the wing disc or wing-disc derived Cl8+ cells.

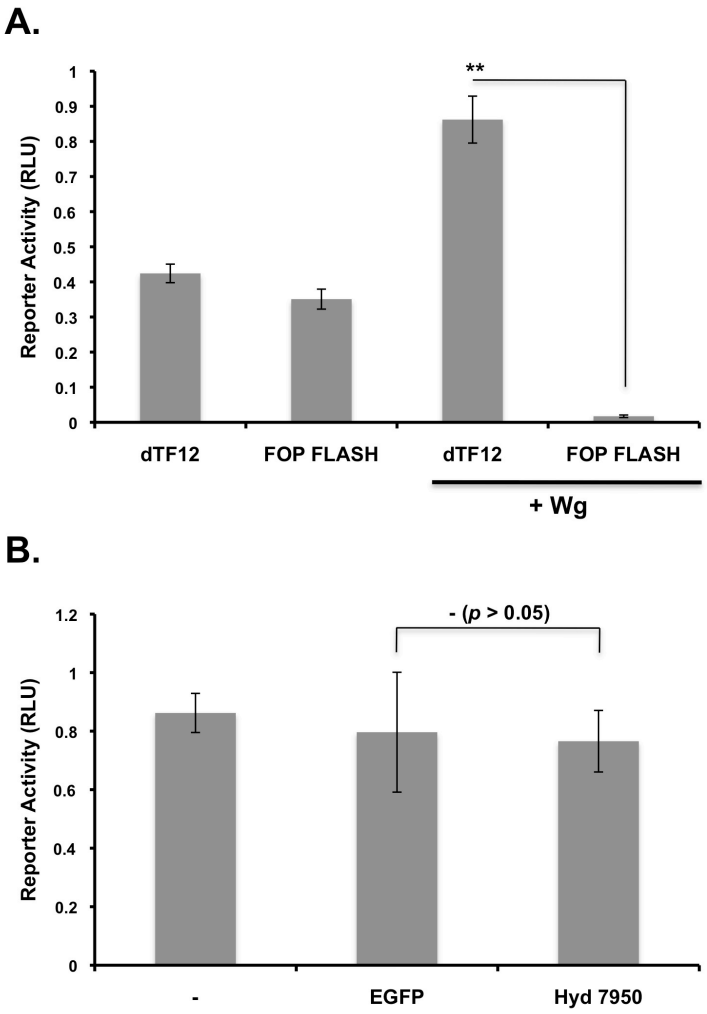

Figure 4.14: Hyd knockdown does not affect Wg pathway activity in Cl8+ cells. (**A**) Wg pathway activation in Cl8+ cells. Cl8+ cells were transfected with Wg ligand, and the TCF luciferase reporters dTF12 and FOPFLASH (negative control). **t-test $p = 0.002$; n=3. (**B**) Treatment with Hyd 7950 dsRNA has no effect on Wg pathway activity. Cl8+ cells were transfected with dsRNA, Wg, and dTF12 reporter. **t-test $p = 0.83$; n=3. All error bars represent standard deviation from three independent transfection replicates. All luciferase readings were normalized to Renilla luciferase activity.

4.7 Hyd interacts with Ci in Cl8+ cells but does not affect Ci levels

Both the *in vivo* and *in vitro* data implicate Hyd in the regulation of Hh pathway activity, with the *in vivo* results clearly suggesting a role for Hyd in the regulation of full-length Ci_{155} levels and/or activity. In order to determine whether Hyd regulates Ci indirectly, or directly through a physical interaction, I first investigated whether Hyd can interact with Ci.

4.7.1 Hyd interacts with Ci_{155} in Cl8+ cells

S2 cells were co-transfected with HA-Strep Hyd and an amino-terminal (NT) HA-tagged Ci construct (HA-Ci). Although S2 cells do not express Ci endogenously, they were chosen for binding assays due to their ease of transfection and handling, as the chances of detecting an interaction are generally higher when using over-expressed proteins. In addition, the catalytic inactive Hyd mutant, Hyd C>A, was also used in these Ci binding assays; the rationale behind this being that it would be very hard to detect an interaction if Hyd degraded Ci.

Although Ci was pulled down with both WT and C>A Hyd, the binding was weak, but potentially more than the background binding of Ci to the StrepTactin Sepharose resin (**Figure 4.15** A). As assessed by measuring band intensity in ImageJ, Ci binding to WT Hyd was the same as background Ci binding, whereas binding to C>A Hyd was about 1.5x over background. Although Ci binding to WT Hyd was not convincing, Ci binding to C>A Hyd looked more promising and suggested that Hyd could be directly involved in positively regulating Ci degradation. Importantly, the HA tag on exogenous Ci is located at the carboxy-terminal, which means that any Ci

that is converted to the Ci_{75} repressor form cannot be detected using the HA antibody. Therefore, another possibility is that Hyd promotes conversion to the repressor form by ubiquitylation of full-length Ci_{155}. However, the levels of Ci_{155} in the input samples appear unchanged in the presence or absence of WT and C>A Hyd (see **Figure 4.15** A, lanes 1, 2 and 4).

In a parallel approach to test Ci binding to Hyd, I also used mammalian 293 cells, as they are known to produce large amounts of over-expressed proteins. *Drosophila* cDNAs were cloned into mammalian expression vectors for this purpose and transfected into 293 cells. Following a Streptactin pull down against HSP-Hyd, Ci co-precipitated with WT Hyd. Importantly, no backround Ci binding was detected in the Ci only control (**Figure 4.15** B, 3rd lane).

Although the binding assays using exogenous, over-expressed proteins in S2 and 293 cells indicate that Ci can interact with Hyd, they are not very convincing. I therefore performed another binding assay using Cl8+ cells, which not only express Ci and Hyd endogenously, but are also capable of transducing the Hh pathway. Additionally, my previous results showed, that knockdown of Hyd in these cells negatively affected Hh pathway activity, suggesting that Hyd could regulate Hh pathway activity in these cells by binding to Ci. I therefore immunoprecipitated endogenous Hyd to investigate whether it can bind to endogenous Ci. Indeed, endogenous Ci co-immunoprecipitated with Hyd (**Figure 4.15** C). In summary, these results suggest that Hyd could positively regulate Hh pathway activity through binding Ci_{155}.

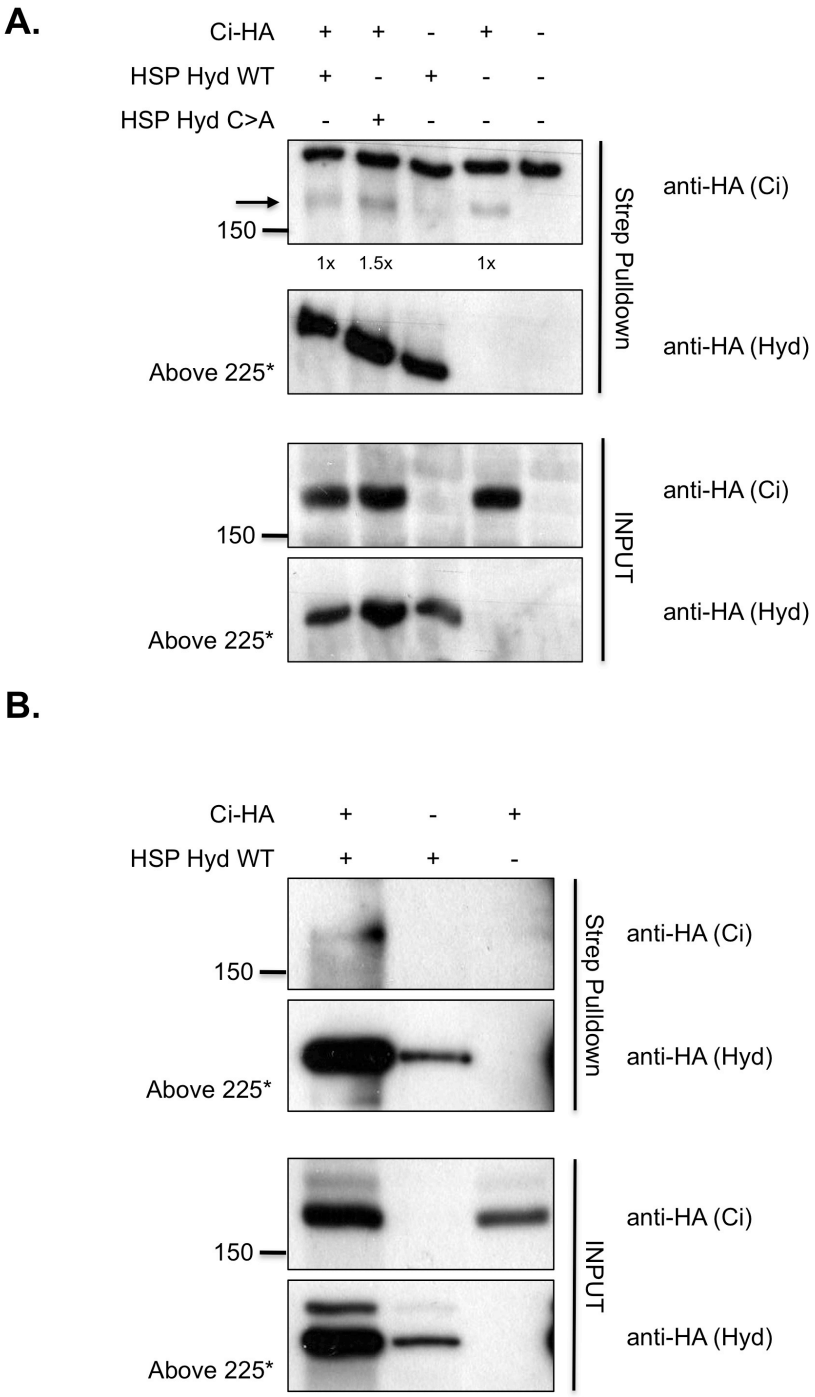
A.
Ci-HA + + - + -
HSP Hyd WT + - + - -
HSP Hyd C>A - + - - -
150
1x 1.5x 1x
Above 225*
Strep Pulldown
anti-HA (Ci)
anti-HA (Hyd)
150
Above 225*
INPUT
anti-HA (Ci)
anti-HA (Hyd)
B.
Ci-HA + - +
HSP Hyd WT + + -
150
Above 225*
Strep Pulldown
anti-HA (Ci)
anti-HA (Hyd)
150
Above 225*
INPUT
anti-HA (Ci)
anti-HA (Hyd)

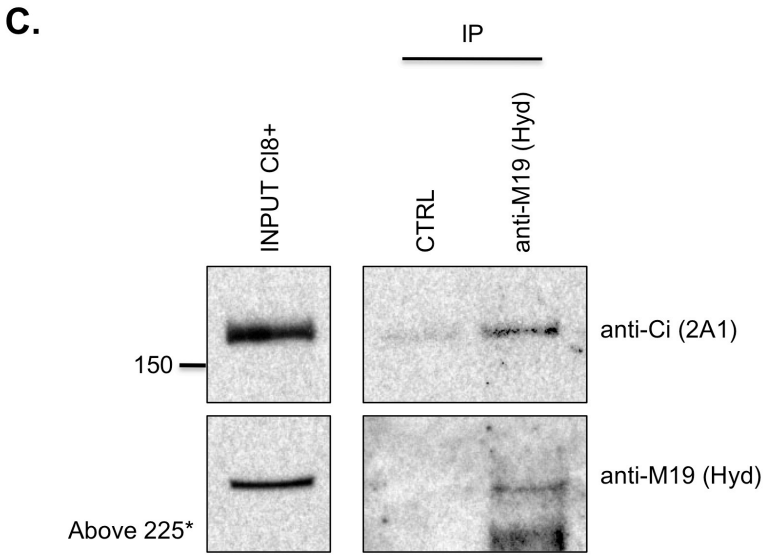

Figure 4.15: Hyd interacts with Ci_{155}. (**A**) StrepTactin pulldown in S2 cells. S2 cells were transfected with HA-Strep(HSP)-Hyd and HA-Ci constructs. (**B**) StrepTactin pulldown in 293 cells. 293 cells were transfected with *Drosophila* HA-Strep(HSP)-Hyd and HA-Ci constructs. (**C**) Immunoprecipitation of endogenous Hyd in Cl8+ cells using the Hyd M19 antibody (Santa Cruz). Endogenous Ci_{155} was co-immunoprecipitated with Hyd, as detected using the 2A1 Ci antibody. Negative control = IgG.

4.7.2 Knockdown of Hyd has no effect on Ci_{155} levels in Cl8+ cells

So far, my data from Cl8+ cells implies that Hyd normally promotes Ci_{155} activity, which may or may not involve regulation of Ci_{155} stability, to positively regulate Hh pathway activity. I next investigated whether knockdown of Hyd affects Ci protein levels, both in the presence and absence of Hh ligand. However, I was only able to analyse full-length Ci_{155} protein levels, as the 2A1 Ci antibody cannot detect the Ci_{75} repressor form. Loss of Hyd does not appear to affect full-length Ci_{155} protein levels, in the presence or absence of Hh ligand and therefore pathway activity (**Figure 4.16**). Although Hyd interacts with Ci_{155}, this does not seem to affect Ci_{155} protein levels. However, Hyd could be directly or indirectly affecting the post-translational

modification (i.e. phosphorylation and/or ubiquitylation) of Ci, and thus regulating Ci_{155} activity independently of any effects on its expression level.

To investigate Hyd's potential role in Wg pathway regulation, I also looked at whether Hyd knockdown could affect the levels of the Wg pathway transcriptional effector Armadillo (Arm). Interestingly, loss of Hyd leads to slightly lower levels of Arm only when the Hh pathway is on (**Figure 4.16**, lane 6). This is in agreement with previous findings that identified Hyd as a positive regulator of Wg signalling through non-degradative ubiquitylation, and subsequent up-regulation of β-catenin (Hay-Koren et al. 2011). Additionally, this result also indicates cross-talk between the Hh and Wg pathways, which has been reported previously (J. He et al. 2006), and suggests that Hyd could be a key protein involved in cross-pathway signalling.

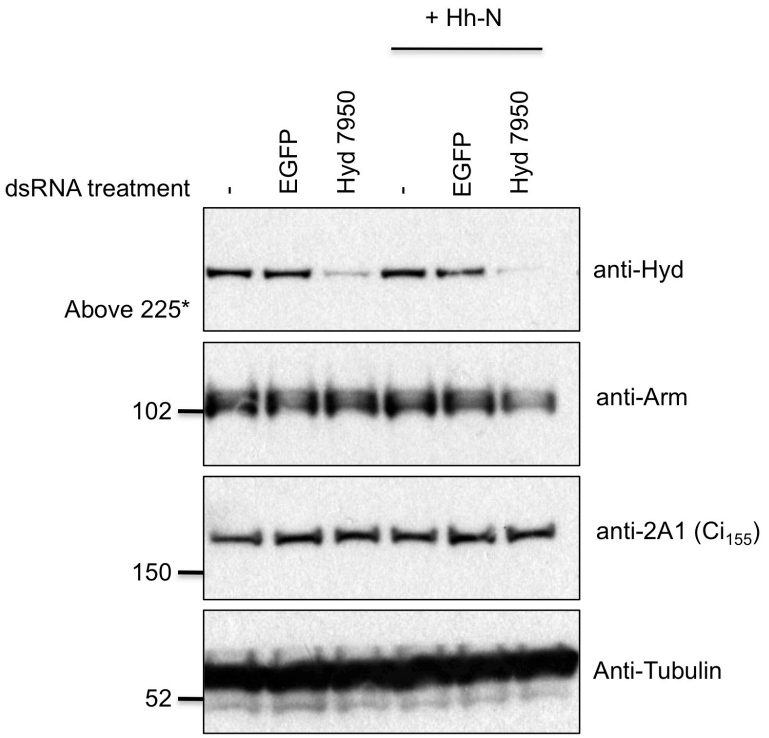

Figure 4.16: Effect of Hyd knockdown on Ci_{155} and Arm protein levels. Cl8+ cells were transfected with EGFP or Hyd 7950 dsRNA and Hh-N ligand.

4.8 Discussion

The findings presented here implicate Hyd in the regulation of both Hh and Wg signalling in the developing *Drosophila* eye and head tissues, and suggest that part of the molecular mechanism may involve regulation of Ci activity through physical interaction of Hyd with Ci. Mutant $hyd^{K7.19}$ clones in the EA disc express a severely truncated Hyd protein that lacks all carboxy-terminal domains except the UBA domain. These clones cause non-autonomous overgrowth of EA disc tissue, as well as overgrowth of head tissue in adults and scarring in adult eyes, although the clones themselves do not persist to adulthood. The adult phenotype is rescued completely by exogenously supplying a wild-type Hyd transgene, whereas a Hyd transgene encoding a catalytically inactive Hyd protein is unable to rescue the phenotype. $hyd^{K7.19}$ clones express significantly higher levels of *hh*, and cause elevated expression levels of both Hh and Wg ligands in EA discs. Accordingly, loss of *hyd* in the clones also affects Hh pathway activity. Loss of *hyd* affects Ci_{155} levels in $hyd^{K7.19}$ clones depending on their location with respect to the MF: Ci_{155} levels are reduced in anterior clones, but are elevated above basal levels in some posterior clones. Additionally, Ptc protein levels accumulate in and around $hyd^{K7.19}$ clones. Finally, Hyd positively regulates Hh pathway activity and interacts with Ci_{155} in wing-disc derived Cl8+ cells, but Hyd does not appear to affect Ci protein levels.

The results clearly show that Hyd is involved in the regulation of both *hh* gene expression, as well as Hh pathway activity in the eye. $hyd^{K7.19}$ clones in the posterior region of the EA disc, which mainly gives rise to the compound eye, express high levels of *hh*, which results in both autonomous and non-autonomous elevation in Hh, Ci_{155}, and Ptc protein levels. Loss of *hyd* in $hyd^{K7.19}$ clones gives rise to an adult eye phenotype that is chiefly characterized by scarring and roughness of the compound eye, but does not often feature hyperplasia of eye tissue. This suggests that Hyd normally negatively regulates both *hh* gene expression and Hh pathway activity in posterior regions of the disc, and that the lack of this repression leads to defects in

eye development. These data are mostly in agreement with previous work that showed ectopic expression of *hh* and *dpp* in $hyd^{K7.19}$ clones, however the $hyd^{K3.5}$ allele used to generate clones in this study gave rise to a distinctly hyperplastic compound eye, which featured non-autonomous outgrowths of excessive eye tissue (J. D. Lee et al. 2002). One common feature between the $hyd^{K3.5}$ and $hyd^{K7.19}$ alleles is that both types of $hyd^{K7.19}$ clones seem to be eliminated in adult eyes. In the case of $hyd^{K3.5}$ clones this is stipulated to be the result of clone elimination due to cell competition, as $hyd^{K3.5}$ clones were found to have a distinct growth disadvantage compared to the surrounding cells (J. D. Lee et al. 2002). It is not known whether $hyd^{K7.19}$ clones are eliminated in the same way, or for different reasons, such as self-directed apoptosis. However, one way to explain the difference in the adult eye phenotypes could be that $hyd^{K7.19}$ clones are eliminated earlier than $hyd^{K3.5}$ clones during eye development, and so the hyperplastic effects on the adult eye tissue, although apparent in EA discs at the third instar, are not as pronounced.

Interestingly, loss of *hyd* in anterior $hyd^{K7.19}$ clones has the opposite effect on Ci_{155} levels, which were clearly reduced below basal levels. This directly contradicts previously published results, which show that anterior $hyd^{K3.5}$ clones accumulate high levels of Ci_{155} (J. D. Lee et al. 2002). During normal eye development, Ci_{155} expression is kept low both posterior and anterior to the MF, with the exception of a D-V strip of high Ci_{155} levels immediately posterior to the MF, where Hh signaling directs the differentiation of photoreceptors. However, Ci_{155} is regulated differently on either side of the furrow. In posterior regions of the eye disc, expression of the Cul3-based E3 ubiquitin ligase Rdx/Hib leads to ubiquitylation and subsequent degradation of full-length Ci_{155}, preventing further activation of the Hh pathway in posterior cells. In anterior regions, expression of the E3 ubiquitin ligase Slmb ensures ubiquitylation of Ci_{155}, which instead results in partial processing of the full-length active protein to a truncated Ci_{75} transcriptional repressor that can no longer activate Hh target genes (Baker et al. 2009). A plausible theory for the differential Hyd-mediated regulation of Ci_{155} levels could therefore be that Hyd normally

antagonizes Slmb function in anterior cells, but potentiates Rdx/Hib function in posterior cells, thereby indirectly regulating Ci_{155} levels during eye development.

This hypothesis is strengthened by the fact that Hyd can interact with Ci. Loss of Hyd in the wing-disc derived Cl8+ cell line results in down-regulation of the Hh pathway, suggesting that Hyd positively regulates Hh pathway activity in this setting. Of course, it must be noted that this setting represents a highly simplified model of Hyd's function in regulating Hh signaling *in vivo*, as the complexity of communication between different cell types within a dynamically developing tissue is completely eliminated. Nevertheless, it appears that Cl8+ cells are responding to a loss of Hyd analogously to anterior cells in the eye disc, in which Ci_{155} is reduced. Hyd could therefore act as a positive regulator of Hh pathway activity in Cl8+ cells by antagonizing Slmb activity, and thus antagonising the processing of C_{155} to the Ci_{75} repressor form. Conversely, the Cl8+ cell luciferase results do not support a role for Hyd in Rdx/Hib potentiation, and thus Ci_{155} degradation. If Hh pathway activity in Cl8+ cells is due to stabilization of Ci_{155} levels as a result of Hyd-mediated antagonism of Slimb-directed Ci_{155} processing, one would expect Ci_{155} levels to be decreased in the absence of Hyd. However, knockdown of Hyd had no effect on Ci_{155} levels in Cl8+ cells, both in the presence and absence of Hh ligand. This could be due to the fact that Ci_{155} protein is constantly replenished as a consequence of continuous Hh ligand stimulation, thereby masking a potential effect on Ci_{155} levels. To test this, the experiment could be improved by blocking protein translation using the drug cyclohexamide (CHX). It is therefore still plausible that Hyd could antagonize Slimb action on Ci_{155}, for example by directly competing for Ci binding, preventing Slimb-mediated ubiquitylation of Ci_{155}, and catalyzing the addition of ubiquitin chains that instead result in stabilization and/or activation of Ci_{155}. This model is supported by the fact that the catalytic inactive Hyd transgene fails to rescue the phenotype, suggesting that Hyd's ubiquitylation activity is crucial for its function in eye development. Additionally, EDD ubiquitylates β-catenin in the Wg pathway by adding K11-and K29-linked ubiquitin chains, which results in up-regulation of β-catenin, and thus Wnt pathway activity. Hyd could therefore act in a smilar way to

ubiquitylate Ci. However, it remains to be determined whether Hyd can ubiquitylate Ci, and what the biochemical nature of these ubiquitin chains would be.

Finally, the results also implicate Hyd in the regulation of Wg signaling during eye development. The Wg and Hh morphogens work in concert during eye development at the third instar to specify cells that will form part of the head cuticle and compound eye, respectively(Royet & Finkelstein 1996). Unlike Hh, which is mostly expressed in posterior regions of the eye disc, Wg expression is restricted to the lateral margins of the anterior eye disc(Cho et al. 2000; Treisman & G. M. Rubin 1995). However, loss of hyd in $hyd^{K7.19}$ clones leads to ectopic and elevated levels of Wg expression throughout anterior regions of the eye disc. As a result, the head cuticle is overgrown in adult heads, and the scarring observed at the margins of adult eyes could therefore represent expanded regions of head cuticle tissue at the expense of the compound eye.

In addition to regulating Wg expression, Hyd also interacts with the Wg pathway components Armadillo and Sgg (see **Chapters 3 and 5**), suggesting that, as for the Hh pathway, Hyd may regulate both Wg-ligand and -pathway activity. This is a novel finding in *Drosophila*, although EDD has previously been shown to interact with β-catenin, the human orthologue of Armadillo, and the kinase GSK3β (Hay-Koren et al. 2011).

The serine-threonine kinase GSK3β, also known as Shaggy in *Drosophila*, plays a key role in both the Hh and Wg signaling pathways (see **Chapter 1, Sections 1.2 and 1.3**). In the Hh pathway, GSK3β/Shaggy contributes to the hyper-phosphorylation of Ci_{155} (J. Jia et al. 2002), which leads to Slmb-directed processing of Ci_{155} to the Ci_{75} repressor form. Similarly, in the Wg pathway GSK3β/Shaggy phosphorylates the transcriptional effector protein β-catenin/Armadillo (S. Ikeda et

al. 1998), which prompts recognition and subsequent degradation of β-catenin/Armadillo by Slimb (Aberle et al. 1997; J. Jiang & Struhl 1998). As such, Shaggy is a negative regulator of both the Hh and Wg pathways, and thus could be a key substrate for Hyd to regulate both signalling pathways.

Having established that the MARCM system is a robust model to study Hyd's function in *hh* gene regulation and Hh pathway activity, the next objective was to determine whether Hyd could negatively regulate Hh signalling during eye development by interacting with Shaggy.

Chapter 5: Hyd regulates Hh signalling by interacting with the protein kinase Shaggy

5.1 Introduction

Glycogen synthase kinase 3 β (GSK3β), also known as zeste-white 3 or Shaggy (Sgg) in *Drosophila*, is a serine/threonine kinase that was initially identified as a key enzyme involved in insulin-mediated glycogen metabolism (reviewed in (Cohen & Frame 2001)). Since then, a multitude of other cellular functions of Sgg/GSK3β have emerged, which include its role as an antagonist of both the Wg/WNT and Hh/SHH signaling pathways (see **Chapter 1, Sections 1.3 and 1.4**). In the Hh pathway, Sgg/GSK3β phosphorylates the full-length transcriptional activator Ci_{155} (J. Jia et al. 2002). Phosphorylated Ci_{155} is targeted for ubiquitylation by the E3 ubiquitin ligase Slimb/βTrCP, and subsequent proteolytic processing to a truncated Ci_{75} protein, which acts to inhibit the transcription of Hh target genes (Méthot & Basler 1999). Similarly, in the Wg pathway Sgg/GSK3β phosphorylates the transcriptional effector protein Armadillo/β-catenin, which prompts recognition and subsequent degradation of Armadillo/β-catenin by Slimb/βTrCP (Aberle et al. 1997). As such, Sgg/GSK3β is a negative regulator of both the Hh and Wg pathways, and thus could be the missing link to explain how Hyd regulates morphogen signaling. In addition to Hyd interacting with Armadillo (see **Chapter 3**), EDD interacts with the human homologue of Sgg, GSK3β, suggesting that Hyd also interacts with Sgg (Hay-Koren et al. 2011).

On this basis, I propose a model in which Hyd negatively regulates both Hh and Wg pathway activity by interacting with Sgg (**Figure 5.1**). Loss of *hyd* up-regulates Ci_{155} levels in posterior $hyd^{K7.19}$ clones, whereas Ci_{155} levels are reduced in anterior clones (see **Chapter 4**). This model would therefore only apply to posterior clones, and is based on the hypothesis that Hyd acts to positively regulate Sgg activity, potentially through non-degradative ubiquitylation. The addition of K63-linked poly-ubiquitin chains has previously been reported as a mechanism for kinase activation (reviewed in (Z. J. Chen & L. J. Sun 2009)). Conversely, in anterior $hyd^{K7.19}$ clones, Hyd would

normally be a negative regulator of Sgg, so that loss of Hyd increases Sgg activity, resulting in Ci_{155} to Ci_{75} processing.

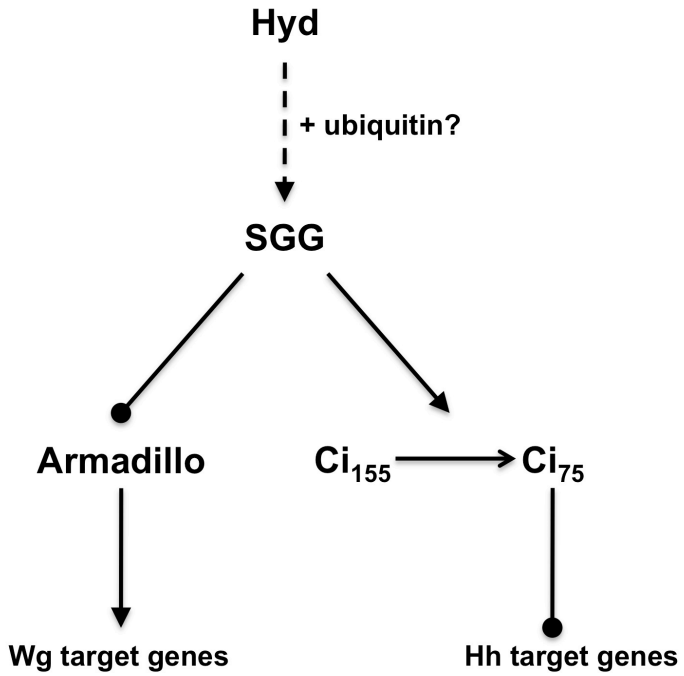

Figure 5.1: Hypothetical model for Hyd-mediated Hh and Wg pathway regulation through interaction with Sgg. Filled arrows and filled circles denote positive and negative regulation, respectively.

The purpose of the work presented here is to determine whether Hyd can interact with and ubiquitylate Sgg, and whether this interaction affects Hh pathway activity. Binding and ubiquitylation assays in both *Drosophila* and human cell lines were used to investigate whether the interaction between the human proteins is conserved in *Drosophila*, to investigate whether Sgg/GSK3β is ubiquitylated, and what role Hyd/EDD plays in any potential Sgg/GSK3β ubiquitylation.

To address whether the interaction has a functional consequence on Hh pathway activity, the MARCM technique (see **Section 4.3.1**) was used to either over-express

or knockdown Sgg in $hyd^{K7.19}$ clones. Since Sgg is not known to be involved in *hh* gene expression, the variation of Sgg levels is not expected to modify ectopic *hh* gene expression in $hyd^{K7.19}$ clones. However, Sgg may modify the $hyd^{K7.19}$ phenotype by affecting the levels of Ci_{155} in $hyd^{K7.19}$ clones. According to the model discussed above (**Figure 5.1**), only the over-expression of Sgg would be expected to rescue the phenotype, as this is expected to reduce ectopic Ci_{155} levels in posterior $hyd^{K7.19}$ clones. In an attempt to increase the chances of rescue, a constitutively active Sgg^{S9A} mutant was used as an over-expression construct in the MARCM analysis. Sgg/GSK3β is negatively regulated by a number of kinases, which phosphorylate Ser9 on its amino-terminus. The phosphorylated Ser9 residue then acts as a 'pseudosubstrate', binding to the priming phosphate site and thereby blocking access of SGG/GSK3β substrates to the active site (see **Chapter 1, Section 1.3.3.2**). In the Sgg^{S9A} mutant, Ser9 is mutated to Ala (Bourouis 2002), which would prevent phosphorylation and de-activation of Sgg/GSK3β through this mechanism.

5.2 Hyd interacts with the protein kinase Sgg *in vitro*

5.2.1 Hyd interacts with Sgg in S2 cells

In order to investigate whether Hyd can physically interact with Sgg *in vitro*, I cloned a carboxy terminally FLAG/V5-tagged Sgg construct into the pMT *Drosophila* and pcDNA3.1 mammalian expression vectors. S2 cells were co-transfected with HSP-Hyd and Sgg-FLAG constructs, and HSP-Hyd was pulled down using StrepTactin beads. A clean interaction was observed between WT Hyd and Sgg, compared to a Sgg only negative control. Interestingly, Sgg did not appear to interact with Hyd C>A, the catalytically inactive Hyd point mutant (**Figure 5.2 A**). The latter result is intriguing, and suggests that perhaps Hyd's ubiquitylation activity is required for the interaction to take place. This could involve multiple possible scenarios, one of which would be that Hyd must first ubiquitylate Sgg before it can interact with Sgg

via its UBA domain binding the newly added ubiquitin moiety. Another possibility would be that the interaction between Hyd and Sgg is indirect, and requires the Hyd-directed ubiquitylation of an intermediate binding partner to recruit Sgg to the complex.

Initially, I wanted to validate that the interaction between Hyd WT and Sgg takes place in an independent experiment. This time, S2 cells were transfected with the Sgg-FLAG construct, and Sgg was immunoprecipitated using anti-FLAG agarose instead. Endogenous Hyd was co-immunoprecipitated with Sgg-FLAG, as detected using the anti-Hyd M19 antibody (**Figure 5.2 B; lane 2**), and the binding was clearly above a low level of background Hyd binding to anti-FLAG agarose (**Figure 5.2 B; lane 1**). This fully validates the interaction between Hyd and Sgg. Interestingly, the immunoprecipitated Sgg-FLAG protein appeared to be heavily modified, as was evident from very pronounced high molecular weight smearing (**Figure 5.2 B; lane 2**). The chemical *N*-ethylmaleimide (NEM), a cysteine protease inhibitor, and thus inhibitor of de-ubiquitinating enzymes (DUBs), as well as a cocktail of phosphatase inhibitors, were added to the lysis buffer prior to immunoprecipitation. This would have resulted in the preservation of phosphorylation and ubiquitylation of Sgg-FLAG, and could explain the high levels of post-translational modification observed. However, high molecular weight smearing is usually indicative of the addition of multiple ubiquitin or UBL chains, rather than the addition of a phosphate group. To address the possible ubiquitylation of Sgg by Hyd, I performed a series of ubiquitylation assays, and this will be discussed in the next section (see **Section 5.3** below).

Next, I wanted to confirm whether the catalytically inactive Hyd C>A mutant was unable to bind Sgg. In addition to the Hyd C>A point mutant, I also included two other Hyd point mutants, harbouring key mutations in the PABC and UBA domains, respectively (these were already mentioned in **Chapter 4**; see **Table 4.2**).

The PABC mutant contains two point mutations: Y2509>A, and L2527>A. Based on structural data of the PABP protein PABC domain, which has very high homology to the Hyd PABC domain, this mutational combination is expected to completely abrogate binding to PAM2 (PABP-interacting motif 2)-containing proteins (Kozlov et al. 2004). As discussed in Chapter 1 (**Section 1.4.1.2**), the PABC domain is a highly conserved protein-protein interaction domain with a high affinity for proteins and peptides containing the 12-amino acid PAM2 motif, such as Paip1, Paip2, Erf3, and Tob2 (Kozlov et al. 2004). However, Sgg does not contain any PAM2 motifs, and so binding of Sgg to the PABC point mutant is not expected to be impaired.

The UBA mutant contains a single point mutation, V166>K. Based on the structure of the EDD UBA domain, and the high homology between the EDD and Hyd UBA domains, this mutation should abrogate binding to both mono- and poly-ubiquitin chains (Kozlov et al. 2007). Consequently, a potentially ubiquitylated Sgg protein that interacts with Hyd via ubiquitin-UBA domain recognition should no longer be able to bind this mutant.

The results from the Sgg binding assay with Hyd point mutants indicate that the interaction between Sgg and Hyd remains intact with all mutants (**Figure 5.2 C; first panel**). S2 cells were co-transfected with HSP-Hyd, HSP-Hyd point mutants, and Sgg-FLAG constructs, and Sgg was immunoprecipitated using anti-FLAG agarose. Although all Hyd proteins were co-immunoprecipitated with Sgg, the binding to the Hyd HECT and Hyd UBA point mutants was slightly stronger. However, looking at the Hyd potein levels in the input, it becomes evident that the transfection efficiency of the various Hyd constructs was extremely variable (**Figure 5.2 C; third panel**), partly explaining the difference in binding levels. The only exception in this case is that, although the Hyd C>A input level is lower than Hyd WT, the levels of Hyd C>A bound to Sgg are higher than Hyd WT. One possible explanation for this could

be that, assuming that Hyd ubiquitylates Sgg, the interaction between Sgg and Hyd is stronger prior to Sgg ubiquitylation, indicating a higher affinity of Hyd for non-ubiquitylated Sgg. Once again, a ubiquitylation assay is necessary to test this hypothesis, and this will be discussed in Section 5.3 below. Importantly, this finding directly contradicts the previous result, which suggested that the Hyd C>A mutant is unable to bind Sgg (**Figure 5.2 A**). Although the binding assays were performed in completely different ways (i.e. StrepTactin pulldown versus anti-FLAG IP), this should theoretically not affect the end result. Unfortunately, I did not have sufficient time to confirm whether an interaction between Sgg and Hyd C>A takes place. In conclusion, the results presented in **Figure 5.2 C** suggest that the Sgg-Hyd interaction is not dependent on Hyd's ubiquitylation activity, does not take place via UBA domain-ubiquitylated Sgg interaction, and, as expected, does not involve Sgg binding to the PABC domain in a PAM2-dependent manner.

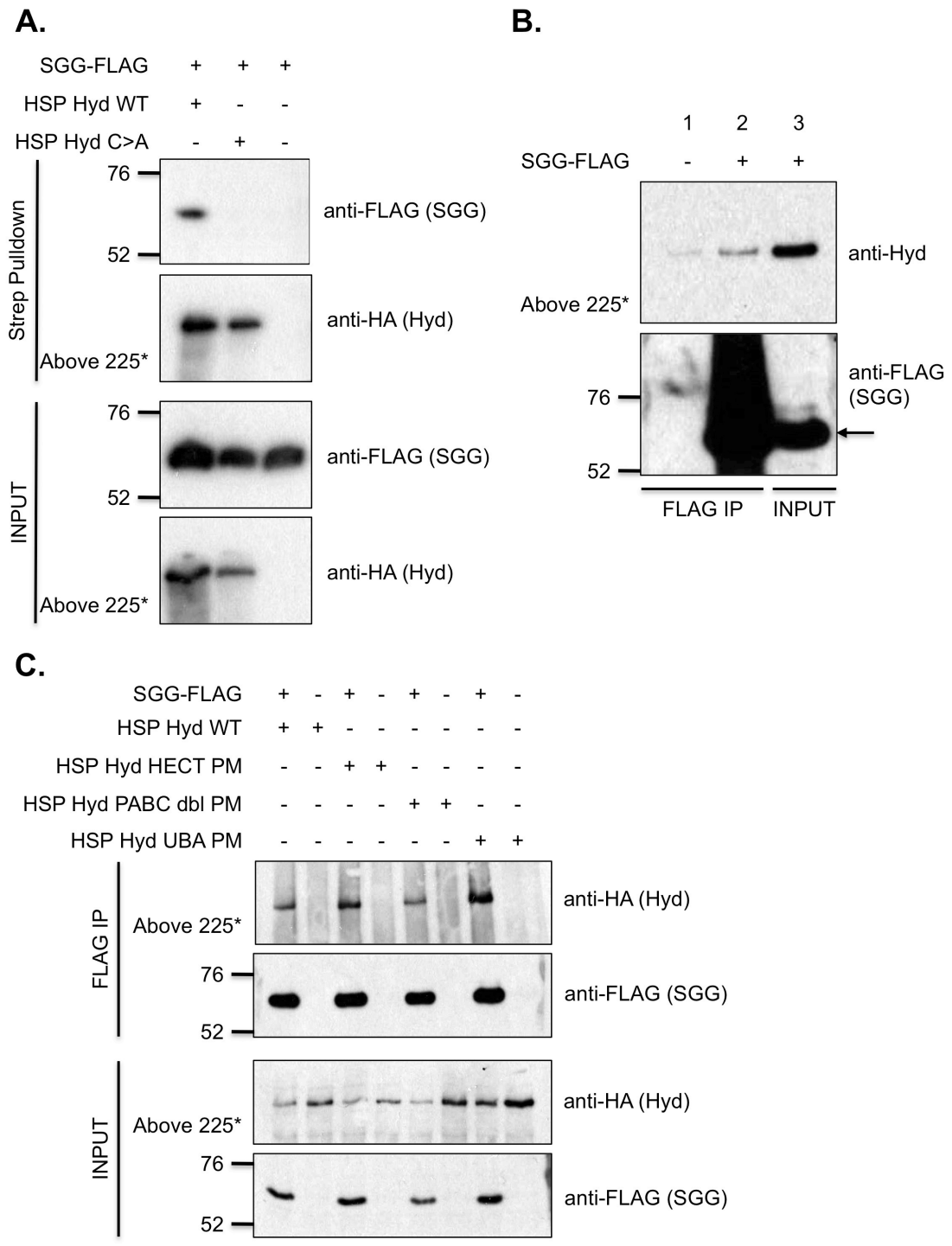

Figure 5.2: Hyd interacts with Sgg in S2 cells. (**A**) StrepTactin pulldown in S2 cells. S2 cells were transfected with HA-Strep(HSP)-Hyd WT, HSP C>A catalytic inactive mutant, and Sgg FLAG constructs. (**B**) anti-FLAG immunoprecipitation in S2 cells. S2 cells were transfected with Sgg FLAG. Endogenous Hyd was co-immunoprecipitated with Sgg-FLAG, as detected using the the Hyd M19 antibody (Santa Cruz). (**C**) anti-FLAG immunoprecipitation in S2 cells. S2 cells were transfected with

Sgg FLAG, and HSP-Hyd point mutants (PMs) containing mutations in the following domains: HECT (C>A), PABC (Y2509>A; L2527>A), and UBA (V166>K).

5.2.2 Generation of Hyd deletion mutants to map the Sgg interaction surface on Hyd

As the Hyd point mutants had proved somewhat uninformative in determining the nature of the Sgg-Hyd interaction, I also designed and cloned a series of Hyd deletion mutants (**Figure 5.3 A**). These were designed in a way that would allow me to map the approximate interaction surface for Sgg binding on Hyd relative to specific domains. To clone the individual Hyd deletion mutants, the original HSP-WT Hyd construct was used as a template for PCR. Forward primers included a KOZAK sequence, to enhance protein expression levels, and reverse primers included a STOP codon to terminate protein expression prematurely in the case of all ΔC mutants lacking a carboxy terminal portion of the full-length Hyd protein. In addition all primers included appropriate restriction enzyme sites to allow cloning into both the pMT *Drosophila* expression vector, as well as the pGEX vector for expression of recombinant GST-tagged proteins in bacterial cells. This is an important design feature, as it is still unknown whether the interaction between SGG and Hyd is direct, or occurs indirectly via an intermediate protein in a multi-protein complex.

Only three of the deletion mutants were successfully cloned (Many thanks to Katharina Krauskopf; Erasmus project student summer 2012), and their expected size was confirmed to be correct through an expression test in S2 cells, although expression levels were sub-optimal (**Figure 5.3 B**). Unfortunately, I did not have time to test the binding between Sgg and the Hyd deletion mutants. However, future experiments would address this by mapping the interaction surface through binding

assays in S2 cells, as well as using recombinant Hyd protein and deletion mutants to investigate whether the interaction between Sgg and Hyd is binary or not.

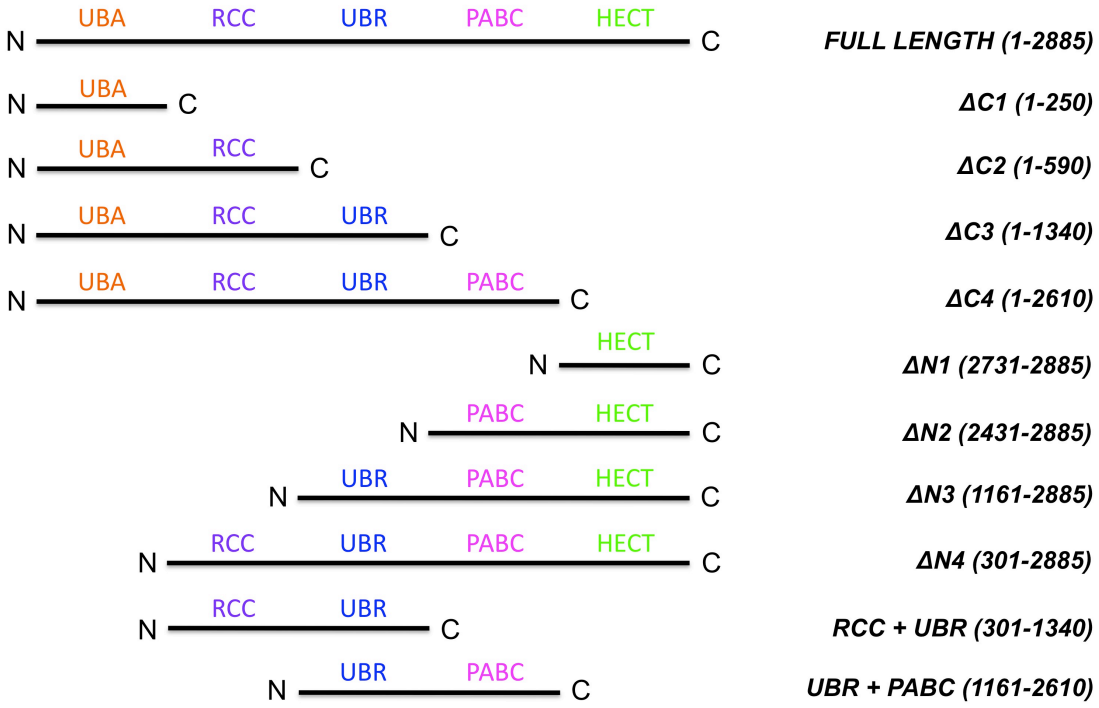

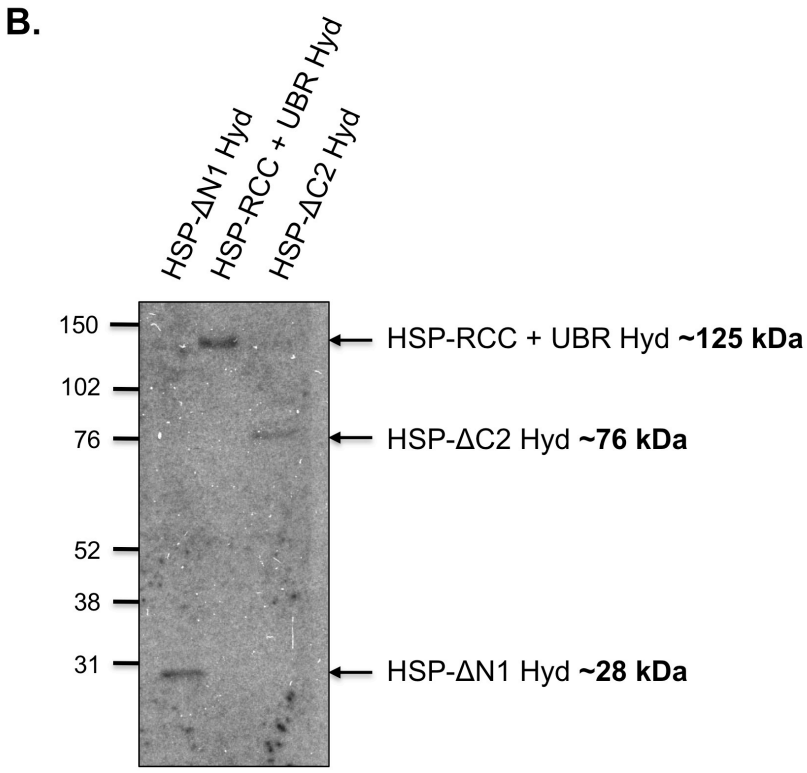

Figure 5.3: Generation of Hyd deletion mutants. (**A**) Schematic of all Hyd deletions mutants. Given names and amino acid coordinates are indicated to the left of each deletion mutant. (**B**) Expression of HSP-Hyd pMT deletion mutant constructs in S2 cells: HSP-ΔN1 Hyd, HSP-RCC + UBR Hyd, and HSP-ΔC2 Hyd. The expected molecular weight of each deletion mutant is indicated on the left.

5.3 Sgg/GSK3β is ubiquitylated in *Drosophila* and human cells

My results so far indicate that Hyd interacts with Shaggy, although it is unclear whether the interaction is direct or occurs indirectly through an intermediate binding partner. As Hyd is an E3 ubiquitin ligase, my next question was to address whether Hyd can also ubiquitylate Shaggy, and whether this affects steady-state levels of the Shaggy protein as a result of Hyd-mediated Shaggy degradation.

5.3.1 Hyd does not affect Sgg protein levels

As discussed above in Section 5.2.1, SGG appears to be post-translationally modified (**Figure 5.2 B**). The nature of the high molecular weight smearing of Sgg suggested that the modification was likely to consist of mono- and poly- ubiquitin chains. If this is indeed correct, and if Hyd is the respective E3 ubiquitin ligase, one of the possible outcomes of Hyd-mediated Sgg ubiquitylation could be its degradation. Therefore, as an initial investigation, I monitored Sgg protein levels in the presence and absence of endogenous Hyd protein in Cl8+ cells. Treatment of Cl8+ cells with dsRNA targeting either EGFP (control) or Hyd did not affect SGG protein levels (**Figure 5.4**).

When the Hh pathway is activated by Hh ligand binding to the Ptc receptor, a sequence of intracellular signaling events leads to inhibition of Sgg. It is possible that Hh pathway activation results in removal, i.e. degradation, of Sgg to prevent Ci_{155} phosphorylation. I therefore also tested whether Sgg protein levels are affected by dsRNA-mediated Hyd knockdown in the presence of Hh-N ligand. However, removal of Hyd had no effect on endogenous Sgg protein levels, regardless of whether the Hh pathway was on or off (**Fig. 5.4**). This suggests that, although Hyd may still be involved in ubiquitylating Sgg, Hyd does not appear to direct the degradation of Sgg.

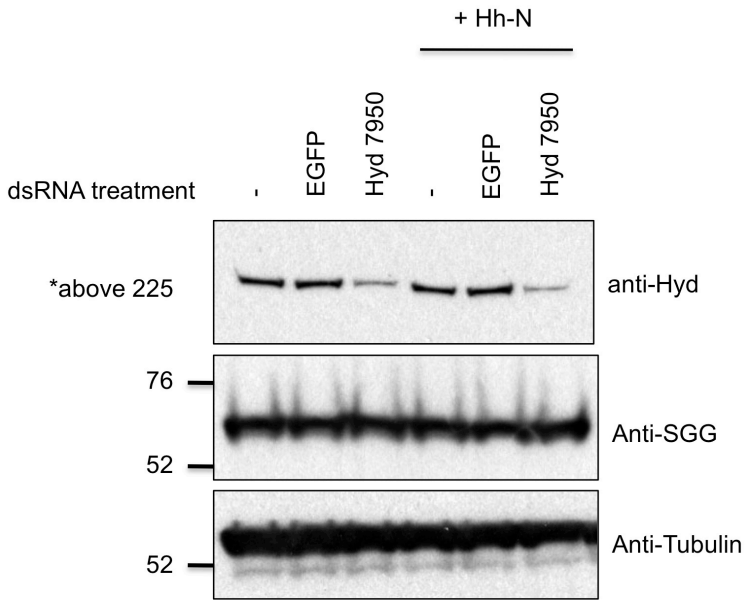

Figure 5.4: Hyd knockdown has no effect on Sgg protein levels. Cl8+ cells were transfected with EGFP dsRNA (control) or Hyd 7950 dsRNA, and Hh-N ligand. Endogenous Hyd and Shaggy protein levels in cell lysates were monitored 48 hours post-transfection by probing with anti-M19 (Hyd) and anti-Sgg antibodies, respectively. Tubulin = loading control.

5.3.1 Sgg is ubiquitylated in S2 cells

To investigate the nature of the Sgg post-translational modification, and whether the high molecular weight modifications can, at least in part, be attributed to the addition of ubiquitin chains, I performed a ubiquitylation assay. To preserve protein ubiquitylation, this assay involves transfection of a His_6-tagged ubiquitin construct, and denaturing cell lysis using a lysis buffer containing 6M Guanidinium hydrochloride. A pulldown of all cellular proteins that have been conjugated with His_6-ubiquitin is then performed using Ni^{2+} agarose beads (see **Chapter 2, Section 2.4.5**). Using an antibody specific for the protein of interest, the presence or absence of this protein (i.e. Sgg) in the pulldown fraction, and thus its ubiquitylation state, can then be determined.

To determine whether Sgg was ubiquitylated, HEK293 cells were co-transfected with *Drosophila* Sgg-FLAG and His_6-ubiquitin constructs. In addition, two positive controls were included to ascertain that the assay was working correctly. One of the positive controls was Myb-FLAG, a *Drosophila* transcription factor that, when co-transfected with His-ubiquitin, was previously found to be heavily ubiquitylated (personal observation). The other positive control was the catalytically inactive apoptotic effector caspase drICE-FLAG (C>A), which is ubiquitylated by co-transfected E3 ubiquitin ligase DIAP1(Ditzel et al. 2008). The catalytically inactive caspase (drICE-FLAG C>A) was used in this case, as transfection of an active caspase would lead to apoptosis of cells. Both positive controls, Myb-FLAG and drICE-FLAG, were ubiquitylated (denoted by * and **, respectively, in **Figure 5.5 A**; upper panel), indicating that the assay can successfully detect protein ubiquitylation. As a result, it was confirmed that over-expressed Sgg-FLAG is also heavily ubiquitylated in HEK293 cells (**Figure 5.5 A**; upper panel, lane 3).

Sgg-FLAG was also co-transfected with HSP-Hyd WT or HSP-Hyd C>A, to determine whether over-expression of Hyd leads to an increase in Sgg-FLAG ubiquitylation. This would identify Sgg as a potential Hyd substrate. Unexpectedly, however, over-expression of Hyd WT drastically reduced Sgg-FLAG ubiquitylation (**Figure 5.5 A**; upper panel, lane 1, compared to lane 3), while over-expression of Hyd C>A resulted in a very slight reduction of Sgg-FLAG ubiquitylation (**Figure 5.5 A**; upper panel, lane 2, compared to lane 3). The lack of Sgg-FLAG in the Ni^{2+} pulldown fraction in the presence of Hyd WT could be a result of Hyd-mediated ubiquitylation and subsequent degradation of Sgg. However, no significant changes in Sgg-FLAG protein levels as a result of Hyd WT expression were detected in the input (**Figure 5.5 A**; third panel, lane 1). Instead, WT Hyd expression levels were noticeably lower in the presence of Sgg-FLAG, compared to Hyd WT expressed on its own (**Figure 5.5 A**; lowest panel, lane 1, compared to lane 4). This raises the possibility that SGG could instead regulate Hyd protein stability, for example, through phosphorylation and in a similar mechanism to Sgg-mediated Ci_{155}

regulation. Alternatively, Hyd could indirectly regulate SGG ubiquitylation by modulating the activity of another E3 ubiquitin ligase involved in Sgg ubiquitylation.

Interestingly, the Ni^{2+} pulldown fraction was also probed with the anti-HA antibody, revealing that both HSP-Hyd WT and HSP-Hyd C>A are themselves ubiquitylated (**Figure 5.5 A**; second panel, lanes 1, 2 and 4). This could be a result of auto-ubiquitylation, which has been previously reported to occur for HECT E3 ubiquitin ligases (Mouchantaf et al. 2006), and would presumably be mediated by endogenous Hyd following dimerisation with HSP-Hyd C>A. On the other hand, the ubiquitylation of Hyd could also be mediated by another E3 ubiquitin ligase.

The experiment was repeated to address whether over-expression of Hyd WT reduces Sgg-FLAG ubiquitylation. Unfortunately, I was unable to reproduce this result, as, in this experiment, Sgg-FLAG ubiquitylation levels, although slightly reduced, were not significantly affected by over-expression of HSP-Hyd WT or HSP-Hyd C>A (**Figure 5.5 B**; upper panel, compare lanes 1, 2 and 3). Similarly, variable levels of Hyd WT in the input no longer appeared to be dependent on the presence or absence of Sgg (**Figure 5.5 B**; lower panel, compare lanes 1 and 4).

Due to inconclusive results when overexpressing Hyd and assessing any changes in overexpressed Sgg ubiquitylation levels, I decided to also investigate the effect of Hyd knockdown on endogenous Sgg ubiquitylation. Based on the previous experiments, this would test the hypothesis that Hyd decreases Sgg ubiquitylation to potentially prevent its degradation. If this were the case, one would expect Sgg ubiquitylation to increase in the absence of Hyd. Over-expressed Sgg-FLAG was co-transfected with His-ubiquitin into S2 cells as a positive control and directly compared with endogenous Sgg ubiquitylation. However, no ubiquitylation of endogenous Sgg could be detected in S2 cells (**Figure 5.5 C**). The Sgg-specific band detected in the pulldown fraction was present in the negative control lacking His-ubiquitin, as well as in all the other samples, suggesting that endogenous Sgg was

simply bound to the Ni^{2+} resin non-specifically (**Figure 5.5 A**; upper panel, compare lane 1 to all others). Although endogenous Hyd was successfully knocked down, no endogenous Sgg ubiquitylation was detected under these circumstances either (**Figure 5.5 A**; upper panel, lane 4).

The fact that no endogenous Sgg ubiquitylation could be detected raised the question of whether the ubiquitylation seen on Sgg-FLAG, although much weaker than in HEK293 cells, could be an artifact or cell-type specific. Unlike HEK293 cells, S2 cells are incapable of transducing the Hh pathway, due to not expressing the transcriptional effector protein Ci. This could explain why Sgg ubiquitylation was much lower, or non-detectable in the case of endogenous SGG, in S2 cells. Although the *Drosophila* Cl8+ cell line is capable of transducing both the Hh and Wg pathways (see **Chapter 4, Section 4.6**), I have to date not been successful in carrying out large-scale transfections on these cells. The transfection efficiency, as assessed by transfection of a GFP construct into Cl8+ cells, and subsequent fluorescence microscopy, was 5-10 % at best, which is not sufficient to carry out a ubiquitylation assay. Due to the comparable ease of working with HEK293 cells, I therefore decided to shift to a mammalian setting to investigate whether the human Sgg orthologue, GSK3β, is also ubiquitylated, and the potential role of the mammalian Hyd orthologue, EDD, in this mechanism.

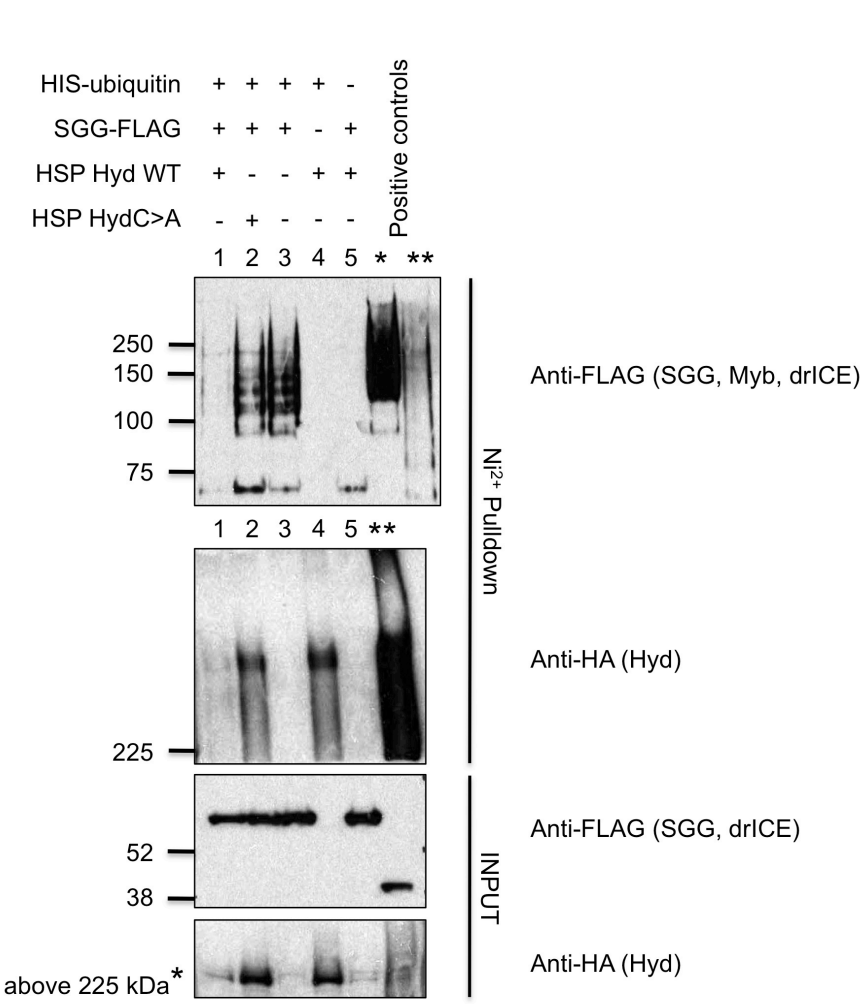
A.
HIS-ubiquitin + + + + -
SGG-FLAG + + + - +
HSP Hyd WT + - - + +
HSP HydC>A - + - - -
Positive controls
1 2 3 4 5 * **
250
150
100
75
Anti-FLAG (SGG, Myb, drICE)
Ni2+ Pulldown
1 2 3 4 5 **
225
Anti-HA (Hyd)
52
38
Anti-FLAG (SGG, drICE)
INPUT
above 225 kDa*
Anti-HA (Hyd)

B.

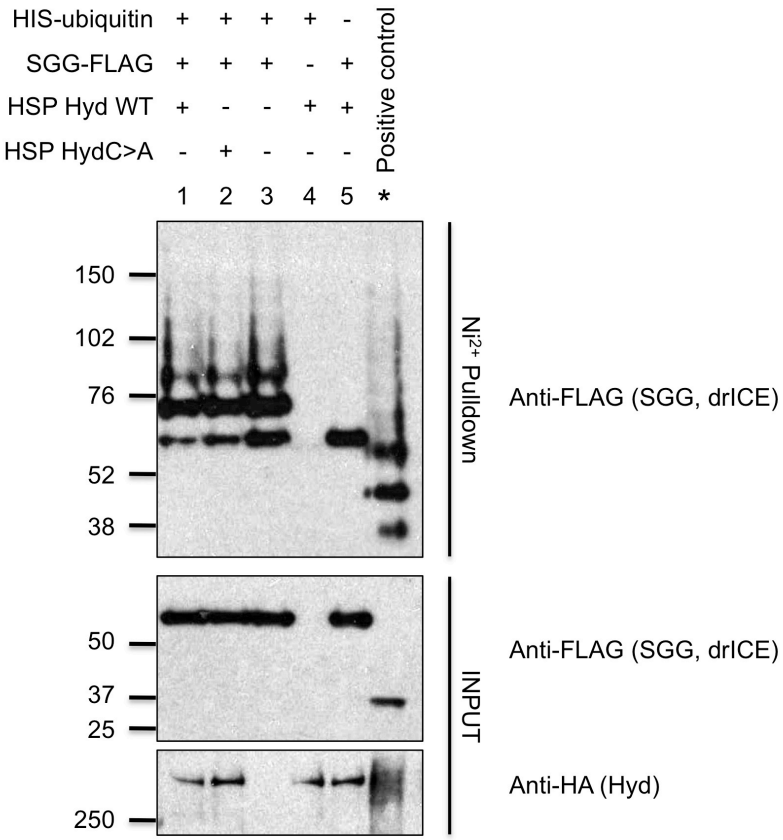
HIS-ubiquitin + + + + -
SGG-FLAG + + + - +
HSP Hyd WT + - - + +
HSP HydC>A - + - - -
Positive control
1 2 3 4 5 *
150
102
76
52
38
Ni2+ Pulldown
Anti-FLAG (SGG, drICE)
50
37
25
INPUT
Anti-FLAG (SGG, drICE)
250
Anti-HA (Hyd)

C.

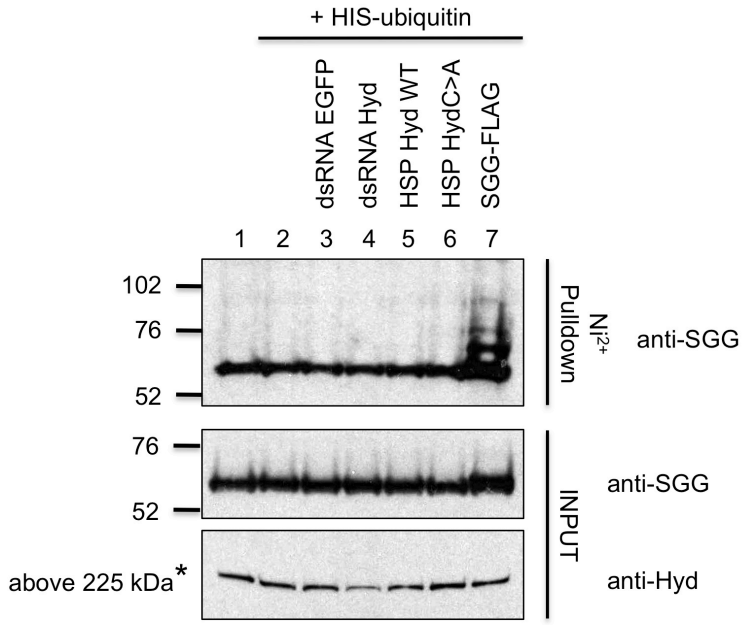
+ HIS-ubiquitin
dsRNA EGFP
dsRNA Hyd
HSP Hyd WT
HSP HydC>A
SGG-FLAG
1 2 3 4 5 6 7
102
76
52
Ni2+ Pulldown
anti-SGG
76
52
INPUT
anti-SGG
above 225 kDa*
anti-Hyd

Figure 5.5: Sgg is ubiquitylated. HEK293 and S2 cells were subjected to denaturing lysis and a Ni^{2+} pulldown of all His-ubiquitin-conjugated proteins. (**A**) Sgg-FLAG ubiquitylation in HEK293 cells. HEK293 cells were transfected with varying combinations of His-ubiquitin, Sgg-FLAG, and HSP-Hyd over-expression constructs. Positive controls were: *Myb-FLAG co-transfected with His-ubiquitin (note no input samples shown); **FLAG-drICE C>A and nude DIAP1 co-transfected with His-ubiquitin. (**B**) Sgg-FLAG ubiquitylation in HEK293 cells. HEK293 cells were transfected with varying combinations of his-ubiquitin, Sgg-FLAG, and HSP-Hyd over-expression constructs. The positive control (*) was: FLAG-drICE C>A and nude DIAP1 co-transfected with His-ubiquitin. (**C**) Endogenous Sgg ubiquitylation in S2 cells. S2 cells were transfected with varying combinations of dsRNA (EGFP control or targeting Hyd), and His-ubiquitin and HSP-Hyd over-expression constructs. The positive control (lane 7) was: Sgg-FLAG co-transfected with His-ubiquitin.

5.3.2 EDD negatively regulates GSK3β ubiquitylation in 293 cells

Initially, to investigate whether GSK3β is also ubiquitylated, HEK293 cells were co-transfected with HA-tagged GSK3β and His-ubiquitin constructs. As expected, GSK3β was also heavily ubiquitylated in HEK293 cells (**Figure 5.6 A**; upper panel, lane 3). Further to this, expression of HSP-EDD WT and HSP-EDD C>A resulted in a small reduction of GSK3β ubiquitylation levels (**Figure 5.6 A**; lanes 1 & 2, compared to lane 3). This result is in agreement with a similar reduction of Sgg-FLAG ubiquitylation seen in HEK293 cells in the presence of HSP-Hyd (**Figure 5.5 A & B**). Interestingly, HSP-EDD C>A was also found to be ubiquitylated (**Figure 5.6 A**; upper panel, red arrow, lane 2), which, as discussed above, could indicate auto-ubiquitylation by endogenous Hyd/EDD, or ubiquitylation by another E3 ubiquitin ligase.

Next, I tested whether endogenous GSK3β is ubiquitylated in HEK293 cells, and whether the presence or absence of EDD can alter the ubiquitylation state of GSK3β. HEK293 cells were transfected with varying combinations of His-ubiquitin, control or EDD siRNA, or HSP-EDD constructs. Indeed, endogenous GSK3β was

ubiquitylated compared to a negative control lacking His-ubiquitin, although endogenous GSK3β ubiquitylation levels were markedly reduced compared to over-expressed HA-GSK3β ubiquitylation levels (**Figure 5.6 B**; upper panel, compare lanes 1, 2, and 9). Importantly, siRNA-mediated knockdown of endogenous EDD resulted in a significant increase of endogenous GSK3β ubiquitylation levels (**Figure 5.6 B**; upper and lower panels, lane 4), although this had no effect on steady-state levels of GSK3β in the input (**Figure 5.6 B**; middle panel, lane 4). Over-expression of EDD did not appear to have any significant effects on endogenous GSK3β ubiquitylation (**Figure 5.6 B**; upper panel, lanes 5-8). Contrary to what one would expect, in this case removal of an E3 ubiquitin ligase increases ubiquitylation, suggesting that EDD does not promote GSK3β high molecular weight ubiquitylaion. Instead, this result suggests that perhaps EDD is involved in regulating the addition of ubiquitin onto, or promoting its removal from, GSK3β. In the former scenario EDD may be involved in suppressing the activity of an additional E3 involved in GSK3β regulation, while EDD-mediated recruitment of a deubiquitylase could explain the latter. In addition, the fact that EDD does not appear to affect steady-state levels of GSK3β suggests that the nature of the GSK3β ubiquitylation affected by EDD is more likely to play a role in GSK3β's activity, rather than its degradation.

As the experiment was performed only once, it was repeated in order to confirm the effect of EDD knockdown on endogenous GSK3β ubiquitylation levels. However, although removal of EDD resulted in a slight increase of GSK3β ubiquitylation (**Figure 5.6 C**; upper panel, lane 4), I was not able to reproduce the same level of GSK3β ubiquitylation increase over baseline levels seen in the previous experiment. Therefore, although this is a very interesting result that could provide insight into the mechanism by which Hyd/EDD could regulate SGG/GSK3β activity, the results do not conclusively support a role for EDD in altering the GSK3β ubiquitylation state.

In conclusion, the results presented here show that both Sgg and GSK3β are ubiquitylated. They also suggest that Hyd does not affect Sgg protein expression levels, and that Hyd/EDD is not likely to be directly involved in ubiquitylating SGG/GSK3β. However, Hyd/EDD may be involved in indirectly regulating protein ubiquitylation, and thus perhaps the activity, of SGG/GSK3β indirectly through interaction with another E3 ubiquitin ligase or DUB.

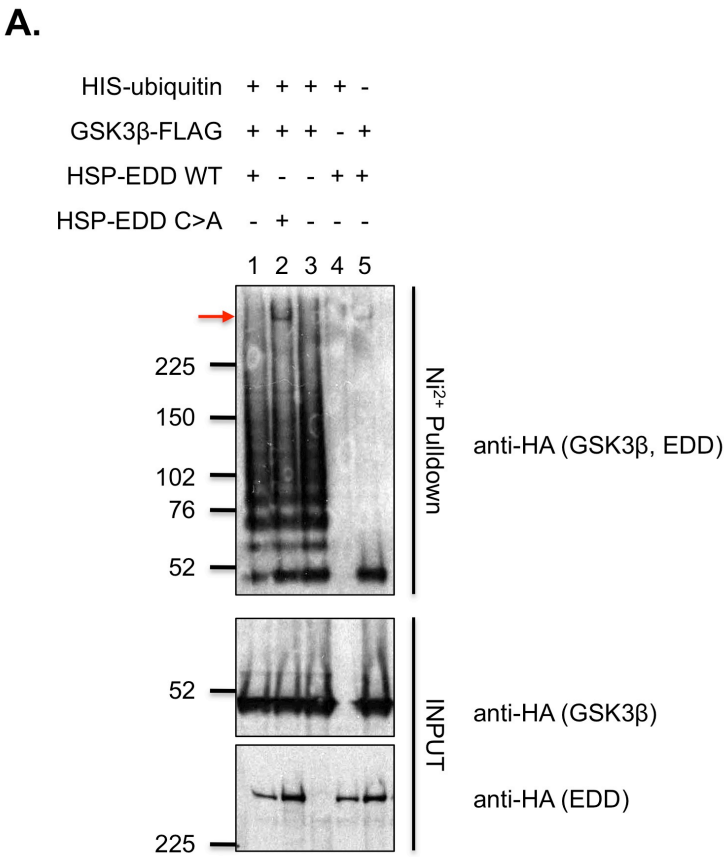

B.

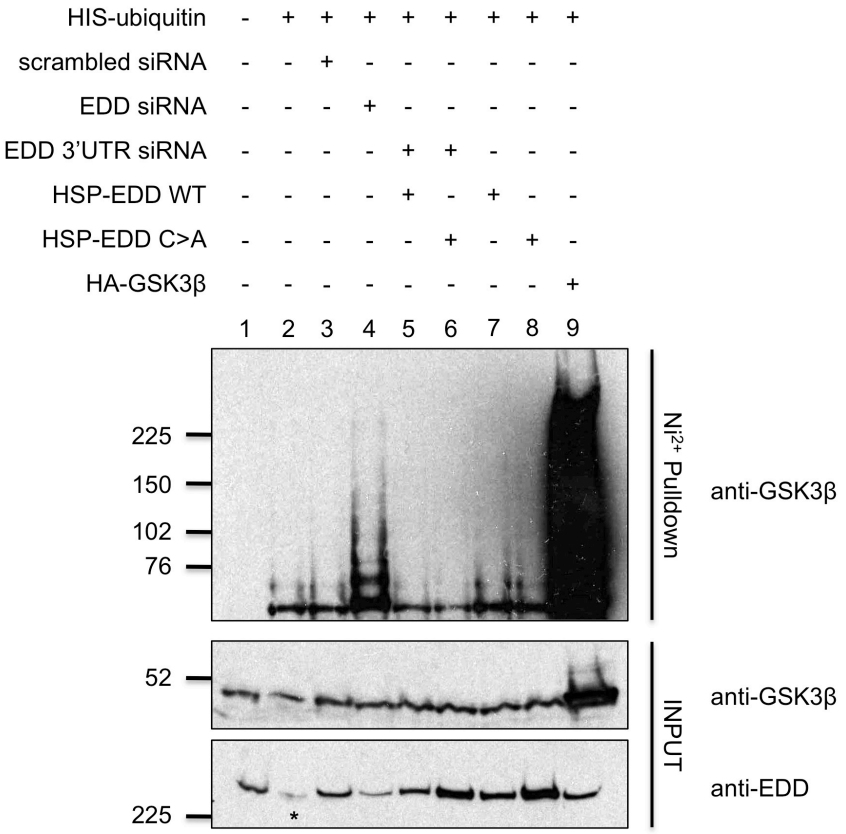
HIS-ubiquitin - + + + + + + + +
scrambled siRNA - - + - - - - - -
EDD siRNA - - - + - - - - -
EDD 3'UTR siRNA - - - - + + - - -
HSP-EDD WT - - - - + - + - -
HSP-EDD C>A - - - - - + - + -
HA-GSK3β - - - - - - - - +
1 2 3 4 5 6 7 8 9
225
150
102
76
Ni2+ Pulldown
anti-GSK3β
52
INPUT
anti-GSK3β
anti-EDD
225
*

C.

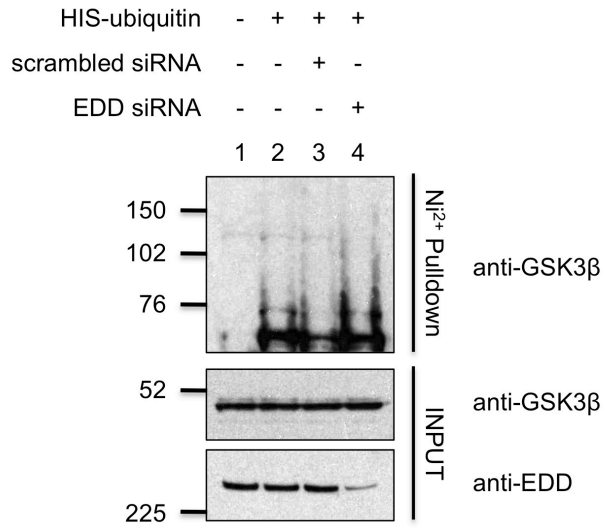
HIS-ubiquitin - + + +
scrambled siRNA - - + -
EDD siRNA - - - +
1 2 3 4
150
102
76
Ni2+ Pulldown
anti-GSK3β
52
INPUT
anti-GSK3β
anti-EDD
225

Figure 5.6: Effect of EDD over-expression or knockdown on GSK3β ubiquitylation. HEK293 cells were subjected to denaturing lysis and a Ni^{2+} pulldown of all His-ubiquitin-conjugated proteins. (**A**) HA-GSK3β ubiquitylation in HEK293 cells. HEK293 cells were transfected with varying combinations of His-ubiquitin, HSP-EDD, and HA GSK3β over-expression constructs. (**B**) Endogenous GSK3β ubiquitylation in HEK293 cells. HEK293 cells were transfected with varying combinations of siRNA (scrambled, and targeting EDD or EDD 3'UTR), and His-ubiquitin, HSP-EDD, or HA GSK3β over-expression constructs. Asterisk (*) on lane 2 indicates a loading problem with the input samples for that lane, which were accidentally lost during loading, thus explaining lower levels of endogenous GSK3β and EDD input in this sample. Please note: this does not affect the pulldown sample. (**C**) Endogenous GSK3β ubiquitylation in HEK293 cells. HEK293 cells were transfected with varying combinations of siRNA (scrambled, and targeting EDD or EDD 3'UTR).

5.4 Variation in Sgg levels and activity *in vivo* rescues the adult *hyd*$^{K7.19}$ phenotype

The results presented so far have focused on the use of biochemistry, in the form of binding and ubiquitylation assays, to attempt to gain insight into the potential mechanism of Hyd-mediated Sgg regulation. These results indicate that an interaction between Hyd and Sgg takes place, and that Hyd is likely to play a role in Sgg regulation, possibly through modifying Sgg ubiquitylation. However, it is not known what the functional consequence of this interaction is *in vivo*. Therefore, I decided to address this by using the MARCM system to query whether Sgg can modify the *hyd*$^{K7.19}$ phenotype in the eye, which has already been extensively described in **Chapter 4**.

As described in Section 4.3.1, MARCM is a genetic technique that allows the tissue-specific generation of *hyd*$^{K7.19}$ clones, which can also over-express any GAL4-regulated transgene. These transgenes can include over-expression constructs, as well as sequences encoding shRNAs that target specific mRNAs for degradation. To assess whether Sgg can modify the *hyd*$^{K7.19}$ phenotype in the eye, I chose two *sgg* transgenes to co-express in *hyd*$^{K7.19}$ clones: UAS-*sgg*^{S9A} and UAS-*sgg*^{RNAi}. The UAS-

sgg^{S9A} transgene expresses a constitutively active Sgg kinase, which can no longer be inactivated by phosphorylation due to the mutation of Ser9 to Ala (Bourouis 2002). The second transgene, UAS-*sgg*^{RNAi}, encodes an inverted repeat, which specifically targets *sgg* mRNA for degradation and thus results in knockdown of endogenous Sgg protein levels in *hyd*$^{K7.19}$ clones. According to the hypothesis discussed in the introduction to this chapter (see **Figure 5.1**), Hyd could negatively regulate Hh and/or Wg pathway activity by enhancing Sgg activity. Therefore, loss of Hyd would reduce Sgg activity, and over-expression of a constitutively active Sgg kinase would be expected to rescue the phenotype. Similarly, RNAi-mediated knockdown of *sgg* in *hyd*$^{K7.19}$ clones would be expected to have the opposite effect, failing to rescue the phenotype, or possibly even exacerbating it.

5.4.1 Effect of Sgg protein levels and activity on the adult eye phenotype

MARCM was used to generate *hyd*$^{K7.19}$ clones in eye-antennal discs, which were either over-expressing Sgg^{S9A}, or were deficient in endogenous Sgg protein. The adult flies were then assessed for both eye and head phenotypes. To control for any Hyd-independent effects of Sgg over-expression and knockdown, clones solely expressing Sgg^{S9A} or *sgg*^{RNAi} only were also generated. As would be expected according to the hypothesis that Hyd positively regulates Sgg activity, over-expression of Sgg^{S9A} in *hyd*$^{K7.19}$ clones can rescue the *hyd*$^{K7.19}$ eye phenotype (**Figure 5.7 A**; panel c). Intriguingly, however, knockdown of endogenous Sgg protein in *hyd*$^{K7.19}$ clones also rescues the phenotype (**Figure 5.7 A**; panel e). In both cases, a complete rescue occurred in 50% of all adult flies analysed (n=10), in which eyes resembled those of control animals. Further to this, by analyzing adult eyes of over-expression-only controls, it was confirmed that neither over-expression of Sgg^{S9A} or *sgg*^{RNAi} alone, in otherwise wild-type clones, had any visible effects on adult eyes (**Figure 5.7 A**; panels d and f). These results suggest a strong and complex genetic

interaction between *sgg* and *hyd*. In addition, epistatically, Sgg function lies downstream of, or in a parallel pathway to, Hyd.

As mentioned before, the $hyd^{K7.19}$ phenotype varies in severity from individual to individual (see **Chapter 4**). To quantify the extent of rescue seen in adult eyes, the incidence of scars, being a major feature in the $hyd^{K7.19}$ mutant phenotype, was noted in all examined flies (n=10 per genotype) (**Figure 5.7 B**). These results confirmed the results of the visual analysis outlined above. The average number of scars in $hyd^{K7.19}$ animals was 2.3, with the total number of scars per eye ranging from one in mild cases to five in the most severe cases (**Figure 5.7 B**; b). Rescued $hyd^{K7.19}$ animals had an average number of 0.7 scars, if expressing UAS-sgg^{S9A} ($p = 0.005$), and 1.1 scars, if expressing UAS-sgg^{RNAi} ($p = 0.05$). For both genotypes, the maximum number of scars never exceeded three (**Figure 5.7 B**; c and d). No scars were observed in any of the control flies, with the exception of a single UAS-sgg^{RNAi}-expressing fly, which had one scar (**Figure 5.7 B**; f).

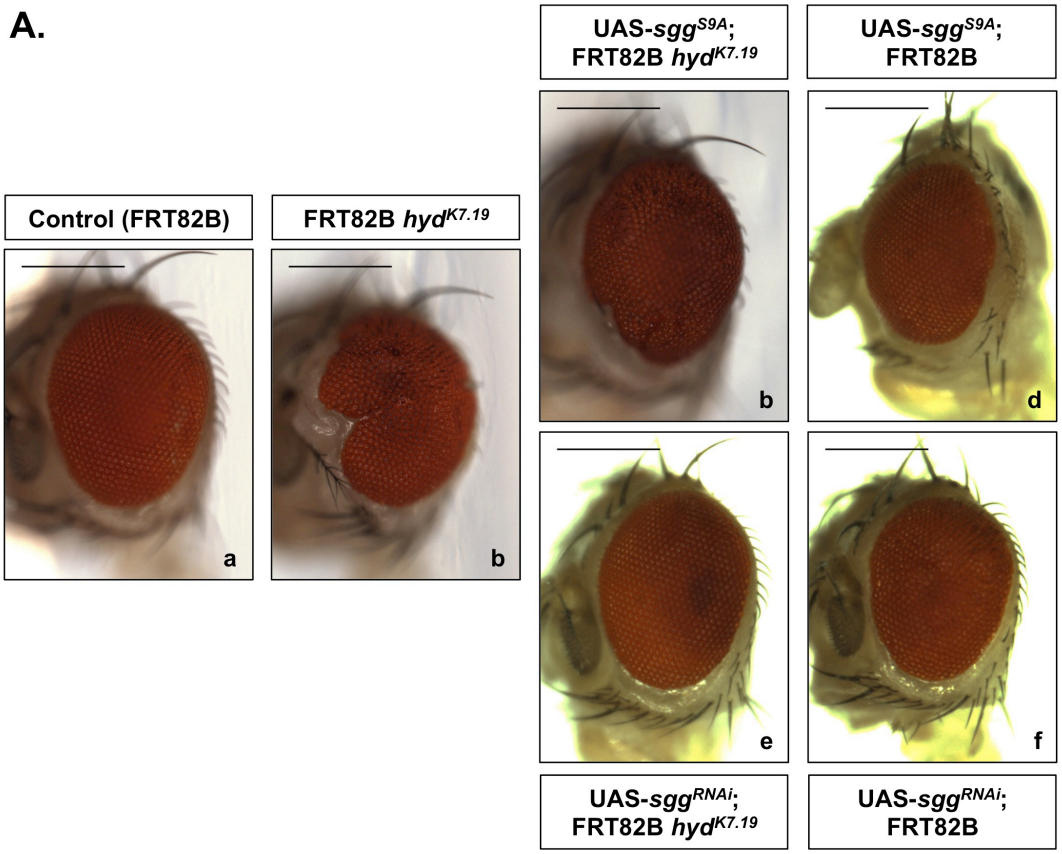

Figure 5.7: Modification of Sgg levels and activity recues the adult *hyd*^{mt} eye phenotype. (**A**) Side view of compound eyes containing the following genotypes of clones: a - FRT82B (control), b - FRT82B *hyd*$^{K7.19}$, c – UAS-*sgg*^{S9A}; FRT82B *hyd*$^{K7.19}$, d - UAS-*sgg*^{S9A}; FRT82B, e - UAS-*sgg*^{RNAi}; FRT82B *hyd*$^{K7.19}$, f - UAS-*sgg*^{RNAi}; FRT82B. Scale bars are 250µm. (**B**) Incidence of scars in adult eyes. Scars were counted in adult eyes containing clones with genotypes a-f (detailed above). Black

squares indicate average number of scars; lines indicate range, starting from minimum number, and ending at maximum number of scars. n=10 (per genotype). *t-test genotype b versus c, $p = 0.005$; *t-test genotype b versus e, $p = 0.05$.

5.4.2 Effect of Sgg protein levels and activity on the *hyd*$^{K7.19}$ head phenotype

As discussed in Chapter 4, the presence of *hyd*$^{K7.19}$ clones in EA discs not only results in scarring of the compound eye, but also causes a significant increase in the amount of non-eye head tissue in adults (**Section 4.3.2**). It was argued that this is more closely linked to effects on Wg pathway activity, whereas the compound eye phenotype is more likely to be dependent on Hh pathway activity (see **Chapter 1, Sections 1.2.5 and 1.3.4**). Because Sgg is a key regulator of both pathways, the expression of Sgg^{S9A} in *hyd*$^{K7.19}$ clones was also expected to affect head size. Indeed, expression of both UAS-*sgg*^{S9A} and UAS-*sgg*^{RNAi} transgenes in *hyd*$^{K7.19}$ clones reduced the amount of non-eye head tissue (**Figure 5.8 A**; panels c and e), although the effects were not found to be significant when quantified (**Figure 5.8 B**; t-test b versus c, $p = 0.1$; t-test b versus e, $p = 0.15$). This suggests that the functional consequence of the Hyd-Sgg interaction is likely to affect both Hh (eye effects) and Wg (head capsule effects) pathway activity. The results were quantified by measuring the eye-to-eye distance of non-eye head tissue at a fixed point (**Figure 5.8 B**). Interestingly, this suggests that Sgg^{S9A} clones significantly reduce the amount of non-eye head tissue compared to control animals containing wild-type clones ($p = 0.03$) (**Figure 5.8 B**; compare d and a). From a molecular point of view, over-expression of Sgg would suppress Wg pathway activity and thus the growth and development of head tissue, which could explain this result.

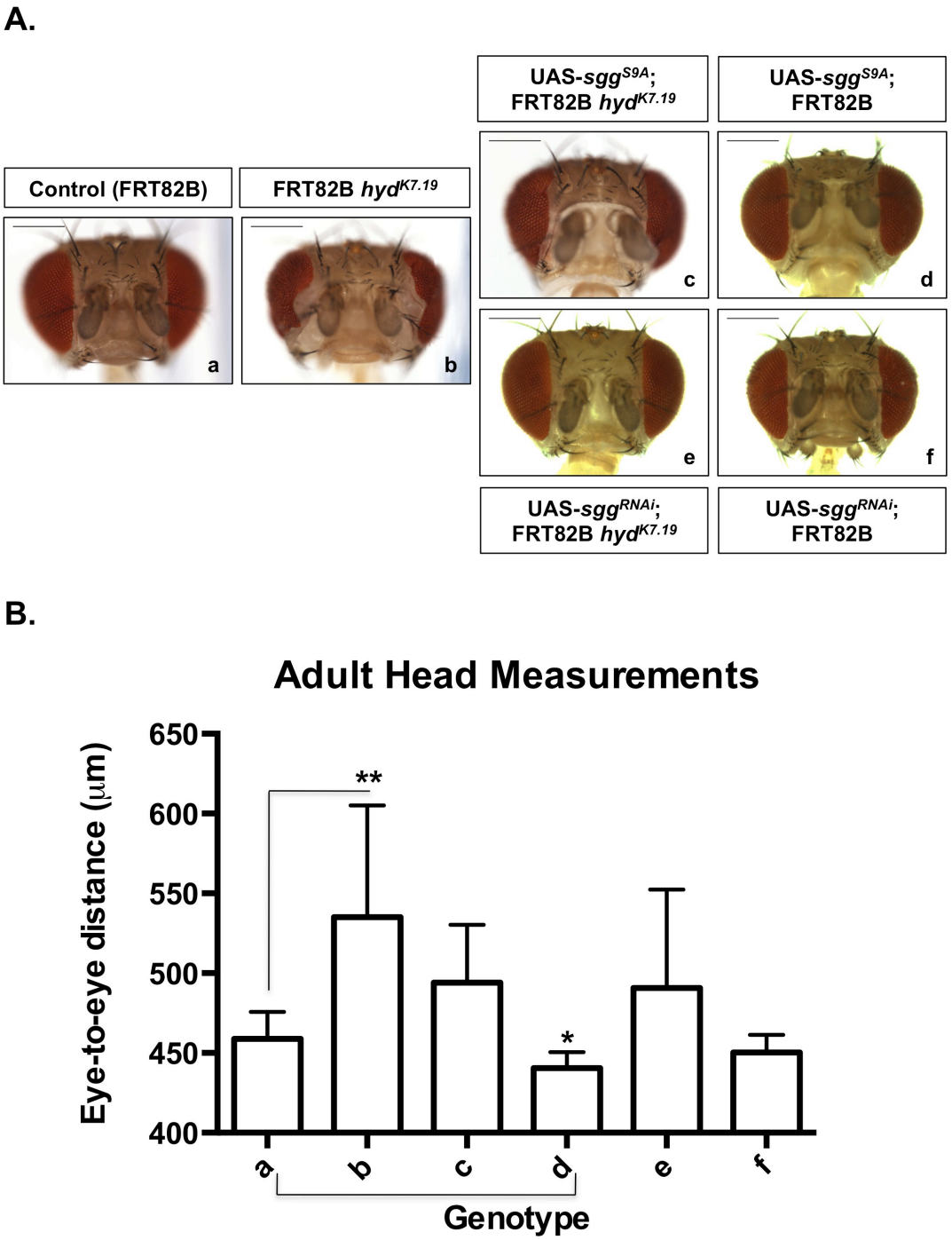

Figure 5.8: Modification of Sgg levels and activity recues the adult *hyd*^{mt} head phenotype. (**A**) Front view of adult heads containing the following genotypes of clones: a - FRT82B (control), b - FRT82B *hyd*$^{K7.19}$, c – UAS-*sgg*^{S9A}; FRT82B *hyd*$^{K7.19}$, d - UAS-*sgg*^{S9A}; FRT82B, e - UAS-*sgg*^{RNAi}; FRT82B *hyd*$^{K7.19}$, f - UAS-s*sgg*^{RNAi}; FRT82B. Scale bars are 250μm. (**B**) Head measurements (μm) were taken from eye-to-eye at a fixed point just above the antennae, and were significantly wider in

FRT82B $hyd^{K7.19}$ animals (**p = 0.004; t-test), and significantly lower in UAS-sgg^{S9A}; FRT82B animals (*p = 0.03; t-test) compared to FRT82B control animals. Genotypes are indicated a-f, and were as described in (A). n=10 (per genotype).

5.4.3 Effect of Sgg protein levels and activity on survival of GFP clones to adulthood

In Chapter 4, I showed that, although there was no obvious difference in the number of $hyd^{K7.19}$ clones versus control clones in age-matched third instar discs, the $hyd^{K7.19}$ clones present in the EA discs did not persist to adulthood in most cases (**Section 4.3.4, Figure 4.5 B** and **Figure 5.9** panels b1 and b2). This has been reported previously for $hyd^{K3.5}$ clones (J. D. Lee et al. 2002). $hyd^{K3.5}$ clones generated in a *Minute* genetic background, a mutation that confers a growth disadvantage (Morata & Ripoll 1975), are not eliminated and survive to adulthood, forming compound eyes that are drastically reduced in size, but nonetheless have correctly formed $hyd^{K7.19}$ ommatidia (J. D. Lee et al. 2002). This suggests that $hyd^{K7.19}$ clones may have a growth disadvantage (i.e. reduced fitness) and, as a result, are eliminated by the surrounding non-clonal tissue through cell competition.

To assess whether over-expression or knockdown of Sgg in $hyd^{K7.19}$ clones affects or rescues their reduced fitness, adult heads and eyes containing GFP positive clones of the respective genotypes were imaged using a fluorescence microscope (**Figure 5.9**). Although over-expression of UAS-sgg^{S9A} in $hyd^{K7.19}$ clones rescues the adult eye phenotype as judged by the obvious reduction in scarring and head size (**Figures 5.7** and **5.8**), UAS-sgg^{S9A}; FRT $hyd^{K7.19}$ clones were completely absent from the adult head (**Figure 5.9**; panel c). This suggests that over-expression of UAS-sgg^{S9A} in addition to loss of *hyd* reduces the fitness of clones even further than in $hyd^{K7.19}$ clones alone. Importantly, the fitness of UAS-sgg^{S9A}–only clones was not significantly affected as they were readily detected in adult heads (**Figure 5.9**; panel d). On the other hand, UAS-sgg^{RNAi}; FRT $hyd^{K7.19}$ clones survived to adulthood (**Figure 5.9**; panel e), and this also resulted in rescue of the scarring and increased

head size seen in animals containing *hyd*$^{K7.19}$ clones (**Figures 5.7** and **5.8**). Similarly, UAS-*sgg*^{RNAi} clones were also present in adult eyes (**Figure 5.9**; panel f). Taken together, these results suggest that the knockdown of endogenous Sgg in *hyd*$^{K7.19}$ clones reverses the reduced fitness of *hyd*$^{K7.19}$ clones compared to the surrounding wild type cells, and that therefore a functional interaction takes place between *hyd* and *sgg*.

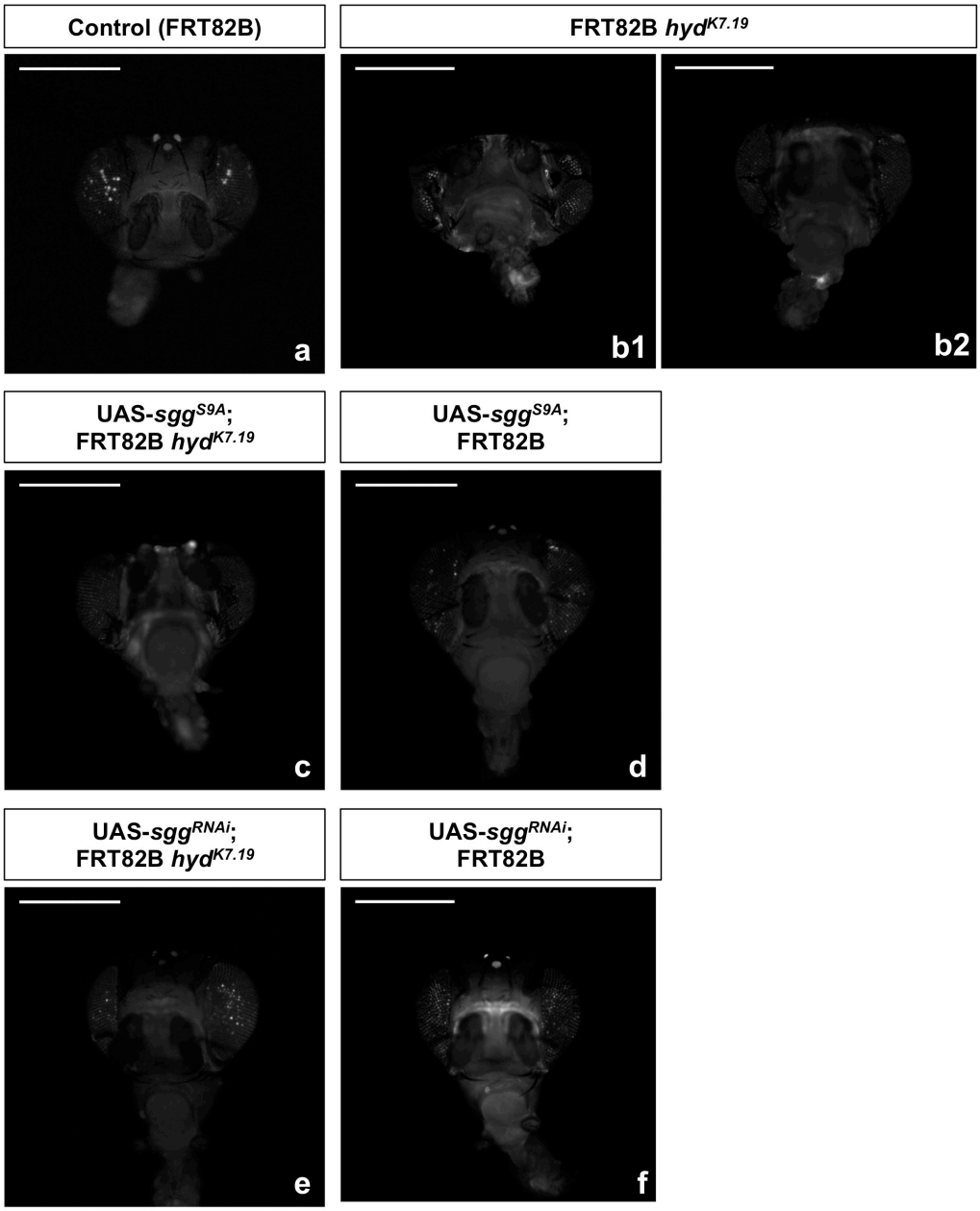

Figure 5.9: Effect of Sgg on clone survival. Front view of adult heads showing eyes containing GFP-positive clones with the following genotypes of clones: a - FRT82B (control), b1 and b2 - FRT82B $hyd^{K7.19}$, c – UAS-sgg^{S9A}; FRT82B $hyd^{K7.19}$, d - UAS-sgg^{S9A}; FRT82B, e - UAS-sgg^{RNAi}; FRT82B $hyd^{K7.19}$, f - UAS-sgg^{RNAi}; FRT82B. Scale bars are 500μm. n = 4; representative image taken for each genotype.

5.5 Effect of Sgg levels and activity on morphogen expression in third instar EA discs

The expression of both UAS-sgg^{S9A} and UAS-sgg^{RNAi} in $hyd^{K7.19}$ clones in EA discs ultimately leads to the rescue of the adult eye and head phenotypes. However, the molecular mechanism by which this rescue occurs is unknown. However, we do know that a major feature of the $hyd^{K7.19}$ phenotype is the ectopic expression of the morphogens Hh and Wg due to the presence of $hyd^{K7.19}$ clones in third instar EA discs (see **Chapter 4, Section 4.4**). Since both of these morphogens play crucial roles in directing the growth and differentiation of head and eye tissue, I investigated the effect of Sgg over-expression or knockdown in $hyd^{K7.19}$ clones on ectopic morphogen expression.

5.5.1 Sgg and *hh* gene expression

Although Sgg is known to be involved in regulating Hh pathway activity (J. Jia et al. 2002), a potential involvement in regulating *hh* ligand expression has not been reported. Therefore, the expression of the constitutively active Sgg kinase, or knockdown of *sgg*, in clones was not expected to affect the ectopic expression of *hh* by $hyd^{K7.19}$ clones. Surprisingly, however, both over-expression and knockdown of *sgg* appeared to affect *hh* gene expression levels in L3 EA discs.

Posterior *hyd*$^{K7.19}$*; hh-lacZ* clones express high levels of *hhlacZ* compared to control clones, and some anterior mutant clones also ectopically express *hhlacZ* (see Section 4.4 and **Figure 5.10 A**). 40% of discs containing UAS-*sgg*^{S9A}; *hyd*$^{K7.19}$ *hhlacZ* clones displayed lower levels of *hhlacZ* expression compared to discs containing *hyd*$^{K7.19}$ *hhlacZ* clones (**Figure 5.10**). Quantitative analysis, in which the intensity of B-gal staining was measured in groups of GFP-positive clones and compared across genotypes, confirmed that the maximum level of *hhlacZ* expression in UAS-*sgg*^{S9A}; *hyd*$^{K7.19}$ *hhlacZ* clones, although still high in some cases, was generally lower than in *hyd*$^{K7.19}$ *hhlacZ* clones (**Figure 5.10**). The wide range of *hhlacZ* expression levels observed indicates some variability in the phenotype, as well as variability in the extent of the rescue of ectopic *hhlacZ* expression. Further to this, over-expression of UAS-Sgg^{S9A} alone can also lead to increased levels of *hhlacZ* expression (**Figure 5.10 A**). Again, quantitative analysis revealed that, on average, UAS-*sgg*^{S9A}; FRT *hhlacZ* clones expressed higher levels of *hhlacZ* compared to FRT *hhlacZ* control clones (**Figure 5.10**).

Interestingly, knockdown of *sgg* in UAS-*sgg*^{RNAi}; *hyd*$^{K7.19}$ *hhlacZ* clones also rescues ectopic *hhlacZ* expression in posterior clones in about 50% of cases (**Figure 5.10**). However, anterior UAS-*sgg*^{RNAi}; *hyd*$^{K7.19}$ *hhlacZ* clones express high levels of ectopic *hh*, and this phenomenon is generally more frequent and widespread than in discs containing *hyd*$^{K7.19}$ *hhlacZ* clones (**Figure 5.10**). Finally, UAS-*sgg*^{RNAi}; FRT *hhlacZ* clones alone express lower levels of *hhlacZ* in posterior regions, which in some cases drop below the levels seen in control discs (**Figure 5.10**). However, the notable ectopic *hhlacZ* expression in anterior clones remains in UAS-*sgg*^{RNAi}; FRT *hhlacZ* clones, even though these carry no mutation in the *hyd* gene (**Figure 5.10**).

Contrary to what was expected, these results suggest that Sgg is involved in the regulation of *hh* gene expression. The expression of a constitutively active Sgg kinase leads to increased *hhlacZ* expression in posterior regions, whereas knockdown

of Sgg leads to ectopic *hhlacZ* expression in anterior regions of the disc. This suggests that Sgg has opposite effects on *hh* gene expression depending on the spatial localization of a cell within the disc. It therefore appears that Sgg positively regulates *hh* expression in posterior cells, but negatively regulates *hh* expression in anterior clones. This notion is supported by the fact that (i) the expression of Sgg^{S9A} in $hyd^{K7.19}$ clones rescues *hhlacZ* expression in anterior clones, and that (ii) knockdown of *sgg* in $hyd^{K7.19}$ clones results in a partial to full rescue of abnormal *hhlacZ* expression in posterior cells, but not in anterior cells. However, if Sgg is a positive regulator of *hh* expression, it is not clear why over-expression of Sgg^{S9A} in $hyd^{K7.19}$ clones can sometimes also rescue high *hhlacZ* levels in posterior cells. This could possibly reflect a variation in the *hyd* phenotype itself.

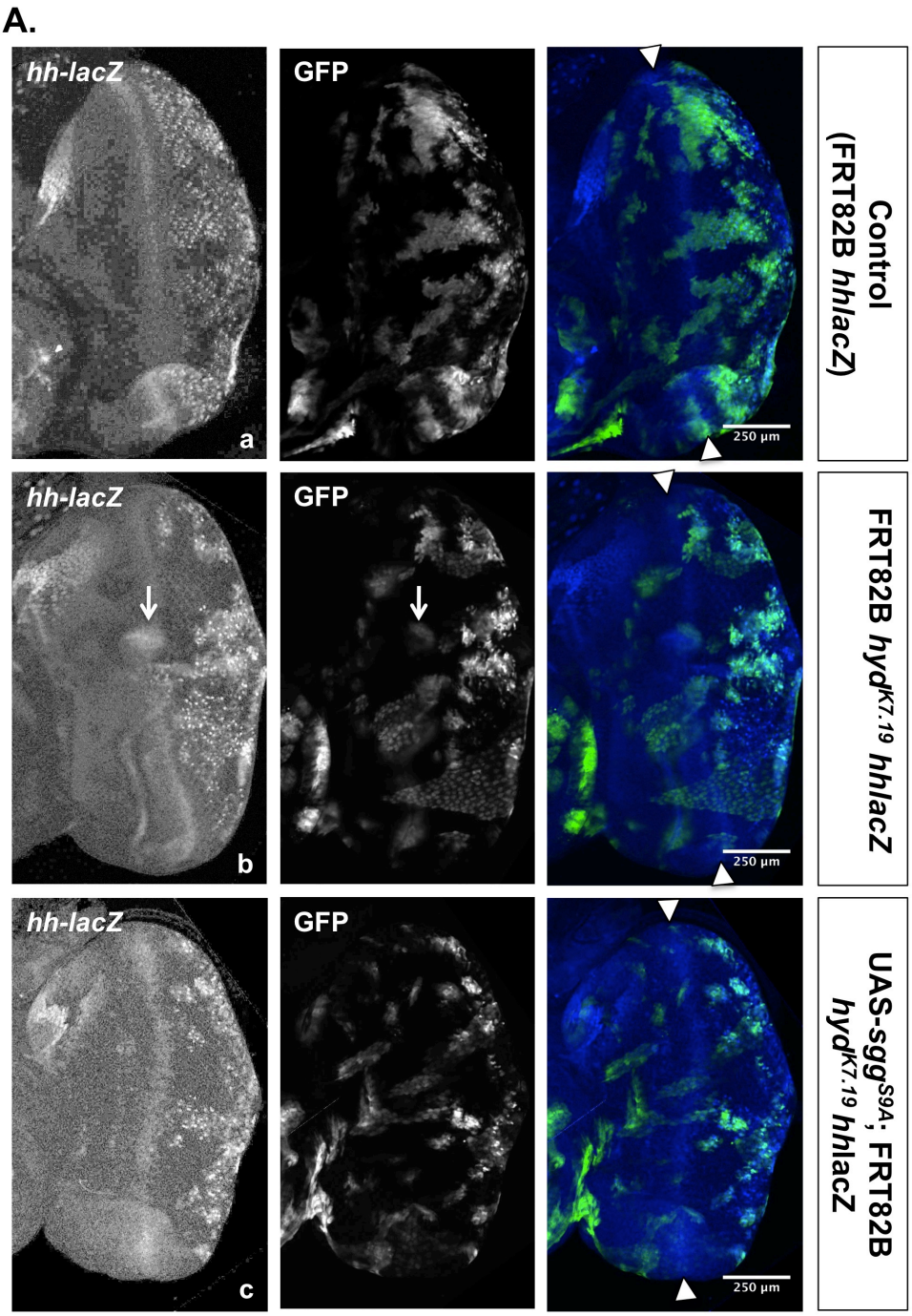
A.
hh-lacZ
GFP
a
b
c
250 µm
Control (FRT82B hhlacZ)
FRT82B hyd^K7.19 hhlacZ
UAS-sgg^S9A; FRT82B hyd^K7.19 hhlacZ

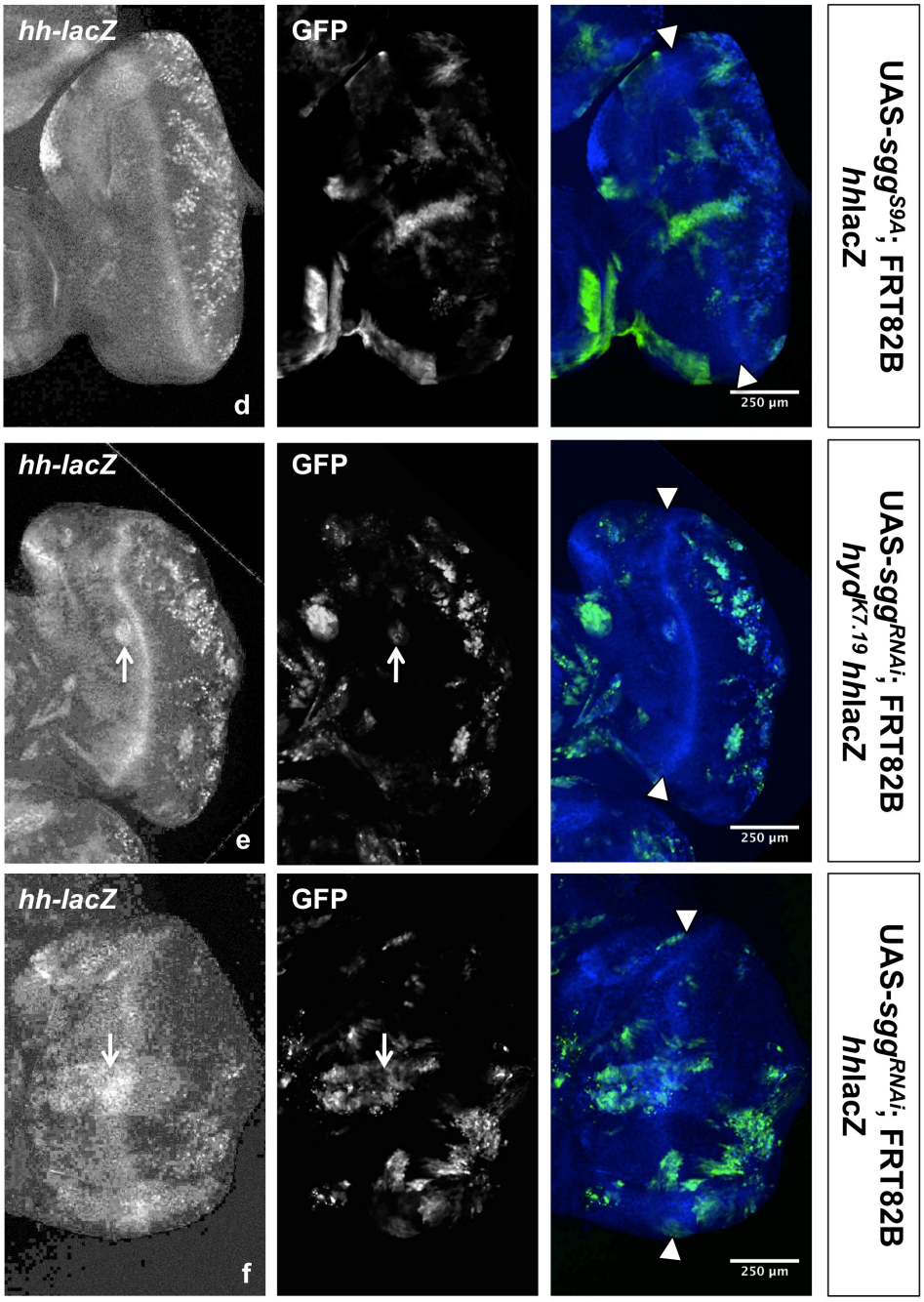
hh-lacZ
GFP
d
250 µm
UAS-sgg^{S9A}; FRT82B hhlacZ
hh-lacZ
GFP
e
250 µm
UAS-sgg^{RNAi}; FRT82B hyd$^{K7.19}$ hhlacZ
hh-lacZ
GFP
f
250 µm
UAS-sgg^{RNAi}; FRT82B hhlacZ

B.

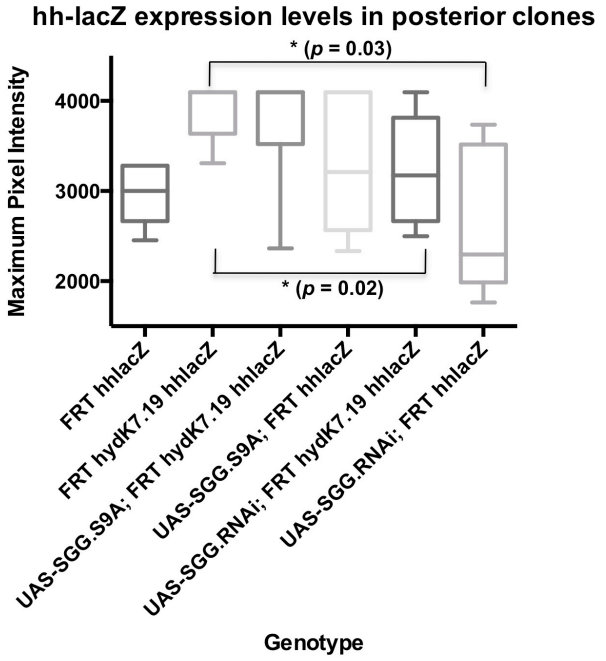

C.

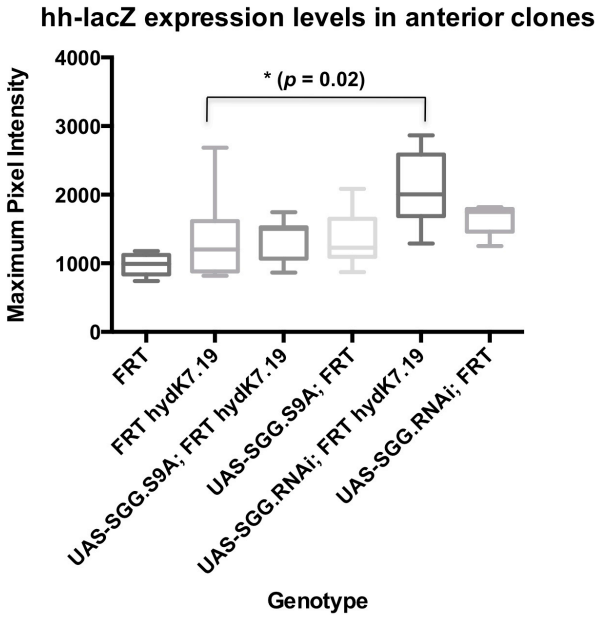

Figure 5.10: **Effect of Sgg on *hhlacZ* expression L3 EA discs.** Anterior is to the left, posterior is to the right, dorsal is up, and ventral is down in all subsequent immunofluorescence (IF) images. (**A**) IF of L3 EA discs containing GFP clones (green), stained for *hhlacZ* (blue). White arrows indicate ectopic *hhlacZ* expression in anterior clones. The morphogenetic furrow (MF) is marked by white triangles in all merged images. Scale bars are 250 μm. (**B**) Measurements of maximum pixel intensities in single ROIs containing groups of posterior GFP-positive clones in L3 EA discs. T-test

was performed on genotypes in brackets. n = 8. (**C**) Measurements of maximum pixel intensities in single ROIs containing groups of anterior GFP-positive clones in L3 EA discs. T-test was performed on genotypes in brackets. n = 8.

5.5.2 Sgg and Hh morphogen expression

Next, I used an antibody specific for Hh-N (Gallet et al. 2003), the Hh protein ligand that is secreted by *hh* expressing cells, to determine whether, as would be expected, Sgg has the same effects on Hh protein expression levels. Although one would expect this to reproduce the *hhlacZ* data, it is important to note that the Hh protein, unlike the *hhlacZ*-derived β-gal protein, can diffuse across the disc and bind to neighbouring cells displaying its receptor Ptc. Therefore, increased levels of Hh staining could be indicative of both high levels of Hh expression, as well as high levels of Ptc and Hh pathway activity.

All genotypes displayed elevated expression patterns of Hh staining compared to control discs (**Figure 5.11**). In addition to a higher level of all over Hh staining, these discs also had regions of localized high intensity Hh staining in clones (**Figure 5.11**). A notable exception to this trend, were discs containing UAS-*sgg*^{S9A} clones, which had levels of Hh protein comparable to levels in control discs (**Figure 5.11**). This was unexpected, because UAS-*sgg*^{S9A} clones were found to express increased levels of *hhlacZ* in posterior cells (**Section 5.5.1**). One possible explanation for this could be that over-expression of Sgg^{S9A} in these discs leads to down-regulation of the Hh pathway and decreased expression of *ptc*, which is then no longer displayed on the cell surface. Any secreted Hh protein therefore has no target to bind to and may subsequently be degraded, potentially explaining the low levels of Hh staining observed in these discs.

Overall, these results indicate that the increased Hh staining seen in the remaining discs is most probably a result of the mis-regulation of both *hh* gene expression and Hh pathway activity.

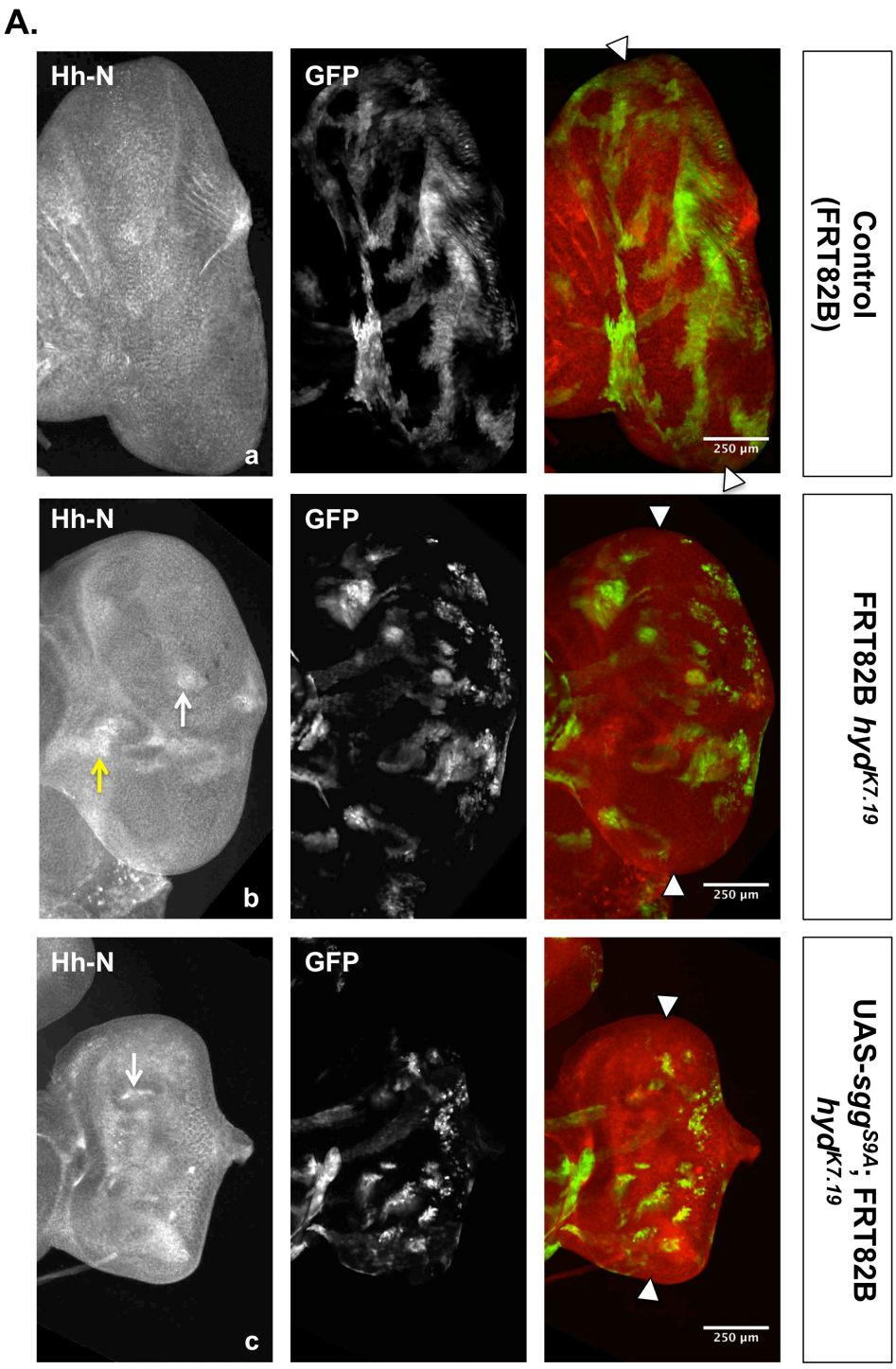

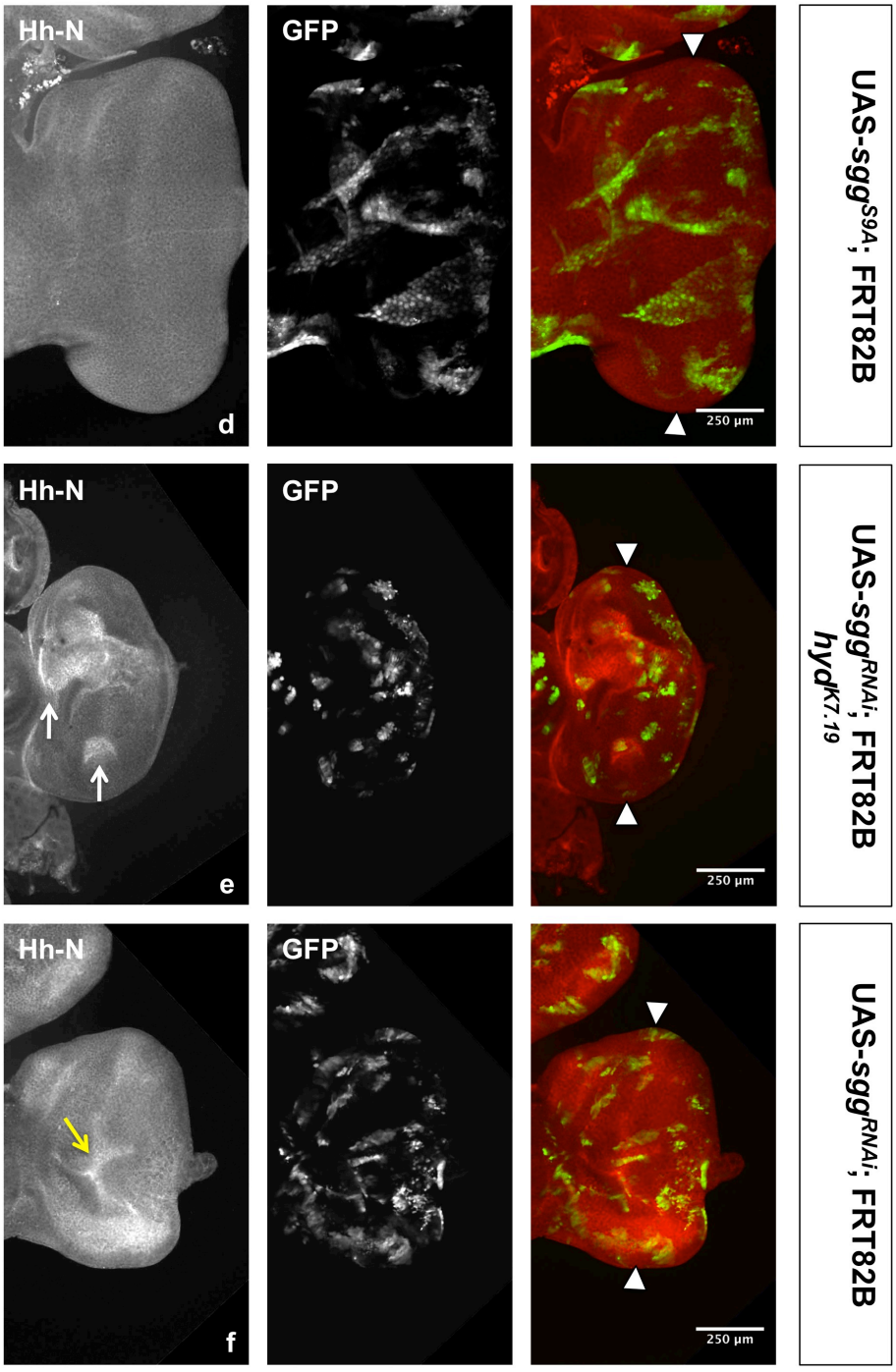
Hh-N
GFP
250 µm
d
UAS-sgg^{S9A}; FRT82B
Hh-N
GFP
250 µm
e
UAS-sgg^{RNAi}; FRT82B hyd$^{K7.19}$
Hh-N
GFP
250 µm
f
UAS-sgg^{RNAi}; FRT82B

B.

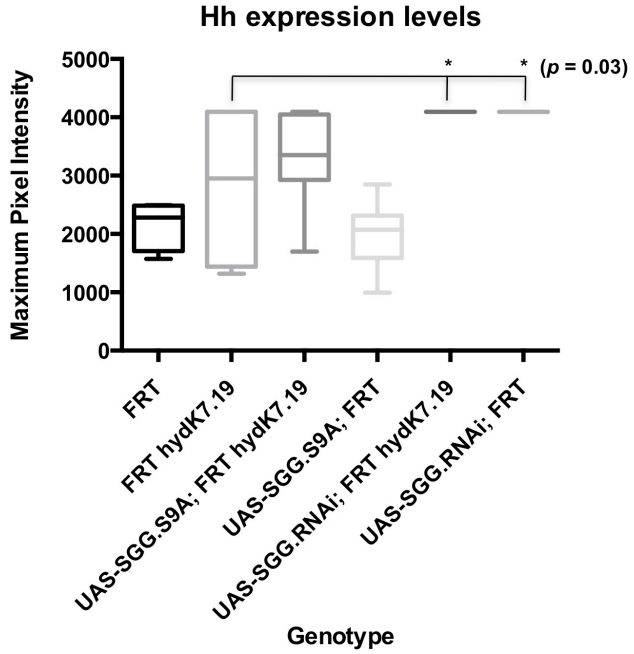

Figure 5.11: Effect of Sgg on Hh expression in L3 EA discs. (**A**) IF of L3 EA discs containing GFP clones (green), stained for Hh-N (red). Arrows indicate ectopic Hh expression in and around clones. The morphogenetic furrow (MF) is marked by white triangles in all merged images. Scale bars are 250 µm. (**B**) Measurements of average maximum pixel intensities in L3 EA discs. T-test was performed on genotypes in brackets. n = 7.

5.5.3 Sgg and Wg morphogen expression

Finally, I also investigated whether over-expression of Sgg^{S9A} could affect the high autonomous and non-autonomous Wg levels previously seen in discs containing $hyd^{K7.19}$ clones (Section 4.4 and **Figure 5.12**). However, expression of Sgg^{S9A} in $hyd^{K7.19}$ clones did not appear to alter the elevated Wg expression levels seen in discs containing $hyd^{K7.19}$ clones alone (**Figure 5.12**). This was further supported by quantitative analysis of the pixel intensity, which also suggested that expression of Sgg^{S9A} fails to rescue ectopic Wg expression in discs containing $hyd^{K7.19}$ clones (**Figure 5.12**). Further to this, no significant change in Wg protein levels was detected in discs containing UAS-sgg^{S9A} clones (**Figure 5.12**). This suggests that,

although previous results implicate Sgg in the regulation of Hh expression, Sgg does not appear to be involved in the regulation of Wg expression.

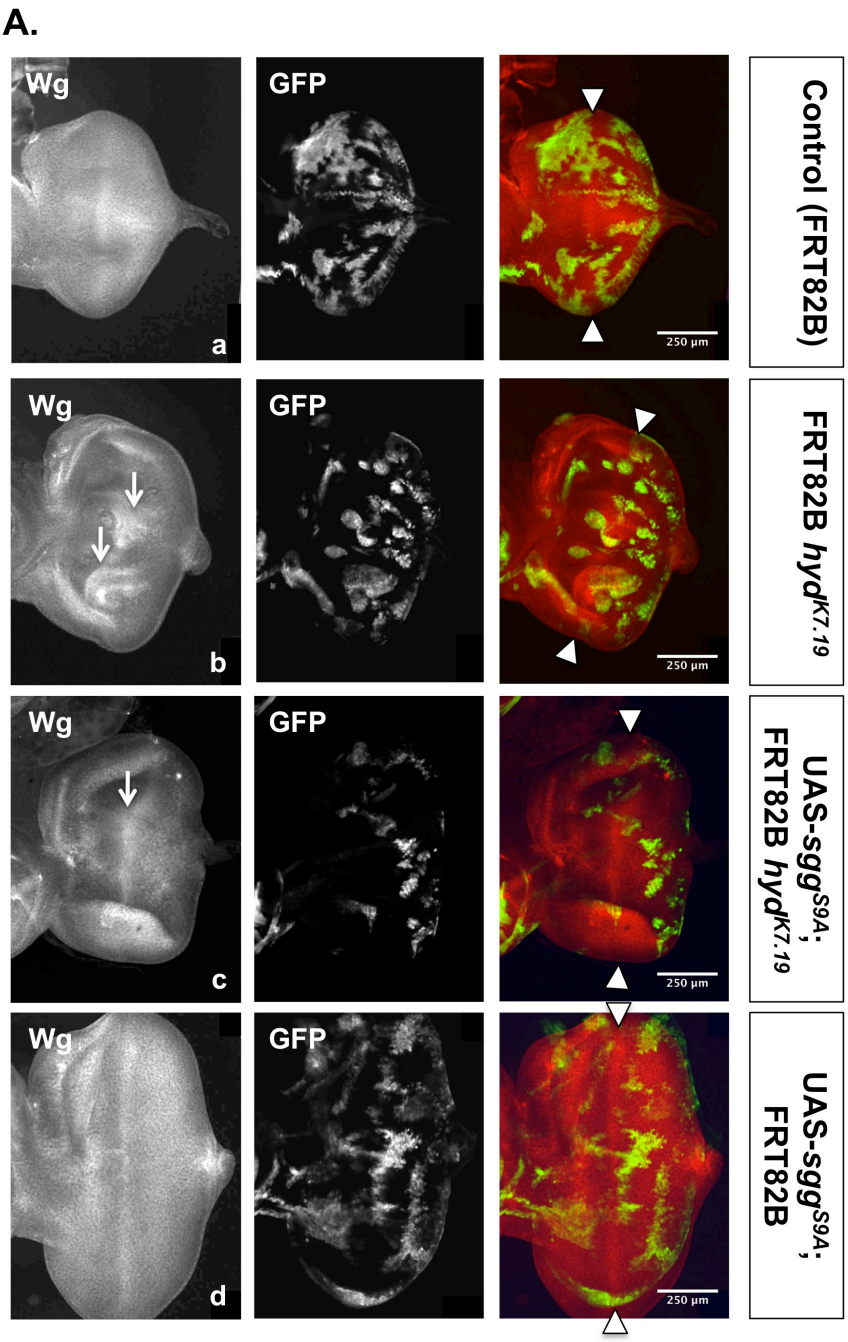

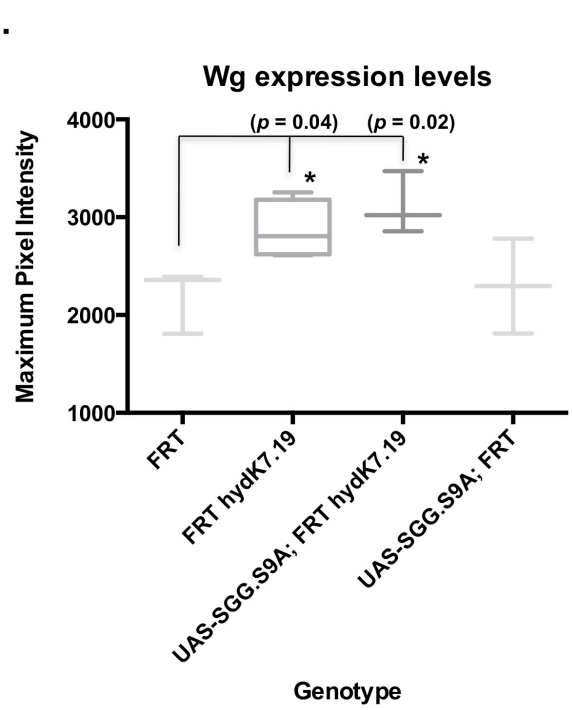

Figure 5.12: Effect of Sgg on Wg expression in L3 EA discs. (**A**) IF of L3 EA discs containing GFP clones (green), stained for Wg (red). White arrows indicate ectopic Wg expression in and around clones. The morphogenetic furrow (MF) is marked by white triangles in all merged images. Scale bars are 250 µm. (**B**) Measurements of average maximum pixel intensities in L3 EA discs. T-test was performed on genotypes in brackets. n = 4.

5.6 Effect of Sgg levels and activity on Hh pathway activity

As discussed in Chapter 4, loss of Hyd results in de-regulation of Hh pathway activity in third instar EA discs, which manifests as ectopic Ci_{155} and Ptc expression in $hyd^{K7.19}$ clones. Sgg is a key regulator of Ci_{155} activity, directing the processing of the active Ci_{155} protein to the Ci_{75} repressor protein. The results presented here so far clearly indicate that both a physical and functional interaction takes place between Hyd and Sgg. It is therefore likely that the rescue of the $hyd^{K7.19}$ phenotype by modifying Sgg levels and/or activity is, at least in part, a result of a direct effect on Ci_{155} protein levels. I therefore assessed the effects of Sgg over-expression and *sgg* knockdown on Ci_{155} and Ptc expression in $hyd^{K7.19}$ clones.

Loss of *hyd* results in elevated Ci_{155} expression levels in posterior clones, whereas anterior clones have reduced Ci_{155} expression levels (**Figure 5.13 A**, yellow and white arrows, respectively). Over-expression of sgg^{S9A} in $hyd^{K7.19}$ clones rescued the phenotype in 30-40% of cases. In a rescued disc, the characteristic D-V stripe of Ci_{155} staining was no longer disrupted or irregular, and the incidence of ectopic Ci_{155} expression was greatly reduced (Data not shown). However, in the majority of discs (~60%) containing UAS-sgg^{S9A}; FRT $hyd^{K7.19}$ clones, Ci_{155} expression was not rescued or only partially rescued. More specifically, these discs still had disrupted and/or an irregular D-V stripe pattern of Ci_{155} staining, as well as some anterior and posterior clones ectopically expressing low or high levels of Ci_{155}, respectively (**Figure 5.13 A**, white and yellow arrows, respectively). On the other hand, over-expression of Sgg^{S9A} in wild-type clones has no significant effect on the normal Ci_{155} staining pattern, apart from low Ci_{155} expression levels in some anterior clones (**Figure 5.13 A**, white arrow).

My previous results suggested Sgg to be a positive regulator of *hh* gene expression, as over-expression of Sgg^{S9A} resulted in high *hhlacZ* expression levels in posterior regions of the eye disc. This is a common feature with the $hyd^{K7.19}$ phenotype, in which posterior $hyd^{K7.19}$ clones also express high levels of *hhlacZ* (**Section 5.5**). I therefore wondered whether there could be a correlation between ectopic *hh* expression and Ci_{155} levels in clones. Indeed, double staining for β-gal and Ci_{155} revealed that high Ci_{155} levels in posterior $hyd^{K7.19}$ clones frequently correlated with high *hhlacZ* expression levels in the same clones (**Figure 5.13 B**, white arrow).

This could indicate that high levels of Ci_{155} in posterior $hyd^{K7.19}$ clones are a direct result of ectopic *hh* expression in the same cells, suggesting that the Hh pathway is activated autonomously. Conversely, in UAS-sgg^{S9A}; $hyd^{K7.19}$ clones high *hhlacZ* expression in posterior clones does not generally correlate with Ci_{155} levels.

Although, in some cases, high *hh* expression in posterior clones correlates with low levels of Ci_{155} levels (**Figure 5.13 B**, white arrow). This negative correlation between hhlacZ and Ci_{155} levels is the opposite trend to the positive correlation seen in $hyd^{K7.19}$ clones. This suggests that over-expression of Sgg^{S9A} reverses the high levels of Ci_{155}, resulting from induction of the Hh pathway by ectopic Hh ligand production, through conversion of the Ci_{155} activator protein to the Ci_{75} repressor protein, which is not detectable with the Ci antibody that was used. In other words, the rescue of the $hyd^{K7.19}$ phenotype by over-expression of Sgg^{S9A} could be, in part, due to increased processing, and thus reduced levels of Ci_{155} in posterior regions of the disc.

However, as mentioned above, only a small proportion (~30%) of discs containing UAS-sgg^{S9A}; $hyd^{K7.19}$ clones display a rescue of ectopic Ci_{155} expression in posterior clones. In the majority of cases, posterior UAS-sgg^{S9A}; $hyd^{K7.19}$ clones still express high levels of Ci_{155}, with no significant differences detectable when compared to $hyd^{K7.19}$ clones (**Figure 5.14**, yellow arrows). However, the incidence of low Ci_{155} expression, seen in anterior $hyd^{K7.19}$ clones, is significantly reduced in anterior UAS-sgg^{S9A}; $hyd^{K7.19}$ clones (**Figure 5.14**, white arrow). In addition, double staining for Ci_{155} and Ptc confirmed that high or low levels of Ci_{155} co-localised with high or low Ptc protein levels, respectively. This suggests that the Hh pathway was ectopically activated in posterior UAS-sgg^{S9A}; $hyd^{K7.19}$ clones and $hyd^{K7.19}$ clones, and down-regulated in anterior $hyd^{K7.19}$ clones.

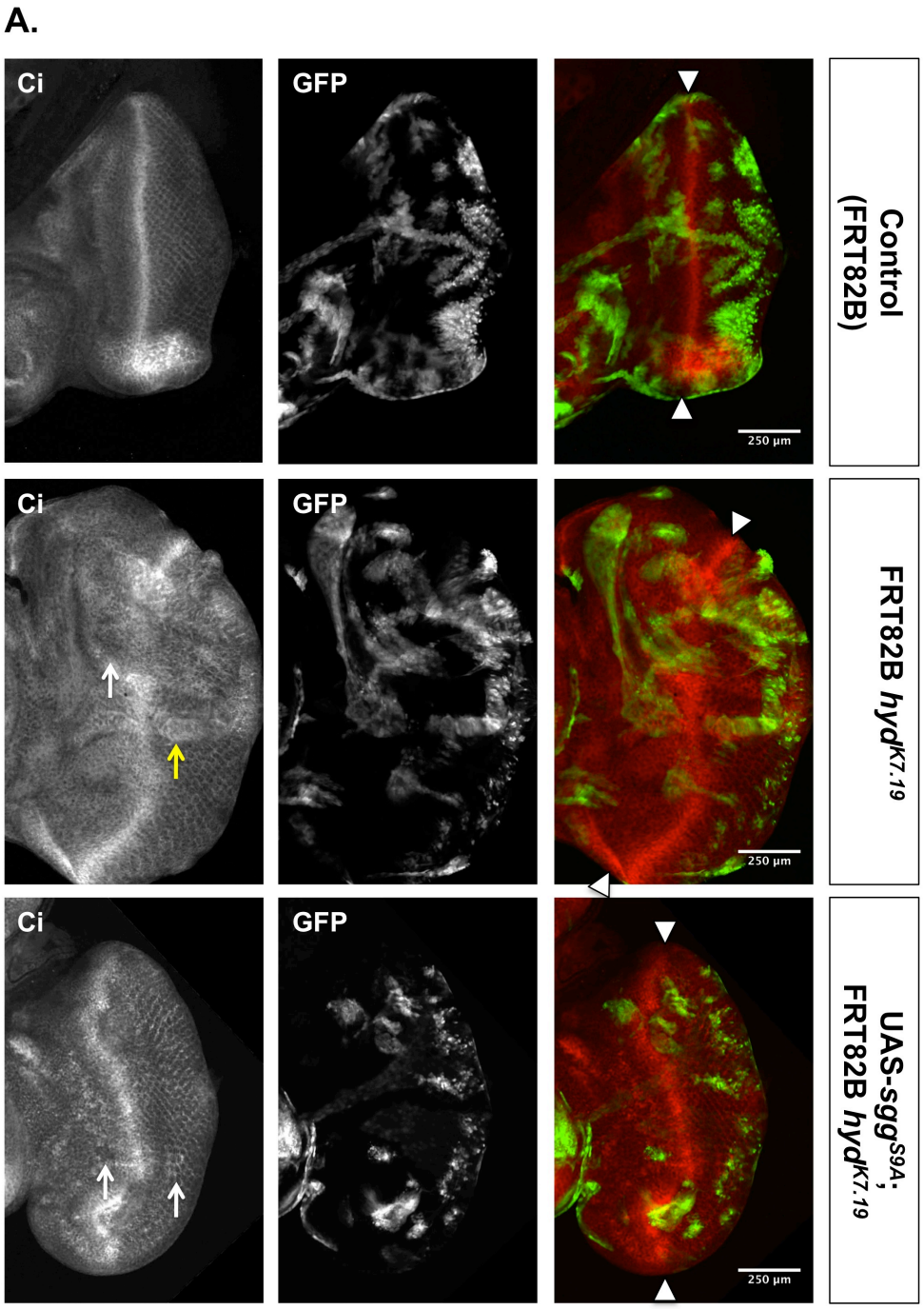
A.
Ci
GFP
Control (FRT82B)
FRT82B hyd^K7.19
UAS-sgg^S9A; FRT82B hyd^K7.19
250 µm

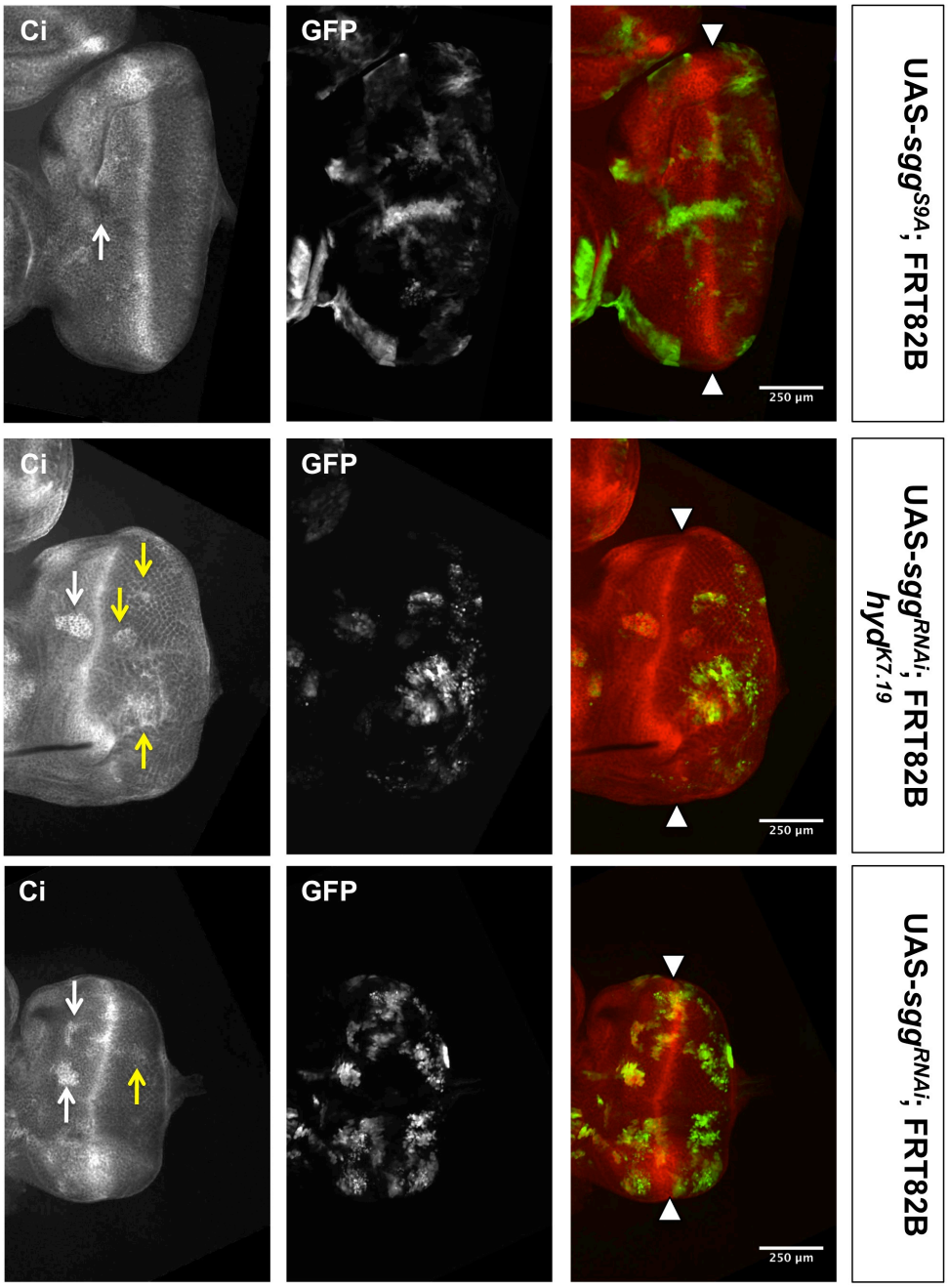
Ci
GFP
250 µm
UAS-sgg^{S9A}; FRT82B
Ci
GFP
250 µm
UAS-sgg^{RNAi}; FRT82B hyd$^{K7.19}$
Ci
GFP
250 µm
UAS-sgg^{RNAi}; FRT82B

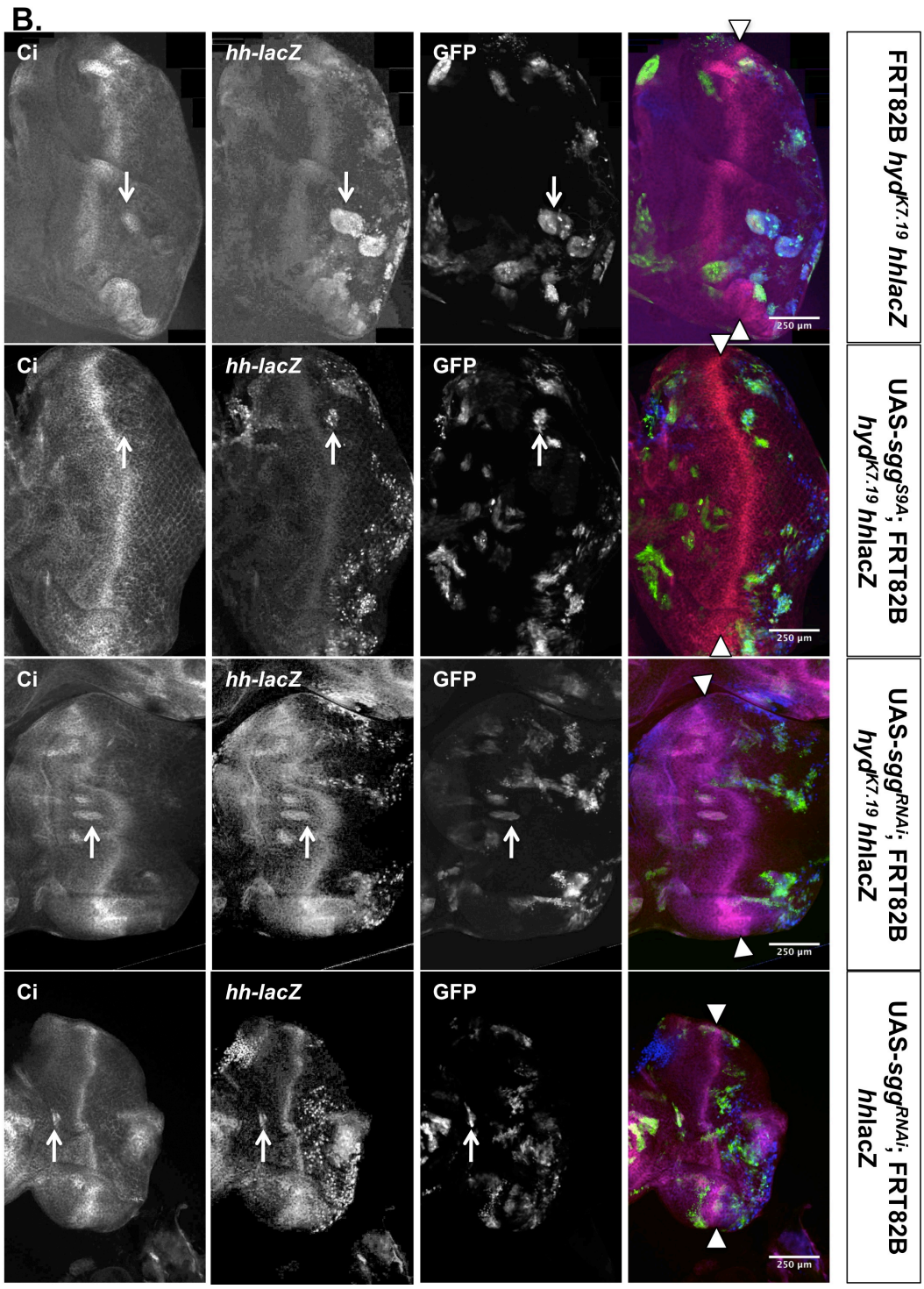

Figure 5.13: Effect of Sgg on Ci_{155} and *hhlacZ* expression L3 EA discs. The morphogenetic furrow (MF) is marked by white triangles in all merged images. Scale bars are 250 µm. (**A**) IF of L3 EA discs containing GFP clones (green), stained for Ci_{155} (red). Arrows indicate ectopic Ci_{155} expression in anterior (white) and posterior (yellow) clones. (**B**) IF of L3 EA discs containing GFP clones (green),

stained for Ci_{155} (red) and *hhlacZ* (blue). White arrows indicate clones in which Ci_{155} and *hhlacZ* expression are correlated.

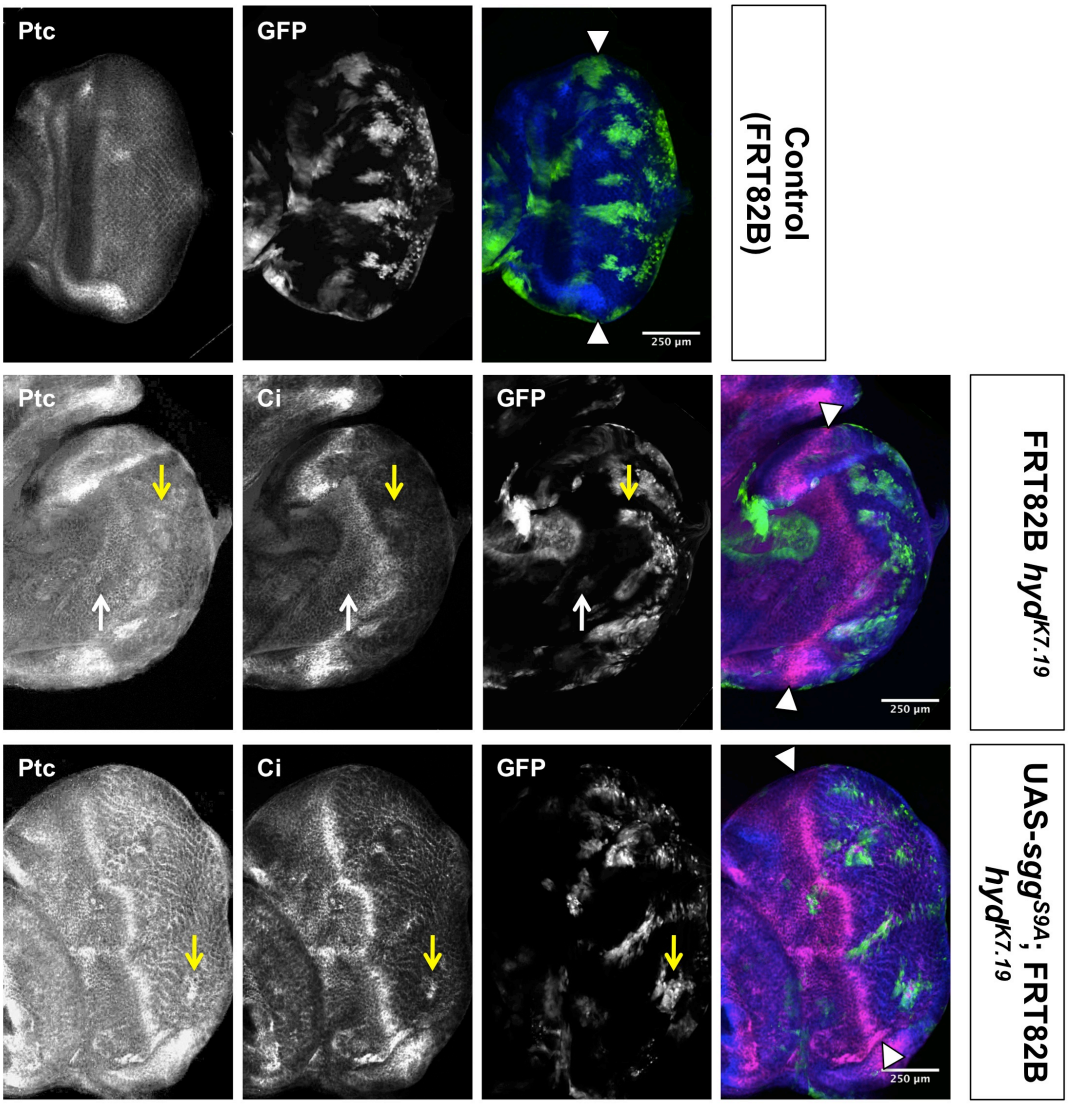

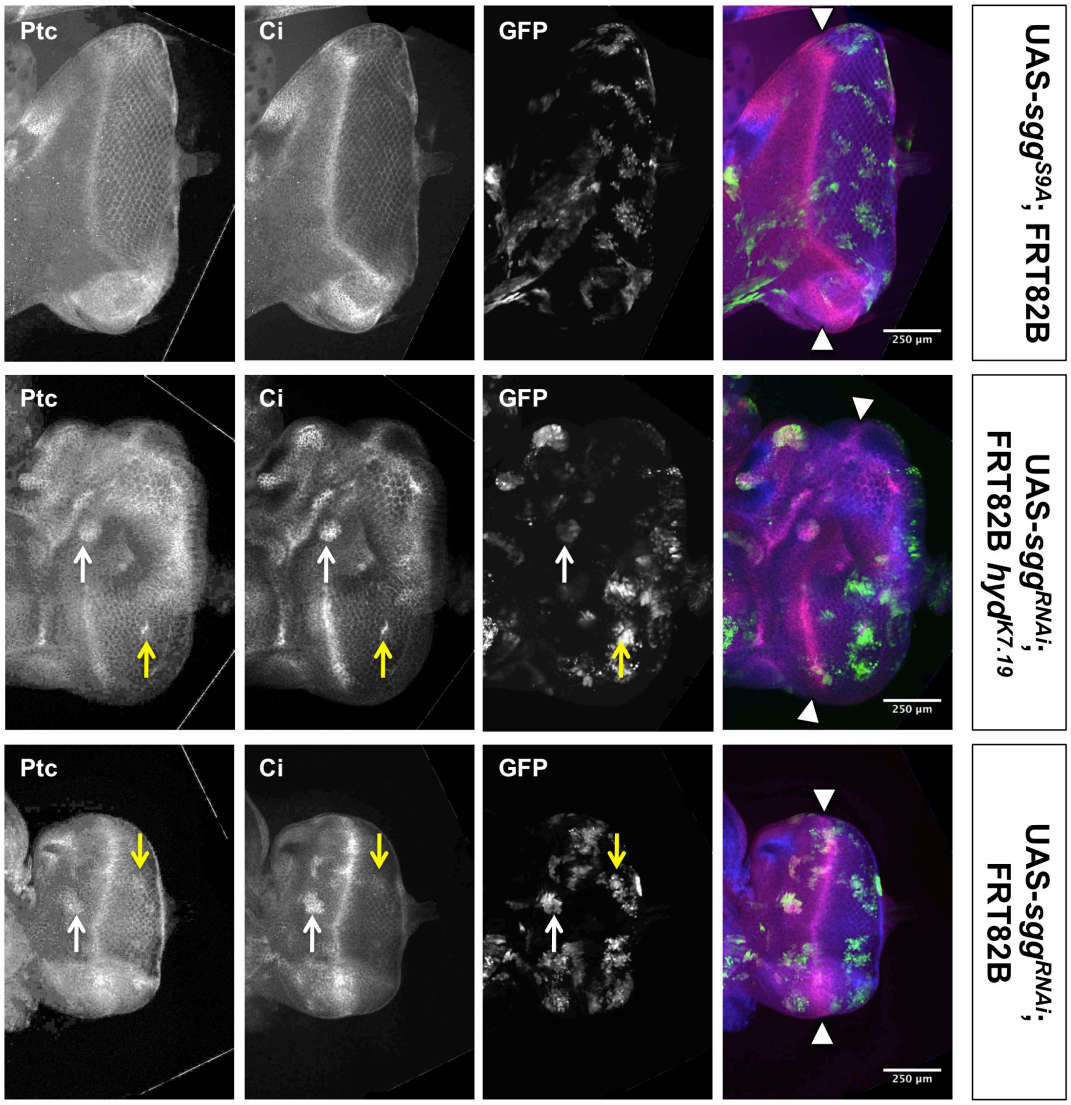

Figure 5.14: Effect of Sgg on Ptc and Ci_{155} expression L3 EA discs. IF of L3 EA discs containing GFP clones (green), stained for Ptc (blue) and Ci_{155} (red). Arrows indicate anterior (white) and posterior (yellow) clones in which ectopic Ci_{155} and Ptc expression are correlated. The morphogenetic furrow (MF) is marked by white triangles in all merged images. Scale bars are 250 µm.

5.6.1 Effect of Sgg knockdown on Hh pathway activity

The RNAi-mediated knockdown of endogenous *sgg* in *hyd*$^{K7.19}$ clones had a much more pronounced and consistent effect on the ectopic Ci_{155} expression profile in

hyd$^{K7.19}$ clones than over-expression of Sgg^{S9A}. In the vast majority of discs examined, anterior UAS-*sgg*^{RNAi}; *hyd*$^{K7.19}$ clones no longer expressed low levels of Ci_{155}, but instead markedly over-expressed Ci_{155} (**Figure 5.13 A**, white arrows). On the other hand, the behaviour of posterior clones remained unchanged. Both posterior *hyd*$^{K7.19}$ and UAS-*sgg*^{RNAi}; *hyd*$^{K7.19}$ clones over-expressed Ci_{155} (**Figure 5.13 A**, yellow arrows). Interestingly, UAS-*sgg*^{RNAi} clones exhibited the same ectopic Ci_{155} expression pattern, with both anterior and posterior clones expressing high levels of Ci_{155} (**Figure 5.13 A**, white and yellow arrows, respectively).

Further to this, in both anterior UAS-*sgg*^{RNAi}; *hyd*$^{K7.19}$ and UAS-*sgg*^{RNAi} clones, high levels of Ci_{155} expression were positively correlated with high levels of ectopic *hhlacZ* expression (**Figure 5.13 B**, white arrows). As discussed in the previous section, Sgg appears to be a negative regulator of *hh* expression in anterior regions of the eye disc (**Section 5.5**). This suggests that the high Ci_{155} levels seen in anterior clones expressing RNAi against *sgg* could be a result of increased autonomous Hh pathway activation as a result of increased *hh* expression in the absence of Sgg. On the other hand, no correlation between high Ci_{155} expression and *hhlacZ* expression was detected in posterior clones, suggesting that increased Ci_{155} levels in these clones were not related to Hh ligand expression. Instead, it is more likely that the absence of Sgg in these cells prevents the conversion of Ci_{155} to Ci_{75} in these clones, resulting in an accumulation of Ci_{155}.

Finally, in both anterior- and posterior UAS-*sgg*^{RNAi}; *hyd*$^{K7.19}$ and -UAS-*sgg*^{RNAi} clones increased Ci_{155} levels were positively correlated with high Ptc levels (**Figure 5.14**, white and yellow arrows, respectively). This suggests that, regardless of the underlying cause of Ci_{155} accumulation in anterior and posterior clones, the downstream effect is the increased activation of the Hh pathway in both cases.

5.7 Discussion

In an effort to elucidate the mechanism by which Hyd negatively regulates Hh pathway activity, I applied both *in vitro* and *in vivo* methods to establish whether Sgg interacts with Hyd, and what the molecular and functional consequences of this interaction are.

Hyd interacts with Sgg in S2 cells, which suggests that the interaction is conserved between *Drosophila* and humans. The interaction between the human orthologue of Hyd, EDD, and GSK3β in HEK293 cells has been reported previously (Hay-Koren et al. 2011). This is encouraging, as it increases the likelihood of conservation of a possible Hyd/EDD-mediated regulation mechanism of Hh/SHH pathway activity involving Sgg/GSK3β in mammalian cells. De-regulation of SHH pathway activity occurs in a wide range of human tumours (reviewed in (L. L. Rubin & de Sauvage 2006)), and this result strengthens the notion that EDD would be a good therapeutic target. The interaction between EDD and GSK3β is binary (Hay-Koren et al. 2011), and although I did not confirm that this is the case in *Drosophila* cells also, I tried to map the interaction surface for Sgg on Hyd. This revealed that Sgg binding does not occur via the recognition of ubiquitin or a PAM2 motif by the UBA and PABC domains, respectively. Nor does the interaction require the catalytic cysteine residue in the HECT domain of Hyd to be present, suggesting that the binding does not occur through this residue. It also suggests that Hyd's ubiquitylation activity is not required. However, S2 cells express endogenous Hyd, which could ubiquitylate Sgg prior to exogenous Hyd C>A binding. This could explain the contradictory results I obtained with Sgg binding to the Hyd C>A mutant. In future, the binding assay should be carried out using recombinant proteins to determine whether the interaction is direct in *Drosophila*, and whether the Hyd C>A mutant can bind Sgg in the absence of endogenous Hyd.

Both Sgg and GSK3β were found to be ubiquitylated, but my results do not support the hypothesis that Hyd/EDD is the E3 ubiquitin ligase responsible for Sgg/GSK3β ubiquitylation. Although Sgg ubiquitylation has not been reported before, GSK3β is ubiquitylated and subsequently degraded by the HECT E3 ubiquitin ligase Smurf2 in mouse chondrocytes, leading to increased Wnt signalling (Q. Wu et al. 2009). In S2 cells, Hyd did not affect Sgg ubiquitylation or Sgg levels, suggesting that Hyd does not ubiquitylate or degrade Sgg. However, loss of EDD in HEK293 cells increased endogenous GSK3β ubiquitylation, which implies that EDD instead antagonizes GSK3β ubiquitylation. This result was not confirmed in S2 cells. However, S2 cells, unlike HEK293 cells do not express the necessary components to transduce the Hh and Wg signaling pathways, and this may explain the discrepancy between these results. Although EDD does not appear to ubiquitylate GSK3β, it does seem to prevent the ubiquitylation of GSK3β.

Since ubiquitylation can have many non-degradative outcomes (see **Chapter 1, Section 1.1.5.2**), EDD could thereby affect GSK3β function independently of changes to its half-life. Over-expression of EDD in HEK293 cells increases the nuclear localization of GSK3β (Hay-Koren et al. 2011), and its nuclear translocation may be regulated by ubiquitylation. This would enable the nuclear phosphorylation of a particular subset of GSK3β substrates, such as GLI-family members (the human Ci homologues). Identification of GSK3β's ubiquitylation sites, specifically those occurring upon EDD RNAi, would allow the creation of non-ubiquitylatable mutants. Various mutants of Sgg/GSK3β, in which all or a sub-set of lysine residues are mutated to alanine, could then be used to determine whether the nuclear uptake of Sgg/GSK3β is dependent on ubiquitylation.

To complement the *in vitro* work, I also successfully used the MARCM technique to vary Sgg levels and activity in $hyd^{K7.19}$ clones in *Drosophila* eye-antennal discs. This

significantly modified the adult *hyd*$^{K7.19}$ hyperplastic phenotype, suggesting that there is also a functional interaction between the two proteins *in vivo*. Intriguingly, both over-expression and RNAi-mediated knockdown of Sgg in *hyd*$^{K7.19}$ clones led to a complete rescue of tissue hyperplasia of the eye and head. While *hyd*$^{K3.5}$/*hh* double mutant clones lead to a partial suppression of the hyperplastic phenotype, the generation of *hyd*$^{K3.5}$/*hh* double mutant clones expressing UAS-Ci$_{75}$ resulted in a complete rescue (J. D. Lee et al. 2002). This suggests that both ectopic *hh* expression and ectopic Hh pathway activation must be rectified in *hyd* mutant clones to reverse the phenotype. My results clearly indicate that Hyd and Sgg regulate both *hh* expression and Hh pathway activity. However, it is also possible that Sgg modifies the *hyd*$^{K7.19}$ phenotype through effects on Wg signalling.

Most of the *hyd*$^{K7.19}$ clones in the adult eye are eliminated, suggesting that the loss of *hyd* may confer a growth disadvantage (see Chapter 4), and the over-expression of Sgg^{S9A} in *hyd*$^{K7.19}$ clones also lead to their elimination prior to adulthood. In a previous study, *hyd*$^{K7.19}$ clones that were generated in a minute background formed adult eyes which were reduced in size, and it was stipulated that *hyd*$^{K7.19}$ clones exhibit a growth disadvantage, leading to their elimination through competition with WT cells (J. D. Lee et al. 2002). To investigate whether the expression of Sgg^{S9A} in *hyd*$^{K7.19}$ cells further reduces the fitness of clones, suggesting that Hyd and Sgg function in the same or parallel pathways, these clones could also be generated in a minute background. If so, it would be expected that UAS-*Sgg*^{S9A}; *hyd*$^{K7.19}$ clones generate even smaller or no adult eyes. Further to this, experiments to address whether the elimination of *hyd*$^{K7.19}$ and UAS-*sgg*^{S9A}; *hyd*$^{K7.19}$ clones occurs through apoptosis could be carried out. This can be achieved by Terminal deoxynucleotidyl transferase dUTP nick end labeling (TUNEL staining) to detect DNA fragmentation following apoptosis, or staining for active caspase-3, or genetically, by generating clones that over-express a caspase inhibitor (e.g. p35), to see whether clones can now survive to adulthood. On the other hand, knockdown of endogenous *sgg* in *hyd*$^{K7.19}$ clones also rescued the hyperplastic phenotype, but these clones were not eliminated. This suggests that an alternate molecular rather than cellular compensation

mechanism is involved, which is most likely attributed to the role of Sgg in regulating the Hh and Wg pathways.

Although my original aim was to determine whether the interaction between Hyd and Sgg affects Hh pathway activity *in vivo*, my results somewhat surprisingly revealed that Sgg also affects *hh* gene expression. Over-expression of Sgg^{S9A} reduces ectopic *hh* expression in posterior $hyd^{K7.19}$ clones, whereas posterior Sgg^{S9A} clones alone express high ectopic levels of *hh*. Conversely, knockdown of Sgg results in ectopic *hh* expression in anterior Sgg^{RNAi}; $hyd^{K7.19}$ and Sgg^{RNAi} clones, whereas this has no effect on posterior $hyd^{K7.19}$ clones, but leads to a reduction in *hh* expression in posterior Sgg^{RNAi} clones (**Figure 5.15 A**). This suggests that Sgg regulates *hh* gene expression, which has not been reported before. Based on these results, I propose a model in which Sgg negatively regulates *hh* expression in anterior regions of the eye disc, as a result of activation by Hyd; whereas Sgg positively regulates *hh* expression in posterior regions, antagonizing the action of Hyd in a separate mechanism (**Figure 5.15 B**). In the anterior compartment of the EA disc, Ci_{75} represses *hh* gene expression (Domínguez et al. 1996; Méthot & Basler 1999). Therefore, Sgg could negatively regulate *hh* expression in anterior cells simply by promoting the processing of Ci_{155} to Ci_{75}. This process, in turn, could be potentiated by Hyd through positive regulation of Sgg activity. On the other hand, in the posterior EA disc compartment, *hh* expression is not regulated by Ci, but instead, the transcripton factor Pointed, a downstream target of the Egfr/Ras pathway, positively regulates *hh* expression (Rogers et al. 2005). Sgg and Hyd could therefore be acting through Pointed to positively and negatively regulate *hh* expression, respectively, in these cells. It would be interesting to determine whether Sgg or Hyd can interact with Pointed, and whether any potential interactions would involve phosphorylation and/or ubiquitylation to regulate Pointed transcriptional activity.

Finally, as expected and reported previously in wing disc *sgg*$^{-}$ clones (J. Jia et al. 2002), RNAi-mediated loss of Sgg also increases the level of Ci_{155} in both anterior and posterior clones (**Figure 5.15 A**). As such, knockdown of Sgg in *hyd*$^{K7.19}$ clones has no effect on ectopic posterior Ci_{155} expression, but reverses the low Ci_{155} expression seen in anterior *hyd*$^{K7.19}$ clones (**Figure 5.15 A**). This would suggest that only the prevention of low Ci_{155} and low Hh pathway activity in anterior clones leads to a rescue in *Sgg*^{RNAi}; *hyd*$^{K7.19}$ animals (**Figure 5.15 C**).

However, on the basis of these results, it is not possible to determine how exactly modification of Hh pathway activity and Ci_{155} levels leads to a rescue of the hyperplastic phenotype following Sgg knockdown. Surprisingly, over-expression of Sgg^{S9A} had no significant effect on Ci_{155} levels in both *Sgg*^{S9A}; *hyd*$^{K7.19}$ and *hyd*$^{K7.19}$ clones (**Figure 5.15 A**). This may be because the RNAi-mediated knockdown of endogenous *sgg* could be more efficient than the over-expression of a *sgg* transgene. Alternatively, protein over-expression can also result in contradictory effects, due to a phenomenon called squelching (Natesan et al. 1997), which occurs when over-expressed proteins compete for a limiting pool of endogenous downstream targets/substrates, resulting in minimal change in downstream effects.

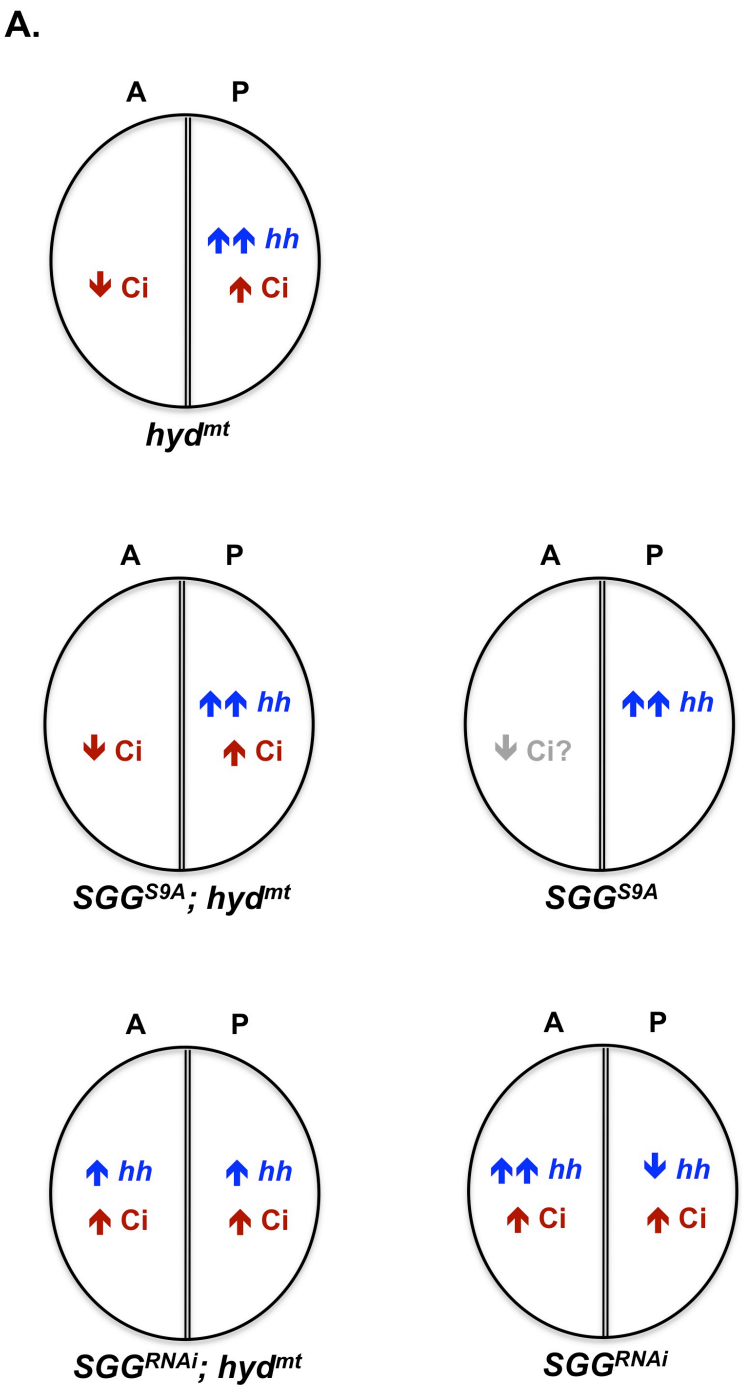
A.
A
P
hh
Ci
Ci
hyd^mt
A
P
hh
Ci
Ci
SGG^S9A; hyd^mt
A
P
hh
Ci?
SGG^S9A
A
P
hh
Ci
hh
Ci
SGG^RNAi; hyd^mt
A
P
hh
Ci
hh
Ci
SGG^RNAi

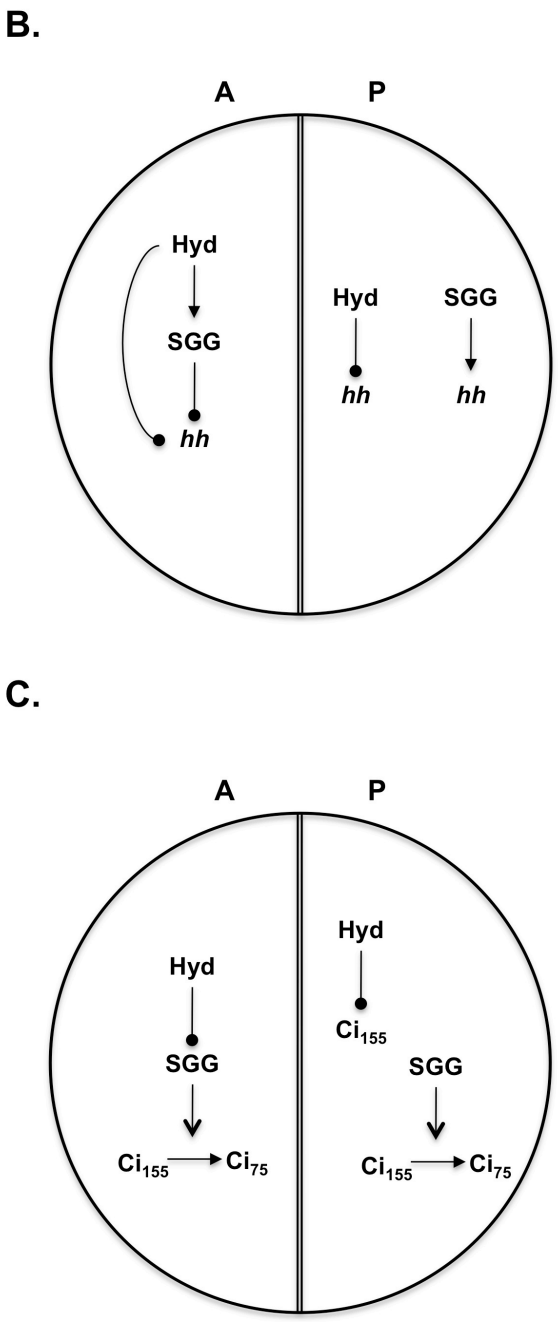

Figure 5.15: Summary of Ci^{155} and *hh* expression in EA discs containing $hyd^{K7.19}$, Sgg^{S9A}, and Sgg^{RNAi} clones. The morphogenetic furrow (MF) is marked by a double line. A = anterior, P = posterior. (**A**) Summary of ectopic autonomous *hh* and Ci_{155} expression in clones. (**B**) Model for the molecular mechanism of *hh* gene regulation in anterior and posterior regions of the eye disc. In anterior regions, Hyd negatively regulates *hh* expression by positively regulating Sgg, which in turn

down-regulates *hh* expression. In posterior regions, Hyd negatively regulates *hh* expression independently of affecting Sgg activity, whereas Sgg positively regulates *hh* expression independently of Hyd. (**C**) Model for the molecular mechanism of Ci_{155} regulation in anterior and posterior regions of the eye disc. In anterior regions, Hyd downregulates Ci_{155} levels by activating Sgg, resulting in increased processing of Ci_{155} to Ci_{75}. Conversely, in posterior regions, Hyd downregulates Ci_{155} levels independently of Sgg in a mechanism that is not dependent on processing of Ci_{155} to Ci_{75}.

Chapter 6: Discussion

6.1 Summary

Hyd is a putative E3 ubiquitin ligase and tumour suppressor protein that negatively regulates Hh signalling in the developing *Drosophila* eye. Hh signalling comprises both *hh* gene expression and the subsequent activation of the Hh pathway, and Hyd regulates both processes by independent, yet unknown, mechanisms (J. D. Lee et al. 2002). Mutations in Hh pathway components are linked to several human tumours (L. L. Rubin & de Sauvage 2006; Scales & de Sauvage 2009). However, recent findings suggest that over-expression of the SHH ligand by either the tumour epithelium or the surrounding stromal cells is much more prevalent in cancer (Fan et al. 2004; Yauch et al. 2008; Dierks et al. 2007; Hegde et al. 2008). As a result, Hyd and its highly conserved human homologue EDD, along with the putative regulatory pathways governing morphogen expression, represent potential targets for the design of novel cancer therapeutics. This is especially important since drugs correcting the cause of *SHH* expression in human tumours are not available. Numerous functional links to morphogen signalling, including the SHH and WNT pathways have been demonstrated for EDD (see **Chapter 1, Sections 1.4.2.3 and 1.4.2.5**), suggesting that Hyd's role in negatively regulating morphogen signalling is likely to be conserved in humans.

The aims of this project were to identify novel Hyd binding partners and/or ubiquitylated substrates that could be involved in putative molecular mechanisms regulating *hh* expression, or in the regulation of Hh pathway activity and possibly other morphogen signalling pathways. More specifically, this involved multiple objectives, including the use of mass spectrometry, bioinformatics and binding/ubiquitylation assays to identify new binding partners, followed by the further investigation of the functional relevance of the interacting proteins in morphogen signalling using a *Drosophila* eye *in vivo* model.

The results presented in this thesis support a significant role for Hyd in the regulation of both Hh and Wg signalling. Tandem affinity purification of exogenous Hyd from *Drosophila* S2 cells and subsequent mass spectrometric analysis of the complexed material revealed several putative novel binding partners, including Armadillo (*Hs* β-catenin), Ran and the SuFu interacting protein of unknown function, PERQ. Binding assays demonstrated that Hyd, unlike EDD, does not bind to the Hh pathway kinase Dyrk2, but may bind the close homologue Dyrk3 in *Drosophila*. In addition, binding assays also confirmed the interaction between Hyd and Armadillo, and showed that Hyd interacts with Shaggy (*Hs* GSK3β) and Ci (Hs GLI). This revealed that Hyd not only interacts with the kinase Shaggy, which is a major regulator in both the Hh and Wg pathways, but also interacts with the transcriptional effector proteins Ci and Armadillo, responsible for the activation of gene transcription in the Hh and Wg pathways, respectively. Although the results show that Shaggy and GSK3β are ubiquitylated, which has been reported previously for GSK3β (Q. Wu et al. 2009), they do not support a role for Hyd in mediating Shaggy ubiquitylation. Instead, my findings suggest that EDD inhibits GSK3β ubiquitylation. Taken together, these results place Hyd firmly in the regulation of Hh and Wg pathway activity at or below the level of Ci and Armadillo phosphorylation by GSK3β, providing a starting point for future investigation of the molecular mechanism underlying Hyd's function in the regulation of these pathways.

I subsequently employed a suitable *Drosophila in vivo* model designed to assess the functional significance of the interaction between Hyd and Shaggy, and its effects on *hh* expression and Hh pathway activity. This model utilized the MARCM technique to generate *hyd* mutant clones in the larval eye antennal imaginal disc, allowing me to assess the spatial expression of morphogens and morphogen pathway components during eye development, as well as the developmental effects on the adult eye and head tissue. The technique further allowed me to knockdown endogenous *sgg* or over-express an exogenous Shaggy protein in *hyd* mutant clones through the simultaneous use of different transgenes.

The generation of homozygous *hyd* mutant clones bearing the previously used $hyd^{K7.19}$ allele resulted in elevated *hh* and full-length Ci_{155} expression in posterior clones, non-autonomous disc tissue overgrowth, and scarring of adult eyes, all of which confirm previous reports of *hyd* mutations in eye disc clones (J. D. Lee et al. 2002). Conversely, I found that Ci_{155} levels were reduced in anterior *hyd* mutant clones, which directly contradicts previous findings where a different *hyd* mutant allele, $hyd^{K3.5}$, was used (J. D. Lee et al. 2002). In addition, *hyd* mutant clones resulted in mis-expression of Wg protein across the eye disc, as well as significantly increased head tissue in adults, an area known to be regulated by Wg signaling at the retinal boundary during eye disc development (Legent & Treisman 2008).

Interestingly, over-expression of exogenous Shaggy protein in *hyd* mutant clones rescued the adult phenotype, resulting in the elimination of eye scarring, reduced head size, as well as significantly reducing *hh* over-expression in posterior *hyd* mutant clones. Conversely, over-expression of Shaggy in anterior *hyd* mutant clones resulted in elevated *hh* expression, suggesting that Shaggy may be a novel regulator of *hh* expression with dual roles in both the positive and negative regulation of *hh* expression depending on the spatial location of eye disc cells.

My sequencing results showed that the $hyd^{K7.19}$ allele contains a pre-mature stop codon, which in theory would result in the expression of a severely truncated Hyd protein lacking all functional domains apart from the UBA domain. Furthermore, while a full-length Hyd transgene rescues the phenotype when expressed in *hyd* mutant clones, a catalytically inactive transgene fails to rescue the phenotype, suggesting that Hyd's E3 ligase activity is crucial for its function in regulating Hh signaling. These findings are in agreement with recent work, which showed that Hyd's E3 ligase activity is essential for its role in regulating Hh signalling (Wang et al. 2014).

Finally, I utilized a wing-disc derived *Drosophila* cell line (Cl8+) in conjunction with a ptc-luciferase reporter to demonstrate that knockdown of endogenous Hyd results in down-regulation of Hh pathway activity, suggesting that Hyd positively regulates Hh pathway activity in this setting.

6.1.1 Hyd function in regulating Hh signaling

My results support a role for Hyd in the regulation of both *hh* expression and Hh pathway activity. While some of my findings are in agreement with previously published data in the literature, others represent a novel contribution to the field and point to intriguing new mechanisms of action for Hyd in these processes. Although previous findings suggest that Hyd is a negative regulator of Hh pathway activity (J. D. Lee et al. 2002), my results suggest that Hyd can both positively and negatively regulate the Hh pathway by affecting full length Ci_{155} levels in the eye-antennal disc, and by positively regulating *ptc* gene expression levels in wing-disc derived *Drosophila* cultured cells. Hyd's dual role in Hh pathway regulation may be tissue- and/or cell type dependent, which may suggest that Hyd employs different effector proteins and mechanisms for different outcomes on Hh pathway activity. Interestingly, this notion is supported by recent work, which showed that Hyd can differentially regulate the transcriptional output of the Hh pathway in wing disc cells (Wang et al. 2014). Furthermore, the interactions between Hyd and Ci and Hyd (*Hs* EDD) and Shaggy (*Hs* GSK3β), which have previously been reported (Wang et al. 2014; Hay-Koren et al. 2011), further suggest that Hyd is involved in regulating Ci levels and or activity to regulate pathway activity. In the eye-antennal disc, *hyd* mutant clones anterior to the morphogenetic furrow exhibit reduced Ci_{155} levels in the region where Ci_{155} is mainly regulated by Slimb-mediated proteolytic processing to Ci_{75}. Interestingly, over-expression of Shaggy in these cells had no effect on Ci_{155} levels, whereas knockdown of endogenous Shaggy protein expression rescued Ci_{155}

levels. As Shaggy is known to promote the processing of Ci_{155} to Ci_{75} (J. Jia et al. 2002), Hyd may prevent Ci_{155} processing by inhibiting shaggy activity, or interfering with Slimb action and/or binding to Ci_{155}. However, knockdown of *hyd* in Cl8+ cells did not appear to affect Ci_{155} levels. Moreover, recent findings suggest that Hyd does not affect Ci_{155} stability, but rather that it acts as a transcriptional co-activator upon Ci_{155} binding to target promoters (Wang et al. 2014).

Further to this, the mass spectrometry results suggest that Hyd, via its interaction with PERQ, could indirectly interact with Sufu, a Ci_{155} negative regulator. Sufu antagonises the transcription of Hh target genes by both preventing the translocation of Ci_{155} (*Hs* Gli) into the nucleus (Kogerman et al. 1999; Ding et al. 1999; Wang et al. 2000; Méthot & Basler 2000), and by recruiting the SAP18-mSin3-histone deacetylase co-repressor complex to Hh target gene promoters (Cheng & Bishop 2002). Hyd and EDD contain nuclear localisation signals and, as a result, were found to localise mostly to the nucleus (Mansfield et al. 1994; Hay-Koren et al. 2011). One possible mechanism of action for Hyd in Hh pathway regulation could therefore be the regulation of the nuclear translocation of Ci_{155}. This would incidentally affect both Hh pathway activity and Ci_{155} levels, as nuclear Ci_{155} activates Hh target gene transcription, but is also subject to degradation by Rdx. For instance, Hyd could oppose the negative regulation of Ci by Sufu by competing for the Sufu binding site on Ci_{155}, and thus facilitating nuclear import. The putative Hyd binding partner Ran, as determined by mass spectrometry, may also be involved in this process, as it is essential for the transport of proteins through the nuclear pore complex (Izaurralde & Adam 1998). In this model of Hyd-mediated Ci_{155} nuclear import, Hyd would bind Ci_{155}, preventing an intraction with SuFu, whilst also recruiting Ran to Ci_{155} to initiate nuclear import. Alternatively, Hyd ubiquitylation of Ci_{155} could prevent binding by Sufu. Interestingly, recent insights into the mechanism of Ci_{155}/Gli nuclear translocation show that *Ds* Transportin (Trn) and *Hs* Importin β1 (Impβ1) positively regulate Ci_{155}/GLI nuclear import. Mechanistically, the two proteins may compete with Sufu for binding to the nuclear localisation sequence (NLS) at the amino-terminal of Ci_{155}/GLI (Shi et al. 2014; Szczepny et al. 2014). Therefore, future

work should address whether Hyd and EDD are involved in this process, and also whether this would involve Hyd-mediated ubiquitylation of Ci_{155}, Sufu, Ran, or Trn/Impβ1.

Finally, the results presented here suggest that Shaggy may have a positive role in promoting *hh* gene expression. From the *in vivo* experiments, the relationship between Hyd and Shaggy mediated regulation of *hh* gene expression, if any, as well as the molecular mechanism, are not clear and would require further investigation (see **Section 5.7** and **Section 6.1.2**).

6.1.2 Hyd function in regulating Wg signaling

Although the main focus of my work was to investigate the role of Hyd in Hh signalling, my results also suggest that Hyd negatively regulates Wg signalling in the developing *Drosophila* eye and head tissues. While the *in vivo* work demonstrated that Hyd negatively regulates Wg protein expression, the data from binding assays also suggest that Hyd engages in the Wg pathway by interacting with both Shaggy (*Hs* GSK3β) and Armadillo (*Hs* β-catenin). As discussed above in relation to Ci, Hyd may have a similar effect on the nuclear translocation of Armadillo. There have been conflicting reports of EDD's role in β-catenin nuclear translocation and WNT pathway regulation, suggesting that EDD can act both as a positive (Hay-Koren et al. 2011) and negative (Ohshima et al. 2007) regulator of these processes. The HECT E3 ubiquitin ligase Smurf2 ubiquitylates and degrades GSK3β, which leads to increased WNT signalling in mouse chondrocytes (Q. Wu et al. 2009). Since my results suggest that EDD antagonises the ubiquitylation of GSK3β, EDD could differentially regulate WNT signalling by (i) preventing the degradation of GSK3β, potentially by antagonizing Smurf-mediated ubiquitylation of GSK3β, and thus down-regulating β-catenin levels, and (ii) ubiquitylating and up-regulating β-catenin, as suggested previously (Hay-Koren et al. 2011).

6.2 Future Perspectives

As well as providing new insights into Hyd's function, the work presented in this thesis raises some interesting questions concerning its molecular mechanism in morphogen signalling. As a result, there are a number of experiments that immediately follow on from this work, some of which I have not been able to carry out in the time available.

6.2.1 How does Hyd regulate *hh* expression?

In order to investigate the molecular mechanism behind Hyd-mediated regulation of *hh* gene expression, and the potential involvement of Shaggy, I would use a more simplified approach to study this process in a cultured cell line model. This would eliminate the complexity of interactions between different cell types that may contribute to *hh* expression patterns in the eye disc. Unfortunately, according to data generated by the modENCODE Fly Transcriptome Project (Celniker et al. 2009), there are currently no *Drosophila* cell lines available that express *hh*. However, there are a number of human cancer cell lines, such as the breast cancer cell line MCF-7 (Cui et al. 2010), which over-express SHH. It would be interesting to analyse the SHH expression profile in these cells by quantitative real-time PCR (qRT-PCR) and Western blotting in the presence and absence of EDD. This would involve the knockdown of endogenous EDD, preferably using an RNAi construct that targets the 3'UTR region of the EDD mRNA to allow simultaneous expression of exogenous wild type or catalytic inactive (C>A) EDD. These experiments would address whether EDD is involved in regulating *shh* expression in human cells, and whether this process involves EDD's E3 ligase activity. Additionally, the potential role of GSK3β in regulating *Shh* expression could also be investigated in this setting using

RNAi, over-expression, or the use of lithium chloride, a specific GSK3β inhibitor (Klein & Melton 1996; Stambolic et al. 1996).

An alternative approach would be to use Chromatin Immunoprecipitation (ChIP) to investigate whether Hyd/EDD and Shaggy/GSK3β can bind to the enhancer regions and/or promoter region of the *hh* and *Shh* genes. For example, Hyd could bind DNA directly through its putative DNA-binding RCC domain, and both Hyd and Sgg could be localised to DNA and regulate the activity of transcription factors, epigenetic regulators and histones through ubiquitylation or phosphorylation, respectively. Briefly, ChIP involves the cross-linking of protein and any bound DNA/chromatin using formaldehyde, followed by shearing of the DNA/chromatin into ~500 bp fragments by sonication, and subsequent immunoprecipitation of specific proteins and sequencing of the associated DNA. This could be performed with EDD and GSK3β in the aforementioned MCF-7 breast cancer cell line, as well as with Hyd and Shaggy in eye-antennal imaginal discs, as specific antibodies are available for all of these proteins (see **Chapter 2**, Materials and Methods).

6.2.2 How does Hyd regulate Hh pathway activity?

Although the absence of *hh*-expressing *Drosophila* cell lines makes the study of the regulation of *hh* gene expression difficult, it is ideal for the purposes of studying Hyd's role in regulating Hh pathway activity, as it effectively uncouples the two processes. Both L3 wing disc derived Cl8+ cells and embryonic derived S2R+ cells are capable of transducing the Hh pathway when stimulated with exogenous Hh-N protein (Cherbas et al. 2011; Lum et al. 2003). They therefore represent a much better model to study the molecular mechanism by which Hyd regulates Hh pathway activity as they are much more likely to express the protein components involved in these putative regulatory pathways. **Table 6.1** summarises the specific Hh pathway components that could interact with Hyd to regulate Hh pathway activity, and their expression levels in the S2, S2R+ and Cl8+ cell lines.

Table 6.1: Expression of Hh signalling components in commonly used *Drosophila* cell lines.

Gene	Cell Line and Expression Level		
	S2	**S2R+**	**Cl8+**
Hh	Absent	Absent	Absent
Ci	Absent	Absent	Medium
Sgg	Medium	Medium	Medium
Sufu	Medium	Low	Low
Slmb	Medium	Medium	Medium
Rdx	Medium	Medium	Medium

The expression levels of Hh pathway components shown in **Table 6.1** suggest that Cl8+ cells are the best model system for studying Hh pathway activity. Therefore, I would use Cl8+ cells to perform the following experiments to address Hyd's function in regulating Hh pathway activity and Ci activity and/or location:

- Immunofluorescence with Cl8+ cells to investigate the effect of Hyd over-expression or knockdown on Ci location in the cell. The Ci antibody (rat Ci 2A1, Developmental Studies Hybridoma Bank) that I used in all experiments presented in this thesis recognises the carboxy terminal portion of full-length Ci, and so only recognises Ci_{155} and not Ci_{75}. Therefore, I would use this antibody in conjunction with another Ci antibody (dl-20) that recognises the amino terminal of Ci, and thus would recognise both Ci_{155} and Ci_{75} (available from Santa Cruz). Additionally, RNAi-mediated knockdown of other components known to affect Ci_{155} localisation, such as Sufu, can be incorporated into these experiments.

- *Drosophila* L3 eye antennal disc immunofluorescence staining of *hyd* mutant clones to determine the expression levels of more proteins using the following additional antibodies: Sgg, Sgg^{S9A}, Sufu, Ci amino-terminal antibody (dl-20), Rdx, Slmb and Dyrk3.

- Luciferase assays with Cl8+ cells to investigate the effects on Hh pathway activity of knocking down Shaggy, Sufu, Roadkill, Slimb, and Ci in combination with knockdown or over-expression of Hyd and/or different Hyd mutant proteins.

- Further binding and ubiquitylation assays to determine whether Hyd interacts with and ubiquitylates Sufu, Transportin, PERQ, Dyrk3, Ran, Roadkill and Slimb.

- Ubiquitylation assays to determine whether Hyd affects Ci ubiquitylation. This would involve ubiquitylation assays with Hyd and Ci in the presence and absence of Roadkill and Slimb.

- *In vitro* binding assays to determine whether the interactions between Hyd and Ci/Shaggy are binary.

- Repeating the TAP mass spectrometry experiment with either Cl8+ cells or eye discs expressing HSP-Hyd in order to target more Hyd interacting partners that are involved in Hh signalling.

6.2.3 How does Hyd regulate Wg signalling?

Finally, some of my data suggests that Hyd regulates Wg signalling, and this would also be an interesting project to pursue. I would use the above-mentioned methods for Hh signalling to investigate both Hyd-mediated regulation of *wg* expression and Wg pathway activity in Cl8+ cells and L3 eye-antennal discs. In addition, I would also use binding and ubiquitylation assays to further characterise the interaction between Hyd and Armadillo, as well as the role of Shaggy in mediating this interaction, and the resulting effect on Armadillo nuclear localisation. The TOPflash luciferase reporter for Wg pathway activity has previously been used successfully in Cl8+ cells (DasGupta et al. 2005), and altering the levels of Hyd by RNAi-mediated knockdown or over-expression would be a good starting point to investigate Hyd's role in Wg pathway regulation.

References

Aberle, H. et al., 1997. beta-catenin is a target for the ubiquitin-proteasome pathway. *The EMBO journal*, 16(13), pp.3797–3804.

Adams, M.D. & Sekelsky, J.J., 2002. From sequence to phenotype: reverse genetics in Drosophila melanogaster. *Nature reviews Genetics*, 3(3), pp.189–198.

Al-Hakim, A. et al., 2010. The ubiquitous role of ubiquitin in the DNA damage response. *DNA repair*, 9(12), pp.1229–1240.

Albrecht, M. & Lengauer, T., 2004. Survey on the PABC recognition motif PAM2. *Biochemical and biophysical research communications*, 316(1), pp.129–138.

Alt, J.R. et al., 2000. Phosphorylation-dependent regulation of cyclin D1 nuclear export and cyclin D1-dependent cellular transformation. *Genes & development*, 14(24), pp.3102–3114.

Bailey, J.M. et al., 2008. Sonic hedgehog promotes desmoplasia in pancreatic cancer. *Clinical cancer research : an official journal of the American Association for Cancer Research*, 14(19), pp.5995–6004.

Baker, N.E., Bhattacharya, A. & Firth, L.C., 2009. Regulation of Hh signal transduction as Drosophila eye differentiation progresses. *Developmental biology*, 335(2), pp.356–366.

Baonza, A. & Freeman, M., 2002. Control of Drosophila eye specification by Wingless signalling. *Development (Cambridge, England)*, 129(23), pp.5313–5322.

Beachy, P.A., Karhadkar, S.S. & Berman, D.M., 2004. Tissue repair and stem cell renewal in carcinogenesis. *Nature*, 432(7015), pp.324–331.

Behrens, J. et al., 1996. Functional interaction of beta-catenin with the transcription factor LEF-1. *Nature*, 382(6592), pp.638–642.

Bejarano, F. et al., 2007. Hedgehog restricts its expression domain in the Drosophila wing. *EMBO reports*, 8(8), pp.778–783.

Berman, D.M. et al., 2003. Widespread requirement for Hedgehog ligand stimulation in growth of digestive tract tumours. *Nature*, 425(6960), pp.846–851.

Bethard, J.R. et al., 2011. Identification of phosphorylation sites on the E3 ubiquitin ligase UBR5/EDD. *Journal of proteomics*.

Bhanot, P. et al., 1996. A new member of the frizzled family from Drosophila

functions as a Wingless receptor. *Nature*, 382(6588), pp.225–230.

Bhatia, N. et al., 2006. Gli2 is targeted for ubiquitination and degradation by beta-TrCP ubiquitin ligase. *The Journal of biological chemistry*, 281(28), pp.19320–19326.

Bienko, M. et al., 2010. Regulation of translesion synthesis DNA polymerase eta by monoubiquitination. *Molecular cell*, 37(3), pp.396–407.

Bigelow, R.L.H. et al., 2004. Transcriptional regulation of bcl-2 mediated by the sonic hedgehog signaling pathway through gli-1. *The Journal of biological chemistry*, 279(2), pp.1197–1205.

Bischoff, F.R. & Ponstingl, H., 1991. Catalysis of guanine nucleotide exchange on Ran by the mitotic regulator RCC1. *Nature*, 354(6348), pp.80–82.

Bourouis, M., 2002. Targeted increase in shaggy activity levels blocks wingless signaling. *Genesis (New York, N.Y. : 2000)*, 34(1-2), pp.99–102.

Boyd, S.D., Tsai, K.Y. & Jacks, T., 2000. An intact HDM2 RING-finger domain is required for nuclear exclusion of p53. *Nature cell biology*, 2(9), pp.563–568.

Briscoe, J. & Thérond, P.P., 2013. The mechanisms of Hedgehog signalling and its roles in development and disease. *Nature reviews Molecular cell biology*, 14(7), pp.416–429.

Bryden, M.M., Evans, H.E. & Keeler, R.F., 1971. Cyclopia in sheep caused by plant teratogens. *Journal of anatomy*, 110(Pt 3), p.507.

Byrd, N. et al., 2002. Hedgehog is required for murine yolk sac angiogenesis. *Development (Cambridge, England)*, 129(2), pp.361–372.

Callaghan, M.J. et al., 1998. Identification of a human HECT family protein with homology to the Drosophila tumor suppressor gene hyperplastic discs. *Oncogene*, 17(26), pp.3479–3491.

Camp, D. et al., 2010. Ihog and Boi are essential for Hedgehog signaling in Drosophila. *Neural development*, 5, p.28.

Cavallo, R.A. et al., 1998. Drosophila Tcf and Groucho interact to repress Wingless signalling activity. *Nature*, 395(6702), pp.604–608.

Celniker, S.E. et al., 2009. Unlocking the secrets of the genome. *Nature*, 459(7249), pp.927–930.

Chamoun, Z. et al., 2001. Skinny hedgehog, an acyltransferase required for palmitoylation and activity of the hedgehog signal. *Science (New York, N.Y.)*, 293(5537), pp.2080–2084.

Chanas, G. & Maschat, F., 2005. Tissue specificity of hedgehog repression by the Polycomb group during Drosophila melanogaster development. *Mechanisms of development*, 122(9), pp.975–987.

Chao, J.-L. et al., 2004. Localized Notch signal acts through eyg and upd to promote global growth in Drosophila eye. *Development (Cambridge, England)*, 131(16), pp.3839–3847.

Chau, V. et al., 1989. A multiubiquitin chain is confined to specific lysine in a targeted short-lived protein. *Science (New York, N.Y.)*, 243(4898), pp.1576–1583.

Chen, C.H. et al., 1999. Nuclear trafficking of Cubitus interruptus in the transcriptional regulation of Hedgehog target gene expression. *Cell*, 98(3), pp.305–316.

Chen, J.K., Taipale, J., Cooper, M.K., et al., 2002a. Inhibition of Hedgehog signaling by direct binding of cyclopamine to Smoothened. *Genes & development*, 16(21), pp.2743–2748.

Chen, J.K., Taipale, J., Young, K.E., et al., 2002b. Small molecule modulation of Smoothened activity. *Proceedings of the National Academy of Sciences of the United States of America*, 99(22), pp.14071–14076.

Chen, M.-H. et al., 2004. Palmitoylation is required for the production of a soluble multimeric Hedgehog protein complex and long-range signaling in vertebrates. *Genes & development*, 18(6), pp.641–659.

Chen, W. et al., 2003. Dishevelled 2 recruits beta-arrestin 2 to mediate Wnt5A-stimulated endocytosis of Frizzled 4. *Science (New York, N.Y.)*, 301(5638), pp.1391–1394.

Chen, X. et al., 2011. Processing and turnover of the Hedgehog protein in the endoplasmic reticulum. *The Journal of cell biology*, 192(5), pp.825–838.

Chen, Y. et al., 2010. G protein-coupled receptor kinase 2 promotes high-level Hedgehog signaling by regulating the active state of Smo through kinase-dependent and kinase-independent mechanisms in Drosophila. *Genes & development*, 24(18), pp.2054–2067.

Chen, Z.J. & Sun, L.J., 2009. Nonproteolytic functions of ubiquitin in cell signaling. *Molecular cell*, 33(3), pp.275–286.

Cheng, S.Y. & Bishop, J.M., 2002. Suppressor of Fused represses Gli-mediated transcription by recruiting the SAP18-mSin3 corepressor complex. *Proceedings of the National Academy of Sciences of the United States of America*, 99(8), pp.5442–5447.

Cherbas, L. et al., 2011. The transcriptional diversity of 25 Drosophila cell lines.

Genome research, 21(2), pp.301–314.

Cho, K.O. et al., 2000. Novel signaling from the peripodial membrane is essential for eye disc patterning in Drosophila. *Cell*, 103(2), pp.331–342.

Clancy, J.L. et al., 2003. EDD, the human orthologue of the hyperplastic discs tumour suppressor gene, is amplified and overexpressed in cancer. *Oncogene*, 22(32), pp.5070–5081.

Clevers, H. & Nusse, R., 2012. Wnt/β-catenin signaling and disease. *Cell*, 149(6), pp.1192–1205.

Cohen, P. & Frame, S., 2001. The renaissance of GSK3. *Nature reviews Molecular cell biology*, 2(10), pp.769–776.

Cojocaru, M. et al., 2011. Transcription factor IIS cooperates with the E3 ligase UBR5 to ubiquitinate the CDK9 subunit of the positive transcription elongation factor B. *The Journal of biological chemistry*, 286(7), pp.5012–5022.

Cooper, M.K. et al., 1998. Teratogen-mediated inhibition of target tissue response to Shh signaling. *Science (New York, N.Y.)*, 280(5369), pp.1603–1607.

Cope, G.A. & Deshaies, R.J., 2003. COP9 signalosome: a multifunctional regulator of SCF and other cullin-based ubiquitin ligases. *Cell*, 114(6), pp.663–671.

Craig, A.W. et al., 1998. Interaction of polyadenylate-binding protein with the eIF4G homologue PAIP enhances translation. *Nature*, 392(6675), pp.520–523.

Cross, D.A. et al., 1995. Inhibition of glycogen synthase kinase-3 by insulin mediated by protein kinase B. *Nature*, 378(6559), pp.785–789.

Cui, W. et al., 2010. Expression and regulation mechanisms of Sonic Hedgehog in breast cancer. *Cancer science*, 101(4), pp.927–933.

Currie, D.A., Milner, M.J. & Evans, C.W., 1988. The growth and differentiation in vitro of leg and wing imaginal disc cells from Drosophila melanogaster. *Development (Cambridge, England)*, (102), pp.805–814.

Dann, C.E. et al., 2001. Insights into Wnt binding and signalling from the structures of two Frizzled cysteine-rich domains. *Nature*, 412(6842), pp.86–90.

DasGupta, R. et al., 2005. Functional genomic analysis of the Wnt-wingless signaling pathway. *Science (New York, N.Y.)*, 308(5723), pp.826–833.

De Angioletti, M. et al., 2004. Beta+45 G --> C: a novel silent beta-thalassaemia mutation, the first in the Kozak sequence. *British journal of haematology*, 124(2), pp.224–231.

de Celis, J.F. & Ruiz-Gómez, M., 1995. groucho and hedgehog regulate engrailed

expression in the anterior compartment of the Drosophila wing. *Development (Cambridge, England)*, 121(10), pp.3467–3476.

Denef, N. et al., 2000. Hedgehog induces opposite changes in turnover and subcellular localization of patched and smoothened. *Cell*, 102(4), pp.521–531.

Deo, R.C., Sonenberg, N. & Burley, S.K., 2001. X-ray structure of the human hyperplastic discs protein: an ortholog of the C-terminal domain of poly(A)-binding protein. *Proceedings of the National Academy of Sciences of the United States of America*, 98(8), pp.4414–4419.

Deshaies, R.J. & Joazeiro, C.A.P., 2009. RING domain E3 ubiquitin ligases. *Annual review of biochemistry*, 78, pp.399–434.

Diehl, J.A. et al., 1998. Glycogen synthase kinase-3beta regulates cyclin D1 proteolysis and subcellular localization. *Genes & development*, 12(22), pp.3499–3511.

Dierks, C. et al., 2007. Essential role of stromally induced hedgehog signaling in B-cell malignancies. *Nature medicine*, 13(8), pp.944–951.

Dikic, I., Wakatsuki, S. & Walters, K.J., 2009. Ubiquitin-binding domains - from structures to functions. *Nature reviews Molecular cell biology*, 10(10), pp.659–671.

Ding, Q. et al., 1999. Mouse suppressor of fused is a negative regulator of sonic hedgehog signaling and alters the subcellular distribution of Gli1. *Current biology : CB*, 9(19), pp.1119–1122.

Dingwall, C. & Laskey, R.A., 1991. Nuclear targeting sequences--a consensus? *Trends in biochemical sciences*, 16(12), pp.478–481.

Ditzel, M. et al., 2008. Inactivation of effector caspases through nondegradative polyubiquitylation. *Molecular cell*, 32(4), pp.540–553.

Dominguez, M. et al., 2004. Growth and specification of the eye are controlled independently by Eyegone and Eyeless in Drosophila melanogaster. *Nature genetics*, 36(1), pp.31–39.

Domínguez, M. & de Celis, J.F., 1998. A dorsal/ventral boundary established by Notch controls growth and polarity in the Drosophila eye. *Nature*, 396(6708), pp.276–278.

Domínguez, M. et al., 1996. Sending and receiving the hedgehog signal: control by the Drosophila Gli protein Cubitus interruptus. *Science (New York, N.Y.)*, 272(5268), pp.1621–1625.

Duman-Scheel, M. et al., 2002. Hedgehog regulates cell growth and proliferation by inducing Cyclin D and Cyclin E. *Nature*, 417(6886), pp.299–304.

Dupont, S. et al., 2009. FAM/USP9x, a deubiquitinating enzyme essential for TGFbeta signaling, controls Smad4 monoubiquitination. *Cell*, 136(1), pp.123–135.

Eaton, S. & Kornberg, T.B., 1990. Repression of ci-D in posterior compartments of Drosophila by engrailed. *Genes & development*, 4(6), pp.1068–1077.

Eblen, S.T. et al., 2003. Identification of novel ERK2 substrates through use of an engineered kinase and ATP analogs. *The Journal of biological chemistry*, 278(17), pp.14926–14935.

Ekas, L.A. et al., 2006. JAK/STAT signaling promotes regional specification by negatively regulating wingless expression in Drosophila. *Development (Cambridge, England)*, 133(23), pp.4721–4729.

Ericson, J. et al., 1996. Two critical periods of Sonic Hedgehog signaling required for the specification of motor neuron identity. *Cell*, 87(4), pp.661–673.

Escudero, L.M. & Freeman, M., 2007. Mechanism of G1 arrest in the Drosophila eye imaginal disc. *BMC developmental biology*, 7, p.13.

Fan, L. et al., 2004. Hedgehog signaling promotes prostate xenograft tumor growth. *Endocrinology*, 145(8), pp.3961–3970.

Farzan, S.F. et al., 2008. Costal2 functions as a kinesin-like protein in the hedgehog signal transduction pathway. *Current biology : CB*, 18(16), pp.1215–1220.

Feldmann, G. et al., 2007. Blockade of hedgehog signaling inhibits pancreatic cancer invasion and metastases: a new paradigm for combination therapy in solid cancers. *Cancer research*, 67(5), pp.2187–2196.

Finley, D., 2009. Recognition and processing of ubiquitin-protein conjugates by the proteasome. *Annual review of biochemistry*, 78, pp.477–513.

Fiol, C.J. et al., 1987. Formation of protein kinase recognition sites by covalent modification of the substrate. Molecular mechanism for the synergistic action of casein kinase II and glycogen synthase kinase 3. *The Journal of biological chemistry*, 262(29), pp.14042–14048.

Firth, L.C. & Baker, N.E., 2005. Extracellular signals responsible for spatially regulated proliferation in the differentiating Drosophila eye. *Developmental cell*, 8(4), pp.541–551.

Fischer, J.A. et al., 1988. GAL4 activates transcription in Drosophila. *Nature*, 332(6167), pp.853–856.

Forbes, A.J. et al., 1993. Genetic analysis of hedgehog signalling in the Drosophila embryo. *Development (Cambridge, England). Supplement*, pp.115–124.

Frame, S., Cohen, P. & Biondi, R.M., 2001. A common phosphate binding site explains the unique substrate specificity of GSK3 and its inactivation by phosphorylation. *Molecular cell*, 7(6), pp.1321–1327.

Franch-Marro, X. et al., 2008. In vivo role of lipid adducts on Wingless. *Journal of cell science*, 121(Pt 10), pp.1587–1592.

Francis, N.J. & Kingston, R.E., 2001. Mechanisms of transcriptional memory. *Nature reviews Molecular cell biology*, 2(6), pp.409–421.

Frank-Kamenetsky, M. et al., 2002. Small-molecule modulators of Hedgehog signaling: identification and characterization of Smoothened agonists and antagonists. *Journal of biology*, 1(2), p.10.

Freeman, M., 1994. The spitz gene is required for photoreceptor determination in the Drosophila eye where it interacts with the EGF receptor. *Mechanisms of development*, 48(1), pp.25–33.

Friedman, A.A. et al., 2011. Proteomic and functional genomic landscape of receptor tyrosine kinase and ras to extracellular signal-regulated kinase signaling. *Science signaling*, 4(196), p.rs10.

Fukumoto, T. et al., 2001. The fused protein kinase regulates Hedgehog-stimulated transcriptional activation in Drosophila Schneider 2 cells. *The Journal of biological chemistry*, 276(42), pp.38441–38448.

Gailani, M.R. et al., 1996. The role of the human homologue of Drosophila patched in sporadic basal cell carcinomas. *Nature genetics*, 14(1), pp.78–81.

Gallet, A. et al., 2003. Cholesterol modification of hedgehog is required for trafficking and movement, revealing an asymmetric cellular response to hedgehog. *Developmental cell*, 4(2), pp.191–204.

Garcia-Bellido, A. & Merriam, J.R., 1969. Cell lineage of the imaginal discs in Drosophila gynandromorphs. *The Journal of experimental zoology*, 170(1), pp.61–75.

Geyer, R.K., Yu, Z.K. & Maki, C.G., 2000. The MDM2 RING-finger domain is required to promote p53 nuclear export. *Nature cell biology*, 2(9), pp.569–573.

Gill, G., 2004. SUMO and ubiquitin in the nucleus: different functions, similar mechanisms? *Genes & development*, 18(17), pp.2046–2059.

Gingras, A.-C. et al., 2007. Analysis of protein complexes using mass spectrometry. *Nature reviews Molecular cell biology*, 8(8), pp.645–654.

Glickman, M.H. & Ciechanover, A., 2002. The ubiquitin-proteasome proteolytic pathway: destruction for the sake of construction. *Physiological reviews*, 82(2), pp.373–428.

Guruharsha, K.G. et al., 2011. A Protein Complex Network of Drosophila melanogaster. *Cell*, 147(3), pp.690–703.

Hahn, H. et al., 1996. Mutations of the human homolog of Drosophila patched in the nevoid basal cell carcinoma syndrome. *Cell*, 85(6), pp.841–851.

Halder, G. et al., 1998. Eyeless initiates the expression of both sine oculis and eyes absent during Drosophila compound eye development. *Development (Cambridge, England)*, 125(12), pp.2181–2191.

Harrison, D.A. et al., 1998. Drosophila unpaired encodes a secreted protein that activates the JAK signaling pathway. *Genes & development*, 12(20), pp.3252–3263.

Hay-Koren, A. et al., 2011. The EDD E3 ubiquitin ligase ubiquitinates and up-regulates beta-catenin. *Molecular biology of the cell*, 22(3), pp.399–411.

He, J. et al., 2006. Suppressing Wnt signaling by the hedgehog pathway through sFRP-1. *The Journal of biological chemistry*, 281(47), pp.35598–35602.

He, X. et al., 2004. LDL receptor-related proteins 5 and 6 in Wnt/beta-catenin signaling: arrows point the way. *Development (Cambridge, England)*, 131(8), pp.1663–1677.

Heberlein, U., Wolff, T. & Rubin, G.M., 1993. The TGF beta homolog dpp and the segment polarity gene hedgehog are required for propagation of a morphogenetic wave in the Drosophila retina. *Cell*, 75(5), pp.913–926.

Hegde, G.V. et al., 2008. Hedgehog-induced survival of B-cell chronic lymphocytic leukemia cells in a stromal cell microenvironment: a potential new therapeutic target. *Molecular cancer research : MCR*, 6(12), pp.1928–1936.

Held, L.I., 2005. *Imaginal Discs*, Cambridge University Press.

Henderson, M.J. et al., 2006. EDD mediates DNA damage-induced activation of CHK2. *The Journal of biological chemistry*, 281(52), pp.39990–40000.

Henderson, M.J. et al., 2002. EDD, the human hyperplastic discs protein, has a role in progesterone receptor coactivation and potential involvement in DNA damage response. *The Journal of biological chemistry*, 277(29), pp.26468–26478.

Heslip, T.R. et al., 1997. Shaggy and dishevelled exert opposite effects on Wingless and Decapentaplegic expression and on positional identity in imaginal discs. *Development (Cambridge, England)*, 124(5), pp.1069–1078.

Hoege, C. et al., 2002. RAD6-dependent DNA repair is linked to modification of PCNA by ubiquitin and SUMO. *Nature*, 419(6903), pp.135–141.

Hofmann, K. & Bucher, P., 1996. The UBA domain: a sequence motif present in

multiple enzyme classes of the ubiquitination pathway. *Trends in biochemical sciences*, 21(5), pp.172–173.

Honda, Y. et al., 2002. Cooperation of HECT-domain ubiquitin ligase hHYD and DNA topoisomerase II-binding protein for DNA damage response. *The Journal of biological chemistry*, 277(5), pp.3599–3605.

Hooper, J.E. & Scott, M.P., 1989. The Drosophila patched gene encodes a putative membrane protein required for segmental patterning. *Cell*, 59(4), pp.751–765.

Hori, T. et al., 1999. Covalent modification of all members of human cullin family proteins by NEDD8. *Oncogene*, 18(48), pp.6829–6834.

Hoshino, S. et al., 1999. The eukaryotic polypeptide chain releasing factor (eRF3/GSPT) carrying the translation termination signal to the 3'-Poly(A) tail of mRNA. Direct association of erf3/GSPT with polyadenylate-binding protein. *The Journal of biological chemistry*, 274(24), pp.16677–16680.

Huang, L. et al., 1999. Structure of an E6AP-UbcH7 complex: insights into ubiquitination by the E2-E3 enzyme cascade. *Science (New York, N.Y.)*, 286(5443), pp.1321–1326.

Hughes, K. et al., 1992. Identification of multifunctional ATP-citrate lyase kinase as the alpha-isoform of glycogen synthase kinase-3. *The Biochemical journal*, 288 (Pt 1), pp.309–314.

Hughes, K. et al., 1993. Modulation of the glycogen synthase kinase-3 family by tyrosine phosphorylation. *The EMBO journal*, 12(2), pp.803–808.

Hui, C.-C. & Angers, S., 2011. Gli proteins in development and disease. *Annual review of cell and developmental biology*, 27, pp.513–537.

Huibregtse, J.M. et al., 1995. A family of proteins structurally and functionally related to the E6-AP ubiquitin-protein ligase. *Proceedings of the National Academy of Sciences of the United States of America*, 92(7), pp.2563–2567.

Huibregtse, J.M., Scheffner, M. & Howley, P.M., 1993. Cloning and expression of the cDNA for E6-AP, a protein that mediates the interaction of the human papillomavirus E6 oncoprotein with p53. *Molecular and cellular biology*, 13(2), pp.775–784.

Ikeda, F. & Dikic, I., 2008. Atypical ubiquitin chains: new molecular signals. “Protein Modifications: Beyond the Usual Suspects” review series. *EMBO reports*, 9(6), pp.536–542.

Ikeda, S. et al., 1998. Axin, a negative regulator of the Wnt signaling pathway, forms a complex with GSK-3beta and beta-catenin and promotes GSK-3beta-dependent phosphorylation of beta-catenin. *The EMBO journal*, 17(5), pp.1371–1384.

Ingham, P.W. & McMahon, A.P., 2001. Hedgehog signaling in animal development: paradigms and principles. *Genes & development*, 15(23), pp.3059–3087.

Iwaki, T. & Castellino, F.J., 2008. A single plasmid transfection that offers a significant advantage associated with puromycin selection in Drosophila Schneider S2 cells expressing heterologous proteins. *Cytotechnology*, 57(1), pp.45–49.

Izaurralde, E. & Adam, S., 1998. Transport of macromolecules between the nucleus and the cytoplasm. *RNA (New York, N.Y.)*, 4(4), pp.351–364.

Jackson, P.K. et al., 2000. The lore of the RINGs: substrate recognition and catalysis by ubiquitin ligases. *Trends in cell biology*, 10(10), pp.429–439.

Janda, C.Y. et al., 2012. Structural basis of Wnt recognition by Frizzled. *Science (New York, N.Y.)*, 337(6090), pp.59–64.

Jarman, A.P. et al., 1994. Atonal is the proneural gene for Drosophila photoreceptors. *Nature*, 369(6479), pp.398–400.

Jarman, A.P. et al., 1995. Role of the proneural gene, atonal, in formation of Drosophila chordotonal organs and photoreceptors. *Development (Cambridge, England)*, 121(7), pp.2019–2030.

Jia, H. et al., 2010. Casein kinase 2 promotes Hedgehog signaling by regulating both smoothened and Cubitus interruptus. *The Journal of biological chemistry*, 285(48), pp.37218–37226.

Jia, H. et al., 2009. PP4 and PP2A regulate Hedgehog signaling by controlling Smo and Ci phosphorylation. *Development (Cambridge, England)*, 136(2), pp.307–316.

Jia, J. et al., 2004. Hedgehog signalling activity of Smoothened requires phosphorylation by protein kinase A and casein kinase I. *Nature*, 432(7020), pp.1045–1050.

Jia, J. et al., 2005. Phosphorylation by double-time/CKIepsilon and CKIalpha targets cubitus interruptus for Slimb/beta-TRCP-mediated proteolytic processing. *Developmental cell*, 9(6), pp.819–830.

Jia, J. et al., 2002. Shaggy/GSK3 antagonizes Hedgehog signalling by regulating Cubitus interruptus. *Nature*, 416(6880), pp.548–552.

Jiang, J., 2002. Degrading Ci: who is Cul-pable? *Genes & development*, 16(18), pp.2315–2321.

Jiang, J., 2006. Regulation of Hh/Gli signaling by dual ubiquitin pathways. *Cell cycle (Georgetown, Tex)*, 5(21), pp.2457–2463.

Jiang, J. & Struhl, G., 1998. Regulation of the Hedgehog and Wingless signalling pathways by the F-box/WD40-repeat protein Slimb. *Nature*, 391(6666), pp.493–496.

Jiang, W. et al., 2011. Acetylation Regulates Gluconeogenesis by Promoting PEPCK1 Degradation via Recruiting the UBR5 Ubiquitin Ligase. *Molecular cell*, 43(1), pp.33–44.

Jin, L. et al., 2008. Mechanism of ubiquitin-chain formation by the human anaphase-promoting complex. *Cell*, 133(4), pp.653–665.

Joazeiro, C.A. & Weissman, A.M., 2000. RING finger proteins: mediators of ubiquitin ligase activity. *Cell*, 102(5), pp.549–552.

Johnson, E.S. et al., 1995. A proteolytic pathway that recognizes ubiquitin as a degradation signal. *The Journal of biological chemistry*, 270(29), pp.17442–17456.

Johnson, R.L. et al., 1996. Human homolog of patched, a candidate gene for the basal cell nevus syndrome. *Science (New York, N.Y.)*, 272(5268), pp.1668–1671.

Kaiser, S.E. et al., 2011. Protein standard absolute quantification (PSAQ) method for the measurement of cellular ubiquitin pools. *Nature methods*, 8(8), pp.691–696.

Kalderon, D., 2004. Hedgehog signaling: Costal-2 bridges the transduction gap. *Current biology : CB*, 14(2), pp.R67–9.

Kamura, T. et al., 2000. Activation of HIF1alpha ubiquitination by a reconstituted von Hippel-Lindau (VHL) tumor suppressor complex. *Proceedings of the National Academy of Sciences of the United States of America*, 97(19), pp.10430–10435.

Karhadkar, S.S. et al., 2004. Hedgehog signalling in prostate regeneration, neoplasia and metastasis. *Nature*, 431(7009), pp.707–712.

Kehoe, J.W. & Kay, B.K., 2005. Filamentous phage display in the new millennium. *Chemical reviews*, 105(11), pp.4056–4072.

Kent, D., Bush, E.W. & Hooper, J.E., 2006. Roadkill attenuates Hedgehog responses through degradation of Cubitus interruptus. *Development (Cambridge, England)*, 133(10), pp.2001–2010.

Kenyon, K.L. et al., 2003. Coordinating proliferation and tissue specification to promote regional identity in the Drosophila head. *Developmental cell*, 5(3), pp.403–414.

Kerscher, O., Felberbaum, R. & Hochstrasser, M., 2006. Modification of proteins by ubiquitin and ubiquitin-like proteins. *Annual review of cell and developmental biology*, 22, pp.159–180.

Khaleghpour, K. et al., 2001. Dual interactions of the translational repressor Paip2 with poly(A) binding protein. *Molecular and cellular biology*, 21(15), pp.5200–5213.

Kim, W. et al., 2011. Systematic and quantitative assessment of the ubiquitin-modified proteome. *Molecular cell*, 44(2), pp.325–340.

Kinstrie, R. et al., 2006. dDYRK2 and Minibrain interact with the chromatin remodelling factors SNR1 and TRX. *The Biochemical journal*, 398(1), pp.45–54.

Kinzler, K.W. & Vogelstein, B., 1996. Lessons from hereditary colorectal cancer. *Cell*, 87(2), pp.159–170.

Kinzler, K.W. et al., 1991. Identification of FAP locus genes from chromosome 5q21. *Science (New York, N.Y.)*, 253(5020), pp.661–665.

Kitagawa, M. et al., 1999. An F-box protein, FWD1, mediates ubiquitin-dependent proteolysis of beta-catenin. *The EMBO journal*, 18(9), pp.2401–2410.

Klein, P.S. & Melton, D.A., 1996. A molecular mechanism for the effect of lithium on development. *Proceedings of the National Academy of Sciences of the United States of America*, 93(16), pp.8455–8459.

Kogerman, P. et al., 1999. Mammalian suppressor-of-fused modulates nuclear-cytoplasmic shuttling of Gli-1. *Nature cell biology*, 1(5), pp.312–319.

Komander, D. & Rape, M., 2012. The ubiquitin code. *Annual review of biochemistry*, 81, pp.203–229.

Komander, D., Clague, M.J. & Urbé, S., 2009. Breaking the chains: structure and function of the deubiquitinases. *Nature reviews Molecular cell biology*, 10(8), pp.550–563.

Korinek, V. et al., 1997. Constitutive transcriptional activation by a beta-catenin-Tcf complex in APC-/- colon carcinoma. *Science (New York, N.Y.)*, 275(5307), pp.1784–1787.

Kozlov, G. et al., 2004. Structural basis of ligand recognition by PABC, a highly specific peptide-binding domain found in poly(A)-binding protein and a HECT ubiquitin ligase. *The EMBO journal*, 23(2), pp.272–281.

Kozlov, G. et al., 2007. Structural basis of ubiquitin recognition by the ubiquitin-associated (UBA) domain of the ubiquitin ligase EDD. *The Journal of biological chemistry*, 282(49), pp.35787–35795.

Kozlov, G. et al., 2001. Structure and function of the C-terminal PABC domain of human poly(A)-binding protein. *Proceedings of the National Academy of Sciences of the United States of America*, 98(8), pp.4409–4413.

Kramps, T. et al., 2002. Wnt/wingless signaling requires BCL9/legless-mediated recruitment of pygopus to the nuclear beta-catenin-TCF complex. *Cell*, 109(1), pp.47–60.

Kumar, J.P. & Moses, K., 2001a. EGF receptor and Notch signaling act upstream of Eyeless/Pax6 to control eye specification. *Cell*, 104(5), pp.687–697.

Kumar, J.P. & Moses, K., 2001b. The EGF receptor and notch signaling pathways control the initiation of the morphogenetic furrow during Drosophila eye development. *Development (Cambridge, England)*, 128(14), pp.2689–2697.

Kurayoshi, M. et al., 2007. Post-translational palmitoylation and glycosylation of Wnt-5a are necessary for its signalling. *The Biochemical journal*, 402(3), pp.515–523.

Lau, A.W., Fukushima, H. & Wei, W., 2012. The Fbw7 and betaTRCP E3 ubiquitin ligases and their roles in tumorigenesis. *Frontiers in bioscience (Landmark edition)*, 17, pp.2197–2212.

Lee, J.D. & Treisman, J.E., 2001. The role of Wingless signaling in establishing the anteroposterior and dorsoventral axes of the eye disc. *Development (Cambridge, England)*, 128(9), pp.1519–1529.

Lee, J.D. et al., 2002. The ubiquitin ligase Hyperplastic discs negatively regulates hedgehog and decapentaplegic expression by independent mechanisms. *Development (Cambridge, England)*, 129(24), pp.5697–5706.

Lee, J.J. et al., 1992. Secretion and localized transcription suggest a role in positional signaling for products of the segmentation gene hedgehog. *Cell*, 71(1), pp.33–50.

Lee, T. & Luo, L., 2001. Mosaic analysis with a repressible cell marker (MARCM) for Drosophila neural development. *Trends in neurosciences*, 24(5), pp.251–254.

Legent, K. & Treisman, J.E., 2008. Wingless signaling in Drosophila eye development. *Methods in molecular biology (Clifton, NJ)*, 469, pp.141–161.

Lewis, P.W. et al., 2004. Identification of a Drosophila Myb-E2F2/RBF transcriptional repressor complex. *Genes & development*, 18(23), pp.2929–2940.

Li, L. et al., 1999. Axin and Frat1 interact with dvl and GSK, bridging Dvl to GSK in Wnt-mediated regulation of LEF-1. *The EMBO journal*, 18(15), pp.4233–4240.

Li, M. et al., 2003. Mono- versus polyubiquitination: differential control of p53 fate by Mdm2. *Science (New York, N.Y.)*, 302(5652), pp.1972–1975.

Li, S. et al., 2012. Hedgehog-regulated ubiquitination controls smoothened trafficking and cell surface expression in Drosophila. *PLoS biology*, 10(1), p.e1001239.

Lim, N.S. et al., 2006. Comparative peptide binding studies of the PABC domains from the ubiquitin-protein isopeptide ligase HYD and poly(A)-binding protein. Implications for HYD function. *The Journal of biological chemistry*, 281(20), pp.14376–14382.

Ling, S. & Lin, W.-C., 2011. EDD inhibits ATM-mediated phosphorylation of P53. *The Journal of biological chemistry*.

Lipinski, R.J. et al., 2008. Dose- and route-dependent teratogenicity, toxicity, and pharmacokinetic profiles of the hedgehog signaling antagonist cyclopamine in the mouse. *Toxicological sciences : an official journal of the Society of Toxicology*, 104(1), pp.189–197.

Liu, C. et al., 2002. Control of beta-catenin phosphorylation/degradation by a dual-kinase mechanism. *Cell*, 108(6), pp.837–847.

Liu, W. et al., 2000. Mutations in AXIN2 cause colorectal cancer with defective mismatch repair by activating beta-catenin/TCF signalling. *Nature genetics*, 26(2), pp.146–147.

Lorick, K.L. et al., 1999. RING fingers mediate ubiquitin-conjugating enzyme (E2)-dependent ubiquitination. *Proceedings of the National Academy of Sciences of the United States of America*, 96(20), pp.11364–11369.

Lu, Z. et al., 2002. The PHD domain of MEKK1 acts as an E3 ubiquitin ligase and mediates ubiquitination and degradation of ERK1/2. *Molecular cell*, 9(5), pp.945–956.

Lum, L. et al., 2003. Identification of Hedgehog pathway components by RNAi in Drosophila cultured cells. *Science (New York, N.Y.)*, 299(5615), pp.2039–2045.

Lustig, B. et al., 2002. Negative feedback loop of Wnt signaling through upregulation of conductin/axin2 in colorectal and liver tumors. *Molecular and cellular biology*, 22(4), pp.1184–1193.

Lv, L. et al., 2011. Acetylation targets the M2 isoform of pyruvate kinase for degradation through chaperone-mediated autophagy and promotes tumor growth. *Molecular cell*, 42(6), pp.719–730.

Ma, C. & Moses, K., 1995. Wingless and patched are negative regulators of the morphogenetic furrow and can affect tissue polarity in the developing Drosophila compound eye. *Development (Cambridge, England)*, 121(8), pp.2279–2289.

Ma, C. et al., 1993. The segment polarity gene hedgehog is required for progression of the morphogenetic furrow in the developing Drosophila eye. *Cell*, 75(5), pp.927–938.

Ma, X. et al., 2006. Hedgehog signaling is activated in subsets of esophageal cancers.

International journal of cancer. Journal international du cancer, 118(1), pp.139–148.

Maddika, S. & Chen, J., 2009. Protein kinase DYRK2 is a scaffold that facilitates assembly of an E3 ligase. *Nature cell biology*, 11(4), pp.409–419.

Mann, R.K. & Beachy, P.A., 2004. Novel lipid modifications of secreted protein signals. *Annual review of biochemistry*, 73, pp.891–923.

Mansfield, E. et al., 1994. Genetic and Molecular Analysis of hyperplastic discs, a Gene Whose Product Is Required for Regulation of Cell Proliferation in Drosophila melanogaster Imaginal Discs and Germ Cells. *Developmental biology*, 165(2), pp.507–526.

Mao, J. et al., 2001. Low-density lipoprotein receptor-related protein-5 binds to Axin and regulates the canonical Wnt signaling pathway. *Molecular cell*, 7(4), pp.801–809.

Martin, P., Martin, A. & Shearn, A., 1977. Studies of l(3)c43hs1 a polyphasic, temperature-sensitive mutant of Drosophila melanogaster with a variety of imaginal disc defects. *Developmental biology*, 55(2), pp.213–232.

Martín, V. et al., 2001. The sterol-sensing domain of Patched protein seems to control Smoothened activity through Patched vesicular trafficking. *Current biology : CB*, 11(8), pp.601–607.

Mas, C. & Ruiz i Altaba, A., 2010. Small molecule modulation of HH-GLI signaling: current leads, trials and tribulations. *Biochemical pharmacology*, 80(5), pp.712–723.

Matsumoto, M.L. et al., 2010. K11-linked polyubiquitination in cell cycle control revealed by a K11 linkage-specific antibody. *Molecular cell*, 39(3), pp.477–484.

Matunis, M.J., Coutavas, E. & Blobel, G., 1996. A novel ubiquitin-like modification modulates the partitioning of the Ran-GTPase-activating protein RanGAP1 between the cytosol and the nuclear pore complex. *The Journal of cell biology*, 135(6 Pt 1), pp.1457–1470.

Maurange, C. & Paro, R., 2002. A cellular memory module conveys epigenetic inheritance of hedgehog expression during Drosophila wing imaginal disc development. *Genes & development*, 16(20), pp.2672–2683.

Maxwell, P.H. et al., 1999. The tumour suppressor protein VHL targets hypoxia-inducible factors for oxygen-dependent proteolysis. *Nature*, 399(6733), pp.271–275.

McLellan, J.S. et al., 2006. Structure of a heparin-dependent complex of Hedgehog and Ihog. *Proceedings of the National Academy of Sciences of the United States of America*, 103(46), pp.17208–17213.

Metcalfe, C. & Bienz, M., 2011. Inhibition of GSK3 by Wnt signalling--two contrasting models. *Journal of cell science*, 124(Pt 21), pp.3537–3544.

Méthot, N. & Basler, K., 1999. Hedgehog controls limb development by regulating the activities of distinct transcriptional activator and repressor forms of Cubitus interruptus. *Cell*, 96(6), pp.819–831.

Méthot, N. & Basler, K., 2000. Suppressor of fused opposes hedgehog signal transduction by impeding nuclear accumulation of the activator form of Cubitus interruptus. *Development (Cambridge, England)*, 127(18), pp.4001–4010.

Molenaar, M. et al., 1996. XTcf-3 transcription factor mediates beta-catenin-induced axis formation in Xenopus embryos. *Cell*, 86(3), pp.391–399.

Moore, M.J., 2000. Intron recognition comes of AGe. *Nature structural biology*, 7(1), pp.14–16.

Morata, G. & Ripoll, P., 1975. Minutes: mutants of drosophila autonomously affecting cell division rate. *Developmental biology*, 42(2), pp.211–221.

Morin, P.J. et al., 1997. Activation of beta-catenin-Tcf signaling in colon cancer by mutations in beta-catenin or APC. *Science (New York, N.Y.)*, 275(5307), pp.1787–1790.

Motzny, C.K. & Holmgren, R., 1995. The Drosophila cubitus interruptus protein and its role in the wingless and hedgehog signal transduction pathways. *Mechanisms of development*, 52(1), pp.137–150.

Mouchantaf, R. et al., 2006. The ubiquitin ligase itch is auto-ubiquitylated in vivo and in vitro but is protected from degradation by interacting with the deubiquitylating enzyme FAM/USP9X. *The Journal of biological chemistry*, 281(50), pp.38738–38747.

Mueller, T.D. & Feigon, J., 2002. Solution structures of UBA domains reveal a conserved hydrophobic surface for protein-protein interactions. *Journal of molecular biology*, 319(5), pp.1243–1255.

Mukherjee, A. et al., 2000. The Drosophila sox gene, fish-hook, is required for postembryonic development. *Developmental biology*, 217(1), pp.91–106.

Mukherjee, S. et al., 2006. Hedgehog signaling and response to cyclopamine differ in epithelial and stromal cells in benign breast and breast cancer. *Cancer biology & therapy*, 5(6), pp.674–683.

Mukhopadhyay, D. & Riezman, H., 2007. Proteasome-independent functions of ubiquitin in endocytosis and signaling. *Science (New York, N.Y.)*, 315(5809), pp.201–205.

Munoz, M.A. et al., 2007. The E3 ubiquitin ligase EDD regulates S-phase and

G(2)/M DNA damage checkpoints. *Cell cycle (Georgetown, Tex)*, 6(24), pp.3070–3077.

Nakano, Y. et al., 1989. A protein with several possible membrane-spanning domains encoded by the Drosophila segment polarity gene patched. *Nature*, 341(6242), pp.508–513.

Natesan, S. et al., 1997. Transcriptional squelching re-examined. *Nature*, 390(6658), pp.349–350.

Nijman, S.M.B. et al., 2005. A genomic and functional inventory of deubiquitinating enzymes. *Cell*, 123(5), pp.773–786.

Nikaido, H., 2011. Structure and mechanism of RND-type multidrug efflux pumps. *Advances in enzymology and related areas of molecular biology*, 77, pp.1–60.

Nishisho, I. et al., 1991. Mutations of chromosome 5q21 genes in FAP and colorectal cancer patients. *Science (New York, N.Y.)*, 253(5020), pp.665–669.

Noureddine, M.A. et al., 2002. Drosophila Roc1a encodes a RING-H2 protein with a unique function in processing the Hh signal transducer Ci by the SCF E3 ubiquitin ligase. *Developmental cell*, 2(6), pp.757–770.

Nüsslein-Volhard, C. & Wieschaus, E., 1980. Mutations affecting segment number and polarity in Drosophila. *Nature*, 287(5785), pp.795–801.

O'Brien, P.M. et al., 2008. The E3 ubiquitin ligase EDD is an adverse prognostic factor for serous epithelial ovarian cancer and modulates cisplatin resistance in vitro. *British journal of cancer*, 98(6), pp.1085–1093.

Ohlmeyer, J.T. & Kalderon, D., 1998. Hedgehog stimulates maturation of Cubitus interruptus into a labile transcriptional activator. *Nature*, 396(6713), pp.749–753.

Ohshima, R. et al., 2007. Putative tumor suppressor EDD interacts with and up-regulates APC. *Genes to cells : devoted to molecular & cellular mechanisms*, 12(12), pp.1339–1345.

Okochi, K. et al., 2005. Interaction of anti-proliferative protein Tob with poly(A)-binding protein and inducible poly(A)-binding protein: implication of Tob in translational control. *Genes to cells : devoted to molecular & cellular mechanisms*, 10(2), pp.151–163.

Ou, C.-Y. et al., 2002. Distinct protein degradation mechanisms mediated by Cul1 and Cul3 controlling Ci stability in Drosophila eye development. *Genes & development*, 16(18), pp.2403–2414.

Page, A.M. & Hieter, P., 1999. The anaphase-promoting complex: new subunits and regulators. *Annual review of biochemistry*, 68, pp.583–609.

Papadopoulou, D., Bianchi, M.W. & Bourouis, M., 2004. Functional studies of shaggy/glycogen synthase kinase 3 phosphorylation sites in Drosophila melanogaster. *Molecular and cellular biology*, 24(11), pp.4909–4919.

Parker, D.S., Jemison, J. & Cadigan, K.M., 2002. Pygopus, a nuclear PHD-finger protein required for Wingless signaling in Drosophila. *Development (Cambridge, England)*, 129(11), pp.2565–2576.

Peifer, M. et al., 1994. wingless signal and Zeste-white 3 kinase trigger opposing changes in the intracellular distribution of Armadillo. *Development (Cambridge, England)*, 120(2), pp.369–380.

Peleg, Y. & Unger, T., 2012. Resolving bottlenecks for recombinant protein expression in E. coli. *Methods in molecular biology (Clifton, NJ)*, 800, pp.173–186.

Peng, J. et al., 2003. A proteomics approach to understanding protein ubiquitination. *Nature Biotechnology*, 21(8), pp.921–926.

Penton, A., Selleck, S.B. & Hoffmann, F.M., 1997. Regulation of cell cycle synchronization by decapentaplegic during Drosophila eye development. *Science (New York, N.Y.)*, 275(5297), pp.203–206.

Perler, F.B., 1998. Protein splicing of inteins and hedgehog autoproteolysis: structure, function, and evolution. *Cell*, 92(1), pp.1–4.

Pertceva, J.A. et al., 2010. The role of Drosophila hyperplastic discs gene in spermatogenesis. *Cell biology international*, 34(10), pp.991–996.

Peters, C. et al., 2004. The cholesterol membrane anchor of the Hedgehog protein confers stable membrane association to lipid-modified proteins. *Proceedings of the National Academy of Sciences of the United States of America*, 101(23), pp.8531–8536.

Petroski, M.D. & Deshaies, R.J., 2005. Function and regulation of cullin-RING ubiquitin ligases. *Nature reviews Molecular cell biology*, 6(1), pp.9–20.

Pietsch, T. et al., 1997. Medulloblastomas of the desmoplastic variant carry mutations of the human homologue of Drosophila patched. *Cancer research*, 57(11), pp.2085–2088.

Pinson, K.I. et al., 2000. An LDL-receptor-related protein mediates Wnt signalling in mice. *Nature*, 407(6803), pp.535–538.

Pola, R. et al., 2001. The morphogen Sonic hedgehog is an indirect angiogenic agent upregulating two families of angiogenic growth factors. *Nature medicine*, 7(6), pp.706–711.

Price, M.A. & Kalderon, D., 2002. Proteolysis of the Hedgehog signaling effector

Cubitus interruptus requires phosphorylation by Glycogen Synthase Kinase 3 and Casein Kinase 1. *Cell*, 108(6), pp.823–835.

Qualtrough, D. et al., 2004. Hedgehog signalling in colorectal tumour cells: induction of apoptosis with cyclopamine treatment. *International journal of cancer. Journal international du cancer*, 110(6), pp.831–837.

Raasi, S. et al., 2005. Diverse polyubiquitin interaction properties of ubiquitin-associated domains. *Nature structural & molecular biology*, 12(8), pp.708–714.

Raburn, D.J. et al., 1995. Stage-specific expression of B cell translocation gene 1 in rat testis. *Endocrinology*, 136(12), pp.5769–5777.

Raffel, C. et al., 1997. Sporadic medulloblastomas contain PTCH mutations. *Cancer research*, 57(5), pp.842–845.

Ready, D.F., Hanson, T.E. & Benzer, S., 1976. Development of the Drosophila retina, a neurocrystalline lattice. *Developmental biology*, 53(2), pp.217–240.

Regl, G. et al., 2004. Activation of the BCL2 promoter in response to Hedgehog/GLI signal transduction is predominantly mediated by GLI2. *Cancer research*, 64(21), pp.7724–7731.

Reifenberger, J. et al., 1998. Missense mutations in SMOH in sporadic basal cell carcinomas of the skin and primitive neuroectodermal tumors of the central nervous system. *Cancer research*, 58(9), pp.1798–1803.

Reifenberger, J. et al., 2005. Somatic mutations in the PTCH, SMOH, SUFUH and TP53 genes in sporadic basal cell carcinomas. *The British journal of dermatology*, 152(1), pp.43–51.

Renault, L. et al., 1998. The 1.7 A crystal structure of the regulator of chromosome condensation (RCC1) reveals a seven-bladed propeller. *Nature*, 392(6671), pp.97–101.

Reya, T. & Clevers, H., 2005. Wnt signalling in stem cells and cancer. *Nature*, 434(7035), pp.843–850.

Reynolds-Kenneally, J. & Mlodzik, M., 2005. Notch signaling controls proliferation through cell-autonomous and non-autonomous mechanisms in the Drosophila eye. *Developmental biology*, 285(1), pp.38–48.

Rieser, E., Cordier, S.M. & Walczak, H., 2013. Linear ubiquitination: a newly discovered regulator of cell signalling. *Trends in biochemical sciences*, 38(2), pp.94–102.

Rietveld, A. et al., 1999. Association of sterol- and glycosylphosphatidylinositol-linked proteins with Drosophila raft lipid microdomains. *The Journal of biological chemistry*, 274(17), pp.12049–12054.

Rijsewijk, F. et al., 1987. The Drosophila homolog of the mouse mammary oncogene int-1 is identical to the segment polarity gene wingless. *Cell*, 50(4), pp.649–657.

Robbins, D.J. et al., 1997. Hedgehog elicits signal transduction by means of a large complex containing the kinesin-related protein costal2. *Cell*, 90(2), pp.225–234.

Rodier, A. et al., 1999. BTG1: a triiodothyronine target involved in the myogenic influence of the hormone. *Experimental cell research*, 249(2), pp.337–348.

Rogers, E.M. et al., 2005. Pointed regulates an eye-specific transcriptional enhancer in the Drosophila hedgehog gene, which is required for the movement of the morphogenetic furrow. *Development (Cambridge, England)*, 132(21), pp.4833–4843.

Roignant, J.-Y. & Treisman, J.E., 2009. Pattern formation in the Drosophila eye disc. *The International journal of developmental biology*, 53(5-6), pp.795–804.

Romer, J.T. et al., 2004. Suppression of the Shh pathway using a small molecule inhibitor eliminates medulloblastoma in Ptc1(+/-)p53(-/-) mice. *Cancer cell*, 6(3), pp.229–240.

Roose, J. et al., 1998. The Xenopus Wnt effector XTcf-3 interacts with Groucho-related transcriptional repressors. *Nature*, 395(6702), pp.608–612.

Rotin, D. & Kumar, S., 2009. Physiological functions of the HECT family of ubiquitin ligases. *Nature reviews Molecular cell biology*, 10(6), pp.398–409.

Royet, J. & Finkelstein, R., 1997. Establishing primordia in the Drosophila eye-antennal imaginal disc: the roles of decapentaplegic, wingless and hedgehog. *Development (Cambridge, England)*, 124(23), pp.4793–4800.

Royet, J. & Finkelstein, R., 1996. hedgehog, wingless and orthodenticle specify adult head development in Drosophila. *Development (Cambridge, England)*, 122(6), pp.1849–1858.

Rubin, L.L. & de Sauvage, F.J., 2006. Targeting the Hedgehog pathway in cancer. *Nature reviews. Drug discovery*, 5(12), pp.1026–1033.

Rubinfeld, B. et al., 1997. Stabilization of beta-catenin by genetic defects in melanoma cell lines. *Science (New York, N.Y.)*, 275(5307), pp.1790–1792.

Ruel, L. et al., 2007. Phosphorylation of the atypical kinesin Costal2 by the kinase Fused induces the partial disassembly of the Smoothened-Fused-Costal2-Cubitus interruptus complex in Hedgehog signalling. *Development (Cambridge, England)*, 134(20), pp.3677–3689.

Saeki, Y. et al., 2009. Lysine 63-linked polyubiquitin chain may serve as a targeting signal for the 26S proteasome. *The EMBO journal*, 28(4), pp.359–371.

Sanchez, P. & Ruiz i Altaba, A., 2005. In vivo inhibition of endogenous brain tumors through systemic interference of Hedgehog signaling in mice. *Mechanisms of development*, 122(2), pp.223–230.

Sanchez, P. et al., 2004. Inhibition of prostate cancer proliferation by interference with SONIC HEDGEHOG-GLI1 signaling. *Proceedings of the National Academy of Sciences of the United States of America*, 101(34), pp.12561–12566.

Saunders, D.N. et al., 2004. Edd, the murine hyperplastic disc gene, is essential for yolk sac vascularization and chorioallantoic fusion. *Molecular and cellular biology*, 24(16), pp.7225–7234.

Scales, S.J. & de Sauvage, F.J., 2009. Mechanisms of Hedgehog pathway activation in cancer and implications for therapy. *Trends in pharmacological sciences*, 30(6), pp.303–312.

Scheffner, M., Nuber, U. & Huibregtse, J.M., 1995. Protein ubiquitination involving an E1-E2-E3 enzyme ubiquitin thioester cascade. *Nature*, 373(6509), pp.81–83.

Schmidt, T.G.M. & Skerra, A., 2007. The Strep-tag system for one-step purification and high-affinity detection or capturing of proteins. *Nature protocols*, 2(6), pp.1528–1535.

Schneider, I., 1972. Cell lines derived from late embryonic stages of Drosophila melanogaster. *Journal of embryology and experimental morphology*, 27(2), pp.353–365.

Schulman, B.A. & Harper, J.W., 2009. Ubiquitin-like protein activation by E1 enzymes: the apex for downstream signalling pathways. *Nature reviews Molecular cell biology*, 10(5), pp.319–331.

Schwartz, C. et al., 1995. Analysis of cubitus interruptus regulation in Drosophila embryos and imaginal disks. *Development (Cambridge, England)*, 121(6), pp.1625–1635.

Sears, R. et al., 2000. Multiple Ras-dependent phosphorylation pathways regulate Myc protein stability. *Genes & development*, 14(19), pp.2501–2514.

Shi, Q. et al., 2011. The Hedgehog-induced Smoothened conformational switch assembles a signaling complex that activates Fused by promoting its dimerization and phosphorylation. *Development (Cambridge, England)*, 138(19), pp.4219–4231.

Shi, Q., Han, Y. & Jiang, J., 2014. Suppressor of fused impedes Ci/Gli nuclear import by opposing Trn/Kapβ2 in Hedgehog signaling. *Journal of cell science*, 127(Pt 5), pp.1092–1103.

Shimura, H. et al., 2000. Familial Parkinson disease gene product, parkin, is a ubiquitin-protein ligase. *Nature genetics*, 25(3), pp.302–305.

Shyamala, B.V. & Bhat, K.M., 2002. A positive role for patched-smoothened signaling in promoting cell proliferation during normal head development in Drosophila. *Development (Cambridge, England)*, 129(8), pp.1839–1847.

Siegfried, E., Chou, T.B. & Perrimon, N., 1992. wingless signaling acts through zeste-white 3, the Drosophila homolog of glycogen synthase kinase-3, to regulate engrailed and establish cell fate. *Cell*, 71(7), pp.1167–1179.

Skaar, J.R. et al., 2009. SnapShot: F Box Proteins II. *Cell*, 137(7), pp.1358–1358.e1.

Skaar, J.R., Pagan, J.K. & Pagano, M., 2013. Mechanisms and function of substrate recruitment by F-box proteins. *Nature reviews Molecular cell biology*, 14(6), pp.369–381.

Smelkinson, M.G. & Kalderon, D., 2006. Processing of the Drosophila hedgehog signaling effector Ci-155 to the repressor Ci-75 is mediated by direct binding to the SCF component Slimb. *Current biology : CB*, 16(1), pp.110–116.

Smith, G.P., 1985. Filamentous fusion phage: novel expression vectors that display cloned antigens on the virion surface. *Science (New York, N.Y.)*, 228(4705), pp.1315–1317.

Sowa, M.E. et al., 2009. Defining the human deubiquitinating enzyme interaction landscape. *Cell*, 138(2), pp.389–403.

Stambolic, V., Ruel, L. & Woodgett, J.R., 1996. Lithium inhibits glycogen synthase kinase-3 activity and mimics wingless signalling in intact cells. *Current biology : CB*, 6(12), pp.1664–1668.

Stanton, B.Z. et al., 2009. A small molecule that binds Hedgehog and blocks its signaling in human cells. *Nature chemical biology*, 5(3), pp.154–156.

Stecca, B. et al., 2007. Melanomas require HEDGEHOG-GLI signaling regulated by interactions between GLI1 and the RAS-MEK/AKT pathways. *Proceedings of the National Academy of Sciences of the United States of America*, 104(14), pp.5895–5900.

Stringer, D.K. & Piper, R.C., 2011. A single ubiquitin is sufficient for cargo protein entry into MVBs in the absence of ESCRT ubiquitination. *The Journal of cell biology*, 192(2), pp.229–242.

Strutt, D.I. & Mlodzik, M., 1996. The regulation of hedgehog and decapentaplegic during Drosophila eye imaginal disc development. *Mechanisms of development*, 58(1-2), pp.39–50.

Su, H. et al., 2011a. Mammalian hyperplastic discs homolog EDD regulates miRNA-mediated gene silencing. *Molecular cell*, 43(1), pp.97–109.

Su, Y. et al., 2011b. Sequential phosphorylation of smoothened transduces graded

hedgehog signaling. *Science signaling*, 4(180), p.ra43.

Suster, M.L. et al., 2004. Refining GAL4-driven transgene expression in Drosophila with a GAL80 enhancer-trap. *Genesis (New York, N.Y. : 2000)*, 39(4), pp.240–245.

Suzuki, T. et al., 2002. Phosphorylation of three regulatory serines of Tob by Erk1 and Erk2 is required for Ras-mediated cell proliferation and transformation. *Genes & development*, 16(11), pp.1356–1370.

Szczepny, A. et al., 2014. Overlapping binding sites for importin β1 and suppressor of fused (SuFu) on glioma-associated oncogene homologue 1 (Gli1) regulate its nuclear localization. *The Biochemical journal*, 461(3), pp.469–476.

Tabata, T. et al., 1995. Creating a Drosophila wing de novo, the role of engrailed, and the compartment border hypothesis. *Development (Cambridge, England)*, 121(10), pp.3359–3369.

Tabata, T., Eaton, S. & Kornberg, T.B., 1992. The Drosophila hedgehog gene is expressed specifically in posterior compartment cells and is a target of engrailed regulation. *Genes & development*, 6(12B), pp.2635–2645.

Tabs, S. & Avci, O., 2004. Induction of the differentiation and apoptosis of tumor cells in vivo with efficiency and selectivity. *European journal of dermatology : EJD*, 14(2), pp.96–102.

Taipale, J. et al., 2002. Patched acts catalytically to suppress the activity of Smoothened. *Nature*, 418(6900), pp.892–897.

Tamai, K. et al., 2004. A mechanism for Wnt coreceptor activation. *Molecular cell*, 13(1), pp.149–156.

Tamai, K. et al., 2000. LDL-receptor-related proteins in Wnt signal transduction. *Nature*, 407(6803), pp.530–535.

Tanaka, K., Kitagawa, Y. & Kadowaki, T., 2002. Drosophila segment polarity gene product porcupine stimulates the posttranslational N-glycosylation of wingless in the endoplasmic reticulum. *The Journal of biological chemistry*, 277(15), pp.12816–12823.

Tasaki, T. et al., 2005. A family of mammalian E3 ubiquitin ligases that contain the UBR box motif and recognize N-degrons. *Molecular and cellular biology*, 25(16), pp.7120–7136.

Tasaki, T. et al., 2012. The N-end rule pathway. *Annual review of biochemistry*, 81, pp.261–289.

Taylor, F.R. et al., 2001. Enhanced potency of human Sonic hedgehog by hydrophobic modification. *Biochemistry*, 40(14), pp.4359–4371.

Taylor, M.D. et al., 2002. Mutations in SUFU predispose to medulloblastoma. *Nature genetics*, 31(3), pp.306–310.

Terakita, A., 2005. The opsins. *Genome biology*, 6(3), p.213.

Terrell, J. et al., 1998. A function for monoubiquitination in the internalization of a G protein-coupled receptor. *Molecular cell*, 1(2), pp.193–202.

Terriente-Félix, A. et al., 2011. A conserved function of the chromatin ATPase Kismet in the regulation of hedgehog expression. *Developmental biology*, 350(2), pp.382–392.

Thayer, S.P. et al., 2003. Hedgehog is an early and late mediator of pancreatic cancer tumorigenesis. *Nature*, 425(6960), pp.851–856.

Theodosiou, N.A. & Xu, T., 1998. Use of FLP/FRT system to study Drosophila development. *Methods (San Diego, Calif.)*, 14(4), pp.355–365.

Thompson, B. et al., 2002. A new nuclear component of the Wnt signalling pathway. *Nature cell biology*, 4(5), pp.367–373.

Tian, H. et al., 2009. Hedgehog signaling is restricted to the stromal compartment during pancreatic carcinogenesis. *Proceedings of the National Academy of Sciences of the United States of America*, 106(11), pp.4254–4259.

Tian, J. et al., 2010. A new method for multi-site-directed mutagenesis. *Analytical biochemistry*, 406(1), pp.83–85.

Tomaic, V. et al., 2011. Regulation of the Human Papillomavirus Type 18 E6/E6AP Ubiquitin Ligase Complex by the HECT Domain-Containing Protein EDD. *Journal of virology*, 85(7), pp.3120–3127.

Tomlinson, A. & Ready, D.F., 1987. Neuronal differentiation in Drosophila ommatidium. *Developmental biology*, 120(2), pp.366–376.

Tostar, U. et al., 2006. Deregulation of the hedgehog signalling pathway: a possible role for the PTCH and SUFU genes in human rhabdomyoma and rhabdomyosarcoma development. *The Journal of pathology*, 208(1), pp.17–25.

Treisman, J.E. & Rubin, G.M., 1995. wingless inhibits morphogenetic furrow movement in the Drosophila eye disc. *Development (Cambridge, England)*, 121(11), pp.3519–3527.

Tremblay, M.R. et al., 2008. Semisynthetic cyclopamine analogues as potent and orally bioavailable hedgehog pathway antagonists. *Journal of medicinal chemistry*, 51(21), pp.6646–6649.

Trempe, J.-F. et al., 2005. Mechanism of Lys48-linked polyubiquitin chain recognition by the Mud1 UBA domain. *The EMBO journal*, 24(18), pp.3178–

3189.

Tsachaki, M. & Sprecher, S.G., 2012. Genetic and developmental mechanisms underlying the formation of the Drosophila compound eye. *Developmental dynamics : an official publication of the American Association of Anatomists*, 241(1), pp.40–56.

Tsai, Y.-C. & Sun, Y.H., 2004. Long-range effect of upd, a ligand for Jak/STAT pathway, on cell cycle in Drosophila eye development. *Genesis (New York, N.Y. : 2000)*, 39(2), pp.141–153.

Tukachinsky, H. et al., 2012. Dispatched and scube mediate the efficient secretion of the cholesterol-modified hedgehog ligand. *Cell reports*, 2(2), pp.308–320.

Tyers, M. & Willems, A.R., 1999. One ring to rule a superfamily of E3 ubiquitin ligases. *Science (New York, N.Y.)*, 284(5414), pp.601–603–4.

Unden, A.B. et al., 1996. Mutations in the human homologue of Drosophila patched (PTCH) in basal cell carcinomas and the Gorlin syndrome: different in vivo mechanisms of PTCH inactivation. *Cancer research*, 56(20), pp.4562–4565.

van Amerongen, R. & Nusse, R., 2009. Towards an integrated view of Wnt signaling in development. *Development (Cambridge, England)*, 136(19), pp.3205–3214.

van de Wetering, M. et al., 1997. Armadillo coactivates transcription driven by the product of the Drosophila segment polarity gene dTCF. *Cell*, 88(6), pp.789–799.

Varjosalo, M. et al., 2008. Application of active and kinase-deficient kinome collection for identification of kinases regulating hedgehog signaling. *Cell*, 133(3), pp.537–548.

Vijay-Kumar, S., Bugg, C.E. & Cook, W.J., 1987. Structure of ubiquitin refined at 1.8 A resolution. *Journal of molecular biology*, 194(3), pp.531–544.

Vorechovsky, I. et al., 1997. Somatic mutations in the human homologue of Drosophila patched in primitive neuroectodermal tumours. *Oncogene*, 15(3), pp.361–366.

Wang, G. et al., 2014. Hyperplastic discs differentially regulates the transcriptional outputs of hedgehog signaling. *Mechanisms of development*.

Wang, G. et al., 2000. Interactions with Costal2 and suppressor of fused regulate nuclear translocation and activity of cubitus interruptus. *Genes & development*, 14(22), pp.2893–2905.

Watkins, D.N. et al., 2003. Hedgehog signalling within airway epithelial progenitors and in small-cell lung cancer. *Nature*, 422(6929), pp.313–317.

Wehrli, M. et al., 2000. arrow encodes an LDL-receptor-related protein essential for

Wingless signalling. *Nature*, 407(6803), pp.527–530.

Welchman, R.L., Gordon, C. & Mayer, R.J., 2005. Ubiquitin and ubiquitin-like proteins as multifunctional signals. *Nature reviews Molecular cell biology*, 6(8), pp.599–609.

Welsh, G.I. & Proud, C.G., 1993. Glycogen synthase kinase-3 is rapidly inactivated in response to insulin and phosphorylates eukaryotic initiation factor eIF-2B. *The Biochemical journal*, 294 (Pt 3), pp.625–629.

Wen, H. et al., 2008. Epigenetic regulation of gene expression by Drosophila Myb and E2F2-RBF via the Myb-MuvB/dREAM complex. *Genes & development*, 22(5), pp.601–614.

Wertz, I.E. et al., 2004. De-ubiquitination and ubiquitin ligase domains of A20 downregulate NF-kappaB signalling. *Nature*, 430(7000), pp.694–699.

Willert, K. et al., 2003. Wnt proteins are lipid-modified and can act as stem cell growth factors. *Nature*, 423(6938), pp.448–452.

Williams, J.A. et al., 2003. Identification of a small molecule inhibitor of the hedgehog signaling pathway: effects on basal cell carcinoma-like lesions. *Proceedings of the National Academy of Sciences of the United States of America*, 100(8), pp.4616–4621.

Wilson, C.W. & Chuang, P.-T., 2010. Mechanism and evolution of cytosolic Hedgehog signal transduction. *Development (Cambridge, England)*, 137(13), pp.2079–2094.

Wolff, T. & Ready, D.F., 1991. The beginning of pattern formation in the Drosophila compound eye: the morphogenetic furrow and the second mitotic wave. *Development (Cambridge, England)*, 113(3), pp.841–850.

Wood, L.D. et al., 2007. The genomic landscapes of human breast and colorectal cancers. *Science (New York, N.Y.)*, 318(5853), pp.1108–1113.

Wu, J.S. & Luo, L., 2006. A protocol for mosaic analysis with a repressible cell marker (MARCM) in Drosophila. *Nature protocols*, 1(6), pp.2583–2589.

Wu, Q. et al., 2009. Smurf2 induces degradation of GSK-3beta and upregulates beta-catenin in chondrocytes: a potential mechanism for Smurf2-induced degeneration of articular cartilage. *Experimental cell research*, 315(14), pp.2386–2398.

Xia, R. et al., 2012. USP8 promotes smoothened signaling by preventing its ubiquitination and changing its subcellular localization. *PLoS biology*, 10(1), p.e1001238.

Xie, J. et al., 1997. Mutations of the PATCHED gene in several types of sporadic

extracutaneous tumors. *Cancer research*, 57(12), pp.2369–2372.

Xiong, Y. et al., 2011. Regulation of glycolysis and gluconeogenesis by acetylation of PKM and PEPCK. *Cold Spring Harbor symposia on quantitative biology*, 76, pp.285–289.

Xirodimas, D.P. et al., 2004. Mdm2-mediated NEDD8 conjugation of p53 inhibits its transcriptional activity. *Cell*, 118(1), pp.83–97.

Xu, P. et al., 2009. Quantitative proteomics reveals the function of unconventional ubiquitin chains in proteasomal degradation. *Cell*, 137(1), pp.133–145.

Xu, T. & Rubin, G.M., 1993. Analysis of genetic mosaics in developing and adult Drosophila tissues. *Development (Cambridge, England)*, 117(4), pp.1223–1237.

Yan, D. & Lin, X., 2009. Shaping morphogen gradients by proteoglycans. *Cold Spring Harbor perspectives in biology*, 1(3), p.a002493.

Yanagawa, S.-I. et al., 2002. Casein kinase I phosphorylates the Armadillo protein and induces its degradation in Drosophila. *The EMBO journal*, 21(7), pp.1733–1742.

Yao, S., Lum, L. & Beachy, P., 2006. The ihog cell-surface proteins bind Hedgehog and mediate pathway activation. *Cell*, 125(2), pp.343–357.

Yauch, R.L. et al., 2008. A paracrine requirement for hedgehog signalling in cancer. *Nature*, 455(7211), pp.406–410.

Ye, Y. & Rape, M., 2009. Building ubiquitin chains: E2 enzymes at work. *Nature reviews Molecular cell biology*, 10(11), pp.755–764.

Yoon, J.W. et al., 2002. Gene expression profiling leads to identification of GLI1-binding elements in target genes and a role for multiple downstream pathways in GLI1-induced cell transformation. *The Journal of biological chemistry*, 277(7), pp.5548–5555.

Yoshida, M. et al., 2006. Poly(A) binding protein (PABP) homeostasis is mediated by the stability of its inhibitor, Paip2. *The EMBO journal*, 25(9), pp.1934–1944.

Yost, C. et al., 1998. GBP, an inhibitor of GSK-3, is implicated in Xenopus development and oncogenesis. *Cell*, 93(6), pp.1031–1041.

Yuan, Z. et al., 2007. Frequent requirement of hedgehog signaling in non-small cell lung carcinoma. *Oncogene*, 26(7), pp.1046–1055.

Zecca, M., Basler, K. & Struhl, G., 1996. Direct and long-range action of a wingless morphogen gradient. *Cell*, 87(5), pp.833–844.

Zecca, M., Basler, K. & Struhl, G., 1995. Sequential organizing activities of

engrailed, hedgehog and decapentaplegic in the Drosophila wing. *Development (Cambridge, England)*, 121(8), pp.2265–2278.

Zhang, Q. et al., 2006. A hedgehog-induced BTB protein modulates hedgehog signaling by degrading Ci/Gli transcription factor. *Developmental cell*, 10(6), pp.719–729.

Zhang, Q. et al., 2009. Multiple Ser/Thr-rich degrons mediate the degradation of Ci/Gli by the Cul3-HIB/SPOP E3 ubiquitin ligase. *Proceedings of the National Academy of Sciences of the United States of America*, 106(50), pp.21191–21196.

Zhang, W. et al., 2005. Hedgehog-regulated Costal2-kinase complexes control phosphorylation and proteolytic processing of Cubitus interruptus. *Developmental cell*, 8(2), pp.267–278.

Zhang, Y. et al., 2011. Transduction of the Hedgehog signal through the dimerization of Fused and the nuclear translocation of Cubitus interruptus. *Cell research*, 21(10), pp.1436–1451.

Zhao, Y., Tong, C. & Jiang, J., 2007. Hedgehog regulates smoothened activity by inducing a conformational switch. *Nature*, 450(7167), pp.252–258.

Zheng, N. et al., 2000. Structure of a c-Cbl-UbcH7 complex: RING domain function in ubiquitin-protein ligases. *Cell*, 102(4), pp.533–539.

Zheng, X. et al., 2010. Genetic and biochemical definition of the Hedgehog receptor. *Genes & development*, 24(1), pp.57–71.

Zhou, Q. & Kalderon, D., 2011. Hedgehog activates fused through phosphorylation to elicit a full spectrum of pathway responses. *Developmental cell*, 20(6), pp.802–814.

Zhou, R. et al., 2008. Comparative analysis of argonaute-dependent small RNA pathways in Drosophila. *Molecular cell*, 32(4), pp.592–599.